



UNIVERSITY OF
LIVERPOOL

Effect of (Poly)phenols on cytokine release and glutathione metabolism in Jurkat T-Lymphocytes.

Siân Helen Rose Richardson

Aug 2016

**A thesis submitted to the University of Liverpool for the doctor of Philosophy in
the Faculty of Health and Life Sciences**

CONTENTS

		Page
	Abstract	17
	Declaration	18
	Copyright statement	18
	Acknowledgement	20
	Dedication	21
	List of abbreviations	22
CHAPTER 1	INTRODUCTION	
1.1	Ageing	27
1.1.1	An increased ageing population leading to a higher incidence of chronic diseases	27
1.1.2	The role of inflammation and immune system dysregulation associated with ageing	27
1.2	Immune system	29
1.2.1	Jurkat cells as a model for inflammation	30
1.2.2	Cytokines, inflammatory markers	31
1.2.3	T-lymphocyte classes: T helper cells (Th1/Th2)	32
1.2.4	Cytokine profiles of Th1/Th2 cells	32
1.2.5	Cytokines modulated with advancing age	33
1.2.6	T-lymphocyte cytokine induction using phorbol esters such as PMA stimulation	34
1.2.7	T-lymphocytes affected by ageing	35
1.2.8	THP-1 monocytes as a model for inflammation	37
1.3	Oxidative stress	38
1.3.1	Free radicals: molecules contributing to oxidative stress	38
1.3.2	Reactive oxygen species	39
1.3.3	Antioxidants maintaining redox homeostasis	40
1.3.4	Superoxide dismutase and catalase	40
1.3.5	Oxidative stress and T cell activation	42
1.3.6	Glutathione antioxidant system	43
1.3.7	Glutathione modulation with advancing age	46
1.3.8	Thioredoxin and peroxiredoxin antioxidant system	47
1.4	Ageing has been associated with dysregulation in redox homeostasis, increased oxidative stress and damage	49
1.5	Dietary (poly)phenols	49
1.5.1	Natural antioxidants generated by plants	49
1.5.2	Dietary polyphenols as antioxidants	50
1.5.3	Polyphenols and their bioavailability	52

1.5.4	Polyphenols are extensively metabolised following ingestion in the stomach, intestines and by gut microflora	53
1.5.5	Phenolic acids and polyphenols ((Poly)phenols) chosen for study in this thesis	56
1.5.6	Polyphenols, inflammation and oxidative stress	58
1.5.8	Polyphenols used in the treatment of diseases	60
1.6	Aims	61
1.7	Hypothesis	62

CHAPTER 2 MATERIALS AND METHODS

2.1	Materials	64
2.2	Methods	68
2.2.1	Jurkat cell culture	68
2.2.2	THP-1 cell culture	68
2.2.3	Thawing frozen cells and maintaining cell culture	68
2.2.4	Cell counting	69
2.2.4.1	Trypan blue exclusion	69
2.2.4.2	MTS (tetrazolium dye) cell proliferation assay	69
2.2.5	Polyphenols	71
2.2.6	Preparation of stimulations PMA/PHA and LPS	71
2.2.7	Cell treatments for multiplex analysis	72
2.2.7.1	Jurkat cell treatments for cytokine measurements	72
2.2.7.2	THP-1 monocyte cell treatments for cytokine measurements	73
2.2.8	Multiplex assay	73
2.2.8.1	Multiplex assay (1) Jurkat	73
2.2.8.2	Multiplex (2) THP-1	77
2.2.9	Multiplex data analysis	78
2.2.10	Jurkat cell treatments for glutathione measurements	79
2.2.11	Glutathione enzymatic recycling assay	80
2.2.12	Glutathione oxidation by diamide and 50µM curcumin	85
2.2.13	Protein quantification using spectroscopic analysis	86
2.2.13.1	Bradford assay	86
2.2.13.2	BCA assay	86
2.2.14	Nuclear and cytoplasmic extraction in Jurkat cells	87
2.2.15	SDS-PAGE and western blotting	89
2.2.15.1	Gel preparation	89
2.2.15.2	Protein transfer using the semi-dry method	90
2.2.15.3	Immunoblotting	93
2.2.15.4	Analysis and normalisation of immunoblotting images	95
2.2.16	Nrf2 DNA binding assay	96
2.2.17	Cell Treatments for Proteomics analysis	97
2.2.18	Liquid Chromatography Mass Spectrometry (LC-MS) of	98

	proteins	
2.2.18.1	Sample digestion	98
2.2.18.2	High resolution LC-MSMS analysis	99
2.2.18.3	LC separation	99
2.2.18.4	Q Exactive set-up	100
2.2.18.5	Database search and Protein identification	101
2.2.19	RNA isolation and quantification of Jurkat cell samples	101
2.2.20	Quantitative polymerase chain reaction (qPCR) to determine mRNA of proteins involved in glutathione metabolism	104
2.2.21	Analysis and normalisation of qPCR data	107
2.2.22	Evaluating suitable housekeeping genes for qPCR analysis	109
2.2.23	Statistical analysis	110
2.2.23.1	Statistical analysis of cytokine data	110
2.2.23.1	Statistical analysis of LC-MS data	101

CHAPTER 3 INVESTIGATION OF A (POLY)PHENOL PANEL TO IDENTIFY MOLECULES THAT MODULATE INFLAMMATION IN JURKAT T LYMPHOCYTE CELLS

3.1	Introduction	114
3.1.1	Cytokine production and regulation in T lymphocytes	114
3.1.2	Effects of T lymphocyte dysregulation and ageing	114
3.1.3	Interleukin 2 (IL2), interleukin 8 (IL8) and TNF α changes with age	115
3.1.4	Dietary (poly)phenols and benefits to health and age	116
3.2	Aims	117
3.3	Results	118
3.3.1	Evaluating cytokine detection in unstimulated and PMA/PHA stimulated cells using multiplex analysis	118
3.3.2	Modification to cytokine release and cell proliferation by Jurkat T-lymphocytes	121
3.3.3	Assessment of cell viability following (poly)phenol treatments	121
3.3.4	Cytokine release by Jurkat T lymphocyte cells following (poly)phenol treatment	123
3.3.5	Decreases in cytokine release by unstimulated cells	124
3.3.6	Increases in cytokine release by unstimulated cells	125
3.3.7	Decreases in cytokine release by stimulated cells	125
3.3.8	Increases in cytokine release by stimulated cells	126
3.3.9	The effect of (poly)phenol mixtures on cytokine release	135
3.4	Discussion	137
3.4.1	The effects of polyphenol on cell viability in Jurkat T lymphocytes	137

3.4.2	Effects of low concentrations of (poly)phenols on cytokine release by Jurkat T lymphocytes	139
3.4.3	Parent compounds and their metabolites comparing cytokine release	141
3.4.4	Inhibition of cytokine release amplified by (poly)phenol mixes	145
3.4.5	Investigating a structure function relationship within the (poly)phenols	146
3.4.6	Methoxy (poly)phenols identified to have greater effects on cytokine release	147
3.4.7	Identifying (poly)phenols that significantly lowering the cytokine release of IL2, IL8 and TNF α in stimulated and unstimulated cells.	151

CHAPTER 4 PROTEOMIC ANALYSIS OF CHANGES IN PROTEIN EXPRESSION CAUSED BY TREATMENT OF JURKAT T-LYMPHOCYTES WITH POLYPHENOLS

4.1	Introduction	155
4.1.1	Proteomic analysis evaluating the changes in protein content following polyphenol treatments	155
4.1.2	Proteomics analysis: Label-free mass spectrometry technique	157
4.1.3	Protein network analysis	157
4.2	Aims	158
4.3	Results	158
4.3.1	Proteomics analysis: number of proteins modulated following polyphenols treatments for 48h in Jurkat T lymphocytes	158
4.3.2	Proteins modified by all three (poly)phenol treatments at either one or both doses	160
4.3.3	Redox-active centres and oxidoreductase activity	163
4.3.4	Oxidative phosphorylation	168
4.3.5	Ribosome modification by the three polyphenol treatments	168
4.3.6	RESVERATROL: proteins modulated follow resveratrol treatment	170
4.3.7	CURCUMIN: proteins modulated follow curcumin treatment	175
4.3.8	ISORHAMNETIN: proteins modulated follow isorhamnetin treatment	179
4.4	Discussion	183
4.4.1	Network analysis of polyphenol proteomics identified NF- κ B to be a central modulated factor	183

4.4.2	Unconventional Myosin-Ia reduction with curcumin	185
4.4.3	Polyphenols and oxidative phosphorylation	186
4.4.4	Modulations with redox homeostasis with the polyphenol treatments	187

CHAPTER 5 THE ANALYSIS OF GLUTATHIONE MODIFICATION BY JURKAT T-LYMPHOCYTES

5.1	Introduction	194
5.1.1	Ageing and elevated levels of oxidative stress	194
5.1.2	Antioxidant proteins maintaining redox homeostasis in the cell	194
5.1.3	Polyphenols regulating cellular redox mechanisms	195
5.2	Aims	196
5.3	Results	196
5.3.1	Glutathione reductase protein expression with polyphenol treatments over time	196
5.3.2	Analysis of glutathione reductase, glutathione synthetase, glutathione peroxidase, and glutamate—cysteine ligase gene expression	200
5.3.3	Glutathione modulation and (poly)phenols	203
5.3.4	Curcumin and isorhamnetin increase Nrf2 activation	206
5.3.5	Immunoblotting for Nrf2, and phosphorylated Nrf2 with isorhamnetin treatments	208
5.3.6	Inhibition of nuclear translocation of Nrf2 by the use of Ochratoxin A	208
5.4	Discussion	211
5.4.1	Polyphenols significantly increased the protein and gene expression of glutathione reductase in Jurkat T lymphocytes	212
5.4.2	Increases in glutathione production and regeneration gene expression	213
5.4.3	Nrf2 activation induced by curcumin and isorhamnetin	216

CHAPTER 6 VALIDATION OF CYTOKINE AND GLUTATHIONE MODULATION IN ANOTHER CELL TYPE, THP-1 CELLS

6.1	Introduction	221
6.2	Aims	224
6.3	Results	224
6.3.1	Optimisation of the culture of THP-1 monocytes with the addition of isorhamnetin	224

6.3.2	Multiplex analysis detecting cytokine release in stimulated and unstimulated THP-1 cells	226
6.3.3	Gene expression analysis of glutathione reductase, glutathione synthase, glutathione peroxidase and glutamate—cysteine ligase	229
6.3.4	Nrf2 activation analysis with isorhamnetin treatment in unstimulated and stimulated THP-1 cells	230
6.4	Discussion	232
6.4.1	Modulations to cytokine release following isorhamnetin treatment in THP-1 cells for 48h	233
6.4.2	Activation of Nrf2 with isorhamnetin, but not induction of glutathione genes	236
CHAPTER 7	DISCUSSION	
7.1	Summary of main findings	238
7.2	Experimental set-up and limitations	240
7.3	Cytokine release was significantly repressed by treatment with polyphenols in Jurkat T lymphocytes	243
7.4	Significant increases in the abundance of redox proteins with polyphenol treatments that were identified through quantitative proteomics	246
7.5	Induction to redox proteins confirmed using protein and gene analysis, along with induction of the antioxidant transcription factor Nrf2	250
7.6	Proposed mechanism antioxidant action of isorhamnetin	253
7.7	Cytokine release was significantly reduced by isorhamnetin in THP-1 cells, but changes to glutathione homeostasis were not confirmed	258
7.8	Summary	259
CHAPTER 8	APPENDIX	
8.1	Polyphenol data sheets	261
8.2	Variability of cytokine data between experiments	271
8.3	Principal component analysis (PCA) for Polyphenol proteomics data	281
8.4	Proteomic data sets for all polyphenol treatments curcumin, isorhamnetin and resveratrol	294
8.5	Proteomics data, number of induced vs repressed proteins with polyphenol treatment	360
8.6	Outcomes	369
 REFERENCES		 372

LIST OF FIGURES

	Page
CHAPTER 1	
Figure	
1.1	Differential secretion of pro- and anti-inflammatory cytokines by T-lymphocyte sub-groups Th1 and Th2. 34
1.2	Co-operative activities of manganese superoxide dismutase (MnSOD) and catalase in neutralising superoxide 41
1.3	Glutathione recycling mechanism 45
1.4	Green tea flavan-3-ols metabolism and breakdown products following consumption 54
1.5	Panel of (poly)phenol compounds chosen for cytokine release investigation 58
1.6	Simplified version polyphenols mechanism of action 59
CHAPTER 2	
Figure	
2.1	Jurkat standard curve used to determine the cell number following the intervention with (poly)phenol 70
2.2	Bio-Plex Pro assay, a flow diagram summarising the steps required for multiple cytokine detection using a multiplex assay 76
2.3	Principles behind the glutathione enzymatic recycling assay 82
2.4	Glutathione redox potential of Jurkat cells 84
2.5	Positive control for oxidised glutathione measurements for glutathione recycling assay 85
2.6	Preparation of gel to allow protein transfer 92
2.7	Ponceau S stain applied to nitrocellulose membrane to allow reversible visualisation of proteins 93
2.8	Bioanalyser example report 103
2.9	Example RNA quantification using NanoDrop 2000 instrument 104
2.10	Changes in CT values of normalising gene TBP over time 109
CHAPTER 3	
Figure	
3.1	Cell viability following the addition of PMA/PHA stimulation by Jurkat T-lymphocytes 123
3.2	Percentage change in cell number with 1 & 30 μ M (poly)phenols in unstimulated cells 127
3.3	Percentage change in interleukin 2 (IL2) release with 1 and 30 μ M (poly)phenols in unstimulated cells 128
3.4	Percentage change in interleukin 8 (IL8) release with 1 and 30 μ M (poly)phenols in unstimulated cells 129

3.5a	Percentage change in IL2 and IL8 with pyrogallol in unstimulated cells	130
3.5b	Percentage change in IL2, IL8 and TNF α with pyrogallol in stimulated cells	130
3.6	Percentage change in cell number with 1 and 30 μ M (poly)phenols in stimulated cells	131
3.7	Percentage change in interleukin 2 (IL2) release with 1 and 30 μ M (poly)phenols in stimulated cells	132
3.8	Percentage change in interleukin 8 (IL8) release with 1 and 30 μ M (poly)phenols in stimulated cells	133
3.9	Percentage change in tumour necrosis factor alpha (TNF α) release with 1 and 30 μ M (poly)phenols in stimulated cells	134
3.10a	Graph shows changes to IL2 release following treatments with mixtures of 4 (poly)phenols, alongside the individual (poly)phenols making up that mixture	136
3.10b	Graph shows changes to IL8 release following treatments with mixtures of 4 (poly)phenols, alongside the individual (poly)phenols making up that mixture	136
3.11	Cytokine release of IL2 and IL8 with 1 μ M (poly)phenols	140
3.12	Phenolic acid breakdown products of quercetin	141
3.13	Quercetin and metabolites effects on inflammation	143
3.14	Curcumin and metabolites effects on inflammation	144
3.15	Resveratrol and metabolites effects on inflammation	145
3.16	Graph shows the lipophilic values of the (poly)phenol compounds (K_{ow}) plotted against the cell viability	147
3.17a	Structural differences between protocatechuic acid and vanillic acid	149
3.17b	Effect 1 and 30 μ M protocatechuic acid and vanillic acid had on cytokine release in unstimulated cells	149
3.17c	Effect 1 and 30 μ M protocatechuic acid and vanillic acid had on cytokine release in stimulated cells	149
3.18	Example of other methoxy (poly)phenols	150
3.19	Significant reduction of (poly)phenols in unstimulated cells	152
3.20	Significant reduction of (poly)phenols in stimulated cells	153

CHAPTER 4

Figure

4.1	Ingenuity network analysis of proteins modulated following 30 μ M treatment of resveratrol	173
4.2	Ingenuity network analysis obtained using the 30 μ M resveratrol data set, identified phospholipase c signalling as a modified pathway	174
4.3	Ingenuity network analysis of proteins modulated following 10 μ M treatment of curcumin	177

4.4	Ingenuity network analysis of proteins modulated following 10 μ M treatment of curcumin	178
4.5	Ingenuity network analysis of proteins modulated following 30 μ M treatment of isorhamnetin	181
4.6	Ingenuity network analysis of proteins modulated following 30 μ M treatment of isorhamnetin	182
4.7	GRK2 signalling in response to ROS leading to activation of NF- κ B, leading to the induction of inflammatory markers	184
4.8	Role of myosin in immune cells	186
4.9	Glutathione metabolism pathway	191

CHAPTER 5

Figure

5.1a	Identifying changes to glutathione reductase (GSR) in Jurkat cells following 48h treatment with 10 μ M curcumin (Cur) and 30 μ M isorhamnetin (Iso) and resveratrol (Res)	198
5.1b	Identifying changes to glutathione reductase (GSR) in Jurkat cells following 48h treatment with 30 μ M isorhamnetin (Iso)	198
5.2	Glutathione reductase protein expression with 24 h treatment with isorhamnetin, curcumin and resveratrol treatments	199
5.3a	Time-course treatments with curcumin, isorhamnetin and resveratrol evaluating the gene expression of GSR	200
5.3b	Time-course treatments with curcumin, isorhamnetin and resveratrol evaluating the gene expression of GPx1	201
5.3c	Time-course treatments with curcumin, isorhamnetin and resveratrol evaluating the gene expression of GSS	201
5.3d	Time-course treatments with curcumin, isorhamnetin and resveratrol evaluating the gene expression of GCLC	202
5.4a	Concentrations of intracellular glutathione (GSH) in nmol/million cells from Jurkat cells treated 1 and 10 μ M curcumin	204
5.4b	Concentrations of intracellular glutathione (GSH) in nmol/million cells from Jurkat cells treated with 1 and 30 μ M isorhamnetin	204
5.4c	Concentrations of intracellular glutathione (GSH) in nmol/million cells from Jurkat cells treated with 1 and 30 μ M resveratrol	204
5.5	Concentration of intracellular oxidised GSSG in nmol/million cells from Jurkat cells treated with 1 and 30 μ M resveratrol	205
5.6	DNA binding assay measuring Nrf2 activation in Jurkat cell samples following treatment with curcumin, resveratrol, and isorhamnetin for 48 h	207
5.7	DNA binding assay measuring Nrf2 activation in Jurkat cell samples following time-course treatment with curcumin,	207

	resveratrol, and isorhamnetin for 1, 3, 9, 24, and 48 h	
5.8a	Western blot for phosphorylated- Nrf2 and Nrf2 following treatment with isorhamnetin for 1, 3, 9, and 24h in Jurkat T-lymphocytes	208
5.8b	Densitometry analysis of Nrf2 following 24h treatment with isorhamnetin	208
5.9	Jurkat cell viability following treatment with 1, 2.5, 5, 10 and 30µM Ochratoxin A over a 72h time period	209
5.10a	Western blot analysis of Nrf2 in nuclear and cytoplasmic extracts in Jurkats treated with 1 and 2.5µM Ochratoxin A for 72h	210
5.10b	Densitometry of Nrf2 in the cytoplasm	210
5.10c	Densitometry of Nrf2 in the nucleus	210
5.11a	Inhibition of Nrf2 translocation into the nucleus by 5µM OTA treatment in Jurkat T lymphocytes	211
5.11b	Nrf2 in the cytoplasm following treatment with 5µM OTA in Jurkat T lymphocytes	211
5.12	Glutathione synthesis and regulation pathway	213
5.13a	Fold changes in Nrf2, glutathione reductase (GSR) and glutamate-cysteine ligase (GCLC) over time with isorhamnetin	217
5.13b	Fold changes in Nrf2, glutathione reductase (GSR) and glutamate-cysteine ligase (GCLC) over time with resveratrol	217
5.13c	Fold changes in Nrf2, glutathione reductase (GSR) and glutamate-cysteine ligase (GCLC) over time with curcumin	218

CHAPTER 6

Figure

6.1	Structure of isorhamnetin, an O-methylated flavonol	222
6.2a	THP-1 cell number following treatment with 1, 10, and 30µM isorhamnetin for 48h (unstimulated cells)	225
6.2b	THP-1 cell number following treatment with 1, 10, and 30µM isorhamnetin for 48h, with a 4 h 1µg/ml LPS stimulation	225
6.3a	Multiplex analysis of MCP-1 following treatment of 1, 10, and 30µM isorhamnetin for 48h in THP-1 monocytes in unstimulated cells	227
6.3b	Multiplex analysis of MCP-1 following treatment of 1, 10, and 30µM isorhamnetin for 48h in THP-1 monocytes with 4h stimulation of LPS prior to the end	227
6.3c	Multiplex analysis of TNFα following treatment of 1, 10, and 30µM isorhamnetin for 48h in THP-1 monocytes in unstimulated cell	227
6.3d	Multiplex analysis of TNFα following treatment of 1, 10, and 30µM isorhamnetin for 48h in THP-1 monocytes with 4h stimulation of LPS prior to the end	227

6.4a	Multiplex analysis of IL1 β following treatment of 1, 10, and 30 μ M isorhamnetin for 48h with 4h stimulation of LPS prior to the end in THP-1 monocytes	228
6.4b	Multiplex analysis of IL6 following treatment of 1, 10, and 30 μ M isorhamnetin for 48h with 4h stimulation of LPS prior to the end in THP-1 monocytes	228
6.4c	Multiplex analysis of IL8 following treatment of 1, 10, and 30 μ M isorhamnetin for 48h with 4h stimulation of LPS prior to the end in THP-1 monocytes	228
6.4d	Multiplex analysis of IL10 following treatment of 1, 10, and 30 μ M isorhamnetin for 48h with 4h stimulation of LPS prior to the end in THP-1 monocytes	228
6.4e	Multiplex analysis of IL12 (p70) following treatment of 1, 10, and 30 μ M isorhamnetin for 48h with 4h stimulation of LPS prior to the end in THP-1 monocytes	228
6.4f	Multiplex analysis of GRO following treatment of 1, 10, and 30 μ M isorhamnetin for 48h with 4h stimulation of LPS prior to the end in THP-1 monocytes	228
6.5	qPCR using primers for glutathione reductase (GSH), glutathione synthase (GSS), glutathione peroxidase (GPX1) and glutamate—cysteine ligase (GCLC) following 30 μ M isorhamnetin treatment over a time-course of 3, 9, 24, and 48 h in THP-1 cells	230
6.6a	DNA binding assay measuring Nrf2 activation in THP-1 monocyte cell samples following treatment with 1, 10, 30 μ M isorhamnetin for 48 h	231
6.6b	DNA binding assay measuring Nrf2 activation in THP-1 monocyte cell samples following treatment with 1, 10, 30 μ M isorhamnetin for 48 h, with LPS treatment 4 h prior to the end	231
6.7	DNA binding assay measuring Nrf2 activation in THP-1 monocyte cell samples following treatment with 1 and 30 μ M isorhamnetin for 3, 9, 24, and 48 h	232
6.8	IPA cytokine network analysis, modulation occurred with isorhamnetin treatment	235

CHAPTER 7

Figure

7.1	RSK (p70 kDa ribosomal protein S6 kinase) a mediator for cell survival, protecting the cell from apoptosis	248
7.2	Proposed mechanism of action for antioxidant and anti-inflammatory effect of Isorhamnetin	256

CHAPTER 8

Figure

8.1	Variability between cell number both within an experiment and also between experiments conducted on different days	271
8.2	Variability between IL2 and IL8 in unstimulated cells both within an experiment and also between experiments conducted on different days	272
8.3	Variability between IL2 and IL8 in PMA/PHA stimulated cells both within an experiment and also between experiments conducted on different days	273
8.4	Variability between TNF α in PMA/PHA stimulated cells both within an experiment and also between experiments conducted on different days	274
8.5	PCA Plots for peptide data generated from proteomics using 1 μ M treatments of curcumin and resveratrol compared with DMSO treated control	281
8.6	PCA Plots for protein data generated from proteomics using 1 μ M treatments of curcumin and resveratrol compared with DMSO treated control	282
8.7	PCA Plots for peptide data generated from proteomics using 1 μ M treatments of curcumin compared with DMSO treated control	283
8.8	PCA Plots for protein data generated from proteomics using 1 μ M treatments of curcumin compared with DMSO treated control	284
8.9	PCA Plots for peptide data generated from proteomics using 1 μ M treatments of resveratrol compared with DMSO treated control	285
8.10	PCA Plots for protein data generated from proteomics using 1 μ M treatments of resveratrol compared with DMSO treated control	286
8.11	PCA Plots for peptide data generated from proteomics using 10 μ M treatments of curcumin and 30 μ M resveratrol compared with DMSO treated control	287
8.12	PCA Plots for protein data generated from proteomics using 10 μ M treatments of curcumin and 30 μ M resveratrol compared with DMSO treated control	288
8.13	PCA Plots for peptide data generated from proteomics using 1 μ M treatments of isorhamnetin compared with DMSO treated control	289
8.14	PCA Plots for protein data generated from proteomics using 1 μ M treatments of isorhamnetin compared with DMSO treated control	290
8.15	PCA Plots for peptide data generated from proteomics using	291

	30µM treatments of isorhamnetin compared with DMSO treated control	
8.16	PCA Plots for protein data generated from proteomics using 30µM treatments of isorhamnetin compared with DMSO treated control	292
8.17	Proteomics data from Isorhamnetin both doses (1 and 30µM) split into function categories	361
8.18	Proteomics data characterised into function categories, Isorhamnetin 1 µM and 30µM	362
8.19	Key for Ingenuity network analysis pathways	363
8.20	Zoomed in version of Ingenuity network analysis for 10µM curcumin data set identified Nrf2 signalling as a modified pathway	365
8.21	Zoomed in version of Ingenuity network analysis for 30µM isorhamnetin data set identified Nrf2 signalling as a modified pathway	367

LIST OF TABLES

	Page	
CHAPTER 1		
Table		
CHAPTER 2		
Table		
2.1	Preparation of glutathione recycling assay buffers	83
2.2	Nuclear/Cytoplasm extract buffers	88
2.3	Buffers for protein transfer during Western blotting	91
2.4	Primary and secondary antibodies used in the immunoblotting	95
2.5	cDNA master mix preparation	105
2.6	Preparation of TaqMan master mix used in the quantitative PCR reaction	107
2.7	Gene primers used in the quantitative PCR reaction	107
2.8	Determining suitable housekeeping genes for qPCR analysis	110
2.9	Programs used to identify function, pathways, clustering of the proteins identified using proteomics	112

CHAPTER 3

Table

3.1	Cytokines induced by PMA/PHA treatment of Jurkat CD4 ⁺ T-lymphocytes	120
-----	---	-----

CHAPTER 4

Table

4.1	Cytokine release following 48h treatment with polyphenols curcumin, isorhamnetin and resveratrol by Jurkat T-lymphocytes	156
4.2	Number of proteins found to have significant fold changes following 48h treatment with the three different (poly)phenols curcumin, resveratrol and isorhamnetin	160
4.3	Quantitative proteomics identified proteins which are common to all three (poly)phenol treatments curcumin, isorhamnetin and resveratrol	163
4.4	Proteins containing redox-active centres or oxidoreductase activity that were significantly modified by the polyphenol treatments	164
4.5	Significant modulation to ribosomal proteins with all three polyphenol treatments	169
4.6	Key for glutathione metabolism pathway diagram on following page and a summary of treatment effects	190

CHAPTER 8

Table

8.1	Polyphenol data: name, structure, molecular weightm food sources and concentrations in plasma	261
8.2	Polyphenol cytokine raw data. 29 different polyphenols at both 1 and 30µM for 48h (unstimulated cells)	275
8.3	Polyphenol cytokine raw data. Polyphenols mixtures at both 1 and 30µM for 48h (unstimulated cells)	276
8.4	Polyphenol cytokine raw data. 29 different polyphenols at both 1 and 30µM for 48h (stimulated cells)	277
8.5	Polyphenol cytokine raw data. Polyphenols mixtures at both 1 and 30µM for 48h (stimulated cells)	278
8.6	Significantly modulated proteins in Jurkat T lymphocytes after 1µM resveratrol identified by label-free LC-MS	294
8.7	Significantly modulated proteins in Jurkat T lymphocytes after 1µM curcumin identified by label-free LC-MS	296
8.8	Significantly modulated proteins in Jurkat T lymphocytes after 30µM resveratrol identified by label-free LC-MS	299

8.9	Significantly modulated proteins in Jurkat T lymphocytes after 10 μ M curcumin identified by label-free LC-MS	322
8.10	Significantly modulated proteins in Jurkat T lymphocytes after 1 μ M isorhamnetin identified by label-free LC-MS	333
8.11	Significantly modulated proteins in Jurkat T lymphocytes after 30 μ M isorhamnetin identified by label-free LC-MS	338

Abstract

Chronic inflammation and increases in oxidative stress are observed in normal ageing and age related diseases, these are characterised by increases in aberrant NF- κ B activation, expression of inflammatory genes and circulating cytokines. Dietary polyphenols found in fruits and vegetables, have been examined for potential antioxidant and anti-inflammatory effects in *in vitro/vivo* studies.

29 (poly)phenols were screened for their anti-inflammatory effects in Jurkat T-cells following 48h treatment. At 1 μ M, a physiologically relevant dose, resveratrol (RES) decreased IL2 release by 42% \pm 7% and IL8 by 32% \pm 8% compared with DMSO treated control ($p < 0.05$). Cells were also stimulated with PMA/PHA to induce cytokine release at the 24h time-point, 1 μ M isorhamnetin (ISO) reduced cytokine release, IL2 by 50% \pm 4%, IL8 by 58% \pm 6% and TNF α by 63% \pm 7%, and curcumin (CUR) reduced IL2 by 43% \pm 14%, IL8 by 30% \pm 7% and TNF α by 22% \pm 5 compared with PMA/PHA treated control ($p < 0.05$). These 3 compounds; CUR, ISO and RES, were investigated further using a proteomic approach. Several proteins were modified in the glutathione metabolism pathway with all treatments significantly (sig.) increasing glutathione reductase (GSR), an enzyme which converts oxidized to reduced glutathione. CUR increased GSR by 1.2 fold, ISO 1.2 fold and RES 1.1 fold ($p < 0.003$). ISO also caused sig. increases in other redox related proteins thioredoxin and peroxiredoxins. These data were validated with sig. increases in GSR gene expression with CUR and ISO at 24h, along with sig. increases in Nrf2 activation, CUR (1.5 fold) and ISO (1.9 fold).

These modulations to inflammatory and redox markers in the Jurkat cell model were replicated in another cell line, THP-1 monocytes. A sig. reduction in cytokine release was observed with 30 μ M ISO for both IL8 and TNF α compared with the DMSO, correlating with the reduction observed in the Jurkat cells. Nrf2 was also sig. activated between 3 and 48h, however no sig. effect on the expression of GSR was observed. This suggests that ISO may have similar effects on inflammation but differed in terms of redox related proteins between the two cell types. CUR, ISO and RES sig. lowered cytokine release in both unstimulated and stimulated T-cells, and proteomics identified sig. increases in GSR. For CUR and ISO this increase was validated using western blot and qPCR analysis, with sig. increases in Nrf2 activation being observed. The reduction in cytokine release was replicated in THP-1 following ISO treatment, along with increases in Nrf2 activation, but no changes in glutathione proteins were observed. These data support the potential use of these compounds in enhancing cellular antioxidant potential and the use of the compounds as part of a healthy ageing diet.

Declaration

No portion of the work described in this thesis has been submitted in support of an application for another degree or qualification of this or any other university or other institute of learning.

Copyright statement

- I. The author of this thesis (including and appendices and/or schedules to this thesis) owns certain copyright or related right in it (the “Copyright”) and has given The University of Liverpool certain rights to use such Copyright, including for administrative purposes.
- II. Copies of this thesis, either in full or in extracts and whether in hard or electronic copy, may be made **only** in accordance with the Copyright, Designs and Patents Act 1988 (as amended) and regulations issued under it or, where appropriate, in accordance with licensing agreements which the University has from time to time. This page must form part of any such copies made.

- III.** The ownership of certain Copyright, patents, designs, trademarks and other intellectual property (the “Intellectual Property”) and any reproductions of copyright works in the thesis, for example graphs and tables (“Reproductions”), which may be described in this thesis, may not be owned by the author and may be owned by third parties. Such Intellectual Property and Reproductions cannot and must not be made available for use without the prior written permission of the owner(s) of the relevant Intellectual Property and/or Reproductions.
- IV.** Further information on the conditions under which disclosure, publication and commercialisation of this thesis, the Copyright and any Intellectual Property and/or Reproductions described in it may take place is available in the University IP Policy (see <https://www.liv.ac.uk/intellectual-property/ip-policy.pdf>), in any relevant Thesis restriction declarations deposited in the University Library, The University Library’s regulations (see <http://www.liv.ac.uk/library/using/regulations.html>) and in The University’s policy on presentation of Theses.

Acknowledgements

I would like to thank my supervisors Dr Christopher Ford, Prof. Anne McArdle and Prof. Malcolm Jackson for their help, guidance and support during my time at Liverpool. I would also like to thank to my industrial supervisor Dr Silvina Lotito for making my industrial placement such an enjoyable experience and for all her advice, support and encouragement thought out the project, along with Jenny and Eleanor who were a great help in co-ordinating and helping me during my time at Unilever. I would like to acknowledge and thank the funders, the BBSRC-DRINC (BB/I005994/1) and Unilever who sponsored this work.

I would also like to thank all of the collaborators, Professor Alan Crozier at the University of Glasgow, Prof. Robert Beynon and Dr Deborah Simpson at the Centre for Proteome Research at University of Liverpool. Also to all the members of the institute past and present that have contributed to this project.

A big thanks to all members of the lab, in particular my office buddies Rachel and Melanie, for always being there, providing daily dramas and countless laughs.

I would like to say a huge thank you to my family for always supporting me. My mum and auntie Heather, my sisters Bethan, Megan and Caitlin who have always been there though all the highs and lows. Thanks to my great friends Shuo and Oktawia, a friendship created when I first started studying 10 years ago, they have always been there, providing support, advice and reassurance when needed and great times away from studying. For my friends in the cycling society and Greenbank hall of residences, thanks for time away from the lab, providing countless laughs and adventures, I will miss you all.

Dedication

I would like to dedicate my work to my loving gran and grandad without their guidance and encouragement I would not be the person I am today. I hope I have made them very proud.



List of abbreviations

A	Amp(s)
ANOVA	Analysis of variance
APS	Ammonium persulfate
B2M	Beta-2 microglobulin
CAT	Catalase
cDNA	Complementary DNA
CO ₂	Carbon dioxide
Ct	Cycle threshold
CUR	Curcumin
dH ₂ O	Distilled water
DMSO	Dimethyl sulfoxide
DPBS	Dulbecco's phosphate-buffered saline
DTNB	5,5'-dithiobis(2-nitro-benzoic acid)
ECL	Enhanced chemiluminescence
EDTA	Ethylenediamine tetra acetic acid
EGCG	Epigallocatechin gallate
FBS	Foetal bovine serum
<i>g</i>	Gravity
g	Gram(s)
GCLC	Glutathione-cysteine ligase
G-CSF	Granulocyte-colony stimulating factor
GM-CSF	Granulocyte macrophage colony-stimulating factor
GPx1	Glutathione peroxidase 1

GRO	Growth-regulated gene product
GSH	Reduced glutathione
GSSG	Oxidised glutathione
GSS	Glutathione synthetase
GSR	Glutathione reductase
h	Hour(s)
HEPES	4-(2-hydroxyethyl)-1-piperazineethanesulfonic acid
H ₂ O ₂	Hydrogen peroxide
IL1 β	Interleukin 1 beta
IL2	Interleukin 2
IL6	Interleukin 6
IL8	Interleukin 8
IL10	Interleukin 10
IL12p40	Interleukin 12 p40
IL12p70	Interleukin 12 p70
ISO	Isorhamnetin
kDa	Kilodaltons
L	Litre(s)
LPS	Lipopolysaccharide
M	Molar (moles/litre)
MCP-1	Monocyte chemoattractant protein-1
μ g	Microgram(s)
mg	Milligram(s)
min	Minute(s)
ml	Millilitre(s)
μ M	Micromole(s) per litre or micromolar

mM	Millimole(s) per litre or millimolar
MTS	3-(4,5-dimethylthiazol-2-yl)-5-(3-carboxymethoxyphenyl)-2-(4-sulfophenyl)-2H-tetrazolium assay
mV	Millivolt(s)
<i>n</i>	Number of replicates
NADP+	Nicotinamide adenine dinucleotide phosphate
NADPH	β -Nicotinamide adenine dinucleotide phosphate, reduced tetra(cyclohexylammonium) salt
NF- κ B	Nuclear factor kappa B
Nrf2	Nuclear factor (erythroid-derived 2)-like 2
OTA	Ochratoxin A
pg	Picogram
PBS	Phosphate buffered saline
PCR	Polymerase chain reaction
PHA	Phytohaemagglutinin
PMA	Phorbol 12-myristate 13-acetate
PMSF	Phenylmethylsulphonyl fluoride
PRDX	Peroxiredoxin
RES	Resveratrol
RNA	Ribonucleic acid
ROS	Reactive oxygen species
rpm	Revolution(s) per minute
RPMI	Roswell Park Memorial Institute
s	Seconds
SDS	Sodium dodecyl sulphate
SDS-PAE	Sodium dodecyl sulphate – polyacrylamide gel electrophoresis

SEM	Standard error of the mean
SSA	Sulphosalicylic acid
TCR	T-cell receptor
TBP	TATA-binding protein
TBS	Tris-buffered saline
TEMED	NNN'N' – tetramethylethylene-diamine
TNF α	Tumour necrosis factor alpha
Tween	Polyoxyethylene – sorbitan monolaurate
TXN	Thioredoxin
μ l	Microlitre(s)
μ M	Micromole(s) per litre
V	Volt(s)
v/v	Volume per volume
w/v	Weight per volume
WHO	World Health Organisation
%	Percentage
$^{\circ}$ C	Degree(s) Celsius
<	Less than
>	Greater than

CHAPTER 1

INTRODUCTION

1.1 Ageing

1.1.1 An increased ageing population leading to a higher incidence of chronic diseases.

The number of people aged over 60 is anticipated to increase globally from 605 million to 2 billion by 2050 (WHO)¹. Improvements in health care have meant people are living longer but the incidence of chronic diseases associated with age such as cardiovascular disease, cancer and Alzheimer's disease are also increasing. The burden the health services supporting the ageing community and treating chronic diseases is therefore becoming a problem. The increasing numbers of elderly people seeking treatments is estimated to cost the UK between £1 billion² and £1.4 billion³ each year. The focus now is on finding ways to improve the quality of life of the ageing population, by promoting healthy ageing and making sure these extra years are healthy years. It is thought that diets rich in antioxidants could help increase lifespan, improve health and prevent disease progression in an ageing population^{4, 5, 6}.

1.1.2 The role of inflammation and immune system dysregulation associated with ageing.

As we age the adaptive and innate immune systems show multiple dysregulations resulting in a chronic systemic pro-inflammatory state, known as inflammaging,

first characterised by C. Franceschi in 2000⁷. Inflammaging is defined by aberrant NF- κ B activation, increases in the gene expression of inflammatory markers, and an elevation in circulating inflammatory cytokines. Along with increases in inflammatory markers, increases in baseline oxidative stress and reactive oxygen species (ROS)⁸ are also observed. ROS acts as signal for inflammation, resulting in the upregulation of pro-inflammatory cytokines, such as tumour necrosis factor (TNF α)⁹. ROS not only act as signals for inflammation but also contribute to the damage with ageing that occurs via oxidation to vital cellular components such as DNA, proteins and lipids, this leads to a build-up of oxidative damage. Over time this build-up of oxidative damage and the inability to repair the damage with age is described as the “free radical theory of ageing”. It was first proposed by Harman in 1956, that molecules with unpaired electrons are highly reactive and cause accumulative damage, leading to the loss of function in ageing and age-related diseases¹⁰. Initially the theory was focused on superoxide free radicals but over time this has included other reactive species such as hydrogen peroxide and peroxynitrite, Harman also later included the role of the mitochondria in oxidative damage, as a further source free radicals¹¹. These changes in the immune system can lead to increases in oxidative stress and inflammation which contribute to the progression of age-related diseases¹². Finding ways to lower inflammation and oxidative stress in the immune system could be beneficial to health of the ageing population and help treat and prevent certain disease.

1.2 Immune system.

The immune system consists of a number of cell types, termed white blood cells and function to protect the body from foreign antigens, tissue injury and infectious diseases. There are several different white blood cells, which all originate from hematopoietic stem cells in the bone marrow. There are two main lineages of white blood cells, the myeloid leukocytes and the lymphocytes. The myeloid leukocytes are defined by the presence of granules in the cytoplasm, neutrophils, monocytes, and basophils are all types of myeloid leukocytes. The lymphocytes lineage contains B-lymphocytes, T-lymphocytes and natural killer cells which are mainly found in the lymphatic system. Immature T-lymphocytes are produced in the bone marrow and mature in the thymus. Naïve T-lymphocytes are activated by antigen presenting cells, e.g. by macrophages or B—lymphocytes, these naïve cells are termed Th0 cells. T_H0 cells can differentiate into a number of subtypes, the main ones e.g. Th1, Th2, and Th17 differentiated depending on the antigen presenting cell. Macrophages induce T_H0 cells to differentiate into Th1 cells, which are induced by interleukin 12 (IL12) production, B-lymphocytes cause differentiation into Th2 cells by induction of interleukin 4 (IL4) and Th17 cells are generated following infection and by either antigen presenting cells, by the presence of interleukin 6 (IL6) and transforming growth factor beta (TGFβ). T-lymphocytes are the main cytokine producing cells in the immune system.

1.2.1 Jurkat cells as a model for inflammation.

T-lymphocytes are among the most affected cells associated with the decline in the immune system with ageing¹³. This is associated with decreases in the number of circulating T cells; along with impairments in T cell function such as activation, differentiation and proliferation. Dysfunction starts with impaired T-cell receptor (TCR) failing to activate T cells, this impairs the TCRs signalling pathway fails to activate the T cell, there have been shown multiple impairments in signalling pathways within T cells with age¹⁴. Prolonged activation of pathways such as NF- κ B, which can be caused by stress and cytokines leads to the upregulation of pro-inflammatory cytokines, increasing circulating inflammatory markers which all contribute to the pro-inflammatory state observed with ageing.

Jurkat cells are an immortalized line of T-lymphocyte commonly used for the *in vitro* study of T-cell signalling and cytokine secretion. In this thesis these cells will be used to evaluate the effects dietary polyphenols have in modulating markers of inflammation and oxidative stress. The Jurkat cells produce a number of different cytokines which can be evaluated and compared with those cytokines modulated with age, other advantages of using the Jurkat cells is that these cells are an immortalised cell line, which meant that large number of comparisons could be made. This allowed the evaluation of a number of different polyphenols, doses and stimulations, which would not have been possible in primary lymphocyte cells. These T-lymphocytes were first isolated from a 14 year old boy with leukemia, over the years there have become various Jurkat T cell lines

developed; the most common is E6.1. These cells express high levels of mature TCR, low levels of cluster of differentiation 4 (CD4), and no cluster of differentiation 8 (CD8) or major histocompatibility complex (MHC) class II¹⁵. T-lymphocytes that present the surface molecules CD4 are known as T helper cells and can be sub-divided. These sub groups include Th1 and Th2 which can be characterised by the inflammatory markers (cytokines) they secrete. In this thesis, Jurkat cells were treated with polyphenols for 48h in order to measure changes to cytokine release following treatment. This time point was chosen to allow treatments to have an effect on gene expression and protein production, to allow the analysis of cytokine release at the 48h time-point. Also, cells were treated with the stimulus PMA/PHA which induces cytokine release in the Jurkat cells. Previous studies showing cytokine signalling pathways such as AP-1 and NF- κ B are activated following treatment with PMA, with their activity peaking at the 24hr time-point¹⁶. These transcription factors activate cytokine production, with their activation peaking at 24hr, this led to the time point 48hr to be chosen to allow for gene transcription and translation of the cytokines.

1.2.2 Cytokines, inflammatory markers.

Cytokines are small proteins (5-20kDa) secreted by a variety of cells in order to signal and communicate between cells with the function of regulation of inflammation, differentiation and proliferation. For immune cells cytokines are essential for cell mediated immunity and allergic responses, with T-lymphocytes being a major source of cytokine release. There are more than 50 secreted factors

termed cytokines¹⁷, which can be grouped into different classes: interleukins, tumour necrosis factors (TNF), interferons (IFN), colony stimulating factors (CSF), transforming growth factors (TGF), and chemokines¹⁸.

1.2.3 T-lymphocyte classes: T helper cells (Th1/Th2).

T-lymphocytes are classified by the surface molecules they present with two main categories, the CD8 presenting cells known as cytotoxic T cells and CD4 presenting T cells are known as T helper cells. A previously discussed T helper cells can be sub-divided into Th1 and Th2 and are distinguished by the different cytokines they secrete.

1.2.4 Cytokine profiles of Th1/Th2 cells.

The two subsets of T helper cells (Th1/Th2) produces different types of cytokines, Th1-type cytokines mainly produce pro-inflammatory cytokines whereas Th2-type cytokines tend to produce more anti-inflammatory cytokines (Fig. 1.1)^{19,20}. Th1 cells produce more cytokines such as interleukin 2, 6, and 12, interferon γ and tumour necrosis factor α , these are considered pro-inflammatory cytokines, whereas Th2 cells produce interleukin 4, 5, 10 and transforming growth factor beta which are anti-inflammatory cytokines. These proteins are important markers that are essential for signalling during inflammation, a number of these markers have been linked through epidemiology studies to ageing and age-related diseases. The most common of these markers are interleukin 6 (IL6) and tumour necrosis factor alpha (TNF α)²¹.

1.2.5 Cytokines modulated with age.

IL6 and TNF α are produced by immune cells but can be produced by other cells such as skeletal muscle, vascular endothelial cells and neural tissues²². In healthy individuals an increase was observed with circulating level of pro-inflammatory cytokines: TNF α ($p = 0.003$), IL1 β ($p = 0.027$) and IL6 ($p = 0.0001$) in those aged > 60 years compared with those < 30 years old²³. Ageing and disease are associated with increases in pro-inflammatory cytokines, increases in circulating levels of TNF α have been reported to significantly increase over time and can effect disease progression. In patients diagnosed with septic shock those aged <50 had TNF α levels of 417 pg/ml, in the serum which was sig. lower than those aged > 50 was 706 pg/ml²⁴. Both show an increase in cytokine release which is what you wouyld expect in septic shock patients, however there was a greater cytokine response to septic shock in the elderly. Further examples of cytokines release modulated with age can be found in Chapter 3 introduction (3.1.3).

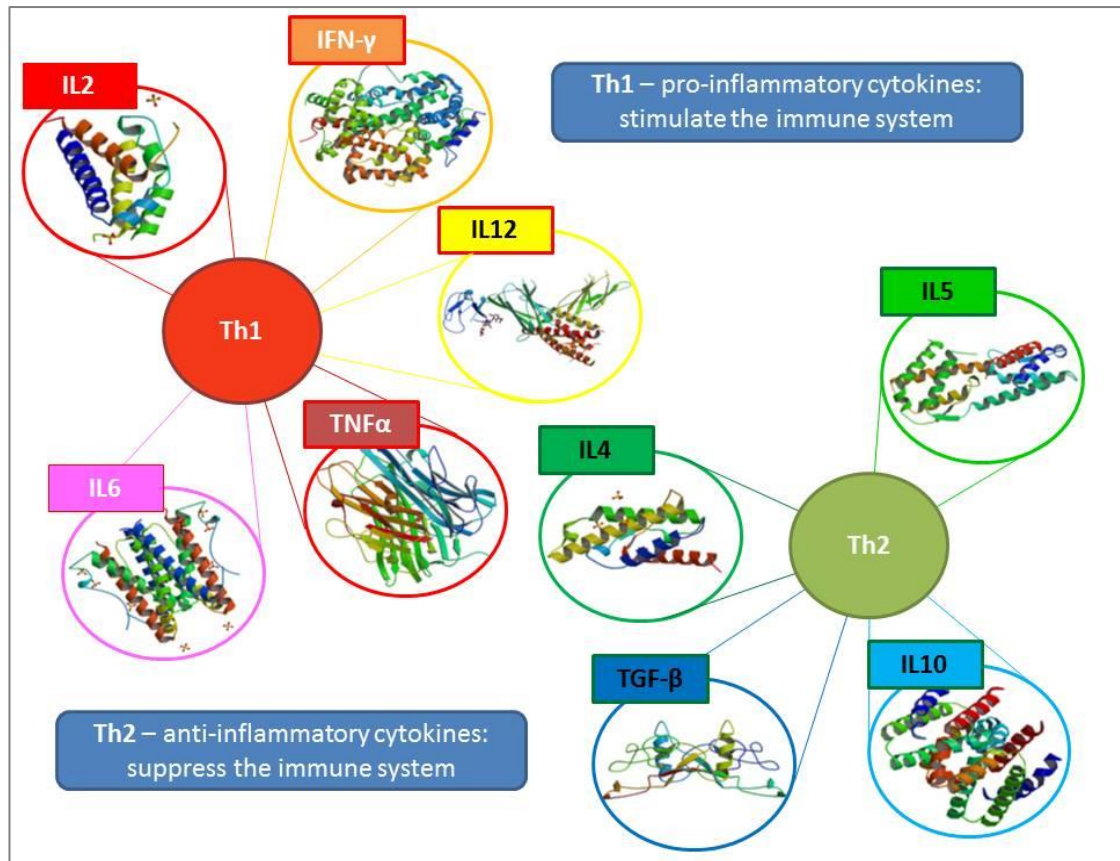


Figure 1.1 – Differential secretion of pro- and anti-inflammatory cytokines by T-lymphocyte sub-groups Th1 and Th2. T-helper cells are sub-divided into Th1 (red) and Th2 (green) cells and are classified by the cytokines they secrete. Th1 cells mainly secrete pro-inflammatory cytokines interleukin 2 (IL2), interleukin 6 (IL6), interleukin 12 (IL12), interferon gamma (IFN γ), and tumour necrosis factor alpha (TNF α). Th2 cells mainly secrete anti-inflammatory cytokines interleukin 4 (IL4), interleukin 5 (IL5), interleukin 10 (IL10), and transforming growth factor beta (TGF β). [Cytokine protein structures obtained from the protein data bank²⁵, figure modified from Beverley, P.C.L. 2007²⁶].

1.2.6 T-lymphocyte cytokine induction using phorbol esters such as PMA stimulation.

Jurkat cells secrete large amounts of the cytokine interleukin 2 (IL2) a cytokine important for T cell differentiation. Production of IL2 can be induced in these cells

following stimulation with phorbol esters such as phorbol 12-myristate 13-acetate (PMA), along with the lectin phytohaemagglutinin (PHA)²⁷. PMA is a phorbol ester and PHA a lectin which work together to activate T-lymphocytes, through the protein kinase c (PKC) pathway, which stimulates cytokine release in particularly interleukin 2²⁸. Stimulating the cells will allow the investigation into whether or not the (poly)phenols were having a protective effect, when the cells were stimulated, mimicking an immune response. At baseline Jurkats produce low levels of cytokines, by inducing cytokines with PMA/PHA, a higher concentration of cytokines will be released, providing greater accuracy when measuring changes to cytokine release.

1.2.7 T-lymphocyte affected by ageing.

IL2 is an important signalling mechanism that is essential for T-lymphocyte activation and differentiation²⁹. During ageing interleukin expression is disrupted, leading to a shift in the proportion of Th1/Th2 cytokine secreting cells, with more cells committed to the Th1 subtype, which secrete more proinflammatory cytokines³⁰. Hoffmann *et al* 2005, showed that CD4+ T-cell cytokine production was significantly increased with age. IL2 production increased from 12.1% in 18-34 year olds to 62.8% in >50 years, in isolated cells stimulated with PMA and ionomycin (% cytokine positive cells). TNF α also increased from 27.28% in 18-34 year olds to 47.81% in >50 year olds³¹. Increases in pro-inflammatory cytokines interleukin 6 and TGF β were also observed in healthy older people; with IL6

significantly increasing from 0.69 pg/ml in people aged 32-59, to 3.16 pg/ml in people aged 86-94, TGF β also significantly increased from 141.5 pg/ml (32-59 years) to 399.9 pg/ml (86-94 years)³². Changes in cytokine release are regulated by a number of pathways, in T lymphocytes cytokine release can be activated either through the AP-1, NF- κ B or NFAT signalling pathways³³. Activation of the TCR, for example by a foreign antigen leads to the activation of transcription factor activator protein 1 (AP-1) through the MAPK cascade, nuclear factor kappa B (NF- κ B) through the PKC θ pathway and nuclear factor of activated T-cells (NFAT) through influxes in intracellular calcium. Activating these transcription factors leads to the induction of cytokine gene expression such as IL2, IL8 and IFN γ , which is a Th1 cytokine profile in lymphocytes^{33,34}. These increases in circulating pro-inflammatory cytokines have been associated with disease, for example atherosclerosis, has been shown to be associated with increases in MCP-1, IL8 and TNF α ³⁵. Treatment of these inflammatory diseases using cytokine inhibitors is being widely researched, with anti-TNF α inhibitors now being used in the treatment of diseases such as rheumatoid arthritis³⁶, inflammatory bowel disease^{37,38} and asthma³⁹. By modulating these inflammatory pathways, the pro-inflammatory profile observed with ageing can be lowered and potentially improve the health of the elderly.

1.2.8 THP-1 monocytes as a model for inflammation.

THP-1 are a human leukaemia monocytic cell line, which are used to study monocyte and macrophage modulations, functions, and signalling mechanism. Monocytes are a type of white blood cells contributing to the innate immune system and making up approximately 5% of all leukocytes in the human body⁴⁰. Monocytes mature in the bone marrow, circulate in the blood and migrate into tissues where they function as macrophages. In cell culture THP-1 monocytes can be differentiated into macrophages by induction using the phorbol ester, PMA (12-myristate 13-acetate)⁴¹. THP-1 monocytes are characterised by the presence of Fc and C3b receptors, the production of IL1 and lysozymes along with phagocytic activity⁴². In this study, the Jurkat T-lymphocytes were the main cell line used, for the inflammatory profile of the cells and contributions to the inflamm-ageing phenotype. THP-1 monocytes will be used to replicate modulations to inflammation and redox found in the Jurkat cell model. Monocytes were chosen as they were another immune cell effected with age but also had a similar cytokine profile such as IL1, IL6, and TNF α which comparisons could be made to the Jurkat cells⁴³; cytokine production can be induced in this cell type through the addition of the endotoxin lipopolysaccharide (LPS) from the Gram-negative bacteria such as *E. coli*⁴⁴. The modulations to cytokines release will be evaluated in both cell types following interventions with polyphenols. Just like with the T-lymphocytes, monocytes are affected during ageing, with sub-sets of monocytic cells being increased, resulting in the increase secretion of pro-

inflammatory cytokines such as monocyte chemoattractant protein-1 (MCP-1)⁴⁵. Evaluating the effects polyphenols have on reducing the pro-inflammatory profile observed with ageing, could potentials aid to protect and reduce age-related diseases by added polyphenols as part of a healthy ageing diet.

1.3 Oxidative stress

1.3.1 Free radicals: molecules contributing to oxidative stress.

Along with the increases in pro-inflammatory cytokines, an increase in oxidative stress by increased activation of free radicals has also been observed with ageing⁴⁶. Free radicals are defined as molecules possessing an unpaired electron, which makes these molecules short-lived and highly reactive. There are many types of free radicals including hydroxyl radicals (OH[•]), superoxide (O^{•-}₂), nitric oxide (NO[•]) and lipid peroxy radical (LOO[•]). Free radical generation mainly occurs in the mitochondria as part of energy generation (ATP), through the electron transport chain⁴⁷. Processes such as inflammation⁴⁸, phagocytosis⁴⁹ and exercise⁵⁰ also generate free radicals as part of their processes and are required for normal function within the cell. However, dysfunction in free radical formation can be caused when production is uncontrolled and build up leads to excess in the cell, resulting in oxidative stress. There are a number of different proteins that are responsible for the removal of free radicals, forming the antioxidant defence.

1.3.2 Reactive oxygen species.

Reactive oxygen species (ROS) are small reactive molecules containing oxygen such as superoxide and peroxides. In the cell ROS are generated during cellular metabolism, during times of environmental stress such as heat or UV, and by ionizing radiation. Exogenous ROS can be produced in the body by external factors such as radiation and smoke, these factors can cause water to lose an electron and form reactive molecules such as hydroxyls, hydrogen peroxide and superoxide. Endogenous ROS are produced within the cell through different processes, such as ATP production in the mitochondria via the electron transport chain, they can produce ROS such as superoxide and hydrogen peroxide⁵⁵. These small molecules when in excess can cause cellular damage and when accumulated in the cell cause oxidative stress. However, small concentrations of ROS are essential for cell signalling and maintaining homeostasis. Nitric oxide⁵¹, superoxide⁵² and hydrogen peroxide⁵³ have all been shown to act as intercellular messengers, regulating cell signalling and function. Antunes and Cadenas⁵⁴, showed that a concentration of 0.7 μ M hydrogen peroxide (H₂O₂) resulted in a proliferative state in Jurkat cells, however higher concentration of 1-3 μ M H₂O₂ caused apoptosis and >3 μ M H₂O₂ resulted in necrosis. Therefore free radical concentrations are tightly controlled and maintained, regulated by antioxidant enzymes that neutralise the radicals. If left uncontrolled build-up of radicals can lead to damage to numerous cellular components such as DNA, lipids and proteins resulting in cellular death and potential disease. The antioxidant defence

system protects the cell for excess ROS and regulates the levels with the use of non-enzymatic molecules such as glutathione and vitamins A, C, and E, along with enzymatic proteins such as glutathione peroxidase, catalase and superoxide dismutase. These mechanisms help keep levels of ROS in a non-toxic level, however in certain circumstances these mechanisms are overwhelmed and cannot maintain this level, leading to build up and oxidative stress.

1.3.3 Antioxidants maintaining redox homeostasis.

In order for cells to maintain a steady state and protect against increases in oxidative stress, antioxidant enzymes are used to regulate and eliminate toxic free radicals and reactive oxygen species, which in excess cause damage to the cells. Intracellular antioxidant enzymes include superoxide dismutase, catalase and glutathione peroxidase, which work together to neutralise and remove ROS, to protect the cell from oxidative stress.

1.3.4 Superoxide dismutase and catalase.

Superoxide dismutase (SOD) and catalase (CAT) act as endogenous cellular defences against free radicals, with SOD converting superoxide ($O_2\bullet$) into molecular oxygen and hydrogen peroxide and CAT converting hydrogen peroxide to molecular oxygen and water (Fig. 1.2).

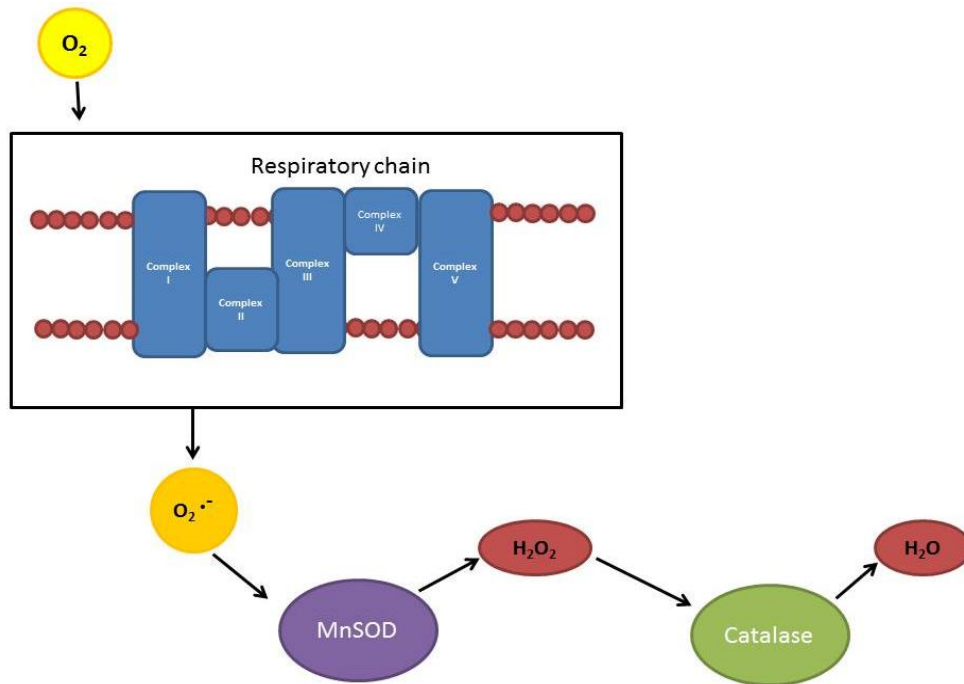
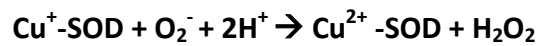
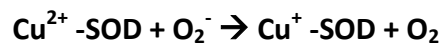


Fig 1.2 – Co-operative activities of manganese superoxide dismutase (MnSOD) and catalase in neutralising superoxide. Conversion of reactive oxygen species ($O_2^{\bullet -}$) generated through the respiratory chain within the mitochondria, into hydrogen peroxide (H_2O_2) via superoxide dismutase (SOD). H_2O_2 is then converted to water and molecular oxygen by the enzyme catalase (CAT)⁵⁵.

Since superoxide is unstable and cannot diffuse through cellular membranes there are different isoforms of SOD depending on the cellular compartment they are located. Copper/zinc superoxide dismutase (Cu,Zn-SOD) is found in the cytoplasm and intermembrane space of the mitochondria, whereas manganese superoxide dismutase (Mn-SOD) is located in the mitochondrial matrix. The SOD enzyme has several cofactor binding sites, where metals bind to the active sites of the enzyme; these include copper, zinc, manganese, iron (eukaryotic) and nickel (prokaryotic)^{56,57,58} hence the different names. The SOD enzyme removes superoxide by adding or removing an electron either generating

molecular oxygen (O₂) or hydrogen peroxide (H₂O₂) depending on the ion state of the metal cofactor.



From this reaction the resulting H₂O₂ can then be neutralised by the enzyme catalase, an ubiquitous protein containing four heme (Fe³⁺) that catalyse the dismutation of hydrogen peroxide to water and molecular oxygen.



Catalase is found throughout the cell, with high concentrations found in the mitochondria and peroxisomes, it also has one of the highest turnovers of enzymes with 6 million molecules of H₂O₂ converted to water and oxygen per min⁵⁹. Catalase has also been identified as an important growth-promoting factor in a number of inflammatory cells including B and T cells, leukaemia cells as well as fibroblast⁶⁰.

1.3.5 Oxidative stress and T cell activation.

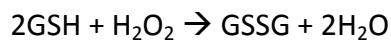
Superoxide and hydrogen peroxide are generated during T cell activation and the inflammatory response; they act as secondary messengers required in signal transduction needed for T cell function and proliferation. However, accumulation of reactive oxygen species (ROS) can lead to apoptosis and necrosis. In T cells,

ROS can activate pathways such as JAK/STAT and (PI3K)/AKT⁶¹. Regulatory T cells require ROS to trigger inflammatory responses; both over- and under-production of ROS have been implicated in inflammatory diseases, such as psoriatic dermatitis⁶². Therefore, maintaining appropriate levels of ROS is important for normal function; with the use of antioxidant enzymes such as SOD and catalase help maintain this balance and control of ROS. Research has been conducted investigating the use of SOD as an antioxidant therapy in the treatment of inflammatory diseases such as skin disorders, pulmonary diseases and arthritis⁶³. Overexpression of Cu,Zn-SOD in mice has been shown to have a protective effect against myocardial ischemia and reperfusion injury⁶⁴, so there is potential for SOD to be used as a therapeutic treatment in inflammatory conditions, where inflammation cannot be maintained and regulated under normal mechanisms.

1.3.6 Glutathione antioxidant system.

Glutathione (GSH) is an important antioxidant responsible for maintaining the redox homeostasis of the cell by neutralising free radicals; it is one of the most abundant intracellular thiols. It acts as an antioxidant, using thiol groups as reducing agents, reducing disulphide bonds on cellular proteins to cysteines, during this process glutathione is oxidised (GSSG). Glutathione is recycled in the cell and with the help of glutathione reductase GSSG can be converted back to GSH, with the addition of NADPH, see Figure 1.3.

Similar to catalase, glutathione peroxidase (GPx) enzymes can reduce hydrogen peroxide into water, and also reduce lipid hydroperoxides to alcohols. Peroxidases have active sites which either contain heme cofactors, redox-active cysteines or selenocysteines residues which catalyse these reactions. Glutathione peroxidases catalyse the reaction below, hydrogen peroxide (H₂O₂) oxidises a selenocysteine residue of the GPx, and this oxidation is then reversed back with the use of reduced glutathione (GSH) molecules, resulting in the formation of oxidised glutathione (GSSG) and water.



There are different isoforms with at least 8 different GPxs. GPx1 is the most common, found in the cytoplasm and prefers the substrate hydrogen peroxide, whereas GPx4 prefers lipid hydroperoxides. GPx2 and 3 are extracellular found in the intestines (GPx2) and plasma (GPx3)^{65,66}. Two glutathione molecules are required for the reduction of hydrogen peroxide into water, with the generation of oxidised glutathione, which now contains a disulphide bond connecting the two glutathione molecules. The oxidised glutathione can then be converted back to reduced glutathione, completing the recycling system.

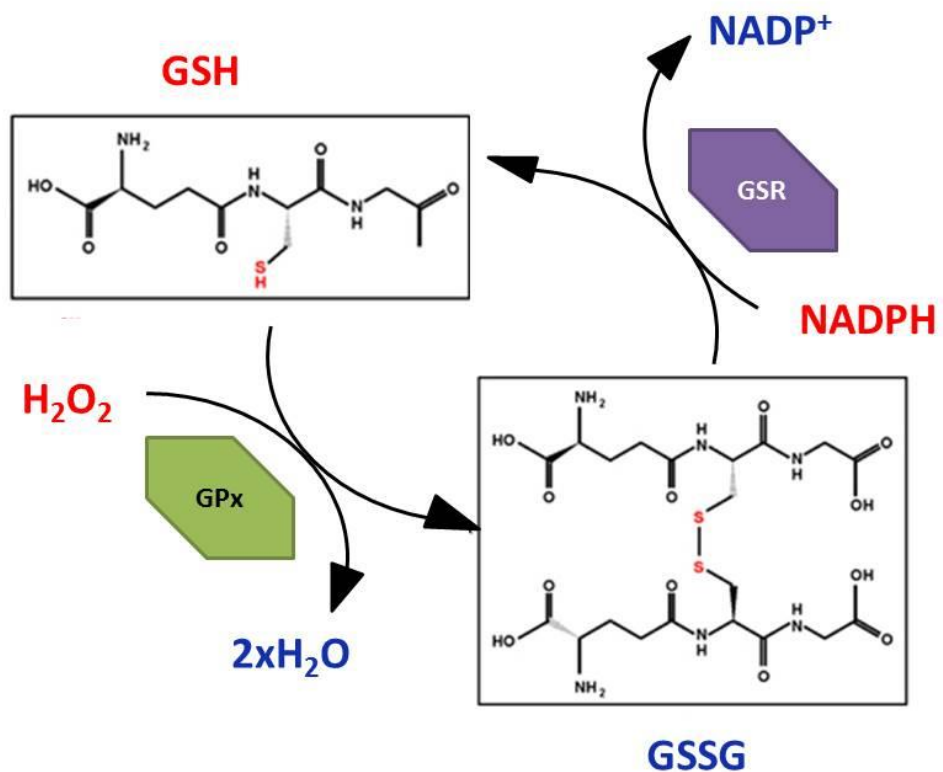


Figure 1.3 - Glutathione recycling mechanism. Hydrogen peroxide (H_2O_2) is removed from the cell by an antioxidant enzyme glutathione peroxidase (GPx) with the use of reduced glutathione (GSH). A disulphide bond is generated between two GSH molecules to create oxidised glutathione (GSSG). GSSG can be recycled in this system back to GSH with the enzyme glutathione reductase (GSR) and NADPH⁶⁷.

The synthesis of glutathione is controlled by two enzymes glutamate cysteine ligase (GCLC), followed by glutathione synthase (GSS). Firstly, GCLC joins glutamate and L-cysteine to produce gamma-L-glutamyl-L-cysteine (γ -EC), followed by GSS which combines the γ -EC with glycine to make reduced glutathione. GCLC is the rate-limiting enzyme in this pathway and controls the concentrations of glutathione within the cell. Diet and fasting can affect the

production of glutathione due to limiting the intake of cysteine⁶⁸ and amino acids⁶⁹ therefore inhibiting the production of glutathione and impairing the cell ability to maintain redox homeostasis.

1.3.7 Glutathione modulations with advancing age.

During ageing, levels of glutathione have been shown to decline in human plasma⁷⁰; this process is thought to occur through a number of different mechanisms. There is a decrease in GSH, through significant lowered rates of glutathione synthesis⁷¹ and increase in GSSG, leading to imbalance. Theories include the loss of glucose-6-phosphate dehydrogenase activity, this enzyme is vital for maintaining levels of NADPH which is essential for glutathione reductase to remove oxidised glutathione⁷². For example, glutathione peroxidase activity has also been shown to decrease with age, GPx activity significantly declines by 2.9 $\mu\text{mol}/\text{min}/\text{L}$ for each additional year after the age of 65⁷³.

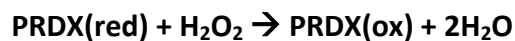
Glutathione is not only utilised by glutathione peroxidase, it is a cofactor for a number of different processes such as glutathione S-transferases (GSTs), which catalyse the conjugation of GSH to xenobiotic substrates⁷⁴, other peroxidases such as peroxiredoxins⁷⁵ and transhydrogenases, which reduced oxidised moieties from DNA and proteins, such as glutathione-insulin transhydrogenase⁷⁶.

1.3.8 Thioredoxin and peroxiredoxin antioxidant system.

Thioredoxins (TXN) is a small, 12kDa oxidoreductase enzyme which facilitates the reduction of other proteins by cysteine thiol-disulfide exchange. TXN has a similar structure to glutaredoxin, peroxiredoxins, and glutathione peroxidase, which is reflected in their functions as thiol-dependant antioxidants⁷⁷. TXN acts as an electron donor to thiol-dependent peroxidases such as peroxiredoxins, in order to remove reactive oxygen. TXN is also believed to have functions in DNA and protein repair by acting as a reducing substrate for ribonucleotide reductase (RNR), an enzyme involved in DNA repair and replication⁷⁸. TXN1 is found in the cytoplasm and nucleus whereas TXN2 is found in the mitochondria. TXN2 only has 2 cysteines, whereas TXN1 has 3 additional cysteine residues which are thought to be regulated by posttranslational modifications⁷⁹. The two forms of TXN have different interaction and functions; TXN2 interacts with methionine sulfoxide reductase (MSR), an antioxidant enzyme restoring the oxidised methionine sulfoxide to methionine⁸⁰, also peroxiredoxin 3 in scavenging of H₂O₂⁸¹. TXN1 in the cytoplasm and nucleus also interacts with MSR, along with peroxiredoxins 1 and 2. TXN2 also interacts with RNR to protect the cell from DNA damage and plays a role in redox signalling. Thioredoxin reductase regulates thioredoxin and catalyses the reduction of thioredoxin, when thioredoxin reductase is inactivated, it triggers the activation of the antioxidant transcription factor Nrf2. Other redox-related transcription factors such as NF-κB, and signalling factors ASK1 are also activated^{82, 83}. Overexpression of TXN in mice has been shown to be induce

resistance to inflammation and these mice had their average lifespan increased to 135% longer than the controls⁸⁴. Therefore, thioredoxins are important proteins influencing inflammation and ageing.

Peroxiredoxins are a family of peroxidases that mainly reduce hydrogen peroxide and alkyl hydroperoxides to water and alcohol⁸⁵. They are classified depended on the number of conserved cysteine residues the peroxiredoxins (PRDX) have either 1-Cys or 2-Cys. There are 6 different PRDXs found in mammals; PRDX1, PRDX2, PRDX3, PRDX4 and PRDX5 are 2-Cys enzymes and use thioredoxin in their catalytic activity, whereas PRDX6 is a 1-Cys enzyme which does not use thioredoxin but catalytic activity is linked to glutathionylation⁸⁶ and phospholipase A₂⁸⁷. All PRDXs have the same basic catalytic function in which active cysteines are oxidised to a sulfenic acid (R-SOH) by peroxide substrate⁸⁸.



Each PRDX has specific roles in regulation and signalling. PRDX1 knockout mice have been shown to have decreased lifespan by up to 15% compared with controls⁸⁹, overexpression of PRDX6 in mice protects against allergic airway inflammation by reducing levels of ROS⁹⁰ and recently oxidised PRDX1 and 2 have been shown to be released from the cell on stimulus with inflammatory molecules such as lipopolysaccharide and TNF α . This stimulates the induction of

inflammatory cytokines and highlights a novel pathway in redox-dependant signalling mechanism in inflammation for human embryonic kidney cells and monocytic cells⁹¹.

1.4 Ageing has been associated with dysregulation in redox homeostasis, increased oxidative stress and damage.

During ageing the ability to maintain these antioxidant proteins and protect the cells against free radicals becomes impaired. Excessive production of free radicals^{92,93}, the inability to regulate antioxidant gene expression^{94,95} and protein dysfunction leads to a build-up in oxidative stress⁹⁶. This leads to damage to vital cellular components such as DNA, proteins and lipids. Protein oxidation can effect signal transduction, the stability of the proteins, degradation and activity there proteins may become inactive, degraded or not produced due to increased oxidative stress with ageing⁹⁷.

1.5 Dietary (poly)phenols.

1.5.1 Natural antioxidants generated by plants.

Polyphenols are naturally occurring compounds, found in a variety of food sources such as fruits, vegetables, beverages, herbs and spices. These compounds are produced in plants in order to defend themselves against oxidative damage by ultraviolet radiation and pathogens⁹⁸. Plants synthesis polyphenols by the

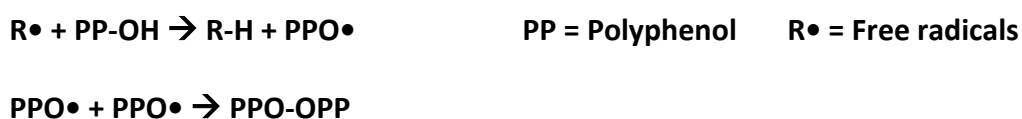
deamination of phenylalanine via the shikimic acid pathway followed various processes depending on the compounds being produced⁹⁹. These compounds are produced as part of the plants defence mechanisms, protecting from biotic and abiotic stress factors and synthesis has been shown by activating wound-inducible polyphenol oxidases (an enzyme involved during synthesis) in tomato plants¹⁰⁰.

Polyphenols are compounds possessing an aromatic ring, including one (phenolic) or multiple (polyphenol) hydroxyl groups; in addition they can contain various functional groups including methyl, glycosides and sulphates. Polyphenols are split into categories based on the number of phenolic rings, structural elements binding the rings and functional groups. There are two main groups flavonoids and non-flavonoids, both have multiple sub-groups such as anthocyanins, flavones, and isoflavones (flavonoids) and phenolic acids, benzoic aldehydes, stilbenes (non-flavonoids)¹⁰¹. There have been over 8000 phenolic compounds identified, with almost half of those consisting of flavonoids^{102, 103, 104}. This study chose (poly)phenols that possessed a variety of these properties, from different food sources and a range of metabolites, to include a broad range of compounds.

1.5.2 Dietary polyphenols as antioxidants.

Dietary (poly)phenols have been extensively studied for their antioxidant and anti-inflammatory effects both in *in vitro* and *in vivo* studies. Studies suggest the consumption of foods high in dietary polyphenols offer protection against the

progression of diseases such as heart disease, cancer and osteoporosis¹⁰⁵. Polyphenols have been reported to be strong antioxidants which can scavenge reactive oxygen species and aid cellular processes to protect against increased levels of oxidative stress. This antioxidant capability is believed to occur via the donation of hydrogen, to neutralise free radicals¹⁰⁶.



The antioxidant potential of these compounds depends on the number of hydroxyl groups and their structure. This can be measured experimentally using the Folin-Ciocalteu reagent, the Trolox equivalent antioxidant capacity or oxygen radical absorbance capacity (ORAC). Ninfali *et al* 2004 identified the antioxidant capacity of a number of different vegetables and spices using the ORAC method, curcumin (spice) had the greatest ORAC value with $76,800 \pm 7500 \mu\text{moleTE}/100\text{g}$, marjoram (herb) $27,297 \pm 2611 \mu\text{molTE}/100\text{g}$ and artichokes (vegetable) $6552 \pm 650 \mu\text{molTE}/100\text{g}$ ¹⁰⁷. The complexity of these compounds and antioxidant capacity is only one component that needs to be considered when evaluating the potential benefits of these compounds. The levels in which these foods are consumed need to be taken into consideration, as herbs and spices may have higher antioxidant capacities but will not be eaten in large quantities unlike fruits and vegetables.

1.5.3 Polyphenols and their bioavailability.

Concentrations of these polyphenols found in the plasma vary depend on the concentration found in the food source, metabolism once within the body and their bioavailability (absorption and uptake into the circulatory system). Pérez-Jiménez *et al* 2010 investigated 502 polyphenols from 452 foods, to rank the 100 richest sources of dietary polyphenols¹⁰⁸. The highest ranking foods included various spices and herbs (15000mg per 100g in cloves), cocoa, dark coloured berries, and also beverages such as wine (10mg per 100ml). Following consumption the polyphenols can be absorbed in the small intestine, colon, and liver, and the polyphenols can be extensively metabolised by gut microflora and in the tissues¹⁰⁹. The human gut consists of a complex mixture of microorganisms, termed microflora and are essential for maintaining human health, aiding in metabolism, nutrition and immune function¹¹⁰. Polyphenols are varied and complex in structure, once they enter the digestion system these compounds are metabolised, into smaller and potentially more bioactive compounds¹¹¹. The structure of the polyphenols can greatly affect absorption and concentrations found in plasma. Bioavailability can be evaluated with the lipophilicity value (log Kow); it can predict the absorption, metabolism, excretion and toxicity of a compound¹¹². Polyphenols are very sensitive to environmental factors affecting their antioxidant ability such as heat, light, water solubility, and pH, which will affect their metabolism and elimination rate. Therefore finding ways to deliver the polyphenols to the body in a way that can increase the bioavailability,

maintain the antioxidant structure and that is palatable to the user. For example curcumin, has a low aqueous solubility and low bioavailability (meaning it is poorly absorbed by the gut). Studies have been looking at nanoparticles to increase curcumins antioxidant potential within the body^{113,114}.

1.5.4 Polyphenols are extensively metabolised following ingestion in the stomach, intestines and by gut microflora.

Once within the body polyphenols undergo a number of biological changes through metabolism in tissues and by colonic microflora¹¹⁵. When polyphenols reach the colon they are metabolised into phenolic acids by the colonic microflora such as *Eubacterium ramulus*, *Bacteroides sp.* and *Enterococcus casseliflavus*¹¹⁶. Quercetin is metabolised in the small intestine and 93% of quercetin found in the plasma is modified to quercetin 3-sulfate, quercetin 3-glucuronide, and 3-methylquercetin 3-glucuronide¹¹⁷. Following consumption of green tea more than 50% of EGCG passes to the large intestines¹¹⁸, where metabolism by colonic microflora occurs, forming epigallocatechin and pyrogallol. Epigallocatechin is then further metabolised into a number of different products including methyl-(-)epigallocatechin and (-)-epigallocatechin-3-O-glucuronide (Fig. 1.4). These metabolites have different antioxidant properties than their parent compounds. Structural changes to polyphenols as a result of metabolism have been shown to alter their antioxidant potential¹¹⁸.

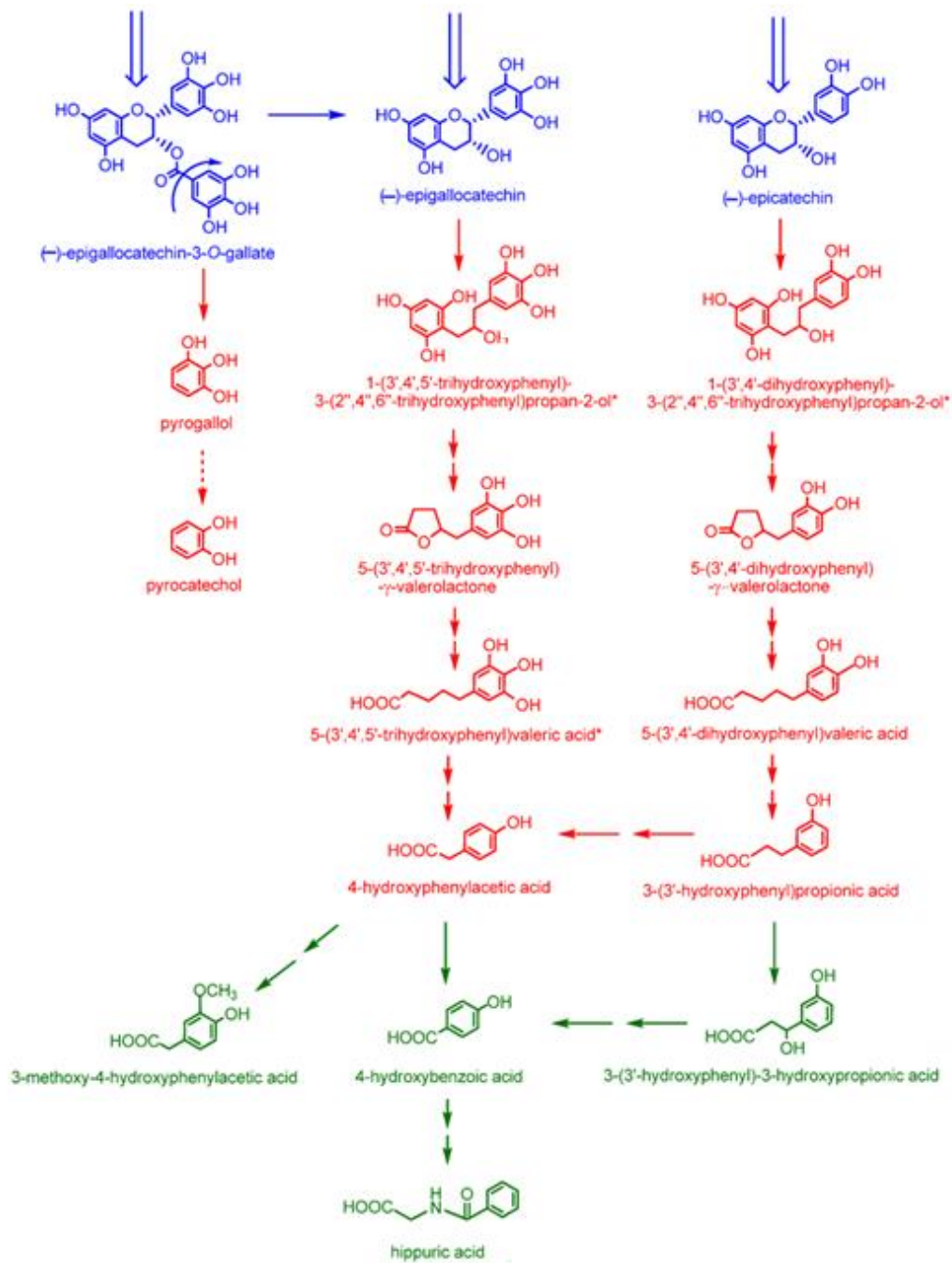


Figure 1.4 - Green tea flavan-3-ols metabolism and breakdown products following consumption. (-)-epicatechin, (-)-epigallocatechin and (-)-epigallocatechin-3-O-gallate (blue) are found in the large intestine, these structures are then broken down by colonic microflora (red). Further metabolites found in the urine after green tea consumption (green) which aren't identified after metabolism via gut microflora, therefore catabolites enter the circulatory and undergo further metabolism before being excreted in urine. (Figure from Del Rio et al, 2010).¹¹⁹

Within the gut, polyphenols are not just metabolised by the microflora, studies have shown that polyphenols also influence what gut microflora are present in the gut. Tzounis et al¹²⁰ showed that the green tea metabolite (+)catechin significantly inhibited the growth of *Clostridium histolyticum* and increased *E. coli* and *Clostridium coccooides-Eubacterium rectale* growth, in an in vitro study using batch-culture model to represent the human large intestine. Therefore there is a two way interaction between the polyphenol intake and the gut microflora present in the gut.

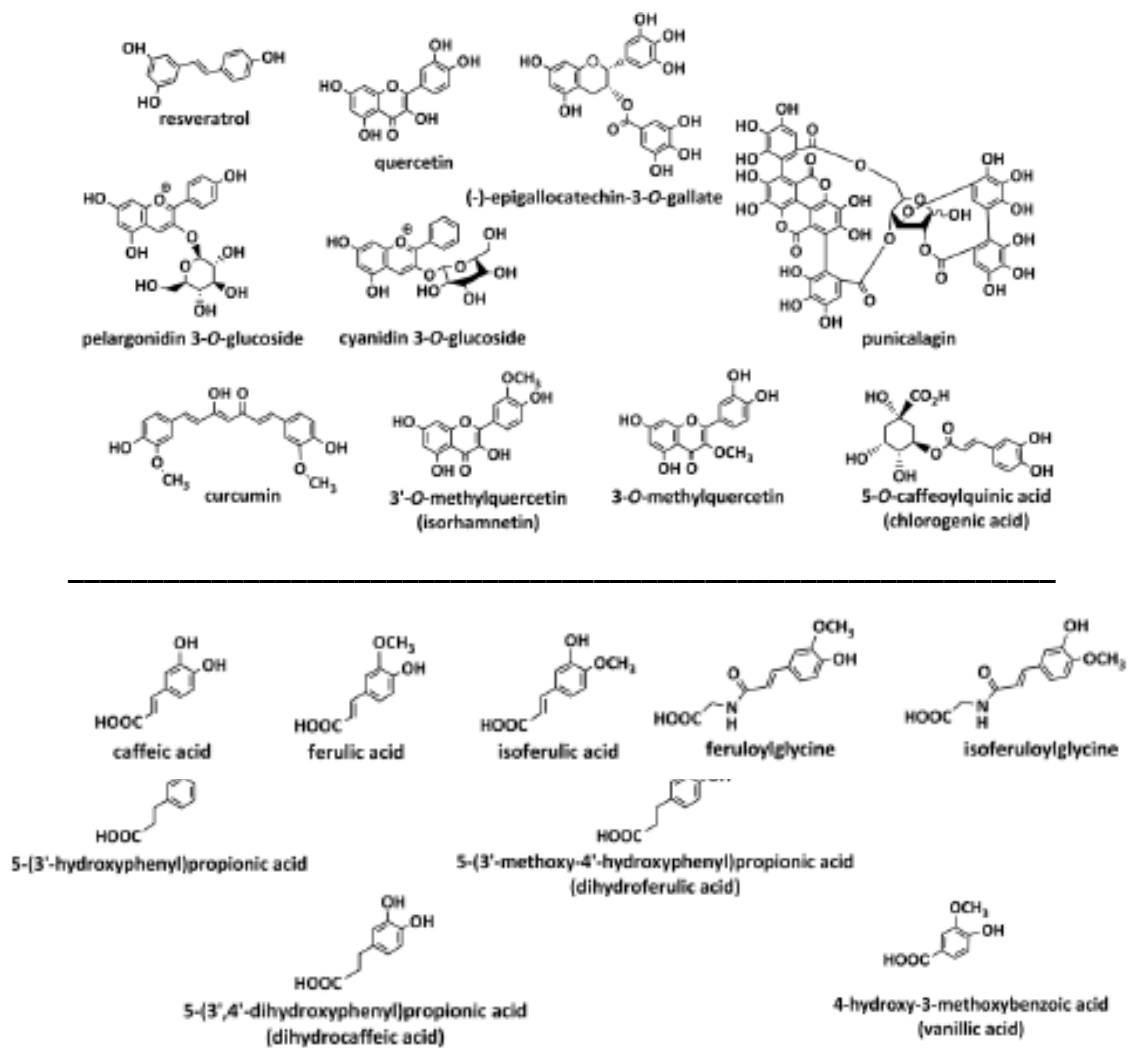
However metabolism of polyphenols doesn't solely occur in the gut. Polyphenols can pass the cell membrane and enter the cell, where phase II enzymes metabolise the polyphenols. The mechanism, rate and concentration of polyphenol absorption depend on the cell type and the polyphenol involved. There has been a large amount of work using Caco-2 cells to investigate polyphenol intake by cells, Caco-2 cells are human epithelial colorectal cells used to represent the small intestine. It has been shown that polyphenols can be taken up by Caco-2 cells by transporters such as SGLT1, MRP2, and P-glycoproteins. This was observed by Teng et al¹²¹, using polyphenols apigenin, resveratrol, emodin, and chrysophanol by using competitive inhibitors of these transporters. They showed that emodin and chrysophanol uptake was inhibited when transporter SGLT1 was inhibited, whereas apigenin and resveratrol was not. Therefore showing different polyphenols have different methods of uptake into the cell. Once within the cell they also showed metabolism of the polyphenols by phase II

enzymes over an hour time period. For emodin and chrysophanol the main metabolites were glucuronides. Polyphenol uptake has also been observed for T lymphocytes, with quercetin accumulation found in the mitochondria of T-lymphocytes by passive diffusion¹²². It is thought that quercetin accumulation in the mitochondria is to protect the mitochondria from ROS.

1.5.5 Phenolic acids and polyphenols ((poly)phenols) chosen for study in this thesis.

A variety of compounds were chosen for this study, covering a broad range of complex polyphenols, with numerous functional groups and multiple metabolites phenolic acids. As previously seen in Fig. 1.4 complex polyphenols such as (–)-epigallocatechin-3-*O*-gallate (EGCG) can be broken down by gut microflora into small phenolics such as pyrogallol and catechol. A number of these catabolites enter the blood stream and are metabolised further into various phenolics such as 4-hydrobenzoic acid, 3-(3'-hydroxyphenyl)-3-hydroxypropionic acid, and hippuric acid. Figure 1.5 shows all the (poly)phenol compounds and their structures chosen for this thesis cytokine release investigation. The term (poly)phenol will be used when discussing both polyphenols and phenolic acids. The panel includes both complex polyphenols which have been well studied in the literature, such as EGCG, curcumin, quercetin, and resveratrol. Compounds with structural analogues of one another such as quercetin, 3-*O*-methylquercetin and isorhamnetin, which include additional functional groups e.g. methoxy group (OCH₃). There is less literature on the smaller phenolic acids and their effect on

inflammatory markers. 19 phenolic acids were included in the panel, this included metabolites of the polyphenols used. For example, curcumin is metabolised into ferulic acid and dihydroferulic acid, pelargonidin 3-O-glucoside is metabolised into 4-hydroxybenzoic acid and quercetin metabolised into isorhamnetin, ferulic acid, dihydrocaffeic acid, 5-(3'-hydroxyphenyl)propionic acid, vanillic acid and protocatechuic acid.



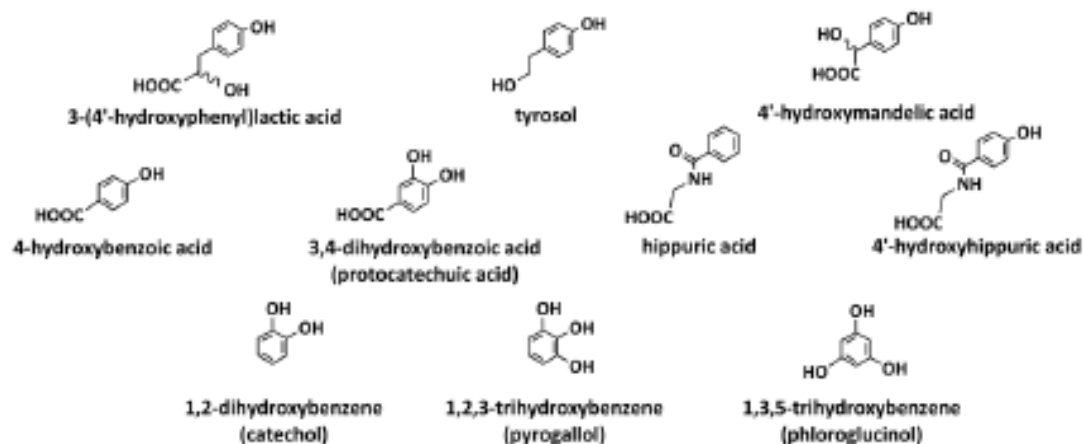


Figure 1.5 – Panel of (poly)phenol compounds chosen for cytokine release investigation. (Poly)phenol name(s) including structure are ordered in size, with the largest polyphenols at the top and the smaller phenolic acids at the bottom.

1.5.6 Polyphenols, inflammation and oxidative stress.

It is believed dietary polyphenols can modulate inflammation and oxidative stress by scavenging ROS, activating or inhibiting signalling pathways and upregulating the gene expression of antioxidant proteins. In the present study twenty-nine different polyphenols and phenolic acids (termed (poly)phenols when discussing both) were used, varying in structure and functional group and also from a variety of different food sources. Full details of each compound used can be found in appendix 1.

It is important to understand the mechanism behind polyphenols mechanism of action, since a better understanding of these compounds will allow more targeted interventions to be derived, since free radicals, oxidation and

inflammation are key to numerous disease states. Figure 1.6, shows a basic schematic view of how polyphenols are thought to act.

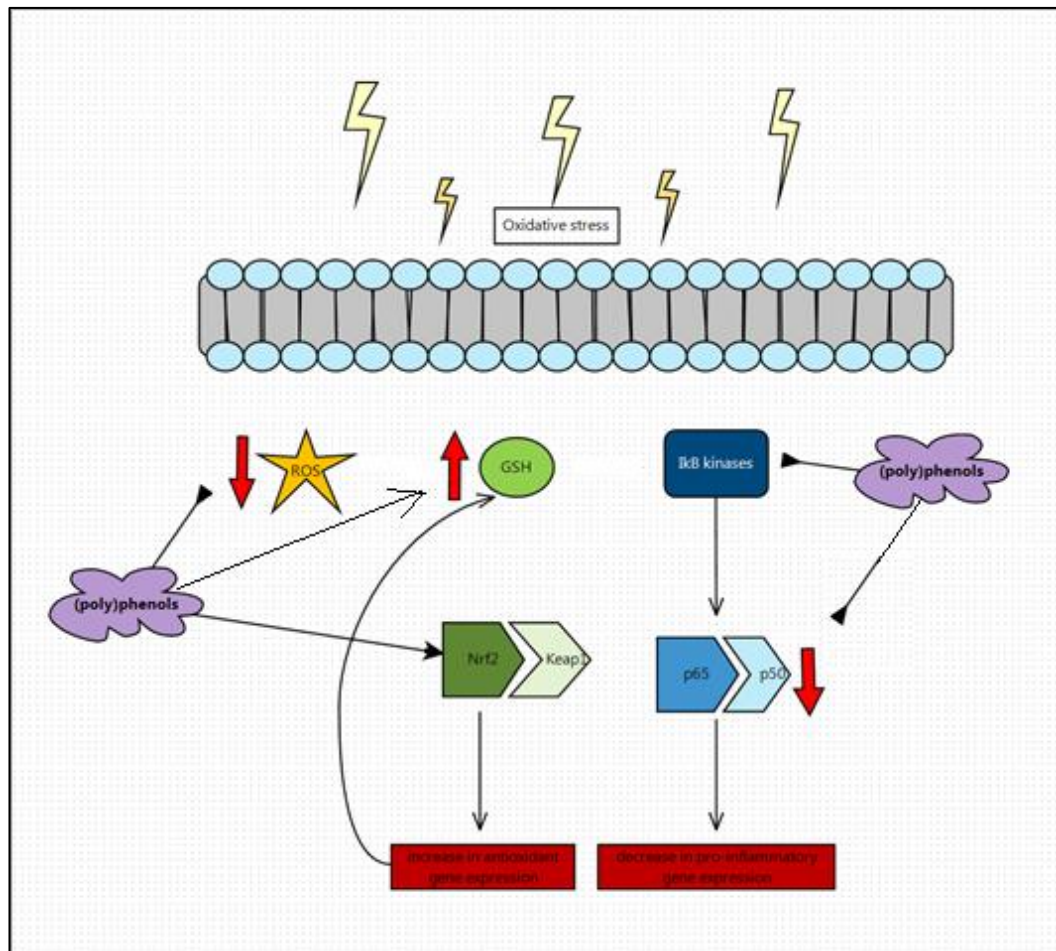


Figure 1.6 - Simplified schematic of potential polyphenol mechanism of action. Polyphenols are thought to inhibit levels of reactive oxygen species (ROS), modulation of antioxidant enzymes gene expression through the transcription factor Nrf2 and modulating and inhibiting IKB kinases, in the NF- κ B pathways, which down regulates the expression of pro-inflammatory cytokines. Modified from Accomando *et al* (2010)¹²³.

Protective mechanisms include the scavenging and detoxification of ROS, blocking the production of ROS, as well as influencing cellular antioxidant enzymes and pathways¹²⁴. Polyphenols can activate antioxidant pathways through the activation of Nrf2, which leads to the upregulation of antioxidant genes such as glutathione reductase, which increases the intracellular concentrations of the antioxidant GSH. Polyphenols are also thought to modulate inflammatory markers by decreasing the production of pro-inflammatory cytokines; this is achieved by inhibiting the NF- κ B pathway. In this study, polyphenols were evaluated for changes in cytokine production and by proteomics to determine how these polyphenols are modulating cytokine release, with the aim to better understand which proteins and pathways are being modulated by polyphenols.

1.5.7 Polyphenols used in the treatment of diseases.

Polyphenols are already in use in the treatment of several conditions. Curcumin, a spice from turmeric is being trialled in the treatment of rheumatoid arthritis; patients receiving curcumin (500 mg) and diclofenac sodium (50 mg) alone or their combination, a significant improvement was noticed in the disease activity score and a reduction in swelling and tenderness in the joints when compared with current treatment methods (diclofenac sodium) for the disease in humans¹²⁵. These effects with curcumin on arthritis have previously been observed in mouse models, where curcumin has been shown to decrease the expression of pro-

inflammatory cytokines such as IL-1beta and TNF-alpha in the ankle joints, and expression of IgG2a in the serum. Showing curcumin can lower the inflammatory response in collagen-induced arthritis in mice by feeding curcumin every day for 2 weeks¹²⁶. Mixtures of polyphenols have been shown to be beneficial in men with prostate cancer, a treatment of pomegranate, green tea, broccoli, and turmeric for 6 months showed a favourable effect on prostate specific antigens when compared with the placebo group¹²⁷. Even though beneficial effects have been observed with these polyphenol treatments, the underlying mechanism of how these compounds work are poorly understood and research is still ongoing to fully evaluate their involvement in modulating cellular processes. This study aims to screen numerous (poly)phenols for the ability to lower pro-inflammatory markers, then to investigate further those compounds with the greatest effects, using proteomics to understand their mechanism of action.

1.6 Aims of this thesis.

The aims of the work that contributes to this thesis were:

- Screen (poly)phenols and phenolic acids to determine which are likely to be anti-inflammatory. A panel of 29 (poly)phenols were investigated to examine effects on interleukin 2, interleukin 8 and tumour necrosis factor alpha release in both unstimulated and PMA/PHA stimulated Jurkat cells.

- (Poly)phenols identified from this cytokine panel as significantly reducing markers of inflammation will be further investigated using proteomic approaches. Label free, liquid-chromatography tandem mass spectrometry will be used to identify changes to protein concentrations following treatment with polyphenols.
- Validation of the changes in protein release observed via the proteomics analysis and identification of a proposed mechanism of action through network and pathway analysis.
- To confirm changes to cytokine release and oxidative stress proteins in an alternative cell type, THP-1 monocytes using the compound that showed the greatest modulation in the previous aims.

1.7 Hypothesis

This study hypothesises that polyphenols will significantly reduce cytokine release, and increase antioxidants markers to reduce oxidative stress in Jurkat and THP-1 cells when compared with the control.

CHAPTER 2

MATERIALS AND METHODS

2.1 Materials.

Abcam (Cambridge, England, UK):

Anti-phosphorylated-Nrf2 antibody, anti-keap1 antibody, anti-TATA binding protein (TBP) antibody, anti-glutathione reductase, anti-catalase, anti-thioredoxin, anti-peroxiredoxin-2, anti-vinculin, anti-Histone H3.

Active motif (La Hulpe, Belgium):

TransAm Nrf2 activation kit.

Bio-Rad (Richmond, California, USA):

Bio-Plex Pro™ Assays, blotting grade non-fat milk, 4x Laemmli sample loading buffer.

Chemicals VWR BDH Prolabo (Lutterworth, Leicestershire, UK):

(Ethylenedinitrilo)tetraacetic acid disodium salt (Na₂EDTA), potassium hydroxide pellets, sodium hydroxide pellets.

Cell signalling technology, Inc (Danvers, MA, USA)

Anti-rabbit antibody, anti-ERK1/2, anti-phosphoERK1/2.

GE Healthcare Life Sciences

Amersham ECL full-range rainbow molecular weight marker, nitrocellulose blotting membrane.

Life Technologies (Paisley, Strathclyde, UK):

Gibco Foetal bovine serum (FBS), Gibco 1M 4-(2-hydroxyethyl)-1-piperazineethanesulfonic acid (HEPES), Gibco RPMI – 1640 (1X) phenol free media containing glutamine, without HEPES, Applied Biosystems High capacity cDNA reverse transcription kit, Applied Biosystems TaqMan universal PCR master mix. TaqMan gene assays – glutathione reductase, glutathione synthetase, glutathione peroxidase, glutamate-cysteine ligase, TATA-binding protein and beta-2 microglobulin.

Lonza (Basel, Switzerland):

L-glutamine.

Millipore (Watford, UK):

Milliplex Map kit (11-plex) – human cytokine/chemokine magnetic bead panel.

National Diagnostics (Atlanta, Georgia, USA):

ProtoGel 30%, ProtoGel Stacking buffer, 4x Resolving Buffer, 10x running buffer,

N,N,N',N'-Tetramethylethylenediamine (TEMED).

PAA Laboratories (Pasching, Austria):

Foetal bovine serum gold (heat inactivated).

Public health England (PHE) culture collection (Salisbury, England, UK):

Jurkat E6.1 T lymphocytes, THP-1 monocytes.

Promega (Madison, Wisconsin, USA):

3-(4,5-dimethylthiazol-2-yl)-5-(3-carboxymethoxyphenyl)-2-(4-sulfoophenyl)-2H-tetrazolium, inner salt (MTS) cell proliferation assay.

Roche Life science (Dubai, UAE):

Glutathione reductase.

Santa Cruz biotechnology, Inc (Dallas, Texas, USA):

Anti-Nrf2 antibody.

Sigma-Aldrich (Poole, Dorset, UK):

2-vinylpyridine, 5,5'-dithiobis(2-nitro-benzoic acid)(DTNB), 5-sulfasalicylic acid, 6-amino n hexanoic acid, ammonium persulfate (APS), anti-mouse antibody, anti-rat antibody, bicinchonic acid solution, β -glycerophosphate, β -Nicotinamide adenine dinucleotide phosphate, reduced tetra(cyclohexylammonium) salt (NADPH), Bradford reagent, diamide, copper(II) sulphate solution, curcumin, dimethyl sulfoxide (DMSO), dithiothreitol, Dulbecco's phosphate-buffered saline (DPBS), *E. coli* B4 lipopolysaccharide (LPS), glutathione reduced (GSH) and oxidised (GSSG), glycerol, hepes-KOH, isorhamnetin, ochratoxin A, magnesium chloride, methanol, p-nitrophenyl phosphate, phorbol 12-myristoyl 13-acetate (PMA), phytohaemagglutinin (PHA), phenylmethanesulfonyl fluoride, phosphatase inhibitor cocktail, proteases inhibitor cocktail, BSA protein standard, resveratrol, RPMI-1640 medium Dutch modification with 1gm/L sodium bicarbonate and 20 mM HEPES, sodium dodecyl sulphate (SDS), sodium fluoride, sodium metavanadate, sodium molybdate, sodium chloride, sodium phosphate dibasic (Na_2HPO_4), tert-butylhydroquinone, tris, trypan blue, tween 20.

Thermo Scientific (Rockford, Illinois, USA):

Super Signal West Dura Chemiluminescent Substrate (ECL).

2.2 Methods.

2.2.1 Jurkat cell culture.

Human Jurkat T-lymphocytes (ATCC, UK) were cultured in RPMI-1640 supplemented with 10% (v/v) fetal bovine serum and 2mM L-glutamine. Cells were cultured in an incubator at 5% (v/v) CO₂, 20% O₂ (v/v) and 37°C. Growing cultures were maintaining between 4-6x10⁵cells/ml¹²⁸.

2.2.2 THP-1 cell culture.

Human monocytic leukaemia cell line (ATCC, UK) were initially cultured in phenol free RPMI-1640 already supplemented with 2mM L-glutamine with 20% (v/v) fetal bovine serum, 100µg/ml Penicillin-Streptomycin, and 2mM. Cells were cultured in an incubator at 5% (v/v) CO₂, 20% O₂ (v/v) and 37°C. Growing cultures were maintaining between 4-6x10⁵cells/ml. When cells reached exponential growth the fetal bovine serum was lowered to 10% (v/v) in media¹²⁹.

2.2.3 Thawing frozen cells and maintaining cell culture.

Frozen aliquots of Jurkat E6.1 or THP-1 cells were thawed from liquid nitrogen storage rapidly in a water bath at 37°C. Aliquots were added to a 25 cm² culture flask with 5 ml of medium prewarmed to 37°C. Cells were continually cultured at 5% (v/v) CO₂ and 37°C, maintaining cultures between 3-9x10⁵ cell/ml. A

sample was taken for counting, using the Trypan Blue exclusion method. Cells were then centrifuged at 224 x *g* for 5 min, old media was discarded and replaced with fresh media to appropriate volume for maintain growing culture.

2.2.4 Cells counting.

2.2.4.1 Trypan Blue exclusion.

Cell number was determined via Trypan Blue exclusion either using a hemeocytometer or automatic cell counter (TC-20, BioRad, California, USA). Typan blue is a diazo dye which is only taken up by dead cells, allowing the dye to cross the cell membrane, distinguishing between live and dead cells.

2.2.4.2 MTS (tetrazolium dye) cell proliferation assay.

Other cell counting methods included the MTS cell proliferation assay, allowing multiple cell counts to be taken, by comparing unknown cell samples to a known cell standard curve. The MTS assay was used during the polyphenol screening due to the large number of treatments being performed (29 polyphenols, 2 doses, with and without stimulation), therefore Trypan Blue exclusion was not possible for this many samples. MTS assay measures cell viability by assessing cell metabolic activity, NAD(P)H-dependent cellular oxidoreductase enzymes reduce the tetrazolium dye to the insoluble formazan, which can be measured spectrophotometrically between wavelengths 490-500nm

A standard curve was made using the Jurkat cells ranging from 2.0×10^6 to 1×10^4 cells per ml (determined by Trypan Blue exclusion) (Fig. 2.1). 100 μ l of unknown cell samples and standards were transferred to a 96 well plate, in duplicate, followed by 20 μ l MTS (tetrazolium dyes) reagents. Plate was incubated for 1.5 h at 5% (v/v) CO₂ and at 37°C, absorbance then measured at 490 nm. The standard curve was used to calculate the unknown cell samples from the absorbance.

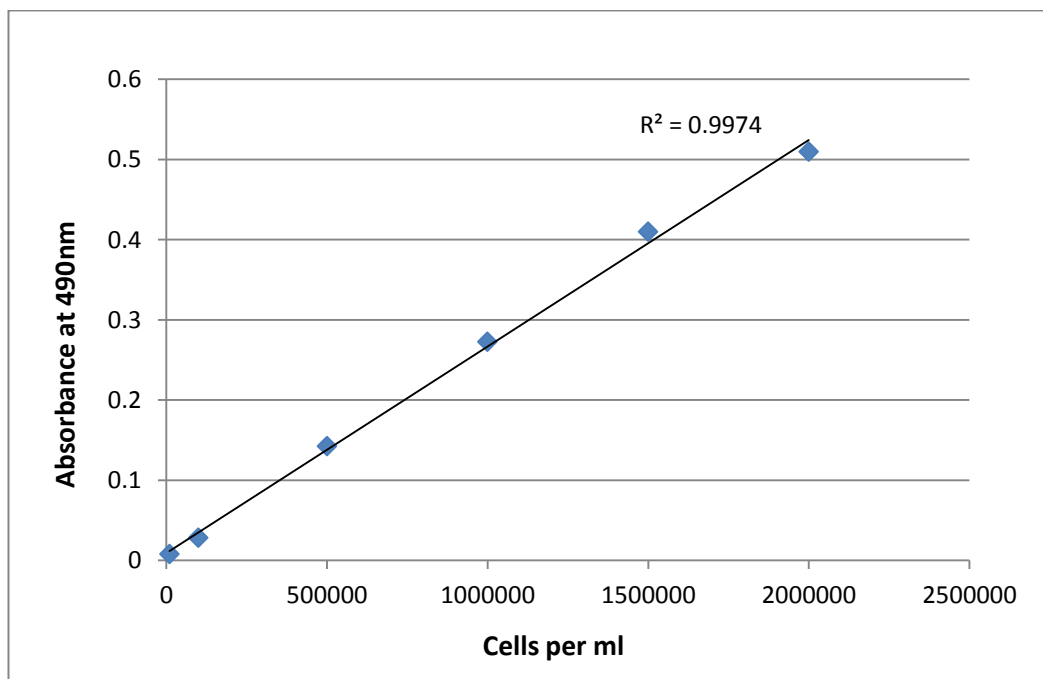


Figure 2.1 – Jurkat standard curve used to determine the cell number following the intervention with (poly)phenol using the MTS method. Absorbance taken at 490nm measuring standards ranging from 2×10^6 to 1×10^4 cell/ml (standards in duplicate). Standard curves were produced for each experiment.

2.2.5 (Poly)phenols.

All (poly)phenols were initially dissolved in dimethyl sulfoxide (DMSO) at 5mM. However, later experiments using just a few polyphenols, higher stock concentrations were produced using 30mM stocks. Catechol, phloroglucinol, pyrogallol, hippuric acid, 4-hydroxybenzoic acid, protocatechuic acid, 4-Hydroxyphenyllactic acid, vanillic acid, 4'-hydroxymandelic acid, 3-(3'-hydroxyphenyl)propionic acid, 3-(3'-hydroxyphenyl)propionic acid, 3-(4'-hydroxyphenyl)lactic acid, caffeic acid, ferulic acid, isoferulic acid, tyrosol, dihydroferulic acid, 4'-hydroxyhippuric acid, feruloylglycine, isoferuloylglycine, resveratrol*, chlorogenic acid, curcumin*, quercetin^o, 3-O-methylquercetin*, isorhamnetin*, epigallocatechin gallate (EGCG)*, kuromanin*, callistephin chloride*, and punicalagin*, stored at -20°C. Phenolic acids and polyphenols (termed (poly)phenols when referring to both) were examined and provided by Professor Alan Crozier (School of Chemistry, University of Glasgow) unless otherwise stated with * (Sigma-Aldrich).

See appendix 1 for information on individual (poly)phenols including structures, molecular weights, foods compounds where they are present and concentrations reported in plasma.

2.2.6 Preparation of stimulations PMA, PHA and LPS.

Compounds were used to induce cytokine release in the cells; this allowed measurements of the protective effect polyphenols had against the stimulations.

At baseline Jurkat and THP-1 cells produce low levels of cytokines, therefore evaluating cytokine reduction may prove problematic, therefore coupling the experiments with stimulation provided greater accuracy to the assays. PMA / PHA treatments used 5 mg / ml phorbol 12-myristoyl 13-acetate (PMA) stock; final concentration 25 ng / ml. Phytohaemagglutinin (PHA) a 5 mg / ml stock; final concentration 5 µg / ml for 24h induces cytokine release in Jurkat cells¹⁶. The PMA/PHA stimulation couldn't be used in the THP-1 cells, as PMA is used in the differentiation of THP-1 monocytes to macrophages, therefore does not have the same effect. Lipopolysaccharide (LPS) was used, as it has been well studied in the induction of cytokines in the THP-1 cell line, there are differences in the treatment times and the pathways they induce, however there is a cross over in the cytokines that are induced by the two treatments, allowing the comparisons between the two cell lines. LPS stock made up 1 mg / ml treated with 1µg / ml LPS and treated for 4h in the THP-1 cells .

2.2.7 Cell treatments for multiplex analysis.

2.2.7.1 Jurkat cell treatments for cytokine measurements.

Cells were seeded at 2×10^6 cells / ml in 48 well plates and incubated overnight. Cells were then treated with DMSO (1µM equivalent = 0.02% v/v, 30µM equivalent = 0.6% v/v), 1 or 30µM (poly)phenols (5mM polyphenol stock) and incubated at 5% CO₂ and 37°C for 48 h. At the 24 h time point cells were treated

with 25 ng/ml PMA and 5 µg/ml PHA. Following incubation cells were resuspended by gently pipetting up and down, 100µl cell suspension was taken for MTS assay. The remaining cell suspension was centrifuged at $224 \times g$ for 5 min and the medium was removed and stored at -80°C for future analysis.

2.2.7.2 THP-1 monocyte cell treatments for cytokine measurements.

Cells were seeded at 1×10^6 cells/ ml in 48 well plates. Cells were treated with dimethyl sulfoxide (DMSO) (0.1% of total media volume) 1, 10 or 30µM isorhamnetin (from 1, 10 and 30mM stock) and incubated at 5% CO_2 , at 37°C for 48 h. Cells were treated with 1µg/ml LPS which was added 4 h prior to the end point. Following incubation cells resuspended by pipetting and 100µl was removed for MTS assay. The remaining cell suspension was centrifuged at $224 \times g$ for 5 min and the media was removed and stored at -80°C for future analysis.

2.2.8 Multiplex assay.

2.2.8.1 Multiplex assay (1) Jurkat.

Multiplex bead analysis was used to measure cytokines IL2, IL8, and $\text{TNF}\alpha$ secreted into the medium obtained following polyphenol treatment by Jurkat T-lymphocytes. Reagents were supplied by Bio-Rad, Hercules, USA unless otherwise stated; the method is illustrated in figure 2.2.

A 96-well filter plate (Millipore, Massachusetts, USA) was pre-washed with assay buffer and removed by vacuum filtration with a pressure of 1-3mmHg. Added to the filter membrane are beads mixed with red and infrared fluorophores which are conjugated with antibodies for IL2, IL8, and TNF α on the surface of the beads, the plate was then washed twice in wash buffer by vacuum aspiration. Standards were made using Bio-Plex Pro™ human cytokine standards (Bio-Rad, Hertfordshire, UK), with a 1:4 serial dilution and were loaded onto the plate along with the samples (undiluted). These were incubated for 1 h under constant agitation at room temperature, protecting the plate from light; this allows the protein of interest to bind to the beads. The plate was washed 3 times in wash buffer using vacuum aspiration before adding a complementary biotinylated detection antibody. The plate was incubated for a further 1h under constant agitation at room temperature, again protecting from the light. Following incubation, 3 more washes were performed using vacuum aspiration and streptavidin-phycoerythrin fluorophore was added, allowing measurement of biotin bound streptavidin-phycoerythrin conjugates. The plate was agitated for a further 10 min at room temperature and protected from light. Three final washes using vacuum to remove liquid, the plate base was blotted dry and samples were resuspended in 150 μ l assay buffer. Plate was then agitated for 30s prior to analysis using Bio-Plex 200 platform (Bio-Rad, Hercules, USA), software was set to record 50 beads per analyte (The Bio-Plex uses lasers to read the colour code of each bead and analyte, e.g. 50 x IL2 beads, 50 x IL8 beads and 50 x TNF α beads

were analysed before moving to next sample on the 96 well plate). This process allows the quantification of multiple molecules within each sample.

See appendix 2, for data on the reproducibility of the assay and correlations between experiments performed on different days.

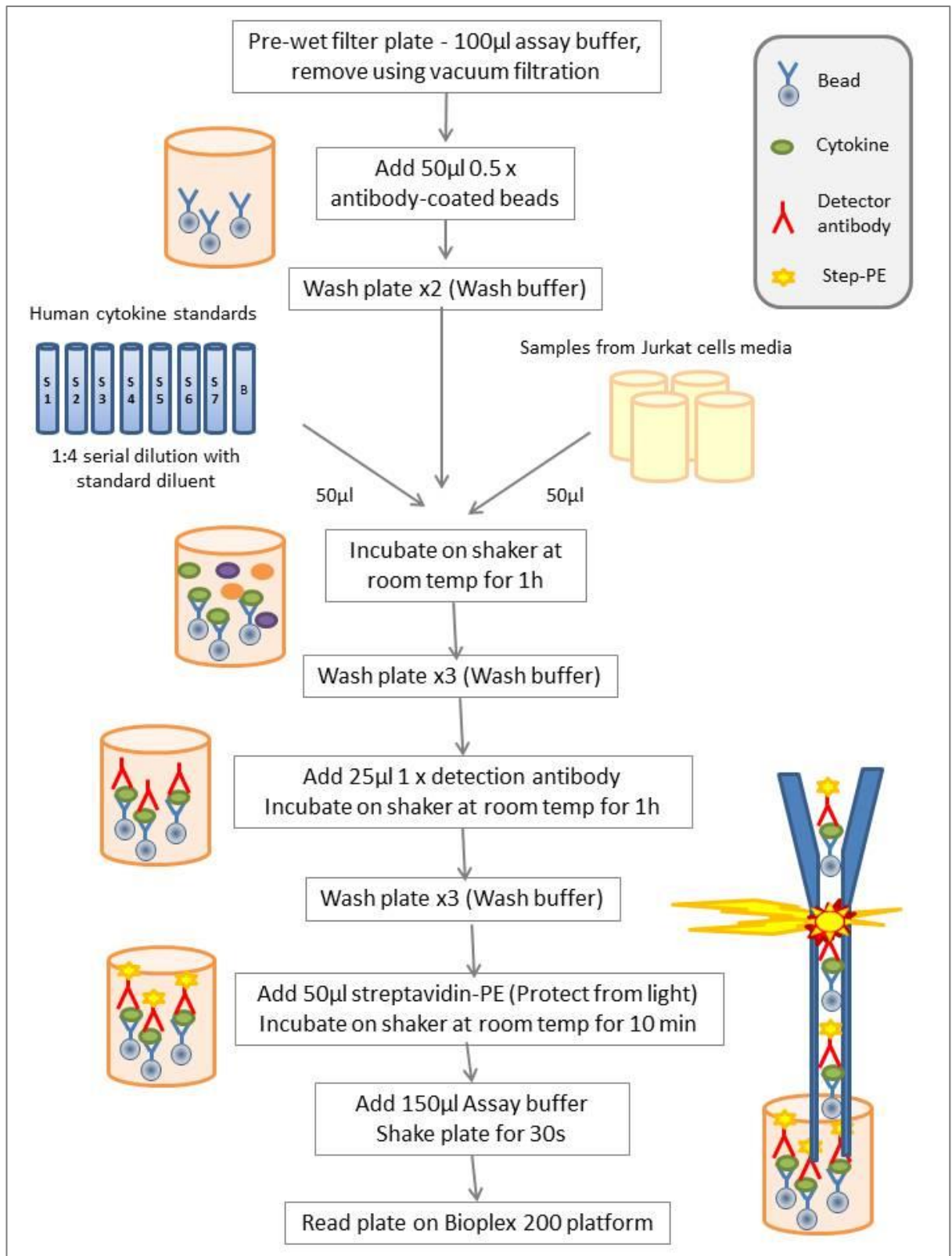


Figure 2.2 – Bio-Plex Pro assay, a flow diagram summarising the steps required for multiple cytokine detection using a multiplex assay (summarised from Bio-Plex Pro assay kit, BIORAD).

2.2.8.2 Multiplex (2) THP-1.

Multiplex bead analysis was used to measure the cytokine content of G-CSF, GM-CSF, GRO, IL1 β , IL6, IL8, IL10, IL12p40, IL12p70, MCP-1, and TNF α in the medium obtained following polyphenol treatment on the THP-1 cells. Reagents were supplied by Mulliplex, Watford, UK, unless otherwise stated. The experiment was similar to BioRad multiplex analysis, with differences in length of incubation, automated plate washing and detection platforms used (detailed below).

Wash buffer was added to a 96 well plate, sealed and agitated for 10min at room temperature. Standards were made human cytokine standards starting at 10,000 pg/ml with 1 in 5 dilution, these were loaded on the plate in duplicate along with 2 quality controls (QC), at a low and high concentration, along with the samples. Assay buffer was added to the sample wells and culture media to the standard and QC wells. The 11 antibody-beads were sonicated in a water bath and vortex for 1 min, to resuspend beads before being diluted and added to the plate. The plate was sealed and incubated overnight at 4°C with agitation.

Following overnight incubation, the plate was washed twice with wash buffer using a magnetic plate washer (BioTek ELx40, setting supplied in manual), detection antibody was added and incubated at room temperature for 1h with agitation. Streptavidin-Phycoerythrin was added and left to incubate for 30 min at room temperature with agitation. The plate was then washed twice with wash buffer, followed by sheath fluid (delivery fluid for the Bioplex platform). The plate analysis was undertaken using Qiagen liquiChip, Luminex xMap technology,

Bioplex Manager, which uses lasers to measure and quantify the colour of individual beads.

2.2.9 Multiplex data analysis.

Raw data generated following multiplex analysis by the bioplex reader, software calculates unknown cytokine samples by using the known cytokine standard curve. Data for unknown samples was given as pg/ml for the chosen cytokines (e.g. IL2, IL8, TNF α). Initial checks to the data were made to ensure a suitable standard curve was generated and that samples fell within the ranges of the standard curve. The data was then normalised to cell number, which was obtained by MTS assay (2.2.4.2) for each polyphenol treatment. The data was then presented as a percentage change from the DMSO treated control. Due to the large amounts of treatments, polyphenols comparisons were conducted in sets of 4 or 5 and statistical analysis was conducted for each separate experiment. Set 1 = Epigallocatechin gallate (EGCG), kuromanin, callistephin chloride, and punicalagin. Set 2 = Phloroglucinol, catechol, protocatechuic acid and 4-hydroxybenzoic acid. Set 3 = 4-Hydroxyphenyllacetic acid, 4'-hydroxymandelic acid, 3-(3'-hydroxyphenyl)propionic acid and 3-(4'-hydroxyphenyl)lactic acid. Set 4 = Caffeic acid, Ferulic acid, Isoferulic acid and isoferuloylglycine. Set 5 = Hippuric acid, 4'-hydroxyhippuric acid, tyrosol and chlorogenic acid. Set 6 = Dihydroferulic acid, feruloylglycine, quercetin and 3-O-methylquercetin. Set 7 = Curcumin,

isorhamnetin, pyrogallol, resveratrol, and vanillic acid. Statistical analysis was performed on normalised raw data, with an ANOVA and Dunnett's post-hoc test which compares multiple treatments against the DMSO treated control. The raw data expressed in pg/ml minus the DMSO control for each cytokine can be found in Appendix 1 (Table 8.2-8.5).

2.2.10 Jurkat cell treatments for glutathione measurements.

Cells were seeded at 2×10^6 cells / ml in 6 well plates. Cells were treated with dimethyl sulfoxide (DMSO), 1 or $30 \mu\text{M}$ (poly)phenol. Cells were then incubated at 5% CO_2 and at 37°C for 48 h. At the 24 h time point cells were treated with 25 ng/ml phorbol 12-myristoyl 13-acetate (PMA) and $5 \mu\text{g/ml}$ phytohaemagglutinin (PHA). Following incubation $100 \mu\text{l}$ was taken in duplicate for MTS assay and the remaining cell suspension was centrifuged at $224 \times g$ for 5 min. The cell pellet was washed in Dulbecco's phosphate-buffered saline (DPBS) and was centrifuged at $224 \times g$ for 5 min. The pellet was resuspended in $100 \mu\text{l}$ extraction buffer (containing sodium phosphate dibasic, sodium EDTA and sulfosalicylic acid hydrate, pH 7.5), then the samples were sonicated $3 \times 5 \text{ s}$ on ice and centrifuged at $20817 \times g$ for 10 min at 4°C . The supernatant was used for glutathione assay, measuring total and oxidised glutathione.

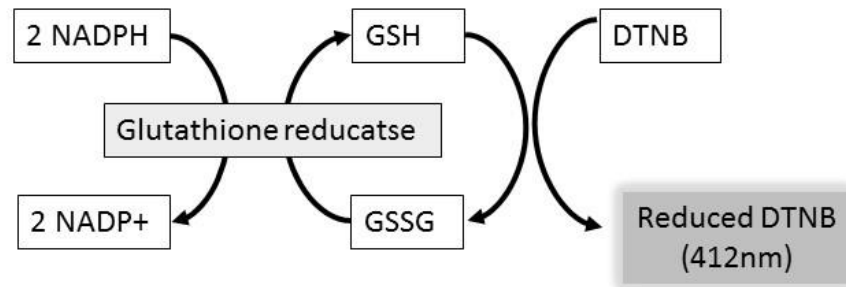
2.2.11 Glutathione enzymatic recycling assay.

The glutathione recycling assay was used to measure intracellular concentrations of total and oxidised glutathione, following treatment of Jurkat cells with (poly)phenols. This method, illustrated in figure 2.3, uses glutathione reductase (ROCHE: Life Sciences, Dubai, UAE) and β -nicotinamide adenine dinucleotide phosphate (NADPH) to convert oxidised (GSSG) to reduced glutathione (GSH), utilising the reduction of 5,5'-dithiobis(2-nitro-benzoic acid) (DTNB) by GSH, forming reduced DTNB which is yellow in colour and can be measured spectrophotometrically at 412nm. The resulting GSSG molecule re-enters the system and the recycling process occurs, kinetic measurements are taken during the exponential phase of the reaction. Using known standards of GSH (10.4 to 0.08 μ M) and GSSG (2.6-0.02 μ M) a standard curve can be used to quantify unknown amounts of total amount of glutathione (GSH and GSSG) in the Jurkat samples. Quantification of GSSG can be measured by masking GSH by pre-incubating samples with 2-vinylpyridine (2-VP). 2-VP does not interfere with glutathione reductase therefore the enzymatic recycling can be done as before but will only be measure GSSG levels in the sample. Oxidised glutathione can be taken away from the total glutathione concentration, giving the levels of reduced glutathione present in the samples.

For total glutathione measurements: 20 μ l of standards and samples (diluted 1 in 10 in extraction buffer) (buffered used are described in table 2.1) were added to a 96 well plate followed by 200 μ l of assay buffer (made up of the

NADPH solution, DTNB solution, glutathione reductase added just before absorbance was taken). Absorbance was read at 412 nm using a kinetic programme, taking absorbance readings every 15s for 10 mins, a standard curve was generated from the exponential phase of the reaction. For oxidised glutathione measurements: 2-vinylpyridine was added to the standards and samples (at 1 in 100 dilutions) and incubated for 1h at room temperature, in order to mask GSH, meaning only GSSG will be present in the sample. Standards and samples were transferred to a 96 well plate, followed by the assay buffer and absorbance taken at 412nm, the same as previously described for total glutathione measurements.

Total glutathione (GSH) assay



Oxidised glutathione (GSSG) assay

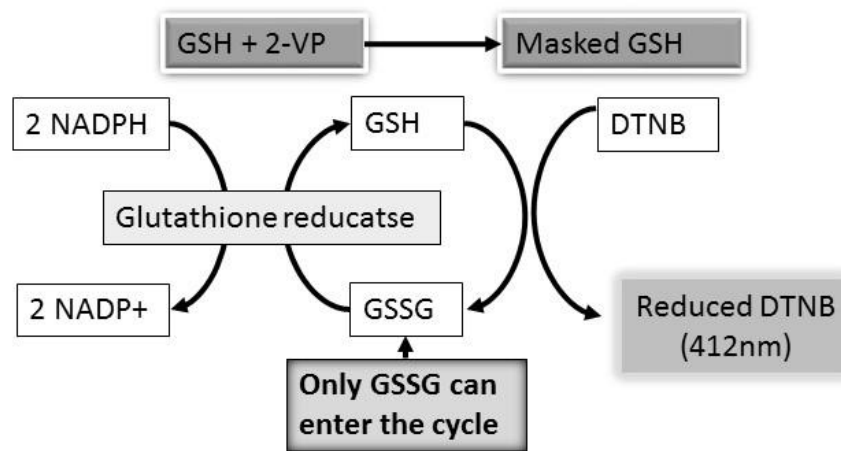


Figure 2.3 – Principles behind the glutathione enzymatic recycling assay. Total glutathione measured using β -nicotinamide adenine dinucleotide phosphate (NADPH) and glutathione reductase to convert oxidised glutathione (GSSG) to reduced glutathione (GSH), which is then recycled back to GSSG, along with the reduction of 5,5'-dithiobis(2-nitro-benzoic acid) (DTNB) which can be measured using a spectrophotometer at 412nm. GSSG can be measured independent of GSH by pre-incubation with 2-vinylpyridine (2-VP) for 1 h, which masks GSH. Recycling assay can then be performed allowing the measurement of GSSG only. (Modified from Moeller, R. and Mason, A.Z.¹³⁰).

Preparation of glutathione recycling assay buffers	
Stock buffer	143mM sodium phosphate dibasic, 124mM sodium EDTA, in distilled water (pH 7.5).
NADPH solution	335.8µM (β-Nicotinamide adenine dinucleotide phosphate, reduced tetra(cyclohexylammonium) salt) in stock buffer.
DTNB solution	6mM 5,5'-dithiobis(2-nitro-benzoic acid) in stock buffer.
Extraction buffer	45.8mM (5-sulfosalicylic acid hydrate) in stock buffer.
Oxidised glutathione	2.6 µM oxidised glutathione in extraction buffer.
Reduced glutathione	10.4 µM reduced glutathione in extraction buffer.
Assay buffer	7:1 ratio of NADPH:DTNB solutions. With 1 in 90 dilution of glutathione reductase enzyme added just prior to absorbance reading.

Table 2.1 – Table detailing the preparation of buffers required for the glutathione recycling assay. Stock buffer is used to make NADPH solution, DTNB solution and extraction buffer, along with oxidised and reduced glutathione which are dissolved in extraction buffer. Assay buffer is comprises of a mixture of NADPH and DTNB solutions, with the addition of the glutathione reductase enzyme.

The concentration of oxidised and reduced glutathione can be represented as a redox potential (mV) calculated using the Nernst equation below.

$$E_h = E_0 + \frac{RT}{nF} \ln \left(\frac{[GSSG]}{[GSH]^2} \right)$$

E_h = redox potential GSH/GSSG (mV), E_0 = standard potential (-264 mV), R = gas constant (8.314 J/°Kmol), T = absolute temperature of analytical measurement (25°C = 298°K), n = number of electrons transferred ($n=2$), F = Faraday's constant (96,485 coulomb/mol).

In humans the intracellular GSH/GSSG redox potential is estimated to range from -260 mV to -230mV for dividing cells¹³¹, in the Jurkat cells the resting redox state was found to be -228mV (Fig. 2). Changes in glutathione with (poly)phenol treatment were compared to a DMSO treated control. No differences in the glutathione redox potentials were observed between untreated cells and DMSO treated cells, significant oxidation was observed with PMA/PHA treatment from -229 mV with DMSO to -211 mV with PMA + DMSO (Fig. 2.4).

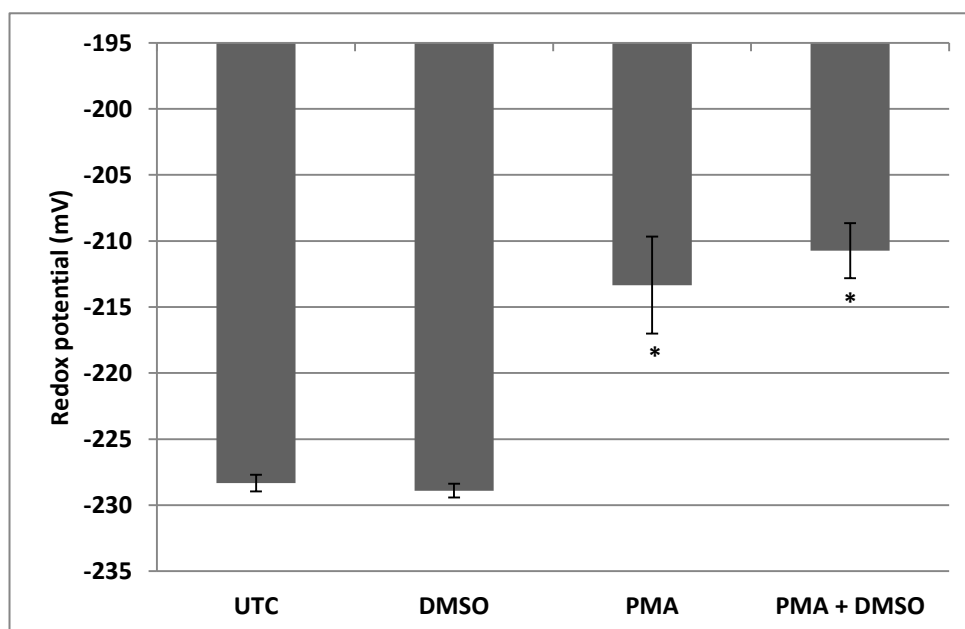


Figure 2.4 - Glutathione redox potential of Jurkat cells comparing untreated cells (UTC) with cells treated with DMSO for 24 h (dose matched to amounts used in (poly)phenol treatments). Cells were also treated with PMA/PHA and with the addition of DMSO for 24 h. Redox potential \pm SEM ($n = 4$).

2.2.12 Glutathione oxidation by diamide and 50 μ M curcumin.

As a positive control for a treatment to oxidative glutathione, cells were stimulated with diamide, which is a strong oxidising agent to induce the formation of oxidised glutathione. Figure 2.5 shows a significant increase in the concentration of oxidised glutathione following 15 minute treatment with 1mM diamide, other time points were examined at 5, 30 and 60 min (data not shown) but only the 15 min showed a significant increase. A high dose of curcumin (50 μ M) for 10 min was also used to give rise to a significant increase in oxidised glutathione, a greater induction of GSSG was observed with curcumin than with the diamide treatment (fig. 2.5B). Satisfied that the glutathione assay was capable of measure changes in reduced and oxidised glutathione in the Jurkat cell model.

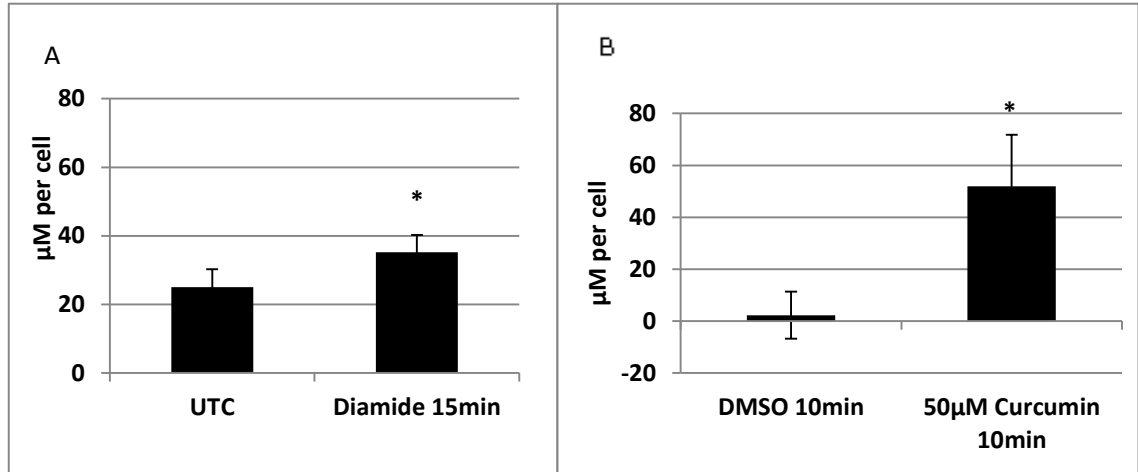


Figure 2.5 – Positive control for oxidised glutathione measurements for glutathione recycling assay. A) Intracellular concentrations of oxidised glutathione in Jurkat cells following treatment with 1mM diamide for 15min. B) Intracellular concentrations of oxidised glutathione in Jurkat cells following treatment with 50 μ M curcumin for 10min. [mean \pm SEM, $n = 4$, $p < 0.05$].

2.2.13 Protein quantification using spectroscopic analysis.

2.2.13.1 Bradford assay.

Standards were prepared from bovine serum albumin stock solution with a 1 in 2 serial dilution starting at 1000µg/ml in water. Samples and standards were transferred to a 96 well plate, 200µl Bradford Ultra reagent (Expedeon, Cambridgeshire, UK) was added and absorbance was read at 595nm using a spectrophotometer.

2.2.13.2 BCA assay.

Standards were prepared in the same way as for the Bradford assay, both standards and samples were transferred to 96 well plate. Copper(II)sulphate was added 1 in 50 to bicinchoninic acid, vortex and 200µl added to the plate, followed by 30 minutes incubation at 37°C, with absorbance being read at 562nm in a spectrophotometer. The BCA assay is based on two reactions, the first reaction is the reduction of Cu^{2+} ions (copper(II)sulfate) by peptide bonds in the proteins, the amount of protein present is direction proportional to the concentration of reduced Cu^+ , this is a temperature dependent reaction, hence the incubation step at 37°C. The second reaction two molecules of the bicinchoninic acid bind to each Cu^+ ion, resulting in the colour change from green to purple, which can be measured spectrophotometrically at 562nm.

The different protein assays were used depended on the concentration of protein in sample and whether the cell lysis buffers contained protein interfering substances, such as SDS, phenol red, reducing or oxidising agents.

2.2.14 Nuclear and cytoplasmic extractions in Jurkat cells.

To measure the nuclear translocation of the activated transcription factor Nrf2, nuclear and cytoplasmic extracts were required from the Jurkat cells. Three methods were evaluated: the subcellular fractionation as described by Dimauro *et al* 2012¹³², 'nuclear protein extraction without the use of detergents' by Sigma Aldrich¹³³, and 'preparation of nuclear extracts' by Active Motif¹³⁴. The Active Motif method was the most accurate and consistent for nuclear and cytoplasmic extracts with Jurkat T lymphocytes using western blotting to evaluate.

Cells were seeded at 2×10^6 /ml in 6 well plates, incubate cells at 37°C, 5% (v/v) CO₂, treated with (poly)phenol of interested with an equivalent DMSO treated control for 48h. Cells were washed 3x in ice cold DPBS and resuspended in 1ml on 5% PIB in DPBS solution, samples were kept on ice throughout. (Buffers described in table below – Table 2.2)

Table 2.2 - Nuclear/Cytoplasm extract buffers	
PIB (phosphatase inhibitor buffer)	125 mM NaF Sodium Fluoride 250 mM β -glycerophosphate 250 mM p-nitrophenyl phosphate (PNPP) 25 mM NaVO ₃ – Sodium metavanadate In distilled water.
HP (hypertonic buffer)	20mM Hepes, pH 7.5 5mM NaF Sodium Fluoride 10 μ M Na ₂ MO ₄ – Sodium molybdate 0.1mM EDTA Ethylenedicmmetetracetate acid. In distilled water.

Samples were centrifuged at 224 x g for 5 min, the supernatant discarded and resuspended in HB buffer, the cells were left to swell on ice for 15 min. 5 μ l of 10% Nonidet P40 substitute (0.5% (v/v) final concentration) was added and vortexed vigorously for 10 sec. The resulting homogenate was then centrifuged at 4^oC, 20817 x g for 30 sec, the supernatant removed and retained (cytoplasmic fraction). Phosphatase and protease inhibitor cocktail were added 1 in 100, to prevent dephosphorylation and proteolytic degradation during cell lysis and stored at -80^oC for future analysis. The resulting pellet was resuspended in 50 μ l 1% (w/v) SDS (also containing protease/phosphatase inhibitor cocktail 1 in 100), samples were sonicated on ice 3 x 5s , then centrifuged at 4^oC for 10 min at 14,000 x g. The supernatant (nuclear fraction) was retained and stored at -80^oC. Protein was quantified using BCA assay.

2.2.15 SDS-PAGE and western blotting.

Protein samples were prepared for western blot analysis by diluting with distilled water to contain appropriate amount of protein (ranging from 7.5 and 30µg of protein), with an appropriate amount of 4x Laemmli sample loading buffer (BioRad, Richmond, USA) (Tris-HC, glycerol, LDS, 1 in 20 dilution of 2-mercaptoethanol, pH6.8). The 2-mercaptoethanol provides a negative charge to the proteins, the loading buffer make the protein sample denser, and allows visualisation of the samples when in the gel, which are important features required when separating protein by electrophoresis. Samples were boiled at 100°C for 5 min to denature the proteins, and allowed to cool before adding to the gel.

2.2.15.1 Gel preparation

Reagents from National Diagnostics (Atlanta, USA) were used unless otherwise stated.

A 12% (w/v) resolving gel was made by mixing 30% (w/v) Protogel, 4x resolving buffer, distilled water, 10% w/v ammonium persulfate (APS) (Sigma Aldrich, Poole, UK) and *N,N,N',N'*-Tetramethylethylenediamine (TEMED) (Sigma Aldrich, Poole, UK) pH to 8.8. The Protogel and resolving contains SDS which provided a negative charge to the proteins, polyacrylamide which forms a matrix of pores upon polymerization by APS and TEMED. The mixture was allowed to polymerize for approximately 20min, with a thin layer of distilled water was placed on top of the

gel while it polymerised, to prevent the gel from drying out and provide a smooth edge. Once set the water was removed and a 4% (w/v) stacking gel is placed on top, this mixture contained 30% (w/v) Protogel and stacking buffer, pH 6.8. The lower percentage obtained with the stacking gel allowed large pores to be generated, which means the proteins move easily through the gel when a current was applied, and allowed the proteins to compact together before entering the resolving gel, where protein separation occurs. A comb was inserted between the glass plates, in order to generate the wells for protein samples to be loaded. Once the gel has set, the comb was removed and apparatus containing the gels was placed into the electrophoresis chamber. The upper and lower chambers were filled with a 1x running buffer, which contained 25 mM Tris, 190 mM glycine, 0.1% (w/v) SDS, and water, pH 8.3 which is stored at 4°C until required. Samples were loaded into the wells along with a molecular weight ladder, which was used to check protein separation and distinguish between different molecular weights. Current was set to 20mA, until the dye front reaches the interface between the stacking and resolving gels, then the amps are increased to 60mA and max volts. When the dye front reaches the bottom of the gel, the current is stopped and the gels removed and prepared for protein transfer.

2.2.15.2 Protein transfer using the semi-dry method

Transfer buffers are prepared as described in table below, Table 2.3.

Anode I buffer	0.3M Tris in 20% methanol. pH to 10.4
Anode II buffer	12mM Tris in 20% methanol. pH to 10.4
Cathode buffer	40mM 6-amino n hexanoic acid in 20% methanol. pH to 7.6
1x Tris buffered saline solution (TBS)	20mM Tris and 150mM sodium chloride (NaCl) pH to 7.6
TBS-Tween (TBST)	1x TBS with 0.005% Tween 20 pH to 7.6

Table 2.3 –Buffers for protein transfer during western blotting. Preparation of protein transfer buffers anode I, anode II and cathode buffers and western blotting buffers TBS, and TBST.

Filter paper was cut to the size of the gel, soaked in appropriate transfer buffer and layered as shown below in fig. 2.6. The gel (with the stacking gel removed) was sandwiched between filter paper soaked in Anode I and II and Cathode Buffer, with a nitrocellulose membrane below the gel and was soaked in Anode II. The nitrocellulose membrane is a matrix used to transfer proteins from the gel on to a medium which can be used in immunoblotting.

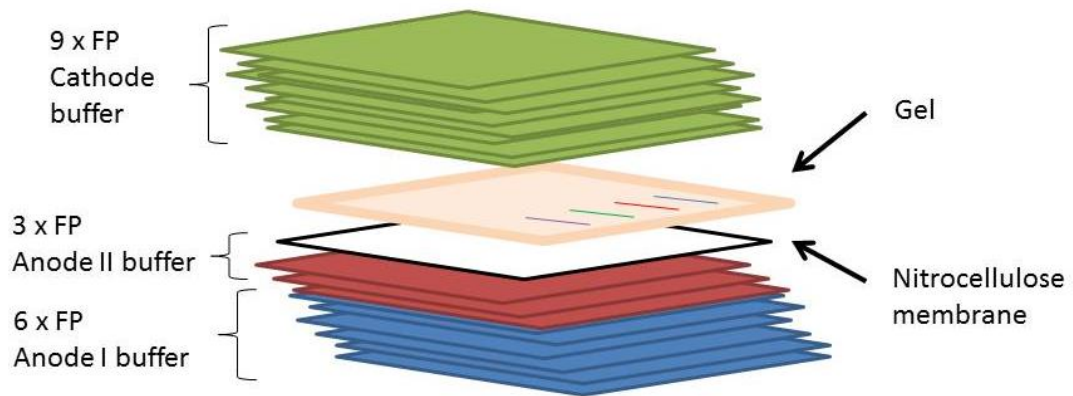


Figure 2.6 – Preparation of gel to allow protein transfer. 6 x filter papers (FP) soaked in Anode I Buffer, with 3 x FP soaked in Anode II on top. Nitrocellulose membrane soaked in Anode II sits below the gel, 9 x FP soaked in Cathode Buffer sit on top.

A roller was used to smooth out the filter papers and remove any air bubbles, the gel and filter papers were sandwiched between two metal plates and a current applied top to bottom, 100mA for each gel for 1 h 15 min. This allowed transfer of the proteins from the gel to the nitrocellulose membrane. Following the transfer the membrane was removed and approx. 10ml of Ponceau S stain was applied to the membrane see figure 2.7. This allows visualization of the proteins to check for successful transfer to the membrane from the gel, even loading of the protein samples into the gel, and cutting of the membrane at different molecular weights to allow the membrane to be analysed for different proteins using antibodies.

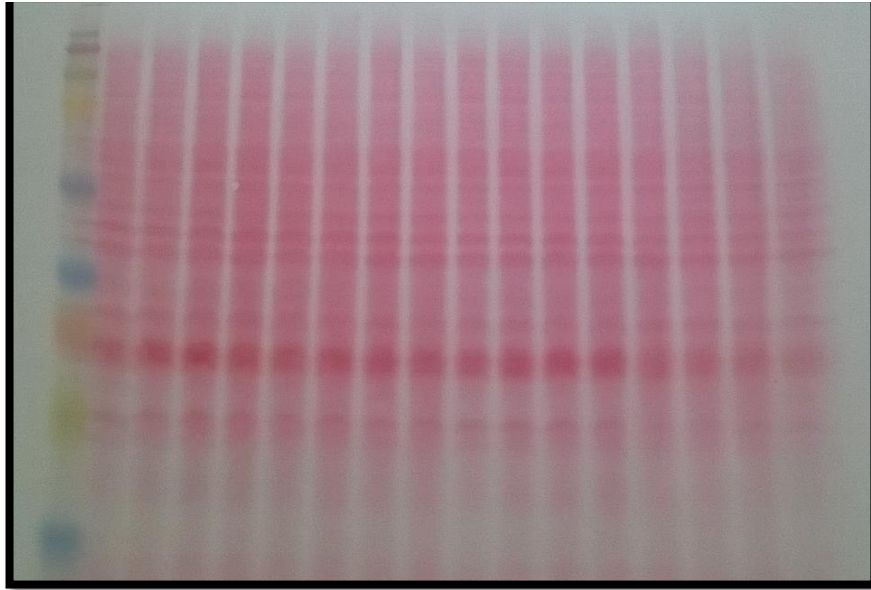


Figure 2.7 - Ponceau S stain applied to nitrocellulose membrane to allow reversible visualisation of proteins. The stain contains a sodium salt, diazo dye, which has a red colour. Stain can be removed using TBS-tween, which allows subsequent immunological detection.

2.2.15.3 Immunoblotting

Once Ponceau S stain has been removed by washes of TBS-T, the membrane was blocked in 5% (w/v) milk for 1 h. The milk was then removed and membrane washed 3x TBST every 10 min, followed by the primary antibody of choice diluted in 3% (w/v) milk, see table below (Table 2.4) for antibodies used and appropriate dilutions. The membrane was incubated with the primary antibody overnight on a rocker at 4^oC. This allows the optimal binding of the antibody to the protein of interest.

Following incubation the primary antibodies was removed (for some antibody these can be kept, stored at -20^oC and reused) and washed 3 x TBST

every 10 min. The secondary antibody which is conjugated to horseradish peroxidase (HRP), was then added, either anti-mouse or anti-rabbit depending on the animal the primary antibody was raised. The secondary antibody was diluted as shown in table 4 in 3% (w/v) milk and incubated for 1 h on a rocker at room temperature. Following incubation the secondary antibody was removed and membrane washed 3x TBST every 10 min.

ANTIBODIES	Animal	MW	Dilution	Code
Primary antibody				
Anti-Nrf2 (C-20)	Rabbit	61kDa	1:500	Santa Cruz biotechnology – sc- 722
Anti-Phospho Nrf2	Rabbit	Predicted: 68kDa Observed: 90kDa	1:1000	Abcam – ab76026
Anti-Keap1	Rabbit	70kDa	1:1000	Abcam – ab66620
Anti-GSR	Rabbit	58kDa	1:1000	Abcam – ab16801
Anti-TXN	Rabbit	12kDa	1:2000	Abcam – ab86255
Anti-TXNRD1	Rabbit	55kDa	1:1000	Abcam – ab16840
Anti-Catalase	Rabbit	60kDa	1:2000	Abcam – ab16731
Anti-PRDX2	Rabbit	22kDa	1:500	Abcam – ab59539
Anti-Vinculin	Mouse	117kDa	1:1000	Abcam – ab18058
Anti-Histone H3	Rabbit	17kDa	1:5000	Abcam – ab1791

Secondary antibody				
Anti-Mouse IgG	Goat		1:50000	Sigma – A2554
Anti-Rabbit IgG	Goat		1:8000	Cell signalling - 7074

Table 2.4 – Primary and secondary antibodies used in the immunoblotting for proteins: nuclear factor (erythroid-derived 2_-like 2 (Nrf2), phosphorylated Nrf2, Kelch-like ECH-associated protein 1 (Keap1), glutathione reductase (GSR), thioredoxin (TXN), thioredoxin reductase 1 (TXNRD1), catalase, peroxiredoxins 2 (PRDX2), vinculin, and histone H3. Table includes the species source of the antibody, the molecular weight, along with the dilution and reference code for the primary and secondary antibodies used.

2.2.15.4 Analysis and normalisation of immunoblotting images.

The membrane was visualised with the addition of an enhanced chemiluminescence ECL reagent (Thermo Scientific, Illinois, USA) using a ChemiDoc XRS system (BioRad, Herts, UK) and analysed using software Quantity One, ChemiDoc XRS. The chemiluminescence reacts with the HRP-conjugated secondary antibody and emits light, which can be visualised and then quantified using software such as Quantity One or Image J. Densitometry values for proteins of interest were normalised to a protein loading control vinculin (cytoplasmic control) or Histone H3 (nuclear control) or normalised to the Ponceau S stain. Vinculin was used as a cytoplasmic control and histone H3 was used as a nuclear control, under some circumstances the Ponceau S stain was used, correcting to total protein in well. Normalisation allows a more accurate representation of

increases or decreases in protein expression is due to the treatments and not due to the amount loaded in the wells. When viewing the bands, membranes are exposed for different time periods to obtain the optimal balance between chemiluminescence signal and background, preventing under- and over-exposure.

2.2.16 Nrf2 DNA binding assay.

All reagents were supplied by Active Motif (La Hulpe, Belgium) unless otherwise stated.

Cell pellets were resuspended in complete cell lysis buffer (containing DTT and protease inhibitor cocktail), samples were sonicated, and then centrifuged at 14,000 xg at 4°C for 10 min, and the supernatant was stored at -80°C. The protein concentration was determined by Bradford assay, 20 μ g was then used to perform the assay.

The 96 well plate provided in the kit has been coated with immobilised oligonucleotide containing the ARE consensus binding site (5'-GTCACAGTGA CT CAGCAGAATCTG-3'). The active form of Nrf2 will bind to this sequence. The plate is prepared by adding binding buffer to the wells required. A positive control is added which is provided by the kit, along with blanks and samples, the plate was then incubated for 1h at room temperature, with mild agitation. Plate was then washed 3x with wash buffer and Nrf2 antibody was

added (1:1,000 dilution) for 1h at room temperature with no agitation. Again the plate was washed 3x with wash buffer before adding the HRP-conjugated antibody (1:1,000 dilution) for 1h at room temperature with no agitation. Following this incubation the plate was washed 4x with wash buffer and a developing solution was added and allowed to develop for ~20 min at room temperature, protected from the light. A blue colour develops over this time and the stop solution was then added, the blue colour turns yellow. The absorbance can now be read at 450nm (with ref wavelength at 655nm).

2.2.17 Cell treatments for proteomics analysis.

Cells were seeded at 2×10^6 cells/ml in 6 well plates, treated with dimethyl sulfoxide (DMSO) (1 μ M equivalent = 0.02% DMSO), or 1 μ M (poly)phenol and 10/30 μ M (poly)phenol and incubated at 5% CO₂ and at 37°C for 48 h. Following incubation cell number was determined using trypan blue exclusion with automatic cell counter. Samples were centrifuged at $224 \times g$ for 5 min and washed 4 times with DPBS. Pellets were frozen and stored in -20°C (n = 5).

Experiments planning:

Initial experiments conducted with DMSO, 1 μ M curcumin and resveratrol. A low number of proteins were identified, therefore follow up experiment included DMSO, 10 μ M curcumin and 30 μ M resveratrol. After reanalysing data,

isorhamnetin was also investigated using DMSO, 1 and 30 μ M isorhamnetin. For all experiments 5 replicates were used.

2.2.18 Liquid Chromatography Mass Spectrometry (LC-MS) of proteins.

LC-MS analysis of Jurkat cells following polyphenol challenge was conducted by

Dr Deborah Simpson, Centre for Proteomics at University of Liverpool.

2.2.18.1 Sample digestion.

Cell pellets (8-11 million cells) were re-suspended in ice-cold 25mM ammonium bicarbonate (0.75mL) and each sample sonicated for three 10s pulses at 30% amplitude followed by a 50s rest period. 0.75 μ L of Benzonase nuclease was added and samples were held on ice. A protein assay was carried out and all sample dilutions were in the linear range of the standard curve (50-fold dilution).

A volume of cell lysate equivalent to 50 μ g of protein was added to a 0.5mL low-bind tubes and the volume of made up to 80 μ L with 25mM ammonium bicarbonate. 5 μ L of 1%(w/v) Rapigest (a surfactant which facilitates digestion) was added and the samples placed in a heating block and held at 80 $^{\circ}$ C for 10min. Dithiothreitol (5 μ L of a 60mM solution in 25mM ambic was added and samples held at 60 $^{\circ}$ C for 10min (reduction of disulphide bridges). Iodoacetamide 5 μ L (178mM in 25mM ammonium bicarbonate) was added and samples incubated in the dark for 30min at room temperature (alkylation of cysteines facilitating MS

analysis). Trypsin (5 μ l of 0.2 μ g/ μ l in 50mM acetic acid) added and samples incubated overnight at 37°C.

Day 2. 1 μ l of Trifluoroacetic acid (TFA) (hydrolysis of Rapigest surfactant) was added and samples were incubated at 37°C for 45min. Centrifugation of samples at 17,300 x g for 30min and clarified digests transferred to fresh low-bind tubes. Centrifugation as above and 10 μ l of sample transferred to 'total recovery autosample vials' for LC-MS analysis.

2.2.18.2 High resolution LC-MS/MS analysis.

1 μ l of digest (500ng protein equivalent) was injected on-column and chromatographed over a 2h gradient using a method whereby following a survey scan at 70,000 resolution the top 10 most abundant peptide ions are fragmented and measured at high resolution (35,000) in the Orbitrap analyser to a mass accuracy of 0.01Da.

2.2.18.3 LC separation.

All peptide separations were carried out using an Ultimate 3000 nano system (Dionex/Thermo Fisher Scientific). For each analysis the sample was loaded onto a trap column (Acclaim PepMap 100, 2cm x 75 μ m inner diameter, C₁₈, 3 μ m, 100Å) at 5 μ l/min with an aqueous solution containing 0.1%(v/v) TFA and 2%(v/v)

acetonitrile. After 3 min, the trap column was set in-line with an analytical column (Easy-Spray PepMap® RSLC 15cm x 75µm inner diameter, C₁₈, 2µm, 100Å) (Dionex). Peptide elution was performed by applying a mixture of solvents A and B. Solvent A was HPLC grade water with 0.1%(v/v) formic acid, and solvent B was HPLC grade acetonitrile 80%(v/v) with 0.1%(v/v) formic acid. Separations were performed by applying a linear gradient of 3.8% to 50% solvent B over 95 min at 300nL/min followed by a washing step (5 min at 99% solvent B) and an equilibration step (15 min at 3.8% solvent B).

2.2.18.4 Q Exactive set-up.

The Q Exactive instrument was operated in data dependent positive (ESI+) mode to automatically switch between full scan MS and MS/MS acquisition. Survey full scan MS spectra (m/z 300-2000) were acquired in the Orbitrap with 70,000 resolution (m/z 200) after accumulation of ions to 1×10^6 target value based on predictive automatic gain control (AGC) values from the previous full scan. Dynamic exclusion was set to 20s. The 10 most intense multiply charged ions ($z \geq 2$) were sequentially isolated and fragmented in the octopole collision cell by higher energy collisional dissociation (HCD) with a fixed injection time of 120ms and 35,000 resolution. Typical mass spectrometric conditions were as follows: spray voltage, 1.9kV, no sheath or auxillary gas flow; heated capillary

temperature, 250°C; normalised HCD collision energy 30%. The MS/MS ion selection threshold was set to 1×10^4 counts and a 2 m/z isolation width was set.

2.2.18.5 Database search and Protein identification.

Raw data files were uploaded into Proteome Discoverer 1.3 and searched against the human UniProt database using the Mascot search engine (version 2.4.1). A precursor ion tolerance of 10ppm and a fragment ion tolerance of 0.01Da were used with carbamidomethyl cysteine set as a fixed modification and oxidation of methionine as a variable modification. The false discovery rate (FDR) against a decoy database was 1-5%.

PCA plots generated to correlate the spread of data and identify significant groups of proteins (Appendix 3)

2.2.19 RNA isolation and quantification of Jurkat cell samples.

The extraction and purification of ribonucleic acids (RNA) from the Jurkat cells was conducted for future quantitative polymerase chain reaction (qPCR) analysis. There are several methods of extracting RNA, but all procedures follow the same basic principles of disrupting the cell membranes to release RNA into solution, separate RNA from protein, DNA and other contaminants, and effectively inhibit

nuclease activity which would otherwise degrade the RNA. In this study RNA was extracted using Qiagen RNeasy Mini kits.

Jurkat cells were seeded at 1×10^6 cells/ml in 24 well plates, incubate cells at 37°C , 5% (v/v) CO_2 , treated with (poly)phenol of interested with equivalent DMSO control for 3, 9, 24, and 48h. Cells were washed 3x in ice cold DPBS and resuspended in $350\mu\text{l}$ of RLT buffer from Qiagen RNeasy Mini kits, then an equal volume of 70% (v/v) ethanol was added, immediately transferred to RNeasy Mini spin column, centrifuge for 15 s at $8,000 \times g$, discarding the flow-through. Buffer RW1 buffer was then added to the column and centrifuged for 15 s at $8,000 \times g$, discarding the flow-through. Buffer RPE is added to the column and centrifuged for 15 s at $8,000 \times g$, discarding the flow-through. Buffer RPE was added and spun for 2 min at $8,000 \times g$. Transfer spin column to a new collection tube and centrifuge for 1 min at full speed to dry the membrane. Again transfer spin column to new collection tube, add $50\mu\text{l}$ of RNase-free water to the spin column membrane and centrifuge for 1 min at $8,000 \times g$. Isolated RNA is then stored at -80°C before RNA quantification and CDNA generation.

RNA quantification and purity was determined using either Bioanalyser or Nanodrop. Bioanalyser is a chip assay which separates ribosomal proteins via electrophoresis, dyes molecules added to the samples intercalate with the RNA which allows detection by laser-induced fluorescence. Software compared unknown samples to a known RNA ladder, determining RNA peaks and sample concentration (Example, Fig. 2.8). The NanoDrop measures nucleic acid

concentration using spectrophometric analysis, using small amounts of sample 0.5 - 2µl of sample. The concentration of RNA can be determined along with purity of the sample, by assessing the ratio of absorbance at 260/280 for protein contamination, a ratio of ~2 is accepted as pure for RNA. The 260/280 absorbance ratio is also assess other molecule contamination such as phenol, a ratio between 2.0-2.2 is considered pure for RNA (Example, Fig. 2.9).

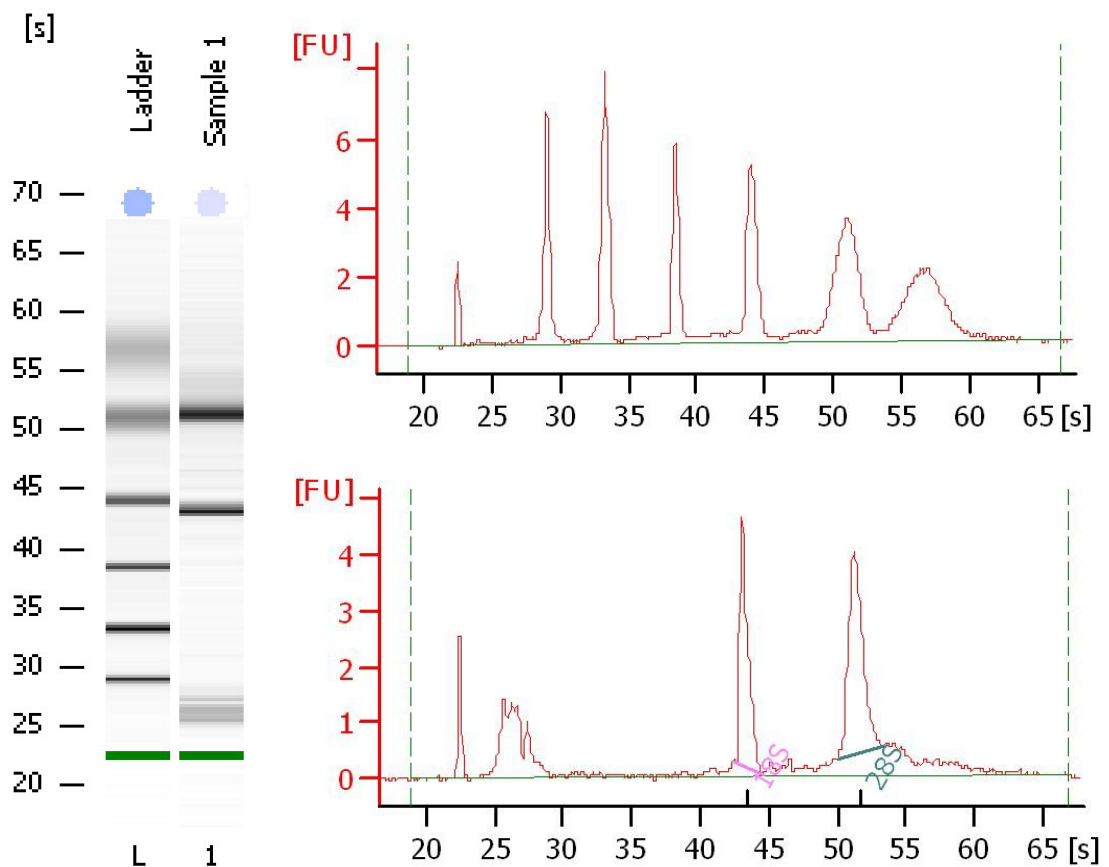


Figure 2.8 – Bioanalyser example report. An RNA 6000 Nano-ladder standard is run on every chip used as a reference for data analysis. The RNA 6000 Nano-ladder contains six RNA fragments ranging in size from 0.2 to 6 kb (0.2 kb, 0.5 kb, 1.0 kb, 2.0 kb, 4.0 kb, and 6.0 kb) at a total concentration of 150 ng/µl.

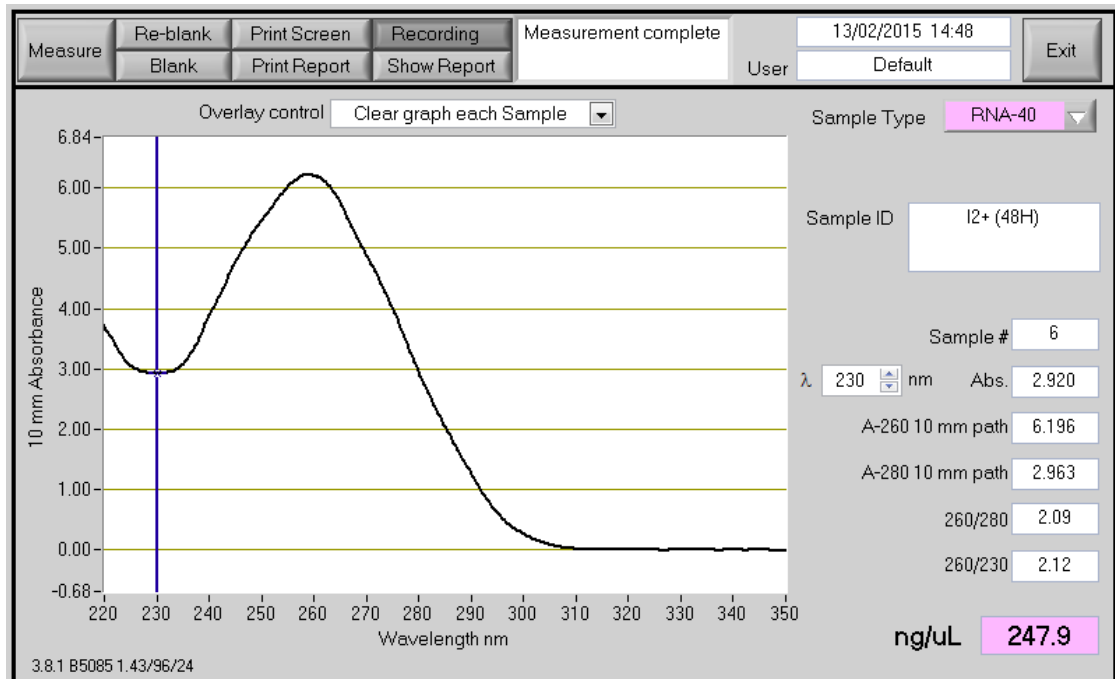


Figure 2.9 – Example RNA quantification using NanoDrop 2000 instrument. Absorbance spectrum is taken of the sample and a curve generated. Purity of the sample can be determined by the 260/280 ratio for (DNA) and 260/230 ratio (Protein) which in pure samples should be approximately 2. The concentration on RNA is also determined (ng/μl).

2.2.20 Quantitative polymerase chain reaction (qPCR) to determine mRNA of proteins involved in glutathione metabolism.

Complementary DNA was prepared from the extracted RNA samples by reverse transcription using high-capacity cDNA reverse transcription kit (Applied Biosystems). A master mix made up of reverse transcriptase (RTase), random primers, and nucleotide bases (dNTP) was prepared as shown in Table 2.5. The master mix contains all the elements required to converted the extracted RNA

into complementary DNA (cDNA), using the enzyme reverse transcriptase. Transcription is initiated by random primers and nucleotide triphosphates are present in excess to allow full transcription of RNA.

Component	Volume x1 (µl)
10x RT buffer	2
25x dNTP mix	0.8
10x RT random primers	2
MultiScribe RTase	1
H ₂ O	4.2
Total per reaction	10

Table 2.5 – cDNA master mix preparation. To reverse transcription buffer and water, nucleotide triphosphate (dNTP), random primers and reverse transcriptase (MultiScribe RTase) were added together to make a master mix used in the generation into CDNA from RNA.

To 10µl of the master mix, 10µl of 30 ng RNA sample was added (diluted using RNA free water), samples were gently mixed following a short centrifuge, then incubated for 10min at 25°C, this allows the primers to anneal to the RNA. The samples were transferred to on a Hybaid Omn-E thermal cycler where the samples were heated to 37°C for 120 min, allowing reverse transcription to take place, then 85°C for 5 min, which terminates the reaction. The sample was then cooled to 4°C, before being stored at -20°C till ready for qPCR analysis.

Following cDNA synthesis, cDNA samples were loaded to a 96-well plate along with a TaqMan universal master mix, prepared as seen in table 2.6. This master mix contained commercially available primers, TaqMan® gene expression assays. In this study 6 different gene expression assays were used (Table 2.7). These included primers for the genes glutathione reductase, glutathione synthetase, glutathione peroxidase 1 and glutamate-cysteine ligase, along with two control genes TATA-binding protein and beta-2 microglobin which were added separately to the cDNA samples.

The 96 well PCR plate was placed in the thermal cycler (BioRad CFX connect real-time system) using TaqMan protocol, which heated the sample to 95°C for 10 min, then proceeds to 50x cycles of 95°C for 15s and 60°C for 60s, CT values are generated. This cycling process allows amplification of DNA, heating the sample to 95°C separates the DNA standards, lowering the temperature to 60°C allows the primers to bind to the gene of interest and DNA polymerase to copy the DNA. Multiple rounds of heating and cooling allow amplification of the DNA, along with the fluorescence probe (TaqMan) which is incorporated into the DNA. Therefore as the number of gene of interest copies increase, so does the amount of fluorescence, which is measured by the instrument over time.

Component	Volume x1 (µl)
20x TaqMan® gene expression assay	1
2x TaqMan® gene expression master mix	10
cDNA template	2
RNase-free water	7
Total per reaction	20

Table 2.6 – Preparation of TaqMan master mix used in the quantitative PCR reaction.

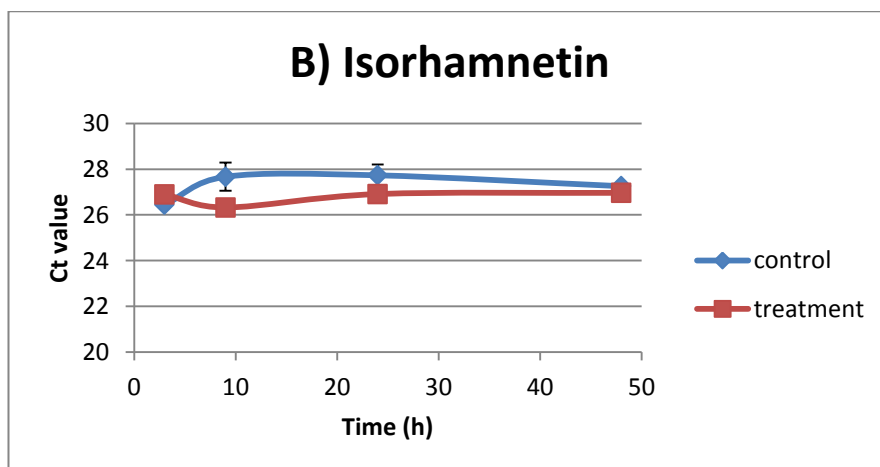
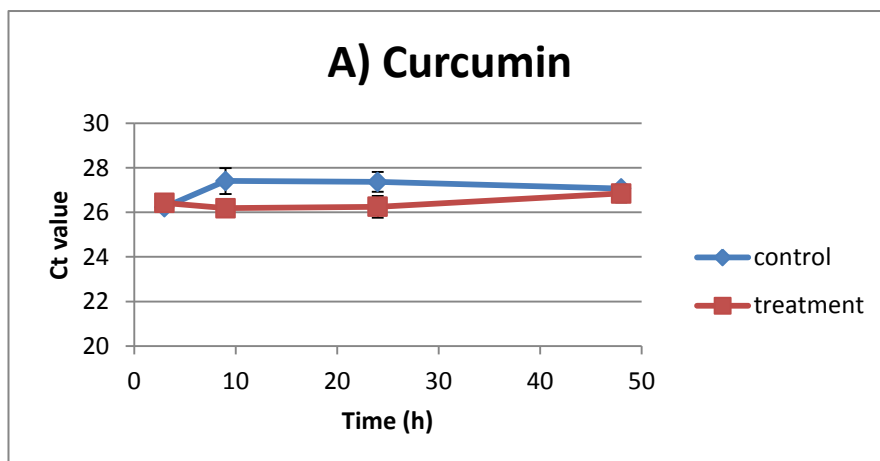
	Gene	20x TaqMan® Gene Expression Assays
GSR	Glutathione reductase	Hs00167317_m1
GCLC	Glutamate-cysteine ligase	Hs00155249_m1
GSS	Glutathione synthase	Hs00609286_m1
GPX1	Glutathione peroxidase 1	Hs00829989_gH
TBP	TATA binding protein	Hs00427620_m1
B2M	Beta-2-microglobulin	Hs00984230_m1

Table 2.7 – Gene primers used in the quantitative PCR reaction. All TaqMan genes were obtained from Life Technologies.

2.2.21 Analysis and normalisation of qPCR data.

Quantification used the comparative CT ($\Delta\Delta CT$) method for calculating relative quantitation of gene expression. Ct values generated by the treatment samples (polyphenol treatments) were compared with control samples (DMSO). Before the fold

change from DMSO was determined values were normalised to an appropriate endogenous housekeeping gene (see 2.2.22) which was TBP, which was evaluated at 3, 9, 24 and 48h. Figure 2.10 shows changes in CT values of TBP over time with the three different treatments and DMSO treated control. At times 3 and 48h there was almost identical readings for DMSO and polyphenols treatment with TBP, there was slight variation at the 9 and 24h time point but T-test showed these were not significant ($p < 0.05$). B2M was also tried in this experiment but TBP was more consistent over time in Jurkat cells and was therefore used as the normalising control for the qPCR experiments.



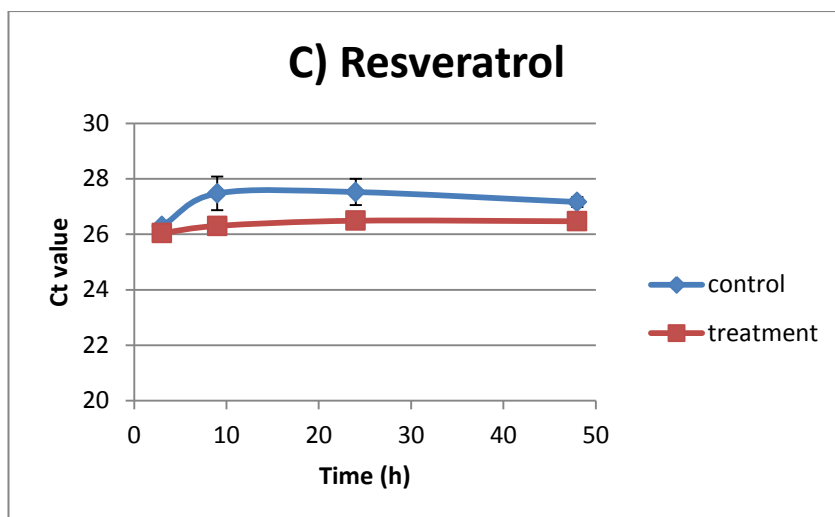


Figure 2.10 – Changes in CT values of normalising gene TBP over time (3, 9, 24 and 48h) following treatment with curcumin (A), isorhamnetin (B) and resveratrol (C) in Jurkat T lymphocytes compared with the DMSO treated control (n=3).

2.2.22 Evaluating suitable housekeeping genes for qPCR and immunoblotting analysis.

Proteomics identified a number of the regularly used normalising controls were modulated following treatment with the three polyphenols curcumin, isorhamnetin and resveratrol. Therefore a list of commonly used qPCR controls were obtained, and cross referenced with the proteomics data and literature searches to identify qPCR controls previously used in Jurkat cells (Table 2.8). The table shows in the first column proteins identified as being modulated by the polyphenols treatments used in this study, the second column then identifies any of the remaining proteins previously used as housekeeping genes in other

studies. These data was also useful when identifying housekeeping genes for western blot analysis. TBP (TATA binding protein) and B2M (β 2 microglobulin) were used as housekeeping genes for qPCR.

	Proteomics	Jurkat		Proteomics	Jurkat
18S		✓ ¹³⁵	MT-ATP6	✓	
ABL1			PES1		
ACTB	✓		PGK1	✓	
B2M		✓ ¹³⁵	POLR2A	✓	
CASC3			POP4		
CDKN1A			PP1A		
CDKN1B			PSMC4		
EIF2B1	✓		PUM1		
ELF1	✓		RPL30	✓	
GADD45A			RPL37A	✓	
GAPDH	✓		RPLPO	✓	
GUSB			RPS17	✓	
HMBS			TBP		✓ ¹³⁵
HPRT1	✓		TFRC	✓	
IP08			UBC		
MRPL19			YWHAZ	✓	

Table 2.8 – Determining suitable housekeeping genes for qPCR analysis. Commonly used qPCR controls (Applied Biosciences), cross referenced with proteins identified through proteomics to be significantly altered with polyphenol treatment and literature searches testing qPCR controls in Jurkat cells.

2.2.23 Statistical analysis.

2.2.23.1 Statistical analysis of cytokine data. Values are most commonly represented as mean \pm standard error of the mean (SEM), although percentage change and fold change are occasionally presented.

Comparisons between the means of the samples were done using SPSS (IBM SPSS statistics 20, New York, USA), and a Student's two-tailed independent samples t-test's were used to identify significant differences between the means. During the polyphenol cytokine screening process, Jurkat T cells were treated with numerous polyphenols and cytokine release measured. With these multiple measurements a one-way ANOVA was used with Dunnett's post-hoc test comparing treatment data to control DMSO treated cell data. Significance was set at $p < 0.05$.

2.2.23.2 Statistical analysis of LC-MS data. Progenesis software was used to determine the significance of the changes to protein expression of the three treatments curcumin, isorhamnetin and resveratrol compared with DMSO treated control; this was done using an ANOVA, with a p-value set to ≤ 0.05 . Also due to proteomics identifying large quantities of proteins being modulated by the treatments, the q-value was also expressed. The q-value is a false discovery rate adjusted p-value. Proteins that were identified to have significant changes in expression were investigated further using a number of different programs (see table 2.9). UniProt was used to determine protein function, GeneCards to convert protein accession number to gene ID, DAVID bioinformatics and Reactome was used to link individual

proteins into a network. Ingenuity uses data from literature to connect proteins in the data set, placing them in signalling pathways and showing the effects when certain compounds are added to the system.

Table 2.9 – Programs used to identify function, pathways, clustering of the proteins identified using proteomics.

Program	Website	Date accessed
UniProt	http://www.uniprot.org/	6/01/14
The GeneCards Human	http://www.genecards.org/	6/01/14
DAVID Bioinformatics Resources 6.7	http://david.abcc.ncifcrf.gov/	6/01/14
STRING 9.05	http://string-db.org/	6/01/14
PANTHER Classification System	http://www.pantherdb.org/	6/01/14
Reactome	http://www.reactome.org/	10/11/14
Ingenuity (Pathway analysis)	http://www.ingenuity.com/	10/02/15

CHAPTER 3

**INVESTIGATION OF A (POLY)PHENOL PANEL TO
IDENTIFY MOLECULES THAT MODULATE
INFLAMMATION IN JURKAT T LYMPHOCYTE CELLS.**

3.1 INTRODUCTION

3.1.1 Cytokine production and regulation in T lymphocytes.

Cytokines are inflammatory molecules secreted by a variety of cell types, these small proteins facilitating signalling both between neighbouring cells and acting on the originating cell. The main function of cytokines is to coordinate the immune response, with pro-inflammatory and anti-inflammatory cytokines mediating these inflammatory mechanisms. Responses vary between the cytokine being released and its target cell. In T-lymphocytes, cytokines are essential for activation, differentiation, and proliferation. However, T-lymphocytes are not the only source of cytokine release; other immune cells including macrophages and B cells¹³⁶ also produce cytokines along with endothelial cells, muscle cells, and fibroblasts^{137,138,139}. Cytokines may behave differently depending on the cell type they are produced in or acting upon.

3.1.2 Effects of T lymphocyte dysregulation and ageing.

T lymphocytes are one of the major producers of cytokines, prompting the focus of this study to use these cells as a model to observe changes in inflammatory markers. During the ageing process the number of T-lymphocytes declines, along with this decline an impaired function and dysregulation is also

observed¹⁴⁰. Dysfunction in the immune system with age is described as 'immunesenescence'¹⁴¹.

This normally tightly regulated system becomes dysregulated with age and increases in baseline pro-inflammatory cytokines are observed. Pro-inflammatory cytokines are produced in a number of responses such as an infection, recognising foreign pathogens, and damage to the cell, these responses are essential to protect the cell/body from damage. This process is highly regulated with pro-inflammatory cytokine induction and feedback mechanisms to quench this induction and restore the resting state of the cells, important to maintain homeostasis. However, during ageing disruptions to this feedback mechanism are observed with over and under production of particular cytokines, affecting the cells ability to respond appropriately. Elevated levels of cytokines such as interleukin 6 (IL6), interleukin 8 (IL8), MCP-1, TNF α , and C - reactive protein (CRP) have been documented in the serum of elderly populations¹⁴².

3.1.3 Interleukin 2 (IL2), interleukin 8 (IL8) and TNF α changes with age.

IL2 is an essential cytokine for T lymphocyte activation and differentiation, during ageing IL2 is reduced due to the decline on the number of T cells. However this decline is only observed in the very elderly >90 years, in those aged between 65-85 the levels of IL2 remained the same as those in the young category aged between 25-34 years, in healthy patients¹⁴³. Increases in pro-inflammatory cytokine such as TNF α have been observed in the plasma of both healthy elderly

patients and those with age-related conditions such as type-2 diabetes¹⁴⁴. IL8 is another pro-inflammatory cytokine observed to be elevated in a number of age-related diseases, such as Alzheimer's disease¹⁴⁵. However, levels in healthy ageing have been shown to vary between the sexes and *in vitro* respond differently when an inflammatory stimulus is added. Clark and Peterson in 1994 observed difference in levels of IL8 between elderly male and female healthy subjects. Women had similar levels to the young control groups, with levels of 57.8 ± 2.1 ng/ml in elderly women compared with 66.4 ± 5 ng/ml in the young control group. Men had significantly lower levels with 8.8 ± 2.1 ng/ml. However, even though they had lower base-line levels, upon stimulation with LPS, they had an 8-fold induction which was significantly increased when compared with stimulated control, women showed no change with stimulation¹⁴⁶.

3.1.4 Dietary (poly)phenols and benefits to health and age.

Polyphenols are naturally occurring compounds which are found in a wide variety of sources including fruits, vegetables, spices, and beverages. These compounds are believed to have benefits to health such as lowering levels of free radicals, inducing protective antioxidant signaling pathways and reducing blood pressure¹⁴⁷. Some of these compounds are already being trialed in the treatment for certain diseases, such as curcumin in patients with rheumatoid arthritis using a daily dose of 500mg capsule¹⁴⁸.

Polyphenols structures are complex and varied, once polyphenols enter the body, they are metabolised either in the stomach or intestines. The complex polyphenols, which come directly from the food source, are modified or broken down into smaller phenolic acids. Some of the more complex polyphenols will make it to the blood stream in low concentrations, along with these the metabolites and phenolic acids will also be present in a higher concentration. In this study a variety of compounds was chosen to include in both a number of polyphenols and phenolic acids (both termed (poly)phenols). Two different concentrations were used, a low dose of 1 μ M which was considered more physiologically relevant and a higher dose of 30 μ M, to evaluate changes to markers of inflammations with these (poly)phenols . This data was also published as part of a paper 'Identification of (poly)phenol treatments that modulate the release of pro-inflammatory cytokines by human lymphocytes' co-authored between myself and Christopher Ford¹⁴⁹.

3.2 AIMS.

The aim of this study was to screen 29 different dietary (poly)phenols for their anti-inflammatory effects in Jurkat T-lymphocytes. This panel of compounds included complex polyphenols, with multiple functional groups, along with small phenolic acids which are metabolites of the polyphenols. The aim was to determine what effect these (poly)phenols would have on the cell viability in this

cell type and determine a suitable treatment dose. This immune cell model was used to evaluate the anti-inflammatory effects these (poly)phenols have on these cells by measuring cytokine release following 48 h treatment with the compounds.

3.3 RESULTS.

3.3.1 Evaluating cytokine detection in unstimulated and PMA/PHA stimulated cells using multiplex analysis.

Jurkat T-lymphocytes were treated with PMA/PHA, a protein kinase C activator and a plant-derived lymphocyte mitogen for 24 h to induce an inflammatory response and cytokine release. Assessments were made to determine the cell viability with DMSO and PMA/PHA, figure 3.1 shows an ~ 45% reduction in cell viability with PMA/PHA. A panel of 13 cytokines were chosen as known cytokines secreted by Jurkat T-lymphocytes and multiplex analysis platform was used to measure the induction of cytokine release following stimulation. The PMA/PHA stimulated cells showed a large increase in the release in a number of cytokines compared with untreated cell and DMSO treated control treatments (Table 3.1). However, there was a large proportion of the cytokines that were undetectable in the untreated cells. There was an induction of cytokine release with cytokines IL2 and IL8. IL2 was 14 ± 1 pg/ml in DMSO treated cells which increased to 6970 ± 304 pg/ml when stimulated with PMA/PHA. IL8 was also expressed at relatively low levels with DMSO treated cells, 34 ± 2 pg/ml,

following induction with PMA/PHA this increased to 1613 ± 93 pg/ml. There was also an induction with TNF α in PMA/PHA cells reaching levels of 260 ± 12 pg/ml, prior to stimulation TNF α was undetectable in the DMSO control cells. Therefore these three cytokines, IL2, IL8, and TNF α were chosen for further experiments due to their high sensitivity to induction by PMA/PHA treatment and the relatively well defined roles of each of these cytokines as pro-inflammatory physiological factors.

Cytokine measured in Jurkat 24 h conditioned medium	Untreated control (pg/ml)	DMSO vehicle control (pg/ml)	24h PMA/PHA stimulated (pg/ml)
Eotaxin-1	ND	2.85 ± 1.47	0.48 ± 0.56
GM-CSF	ND	ND	5.81 ± 0.39*
IFN γ	ND	ND	ND
IL1 β	ND	ND	ND
IL2	13.45 ± 1.39	14.40 ± 1.41	6969.69 ± 303.95*
IL4	21.55 ± 0.35	ND	1.86 ± 5.67
IL6	ND	ND	ND
IL7	0.3 ± 0.06	0.804 ± 0.66	3.52 ± 0.66
IL8	35.25 ± 2.88	34.22 ± 2.32	1612.68 ± 92.71*
IL12p70	ND	ND	ND
IL13	ND	ND	7.68 ± 1.52*
MCP-1	ND	ND	ND
TNF α	ND	ND	259.55 ± 12.36*

Table 3.1 - Cytokines induced by PMA/PHA treatment of Jurkat CD4⁺ T-lymphocytes. Data expressed as means \pm SEM. ND indicates no detection. Abbreviations: Granulocyte macrophage-colony stimulating factor (GM-CSF), interleukin (IL), interferon (IFN), monocyte chemoattractant protein (MCP). Data expressed as mean \pm SEM, * n=4, $p < 0.05$ ¹⁴⁹.

3.3.2 Modification to cytokine release and cell proliferation by Jurkat T-lymphocytes.

Cytokine release was measured following 48h treatment with the chosen phenolic compounds. There were 29 compounds in total, these consisted of small metabolites called phenolic acids, structurally they contain one phenolic ring (C_6H_5OH) and the panel also included larger more complex polyphenols, containing multiple phenol structures and functional groups (full compound details can be found in Appendix 1). A colorimetric assay (MTS) was used to determine the cell viability, along with a multiplex assay to measure changes in cytokine release of interleukin 2 (IL2), interleukin 8 (IL8) and tumour necrosis factor alpha ($TNF\alpha$). The data has been expressed as a percentage change from DMSO treated control.

3.3.3 Assessment of cell viability following (poly)phenol treatments.

Jurkat cells were treated for 48h with the chosen (poly)phenols. Figure 3.2, shows the effect treatments had on cell viability, at both 1 and 30 μ M concentrations of (poly)phenols. Only a couple of the treatments reduced the number of Jurkat cells and in all the cases that had reduced viability, this was with the 30 μ M concentration suggesting toxicity with the higher dose. The largest decrease in cell number was observed with 30 μ M curcumin decreased cell

number by $45\% \pm 3\%$, followed by $30\mu\text{M}$ catechol with $43\% \pm 5\%$, compared with DMSO treated control. However a number of the treatments did cause an increase in cell viability, the greatest increases was observed with $1\mu\text{M}$ kuromanin increasing cell number by $40\% \pm 8\%$ compared with DMSO treated control.

The effect PMA/PHA stimulation had on cell viability was also investigated. The Jurkat cells were treated with the (poly)phenol compounds for 48h the same as before but with the addition of PMA/PHA at the 24 h time point. PMA is a phorbol ester and PHA a lectin which work together to activate T lymphocytes, through the protein kinase c (PKC) pathway, stimulating cytokine release particularly interleukin 2¹⁵⁰. This would allow investigation into whether or not the (poly)phenols were having a protective effect, when the cells were stimulated, mimicking an immune response.

Stimulating cytokine release with PMA/PHA resulted in a decrease in cell number $\sim 45\%$ reduction compared with DMSO treated cells (see fig. 3.1). In stimulated cells there was much more cell death with the polyphenol compounds than observed with unstimulated cells (Figure 3.2 and 3.5); again this was mainly observed with the higher dosage. $30\mu\text{M}$ catechol ($75\% \pm 3\%$), $30\mu\text{M}$ phloroglucinol ($70\% \pm 2\%$), 1 and $30\mu\text{M}$ 4'-hydroxybenzoic acid ($36\% \pm 11$, $68 \pm 2\%$), $30\mu\text{M}$ protocatechuic acid ($56\% \pm 4$), and 1 and $30\mu\text{M}$ 3-O-methylquercetin ($68\% \pm 7\%$, $49\% \pm 8\%$), these compounds had the greatest decrease in cell viability. Only a few compounds had an increase in cell number when combined

with the stimulation, this was 30 μ M punicalagin and 30 μ M feruloylglycine. Feruloylglycine was the only (poly)phenol that had an increase in cell number in both the unstimulated and stimulated cells.

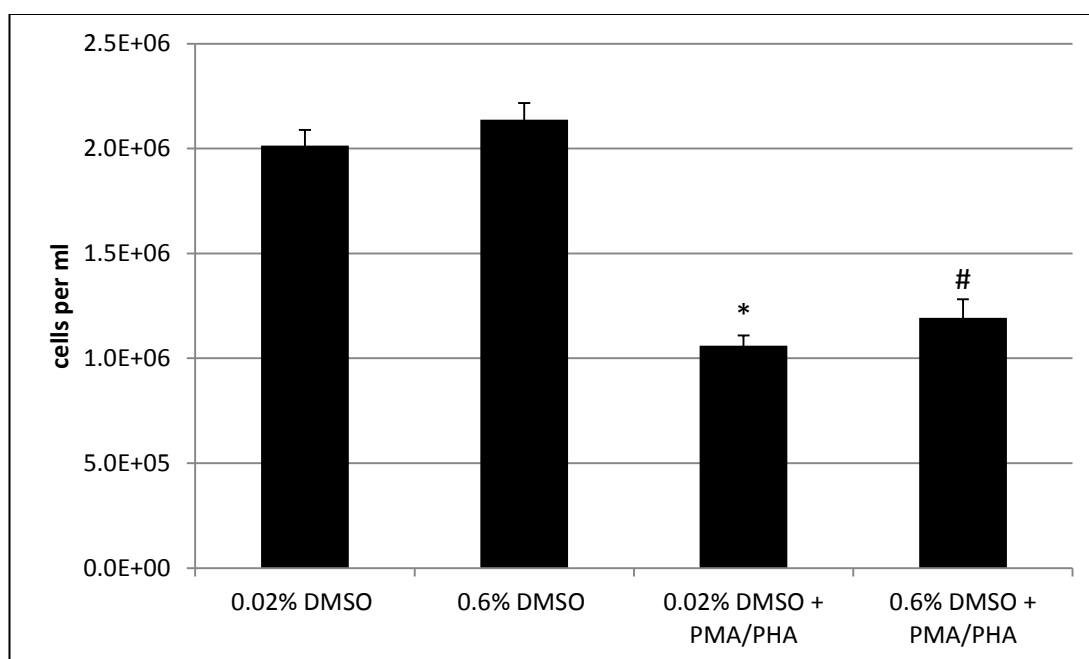


Figure 3.1 - Cell viability following the addition of PMA/PHA stimulation by Jurkat T-lymphocytes. Jurkat cell number following 48h incubation with the two concentrations of DMSO used, with and with PMA/PHA stimulation at the 24h time point. 0.02% is equivalent to 1 μ M (poly)phenol and 0.6% is equivalent to 30 μ M (poly)phenol. The data is expressed as mean \pm SEM (n=6). * Shows significance $p<0.05$ PMA/PHA compared with equivalent DMSO dose 0.02%, # significance $p<0.05$ PMA/PHA compared with equivalent DMSO dose 0.6%.

3.3.4 Cytokine release by Jurkat T lymphocyte cells following (poly)phenol treatment.

Following the 48h treatment with the 29 different polyphenol compounds, cytokines secreted by the Jurkat cells into the culture media were measured using

a multiplex assay. From the pre-screening panel conducted, 3 cytokines could be measured in the Jurkat samples (table 3.1), interleukin 2 (IL2) and interleukin 8 (IL8) in unstimulated cells and in the stimulated cells tumour necrosis factor alpha (TNF α) could be measured. Data is presented as a percentage change from DMSO treated control, raw data can be obtained in appendix 2, fig 8.5 - 8.8.

3.3.5 Decreases in cytokine release by unstimulated cells.

A large proportion of the treatments had an anti-inflammatory effect lowering cytokine release of both IL2 and IL8 in the Jurkat T lymphocytes, following the 48h treatments. The greatest decreases in IL2 were observed with 30 μ M curcumin (99% \pm 2%), resveratrol (70% \pm 6%), and isorhamnetin (61% \pm 5%) figure 3.3, which were significantly decreased compared with DMSO treated control. These decreases were also observed for IL8 with 30 μ M isorhamnetin, lowering IL8 by 66 \pm 4%, 1 μ M EGCG, callisephin chloride, and punicalagin also significantly lowered IL8 in the Jurkat cells compared with DMSO treated control (Fig. 3.4). The lower dose of 1 μ M polyphenols, also had significant reductions in cytokine release. The greatest effects in lowering cytokine release were observed with 1 μ M isoferuloylglycine (68% \pm 2%) and ferulic acid (63% \pm 3%) for interleukin 8. Some of these anti-inflammatory effects were shown to be dose dependent for

example 1 μ M resveratrol lowered IL2 by 42% \pm 7% and IL8 by 32% \pm 6%, and 30 μ M resveratrol lowered IL2 70% \pm 6% and IL8 by 55% \pm 5%.

3.3.6 Increases in cytokine release by unstimulated cells.

For the majority of the treatments a decrease in cytokine release was observed. The most dramatic increase in cytokine release was observed with pyrogallol, a metabolite of green tea. Both 1 and 30 μ M pyrogallol significantly increased cytokine release of IL8 by 334 \pm 50% and 1722 \pm 74% (respectively) compared with the DMSO treated control. The increases were so large data had to be represented in a separate graph, figure 3.5A/B.

3.3.7 Decreases in cytokine release by stimulated cells.

The Jurkat cells were incubated with the (poly)phenols for 48h, with PMA/PHA stimulation at the 24h time-point, this was to induce cytokine release. With the PMA/PHA stimulation, the increase in cytokine release allowed the measurement of TNF α . With the addition of the stimulation it was predicted that the (poly)phenols would have a protective effect against the induction of cytokine release. There were three main (poly)phenols that stood out as particularly good

at lowering cytokine release in the stimulated cells. 30 μ M curcumin lowered IL2 by 98% \pm 0.2%, IL8 by 62% \pm 4%, and TNF α 98% \pm 2%, 30 μ M quercetin lowered IL2 by 84% \pm 3% and TNF α by 89% \pm 3%, and 3-O-methylquercetin lowered IL2 by 84% \pm 2% and TNF α by 92% \pm 1% (Figures 3.7, 3.8, 3.9)

3.3.8 Increases in cytokine release by stimulated cells.

There were more increases in cytokine release with the (poly)phenols in the PMA/PHA stimulated cells than with the unstimulated cells. The largest increase in cytokine release was observed with 1 μ M 3-O-methylquercetin, a metabolite of quercetin, increased IL2 by 459 \pm 38% and IL8 by 160 \pm 7% (Fig. 3.7 and 3.8). Others that increased IL2 were 30 μ M 4'-hydroxybenzoic acid (193 \pm 11%) and 1 μ M feruloylglycine (169 \pm 31%) (Fig. 3.7). 30 μ M Catechol and phloroglucinol increased IL8 release by 254% \pm 11% and 219% \pm 33% (respectively) (Fig. 3.8). Both 1 and 30 μ M punicalagin increased TNF α release by 239% \pm 14% and 508% \pm 18% (respectively), along with 30 μ M phloroglucinol (264% \pm 9%) and 4'-hydroxybenzoic acid (2895 \pm 13%) (Fig. 3.9).

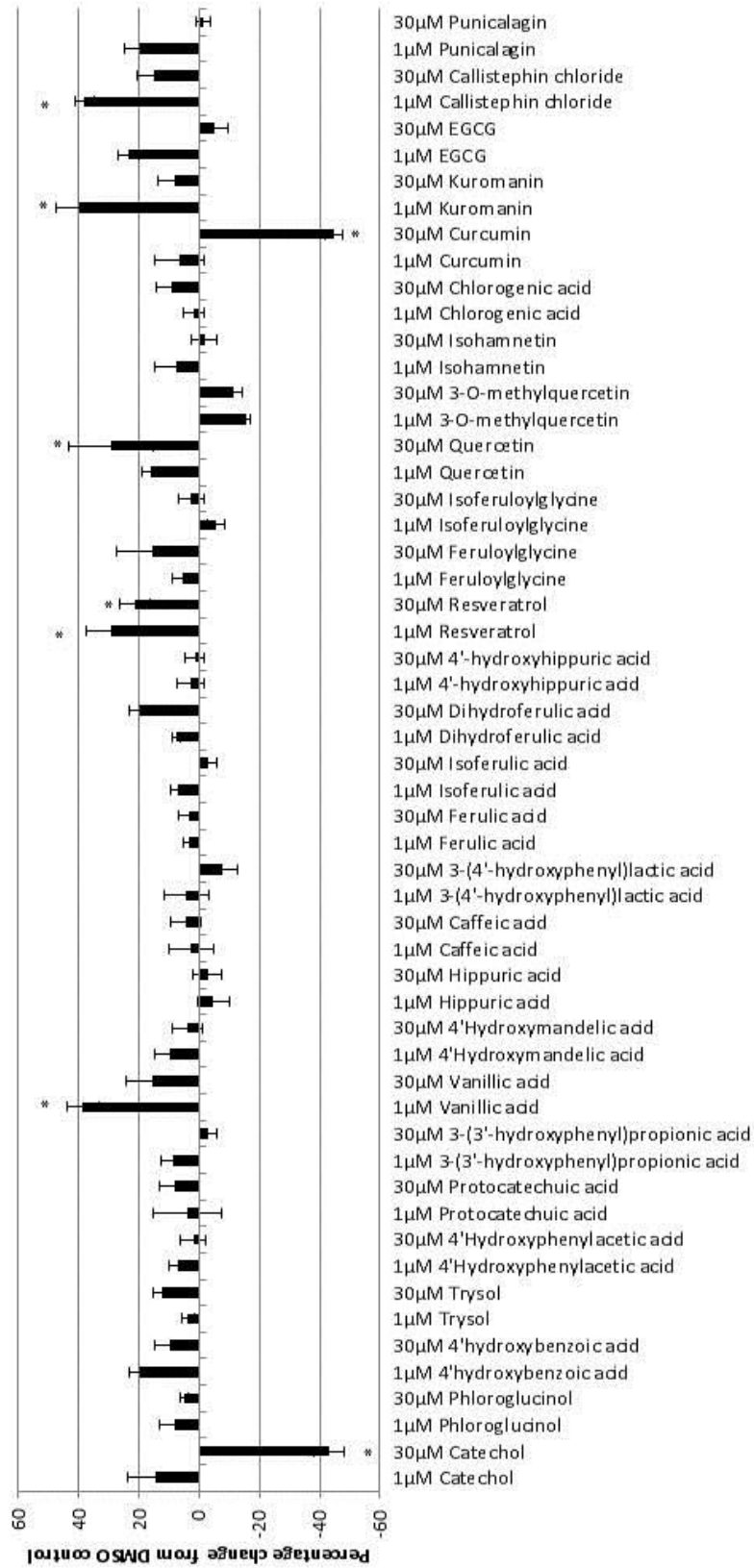


Figure 3.2 – Changes in cell number with 1 & 30 μM (poly)phenols in unstimulated cells, expressed as percentage change from DMSO vehicle control (0% line). (Poly)phenols arranged in molecular weight order starting from the far left (phenolic acids) to the right (polyphenols). Data expressed as mean ± SEM (n=6), One-way ANOVA with Dunnett's post hoc test * p < 0.05 (statistics performed in sets of 4 treatments, see 2.2.9).

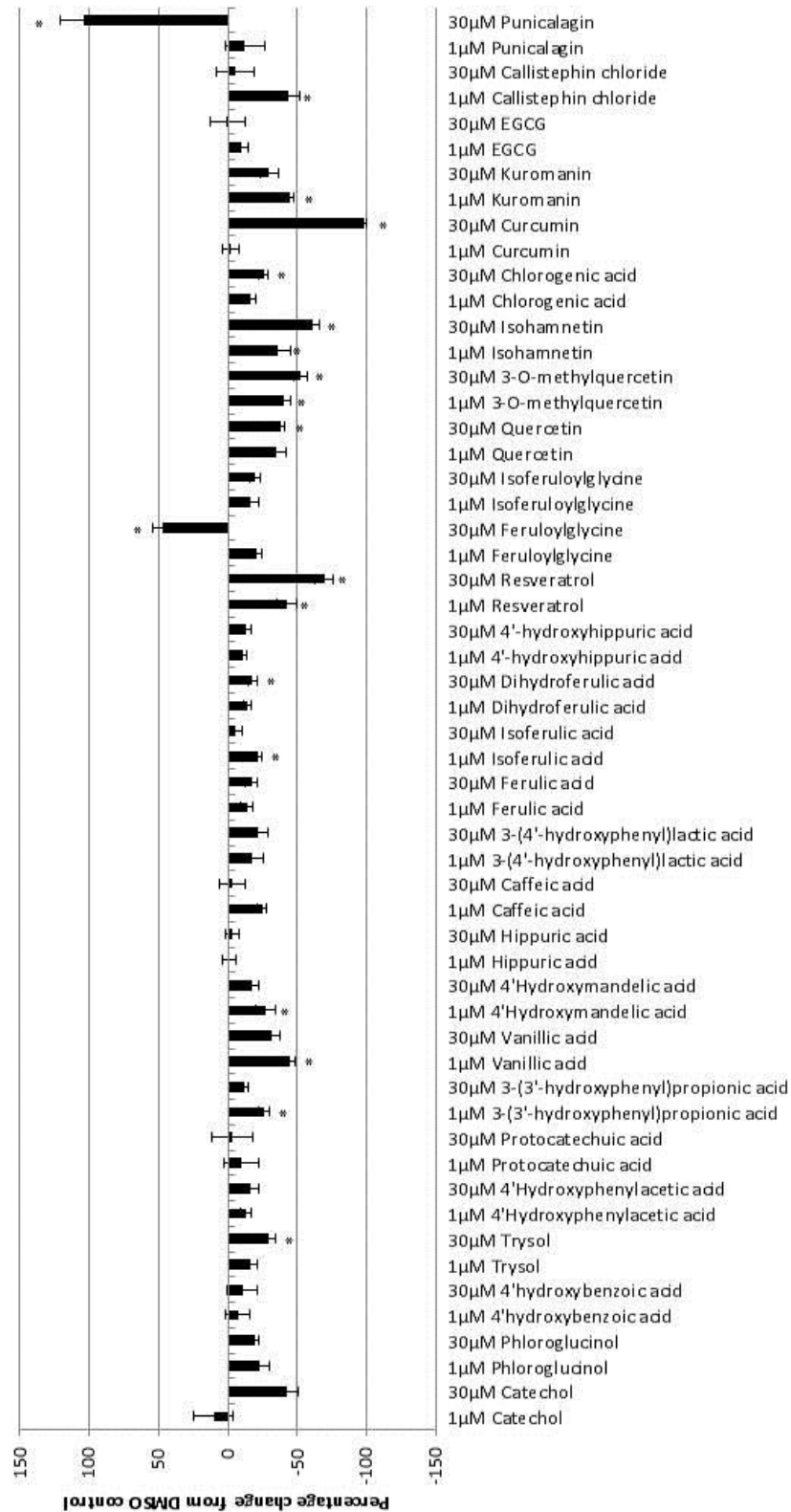


Figure 3.3 – Changes in interleukin 2 (IL2) release with 1 and 30μM (poly)phenols in unstimulated cells, expressed as percentage change from DMSO vehicle control. (Poly)phenols arranged in molecular weight order starting from the far left (phenolic acids) to the right (polyphenols). Data expressed as mean ± SEM (n=6), One-way ANOVA with Dunnett's post hoc test * $p < 0.05$ (statistics performed in sets of 4 treatments, see 2.2.9).

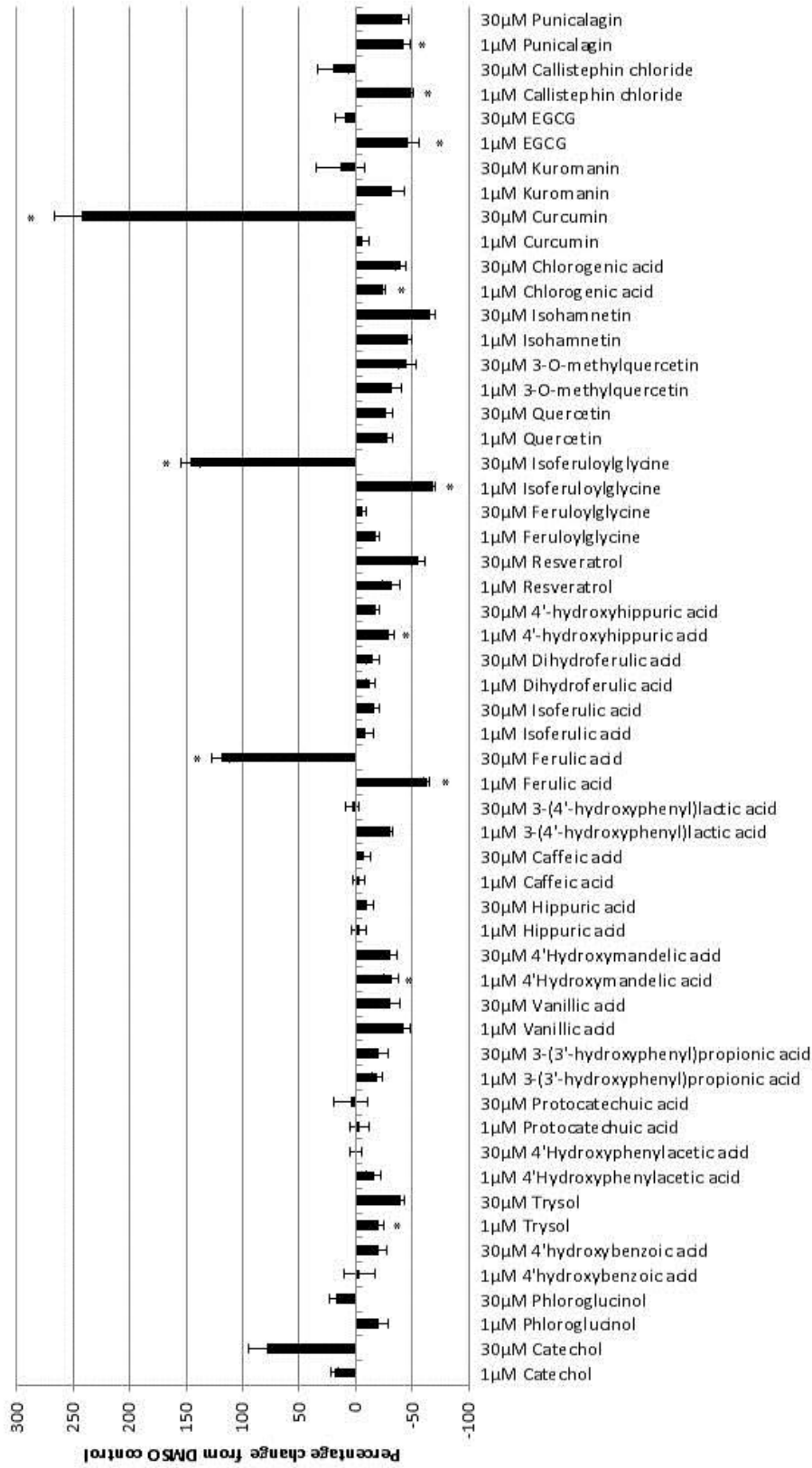


Figure 3.4 – Changes in interleukin 8 (IL8) release with 1 and 30μM (poly)phenols in unstimulated cells, expressed as percentage change from DMSO vehicle control. (Poly)phenols arranged in molecular weight order starting from the far left (phenolic acids) to the right (polyphenols). Data expressed as mean ± SEM (n=6), One-way ANOVA with Dunnett's post hoc test * $p < 0.05$ (statistics performed in sets of 4 treatments, see 2.2.9).

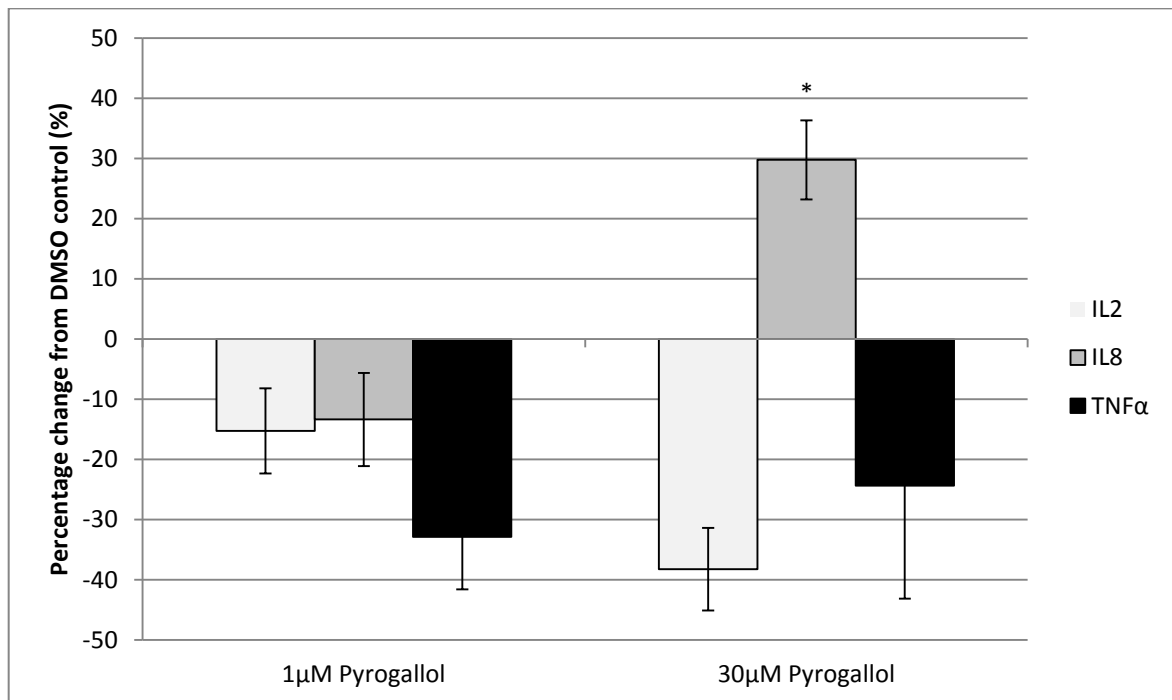
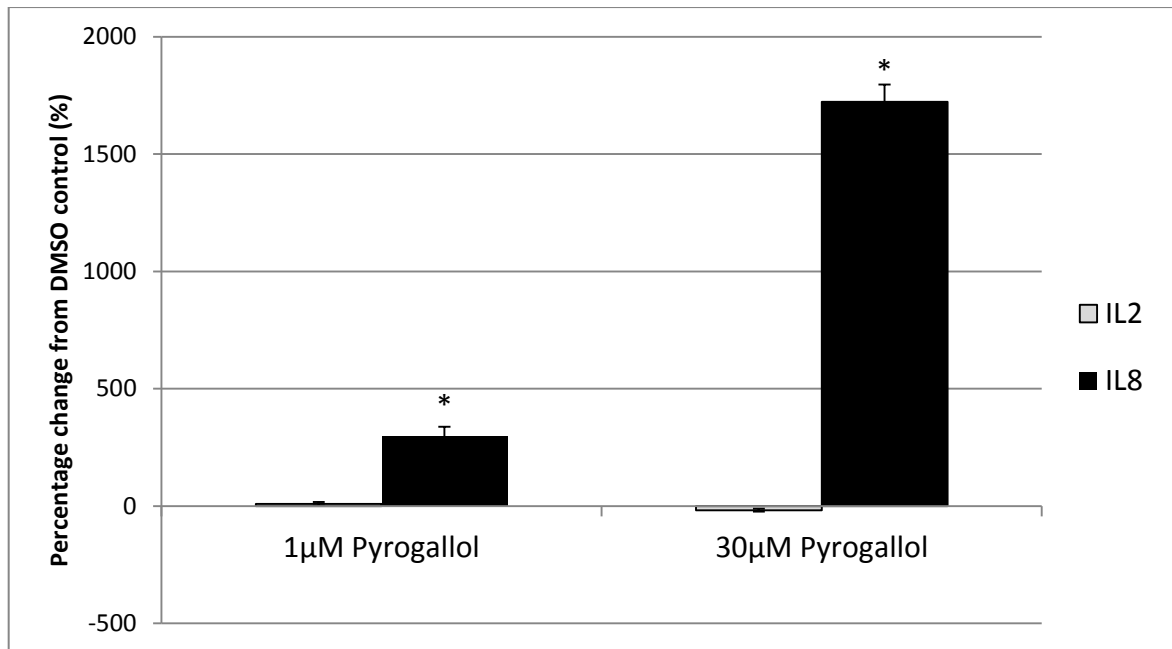


Figure 3.5 – A) Changes in interleukin 2 (IL2) and interleukin 8 (IL8) release with 1 and 30µM pyrogallol in unstimulated cells, expressed as percentage change from DMSO vehicle control. B) Changes in interleukin 2 (IL2), interleukin 8 (IL8) and tumour necrosis factor alpha (TNFα) release with 1 and 30µM pyrogallol in stimulated cells, expressed as percentage change from DMSO vehicle control. Data expressed as mean ± SEM (n=6) , One-way ANOVA with Dunnett’s *post hoc* test * $p < 0.05$ (statistics performed in sets of 4 treatments, see 2.2.9).

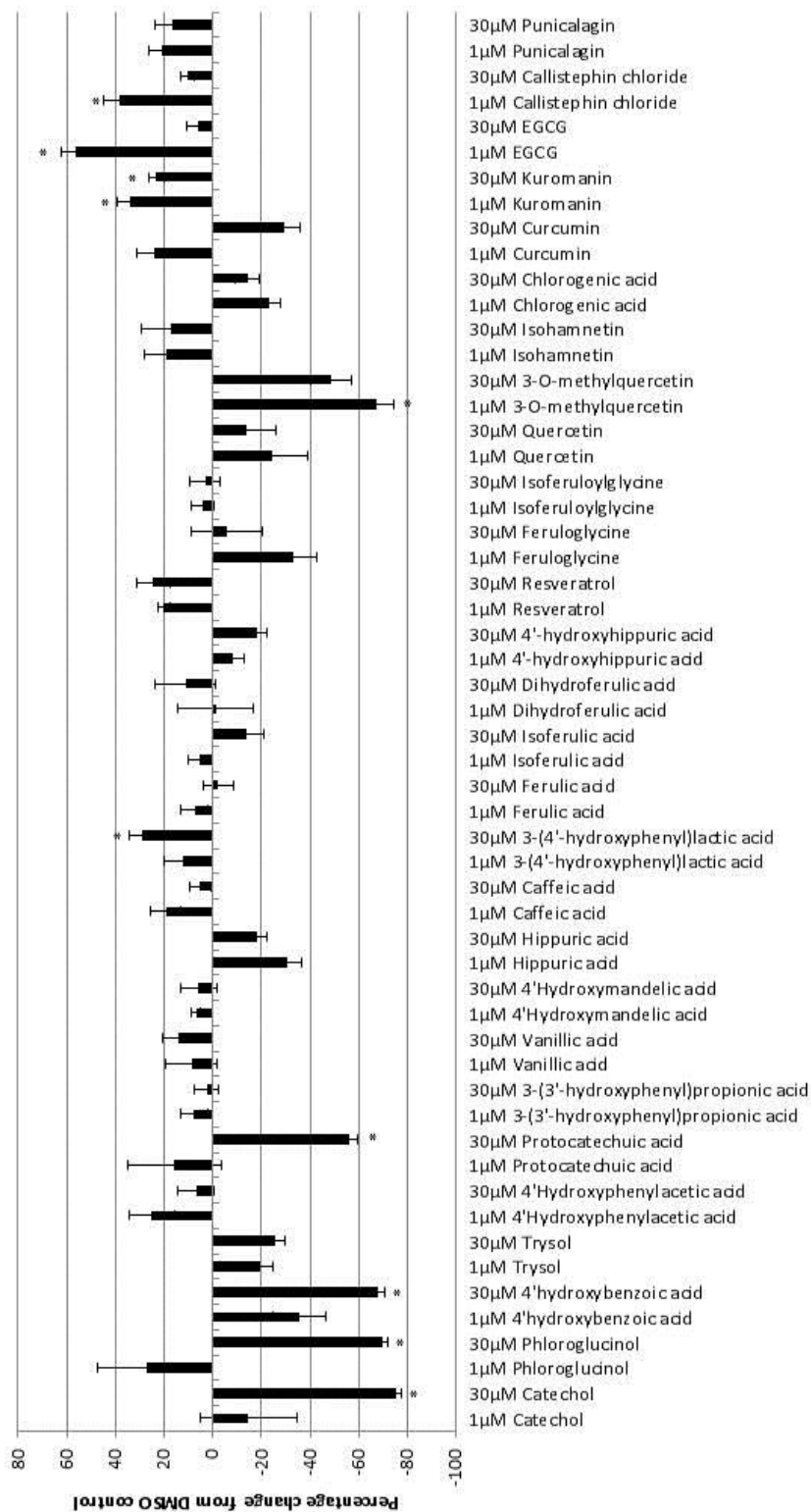


Figure 3.6 – Changes in cell number with 1 and 30 μM (poly)phenols in stimulated cells, expressed as percentage change from DMSO vehicle control. (Poly)phenols arranged in molecular weight order starting from the far left (phenolic acids) to the right (polyphenols). Data expressed as mean ± SEM (n=6), One-way ANOVA with Dunnett's post hoc test * p < 0.05 (statistics performed in sets of 4 treatments, see 2.2.9).

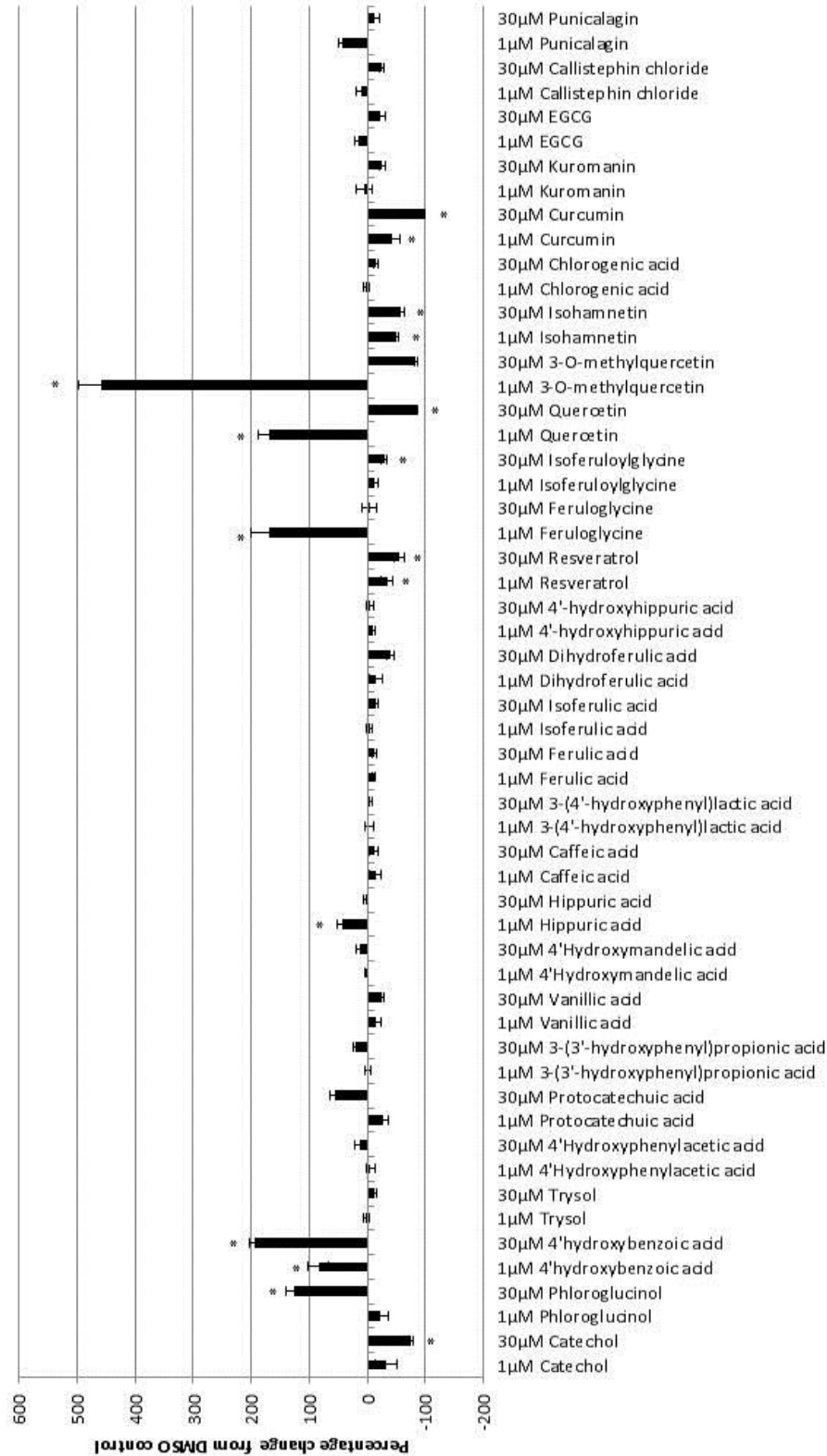


Figure 3.7 – Changes in interleukin 2 (IL2) release with 1 and 30µM (poly)phenols in stimulated cells, expressed as percentage change from DMSO vehicle control. (Poly)phenols arranged in molecular weight order starting from the far left (phenolic acids) to the right (polyphenols). Data expressed as mean ± SEM (n=6), One-way ANOVA with Dunnett's post hoc test * p < 0.05 (statistics performed in sets of 4 treatments, see 2.2.9).

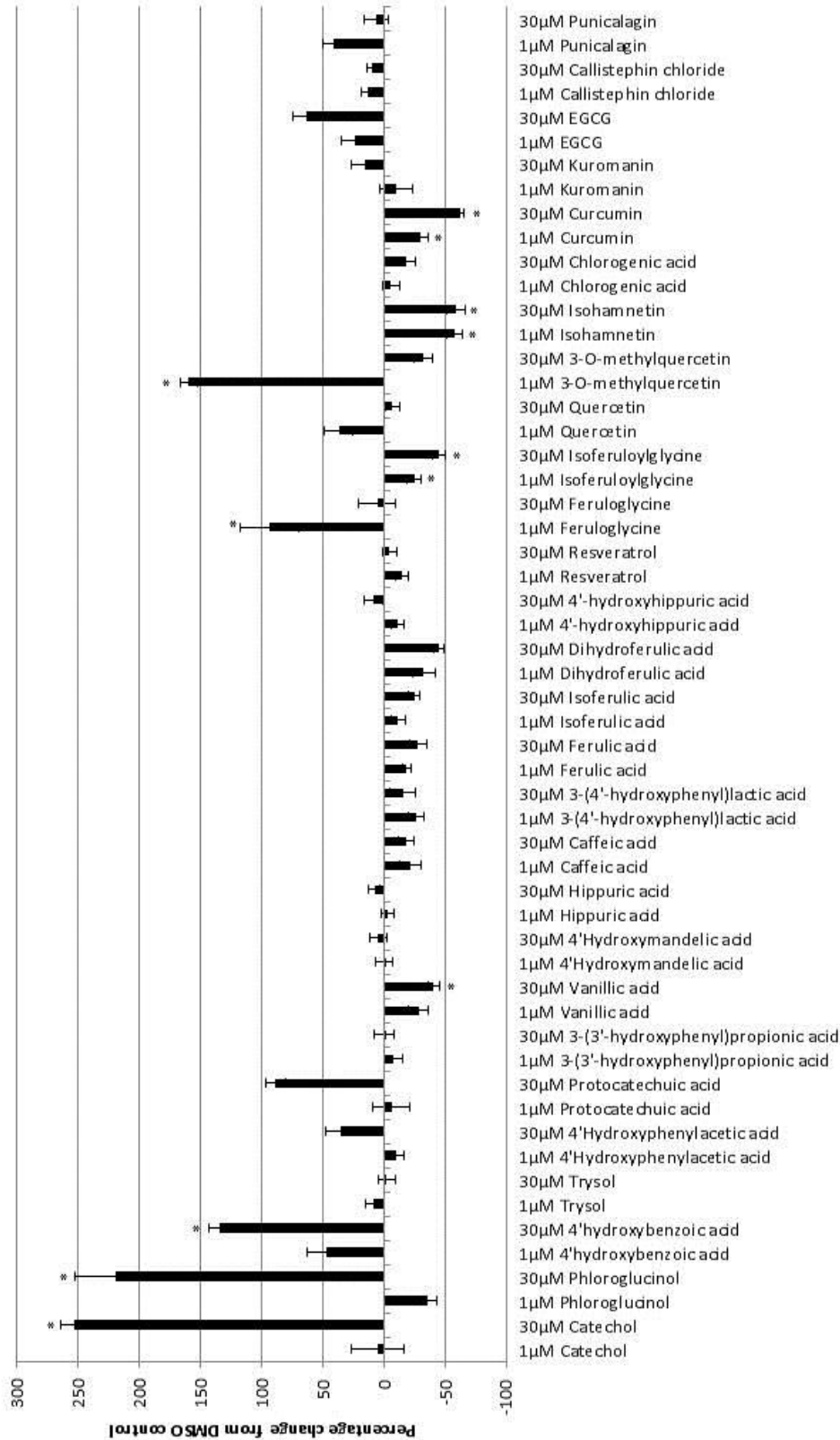


Figure 3.8 – Changes in interleukin 8 (IL8) release with 1 and 30µM (poly)phenols in stimulated cells, expressed as percentage change from DMSO vehicle control. (Poly)phenols arranged in molecular weight order starting from the far left (phenolic acids) to the right (polyphenols). Data expressed as mean ± SEM (n=6), One-way ANOVA with Dunnett's post hoc test. * $p < 0.05$ (statistics performed in sets of 4 treatments, see 2.2.9).

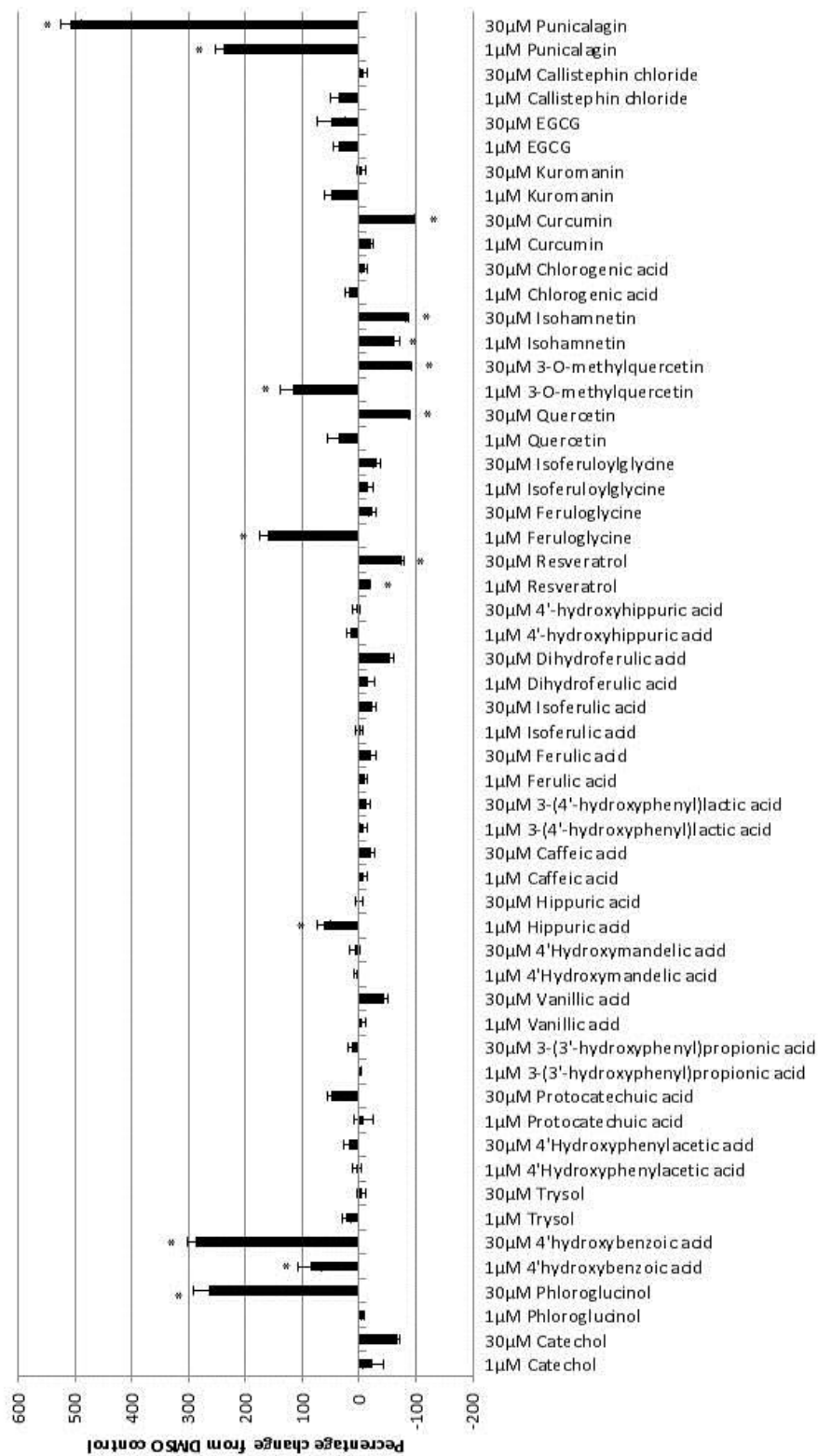


Figure 3.9 – Changes in tumour necrosis factor alpha (TNFα) release with 1 and 30µM (poly)phenols in stimulated cells, expressed as percentage change from DMSO vehicle control. (Poly)phenols arranged in molecular weight order starting from the far left (phenolic acids) to the right (polyphenols). Data expressed as mean ± SEM (n=6) , One-way ANOVA with Dunnett's post hoc test * p < 0.05 (statistics performed in sets of 4 treatments, see 2.2.9).

3.3.9 The effect of (poly)phenol mixtures on cytokine release.

As part of a balanced diet these dietary (poly)phenols would be found in combination with one another. For a more physiological representation of how these compounds are acting, mixtures of four different (poly)phenols were put together and added to the Jurkat cells for 48 h. These compounds are arranged in molecular weight order, with phenolic acids on the left, polyphenols on the right. Figure 10A, shows changes to IL2 release with individual and mixed compounds. In 4/6 cases the mixtures of compounds showed greater anti-inflammatory effects than the compound individually, a greater effect occurred when these compounds were mixed together. In particular a mixture of EGCG, punicalagin, kuromanin, and callistephin chloride had the greatest anti-inflammatory effect ~60% reduction of IL2 compared with DMSO treated control.

In figure 3.10B, 2 out of the 6 mixture combinations had greater anti-inflammatory than the individual compounds for IL8. This greatest effect was observed with a mixture of dihydroferulic acid, ferulic acid, isoferulic acid and isoferulylglycine with a $43\% \pm 5\%$ reduction in IL8.

The (poly)phenol mixes were made up to a total polyphenol content of $1\mu\text{M}$, therefore each individual compound was $0.25\mu\text{M}$. Using the data already produced, individual comparison were made using data from the $1\mu\text{M}$ treatment, ideally for a true representation of the synergistic effect a treatment of $0.25\mu\text{M}$ would be required. A greater synergistic effect maybe observed if a true dose comparison was used.

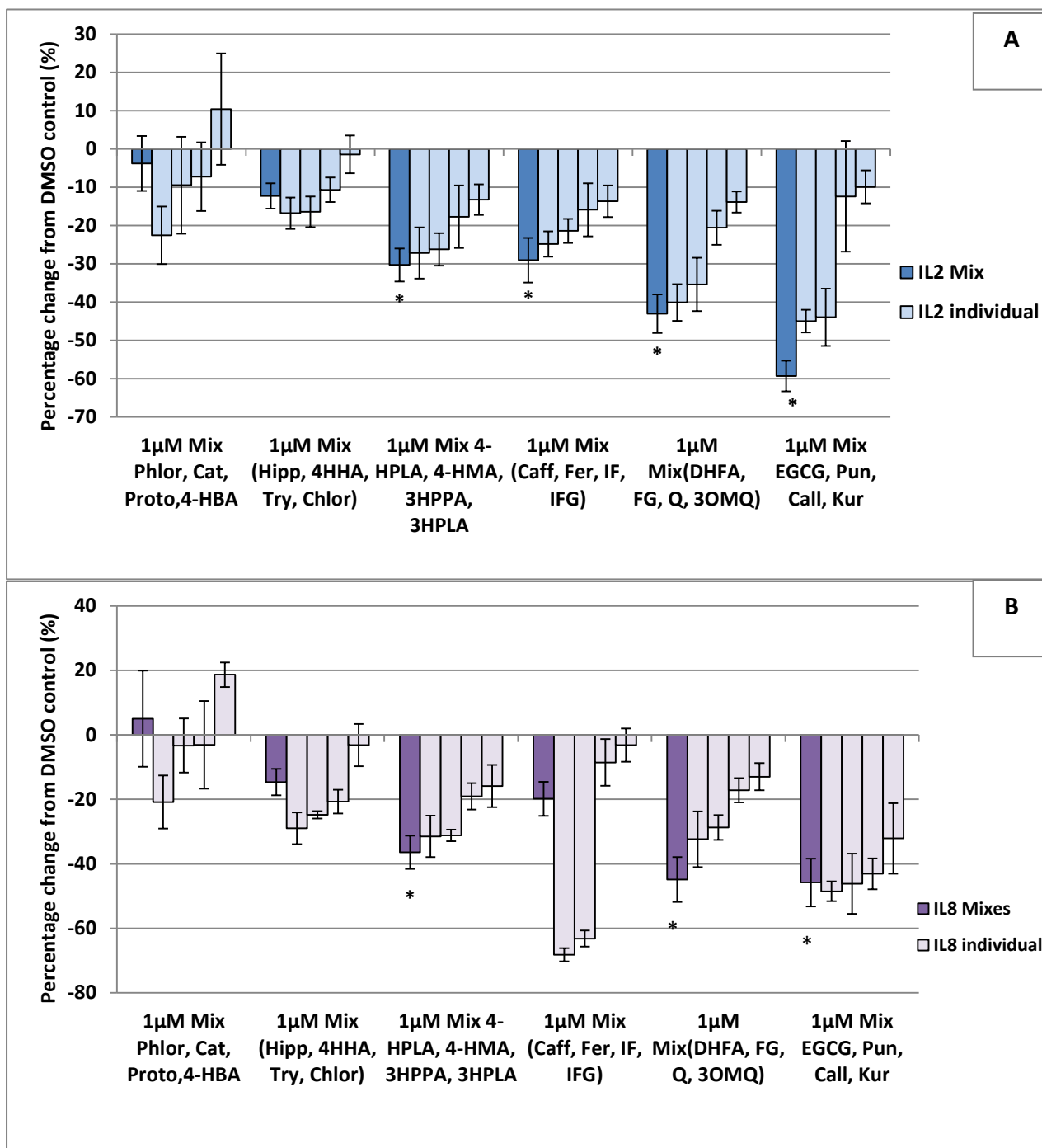


Figure 3.10 –Mixtures of 4 (poly)phenols (total 1µM phenolic content – 0.25 µM individual) alongside the individual (poly)phenols making up that mixture. A) shows changes to IL2 release by unstimulated Jurkat cells compared with DMSO treated control and B) shows changes to IL8 release by unstimulated Jurkat cells compared with DMSO treated control. Graphs represent a percentage change from DMSO treated control (0%) in unstimulated cells. (Poly)phenols arrange in molecular weight order. [Mean ± SEM, n=6. One-way ANOVA with Dunnett’s *post hoc* test * $p < 0.05$ (statistics performed in sets of 4 treatments, see 2.2.9)].

Mix 1 = Phloroglucinol (Phlor), catechol (Cat), protocatechuic acid (Proto) and 4-hydroxybenzoic acid (4-HBA). **Mix 2** = Hippuric acid (Hipp), 4'-hydroxyhippuric acid (4HHA), tyrosol (Try) and chlorogenic acid (Chlor). **Mix 3** = 4-Hydroxyphenyllactic acid (HPLA), 4'-hydroxymandelic acid (4-HMA), 3-(3'-hydroxyphenyl)propionic acid (3HPPA) and 3-(4'-hydroxyphenyl)lactic acid (3HPLA). **Mix 4** = Caffeic acid (Caff), Ferulic acid (Fer), Isoferulic acid (IF) and isoferuloylglycine (IFG). **Mix 5**= Dihydroferulic acid (DHFA), feruloylglycine (FG), quercetin (Q) and 3-O-methylquercetin (3OMQ). **Mix 6** = Epigallocatechin gallate (EGCG), kuromanin (Kur), callistephin chloride (Call), and punicalagin (Pun).

3.5 DISCUSSION.

This project analysed multiple (poly)phenols for their effects on cell viability and modulations to cytokine release in Jurkat T lymphocytes.

3.5.1 The effect of polyphenol on cell viability in Jurkat T lymphocytes.

Overall cell viability was not significantly affected by the (poly)phenol treatments, only in certain cases modulations were observed using the higher dose. Kuromanin (also known as cyaniding 3-O-glucoside) in particular increased cell proliferation by $40\% \pm 8\%$, kuromanin is found in a number of fruits including pomegranates, grapes, and cranberries. Consumption of cranberry polyphenols showed an increase in T cell production in healthy patients following 10 weeks of consumption¹⁵¹. Some treatments also inhibited cell proliferation including curcumin and catechol with a reduction of $\sim 40\%$. Previous studies have investigated the

effects polyphenols have on cell viability, particularly in cancer cell lines. Being able to inhibit cell proliferation specifically in cancer cells is a promising prospect in cancer treatment. However, the current literature can be confusing and have opposing positions regarding cell proliferation, depending on dose or cell type being used. For example, Roe *et al* 2010 found EGCG to inhibit cell proliferation and induce apoptosis in human ovarian cell line¹⁵². However, Yoo *et al* 2010 found EGCG to increase cell proliferation in the brain cell in mice¹⁵³. Depending on the cell type in question, *in vitro* or *in vivo* these compounds have different effects on cell proliferation. The Jurkat cell used in this study are from a cancer cell line, therefore the effect on cell viability may differ in primary T lymphocytes than what was observed *in vitro*. Also, cell viability for the screening study use the MTS assay, which measures viability based on the reduction of tetrazolium dye by the enzyme NAD(P)H-dependent oxidoreductase. This assay depends on the cellular metabolic activity due to the NAD(P)H, for this study the assumption has been made that the (poly)phenols haven't effected cellular metabolic activity but this may not be the case. (Poly)phenols may have increased or decreased cellular metabolic activity therefore cell viability would not correlate with metabolic activity. There were 29 (poly)phenols, 2 treatments doses of 1 and 30 μ M, an n number of 6, and unstimulated and PMA stimulated conditions, this equated to almost 700 data points not including experimental controls. Therefore the MTS assay allows multiple analysis and higher throughput compared with the traditional Trypan blue exclusion method. For the purpose of this study investigating the overall effect these

compounds had in order to determine a suitable treatment dose for further investigations. Once the field has been narrowed down to a few (poly)phenols then more in-depth analysis will be performed on the effect on cell number.

3.5.2 Effects of low concentrations of (poly)phenols on cytokine release by Jurkat T lymphocytes.

1 μ M was considered to be a more physiologically relevant dose to the levels found in the blood plasma, these results were separated from the other data and both IL2 and IL8 were represented together. Figure 3.11 shows the majority of the (poly)phenol treatments showed a reduction in cytokine release of both IL2 and IL8. Only catechol increased cytokine release at this dose and pyrollalol (which isn't shown in this graph, see figure 3.5). Ferulic acid and isoferuloyglycine were the most anti-inflammatory compounds with over 60% reduction in IL8 release; interestingly IL2 did not have the same effect, with a reduction of less than 20%. EGCG and punicalagin also had a stronger reduction with IL8 than IL2; the majority of the other treatments lowered IL2 and IL8 to the same level. This suggests that ferulic acid and isoferuloyglycine may be acting differently than the other compounds, having varying and more specific effects on cytokine release.

There appeared to be greater anti-inflammatory effects with the more complex the polyphenols become. The smaller phenolic acids (left hand-side figure 3.11) seemed to have less reduction, even pro-inflammatory characteristics when

compared with the polyphenols (right hand-side figure 3.11). Polyphenols are more complex and have a greater number of functional groups or modifications to the basic phenol ring. These functional groups maybe having a greater influence on cytokine release and signalling pathways than the phenolic acids investigated. Further work to evaluate a structure function relationship between the complexity of the compound and cytokine release will be investigated (see section 3.5.5/3.5.6).

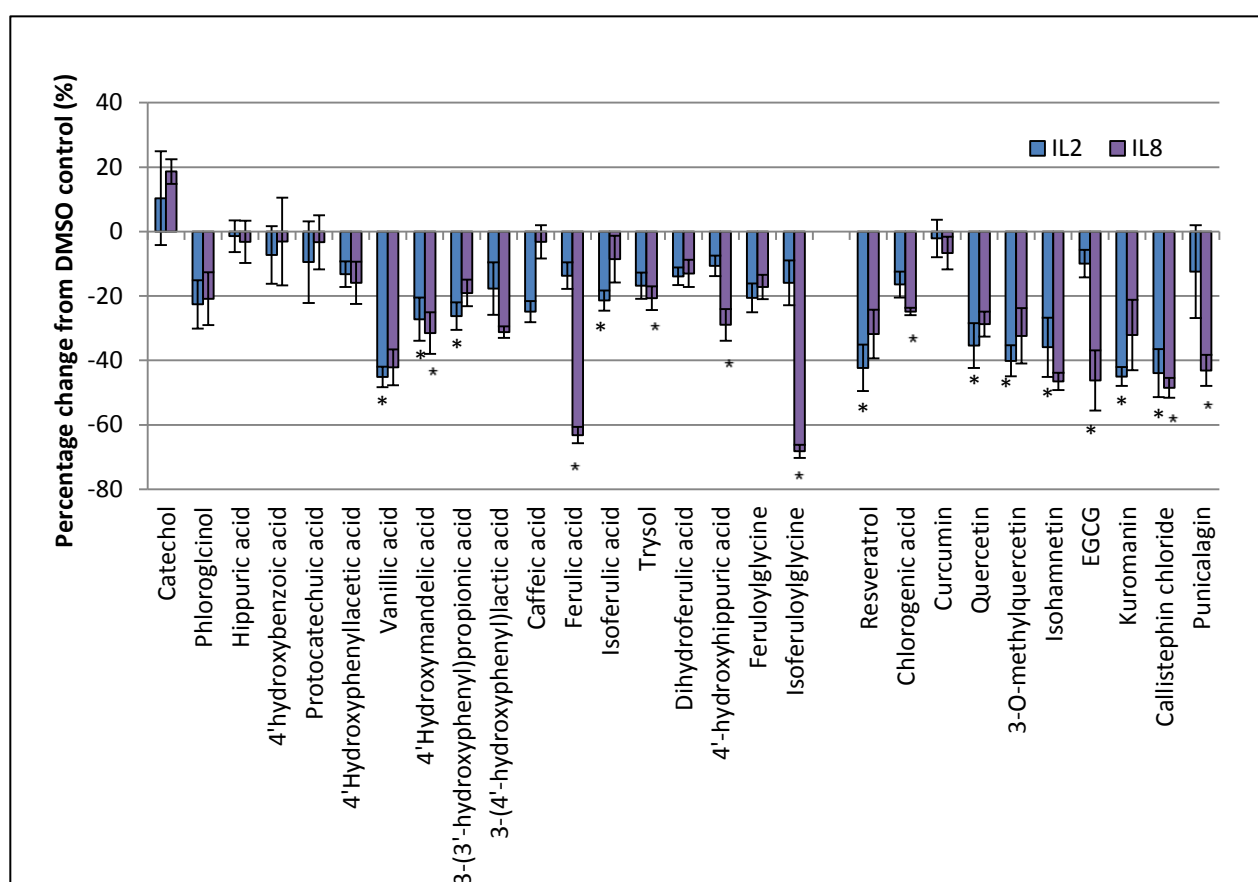


Figure 3.11 – Cytokine release of IL2 and IL8 with 1 μ M (poly)phenols. Graph shows effect of 1 μ M (poly)phenols as a percentage change from DMSO control (0%) in unstimulated cells for interleukin 2 (blue) and interleukin 8 (purple). (Poly)phenols arrange in molecular weight order. [Mean \pm SEM, $n=6$. One-way ANOVA with Dunnett's *post hoc* test * $p < 0.05$ (statistics performed in sets of 4 treatments, see 2.2.9)].

3.5.3 Parent compounds and their metabolites comparing cytokine release.

From the screening process, the most anti-inflammatory (poly)phenols screened were curcumin, resveratrol, quercetin, and isorhamnetin. These (poly)phenols are the parent compounds found in foods they tend to have low bioavailability and are metabolised by colonic microflora and also in the tissues. The polyphenols can be glucuronidated, sulphated and broken down into smaller phenolic acids. Figure 3.12, shows quercetin being broken down into phenolic acids some of which were included in the study, phloroglucinol, protocatechuic acid, and 3-(3'-hydroxyphenyl)propionic acid. The allowed the investigation of whether or not the phenolic acids have the same effects on cytokine release as the parent compounds.

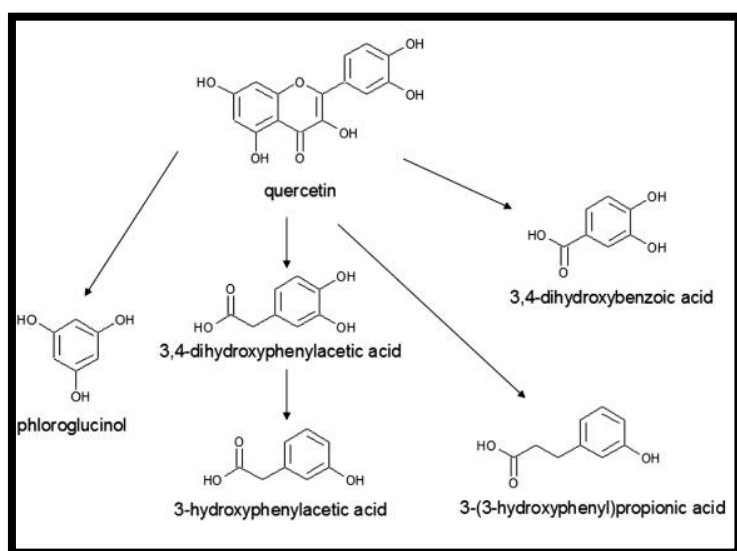


Figure 3.12 – Phenolic acid breakdown products of quercetin¹⁵⁴.

Quercetin and its methylated form isorhamnetin had similar effects in unstimulated cells, lowering both IL2 and IL8 release. However they had dramatically different effects in stimulated cells, with quercetin increasing and isorhamnetin lowering cytokine release. The smaller phenolic acids phloroglucinol, protocatechuic acid, and 3-(3'-hydroxyphenyl)propionic acid all lowered cytokine release in both unstimulated and stimulated cells, but less than the parent compound quercetin (See figure 3.13).

Figure 3.14, shows curcumin, the active principle of the dietary spice turmeric, lowered cytokine release of IL2 by $43\% \pm 14\%$, IL8 by $30\% \pm 7\%$ and TNF α $21\% \pm 4\%$ in stimulated cells. The curcumin metabolites ferulic acid and dihydroferulic acid retained the anti-inflammatory effects observed with curcumin. Curcumin had less of an effect in unstimulated cells, whereas ferulic acid lowered IL8 by $-63\% \pm 3\%$. Curcumin blocks Ca²⁺ mobilization in T cells, preventing activation of nuclear factor of activated T cells (NFAT) and also nuclear factor kappaB (NF- κ B) via T cell receptor¹⁵⁵. This may explain the decreases in both IL2 (expression regulated by NFAT) and IL8 release (expression regulated by NF- κ B)¹⁵⁶.

Resveratrol is found in red wine resulted in a decrease in IL2 release by $42 \pm 7\%$ and IL8 by $31\% \pm 3\%$ in unstimulated cells (Fig. 3.15). The smaller phenolic acids vanillic acid and caffeic had similar effects especially in stimulated cells. Other studies have shown resveratrol to lower inflammation, with 5 μ M resveratrol suppress NF- κ B activation induced by TNF α in Jurkat cells¹⁵⁷.

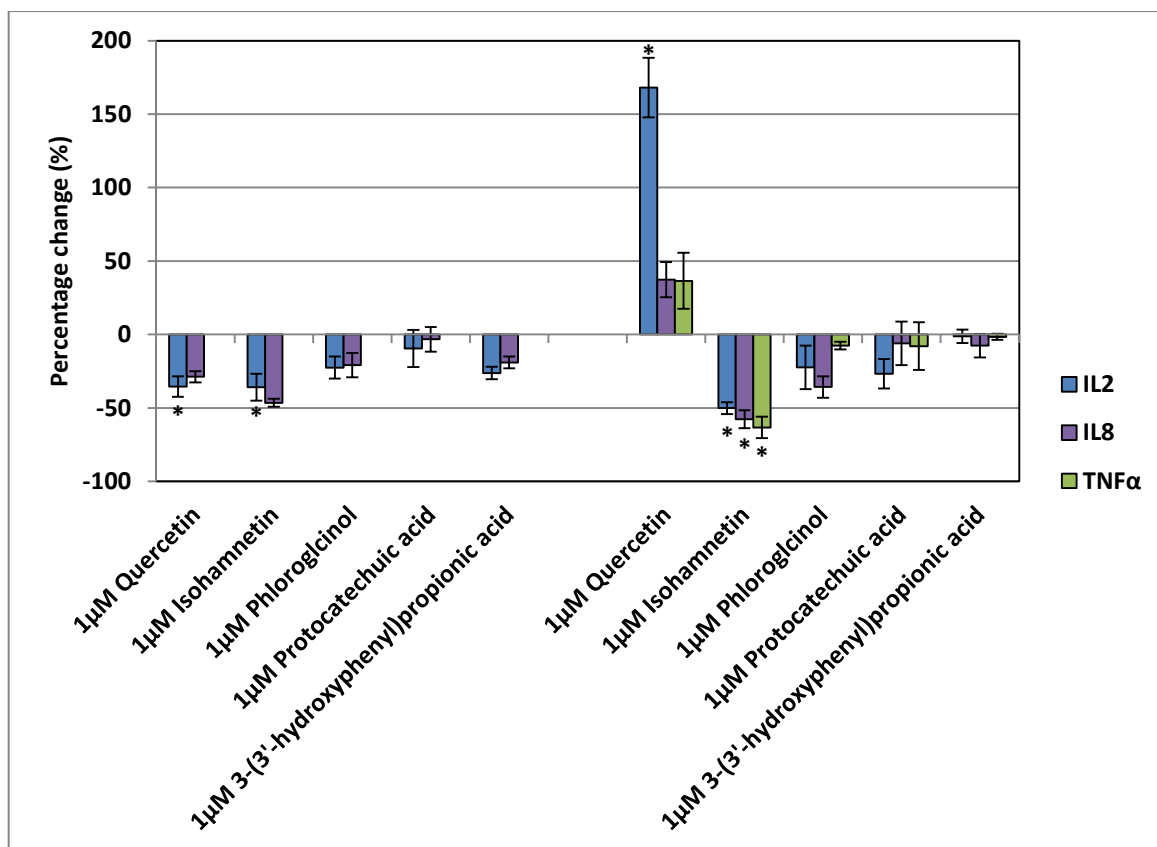


Figure 3.13 – Quercetin and metabolites effects on inflammation. Effect of (poly)phenols on cytokine release from Jurkat cells (expressed as percentage change from DMSO carrier cells). Cells were treated with 1μM parent compound quercetin or metabolites, for 48h with and without PMA/PHA added at the 24h time point.

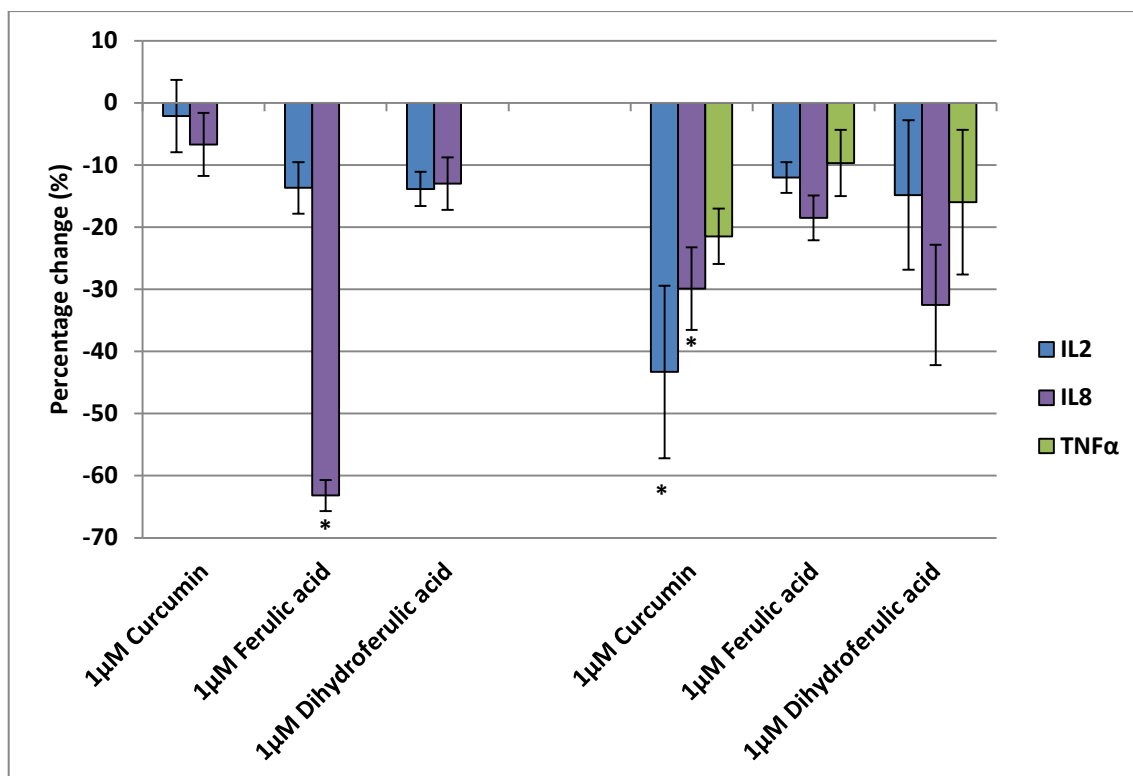


Figure 3.14 – Curcumin and metabolites effects on inflammation. Effect of (poly)phenols on cytokine release from Jurkat cells (expressed as percentage change from DMSO carrier cells). Cells were treated with 1μM parent compound curcumin or metabolites, for 48h with and without PMA/PHA added at the 24h time point.

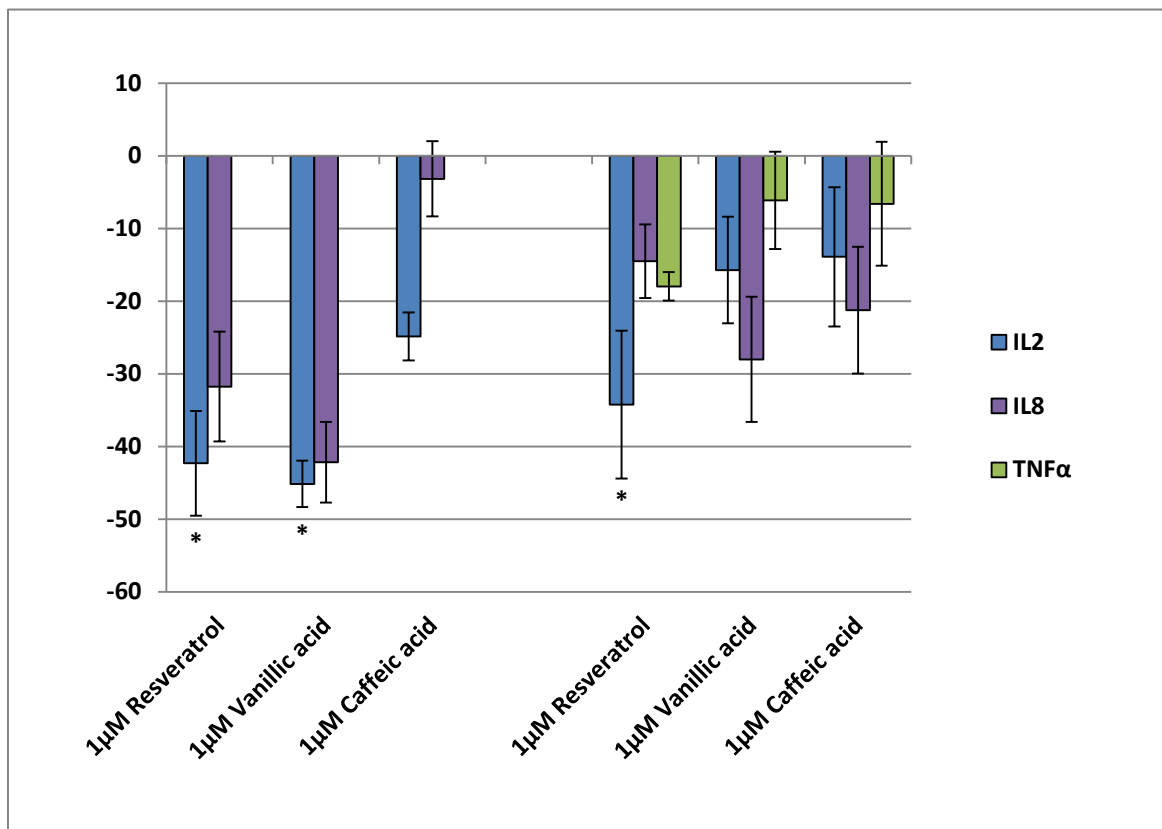


Figure 3.15 – Resveratrol and metabolites effects on inflammation. Effect of (poly)phenols on cytokine release from Jurkat cells (expressed as percentage change from DMSO carrier cells). Cells were treated with 1μM parent compound resveratrol or metabolites and wine phenolic, for 48h with and without PMA/PHA added at the 24h time point.

3.5.4 Lowering of cytokine release was amplified by the mixtures of (poly)phenol.

The mixtures of the polyphenol the compounds aren't necessarily found in the same food source. Compounds EGCG, kuromanin, callistephin chloride, and punicalagin had the greatest decrease in IL2 cytokine release when mixed together

(Fig. 3.10A); they are found in foods such as green tea, raspberries, and pomegranates. Although they aren't found in the same food source, they are most likely eaten together as part of a balanced diet. Other research has observed synergistic effects when investigating (poly)phenols, Shen *et al* 2010 measured lower levels of TNF α gene expression in LPS treated mice which had consumed green tea polyphenols and 1- α -OH- vitamin D3, than each consumed individually¹⁵⁸. These synergistic effects will allow lower doses to be used, to gain equal or greater inflammatory responses.

3.5.5 Investigating a structure function relationship within the (poly)phenols.

The (poly)phenols used had a variety of molecular weights and functional groups, analysis of the data suggested there may be a structure-function relationship, with the more complex polyphenols having greater anti-inflammatory effects than the smaller phenolic acids. To evaluate if the bioavailability of the compounds was affecting the viability of the cells, the lipophilicity (K_{ow}) was plotted against cell viability for all compounds (Figure 3.16). This graph indicated there may be a relationship between the bioavailability of the compounds and the viability of the cells; however certain functional groups will have greater effects than others. Therefore dividing the data into chemical classes such as methoxy groups, nitrogen containing groups, would give better representation of the cell viability effects,

however there were not enough compounds in each category for this analysis to be done.

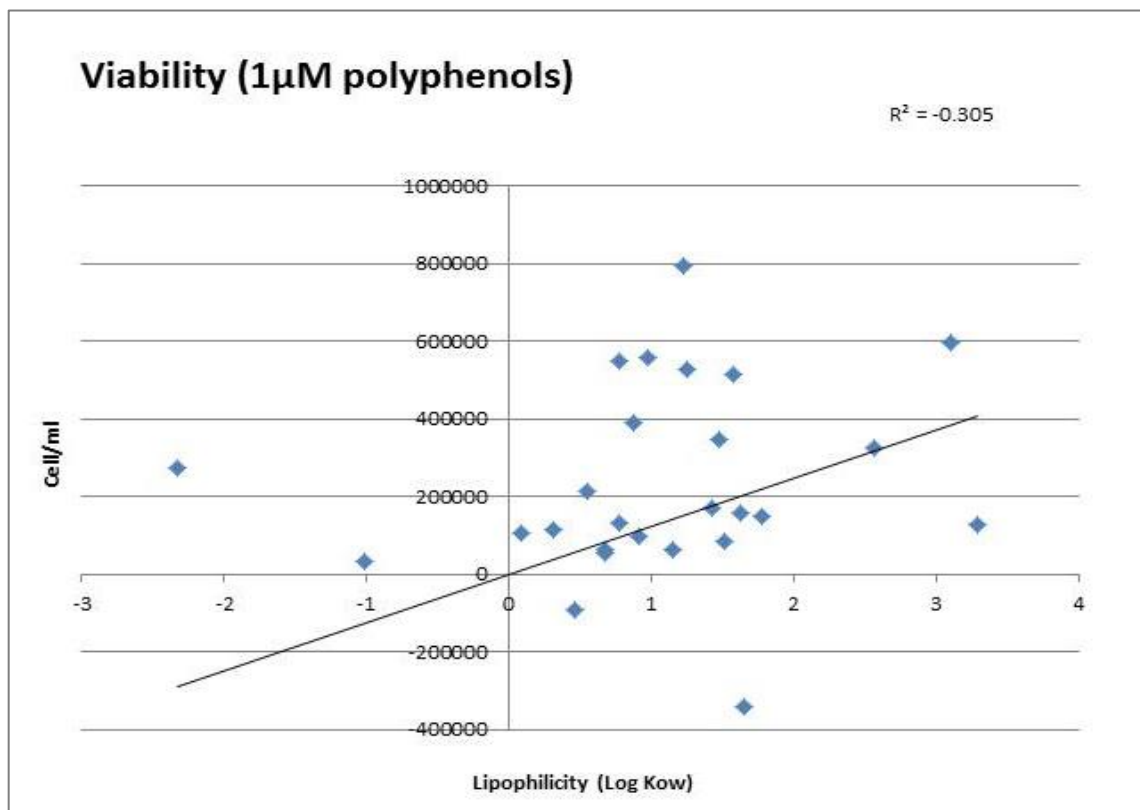


Figure 3.16 – Graph shows the lipophilic values of the (poly)phenol compounds (K_{ow}) plotted against the cell viability following 48h with a 1µM (poly)phenol treatment.

3.5.6 Methoxy (poly)phenols identified to have greater effects on cytokine release.

Greater number of hydroxyl groups and their positioning, have been shown to alter (poly)phenol antioxidant capabilities¹⁵⁹. Methoxy groups are functional groups made up of a methyl group bound to oxygen (OCH_3) and are of particular

interest as they are lipophilic compounds and are more easily absorbed by the cell across the phospholipid bilayer. Therefore methyl groups tend to have a greater bioavailability, crossing the cell membrane easier and potential having a greater effect within the cell, but the drawback is they have decreased antioxidant capacity compared with similar non-methoxy compounds. Compare similar (poly)phenols with and without methoxy groups and evaluating the effects these compounds had on cytokine release.

Figure 3.17B, unstimulated cells the non-methoxy polyphenol protocatechuic acid had little effect on cytokine release at either dose. However, vanillic acid and its methoxy counter-part lowered both IL2 and IL8 at both 1 and 30 μ M. For the lower dose this was a $45 \pm 3\%$ reduction for IL2 and $42 \pm 6\%$ reduction for IL8. With over a 40% reduction in cytokine release shows that the methoxy group is playing an important role in driving the anti-inflammatory response either by its greater presents in the cell or through other signalling pathways. Further investigation would be required to determine the mechanisms behind these effects.

Similar effects were observed with the stimulated cells (Fig. 3.17C), with the protocatechuic acid having a pro-inflammatory effect increasing IL2 by $56 \pm 9\%$, IL8 by $89 \pm 9\%$ and TNF α by $50 \pm 7\%$. However, with vanillic acid an anti-inflammatory effect was observed lowering IL2 by $-26 \pm 3\%$, IL8 by $-40 \pm 5\%$ and TNF α by $-46 \pm 5\%$.

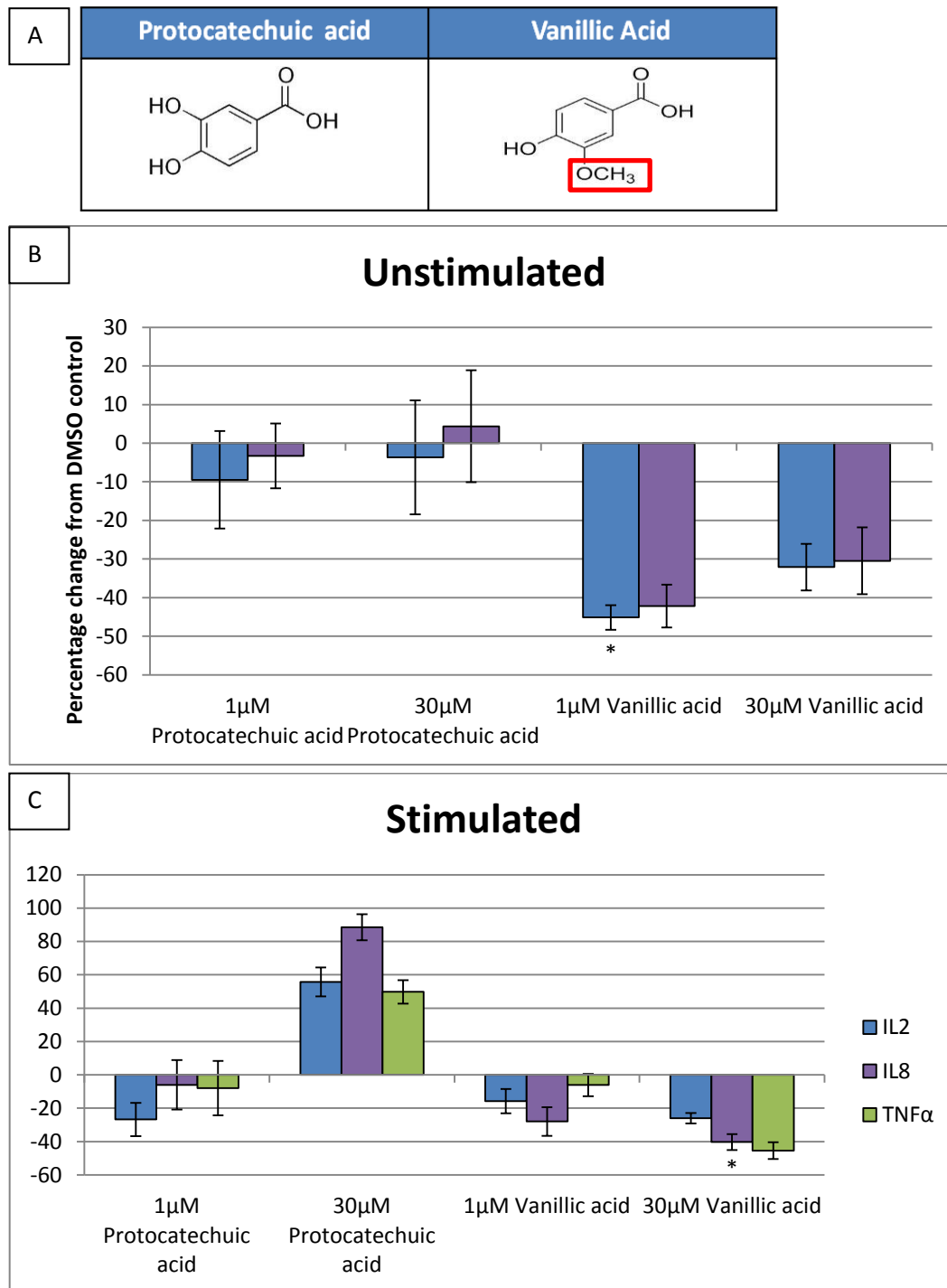
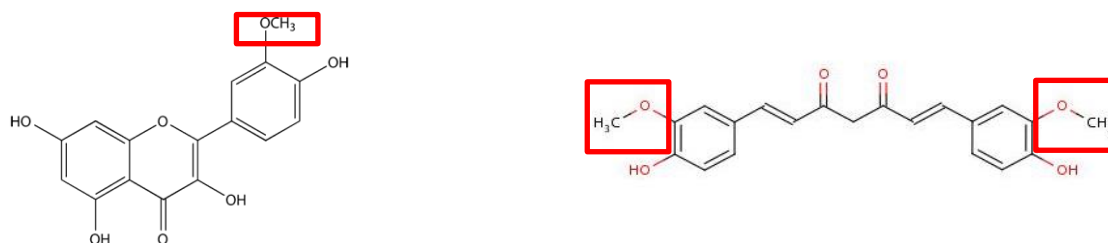


Figure 3.17 – A) Structural differences between protocatechuic acid and vanillic acid. B) Effect 1 and 30µM protocatechuic acid and vanillic acid had on cytokine release from Jurkat cells (expressed as percentage change from DMSO). Cells were treated for 48h with (C) and without PMA/PHA (B) added at the 24h time point.

Vanillic acid was not the only methoxy compounds in the (poly)phenols screening, however it was the only compound with a non-methoxy structural counter-part to compare the result. Other compounds included ferulic acid, isoferulic acid, dihydroferulic acid, feruloylglycine, isorhamnetin and curcumin. We observed large reduction in IL2 with the curcumin treatments; this may be due to curcumin containing two methoxy groups (Fig. 3.18).



Isorhamnetin

Curcumin

Figure 3.18 – Example of other methoxy (poly)phenols included in the screening, isorhamnetin (1 methoxy group) and curcumin (2 methoxy groups).

Pterostilbene, is structurally similar to resveratrol but has two hydroxyl groups replaced with methoxy groups. Studies have compared these two compounds and have shown that pterostilbene had a positive effect on cellular stress and inflammation compared with resveratrol, which had no effect; conducted in mice exhibiting signs of Alzheimer's disease¹⁶⁰.

3.5.7 Identifying (poly)phenols that significantly lowering the cytokine release of IL2, IL8 and TNF α in stimulated and unstimulated cells.

Graphs 3.19 and 3.20 summaries only those (poly)phenols that significantly reduced cytokine release in the Jurkat cells when compared with DMSO treated control. By just looking at the significant ones, the aim was to focus down on just a couple of polyphenols to be used for further investigation. From figure 3.19, 30 μ M curcumin is shown to be the most significant polyphenol reducing IL2 cytokine release in unstimulated cells, followed by 30 μ M resveratrol and isorhamnetin. 1 μ M EGCG, Callisephin chloride and punicalagin also have a greater reduction in IL8, along with the phenolic acid 1 μ M isorferuloylglycine.

Figure 3.20, shows just the significant (poly)phenols that significantly reduced cytokine release in PMA stimulated cells. Again curcumin seems the most significant reducing IL2, IL8 and TNF α , along with both 1 and 30 μ M isorhamnetin significantly lowering all three cytokines. 30 μ M quercetin and 3-O-methylquercetin also had large decrease in both IL2 and TNF α . Resveratrol lowered both IL2 and TNF α with both doses 1 and 30 μ M. It was therefore chosen that curcumin, isorhamnetin and resveratrol would be the three (poly)phenols chosen for further investigation using proteomic approaches. Based on their effecting in lowering cytokines IL2, IL8 and TNF α , with both doses and in unstimulated and stimulated cells.

To evaluate the changes in cytokine release observed with curcumin, isorhamnetin and resveratrol, these compounds were analysed further by evaluating

the changes in protein expression via label free proteomics. This will allow network and pathway analysis to be conducted to evaluate how these compounds may be causing the reduction in cytokine release observed in the Jurkat T-lymphocytes.

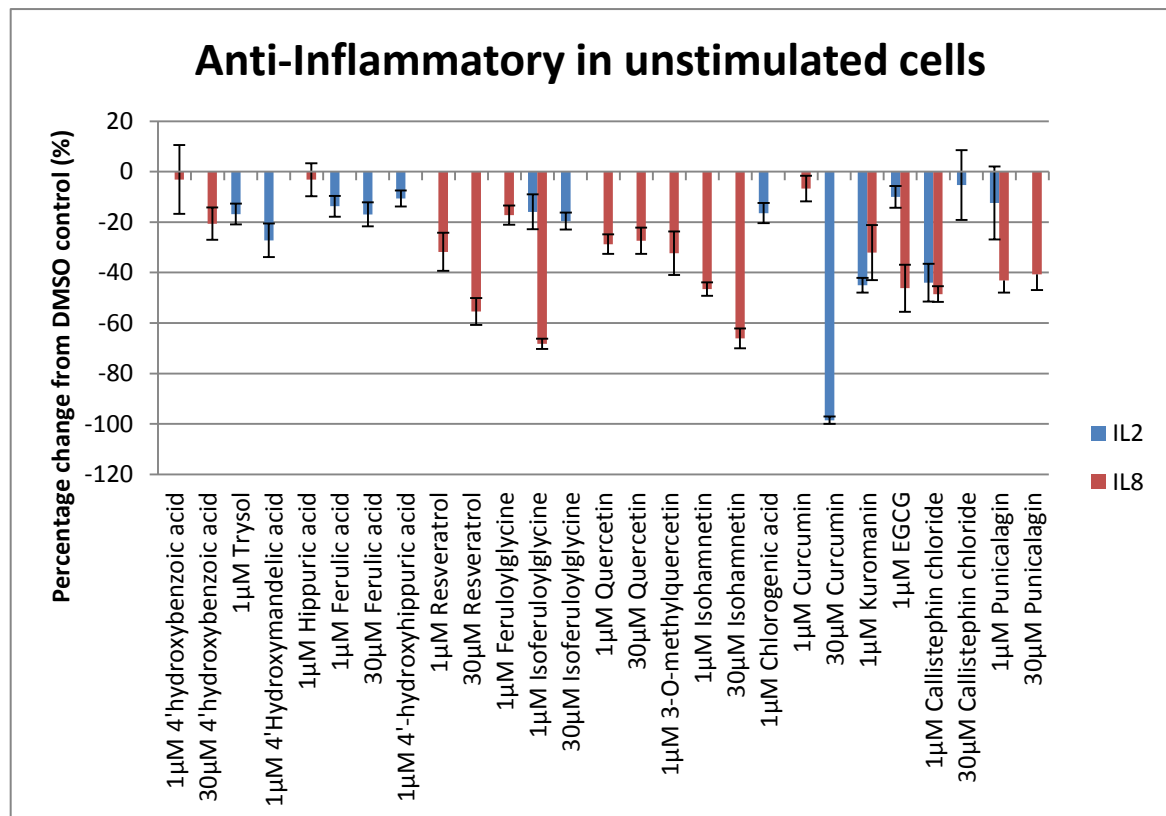


Figure 3.19 – Graph showing just the (poly)phenols that had a significant reduction in cytokine release of IL2 and IL8 with both 1 and 30 μM (poly)phenols in unstimulated cells. Shown as a percentage change from DMSO control (0%) in unstimulated cells for interleukin 2 (blue) and interleukin 8 (purple). [Mean ± SEM, n=6. One-way ANOVA with Dunnett’s *post hoc* test $p < 0.05$ (statistics performed in sets of 4 treatments, see 2.2.9)].

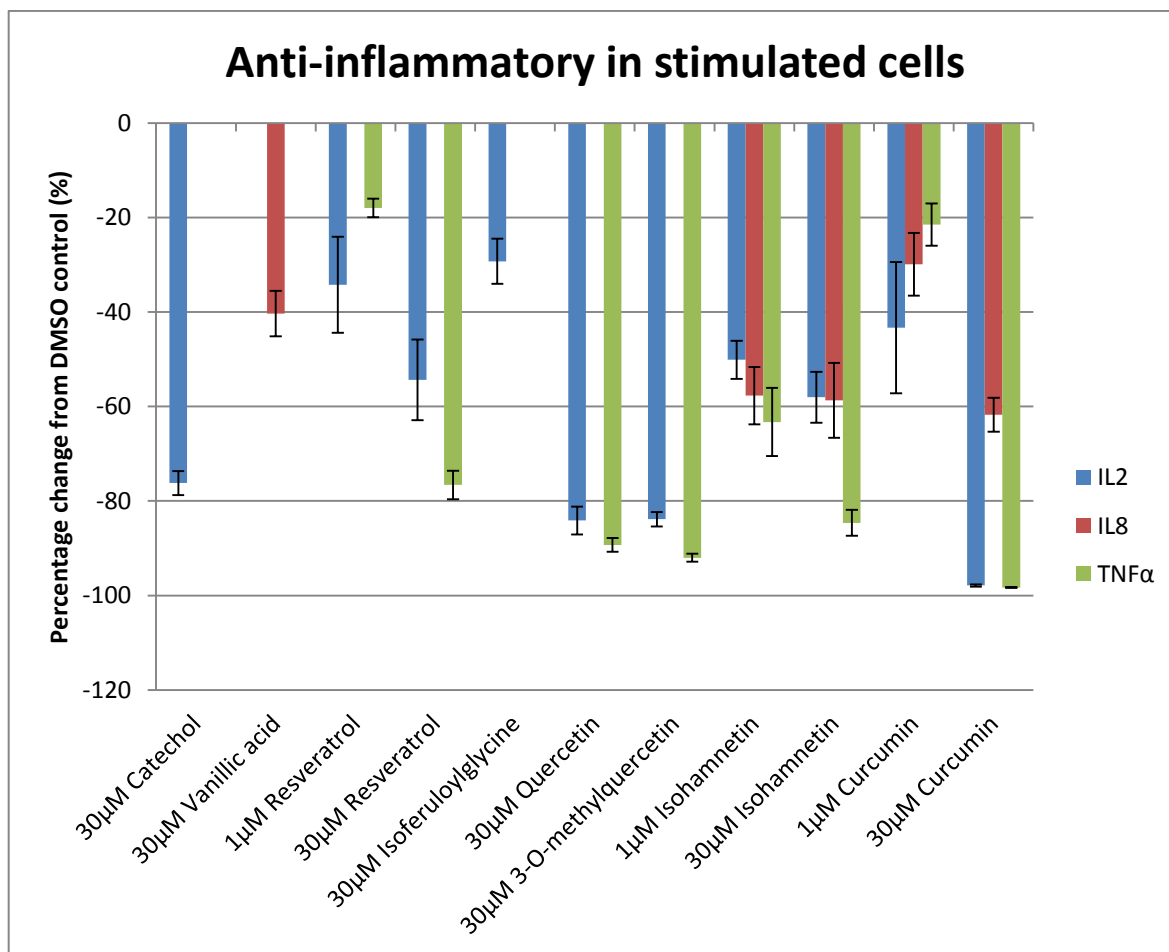


Figure 3.20 – Graph showing just the (poly)phenols that had a significant reduction in cytokine release of IL2, IL8 and TNFα with both 1 and 30 μM (poly)phenols in stimulated cells. Shown as a percentage change from DMSO control (0%) in unstimulated cells for interleukin 2 (blue), interleukin 8 (purple) and TNFα in green. [Mean ± SEM, $n=6$. One-way ANOVA with Dunnett's *post hoc* test $p < 0.05$ (statistics performed in sets of 4 treatments, see 2.2.9)].

CHAPTER 4

**PROTEOMIC ANALYSIS OF CHANGES IN PROTEIN
CONCENTRATION FOLLOWING TREATMENT OF
JURKAT T-LYMPHOCYTES WITH POLYPHENOLS.**

4.1 INTRODUCTION.

4.1.1 Proteomic analysis evaluating the changes to proteins following polyphenol treatments.

Chapter 3 identified polyphenols that significantly lowered markers of inflammation in Jurkat T lymphocytes in both unstimulated and PMA/PHA stimulated cells. In particular curcumin, isorhamnetin and resveratrol were among the compounds that significantly lowered cytokine release by Jurkat T-lymphocytes when stimulated with PMA/PHA (Table 4.1). In this investigation it was chosen to first investigate the effects in unstimulated cells, to observe the effects the polyphenols were having in a non-stressed situation, both unstimulated and stimulated cells shown significant reductions in cytokine release. Further investigation would be interesting to evaluate the change in protein expression with the PMA/PHA stimulus but was not covered in this study. In order to determine the mechanisms regulating the changes in cytokine release, quantitative proteomics was used. Previous proteomic analyses have examined changes in protein levels due to polyphenol treatment in a variety of cell types, however, these studies have tended to focus on extremely high doses of polyphenols to induce protein changes. For example, Díaz-Chávez *et al* 2013 used 250µM resveratrol in MCF-7 breast cancer cells for 48 h, while investigating the chemopreventive and anti-tumour effect of resveratrol¹⁶¹. Achieving this level of resveratrol in vivo is unlikely, since in rats administered an oral dose of 5 mg/kg resveratrol, levels in the plasma were 1.5µM, including resveratrol-conjugates and metabolites at 4h after consumption, with only

0.08 μ M of this being free resveratrol¹⁶². Higher doses in the plasma can be achieved, for example mice given 75 mg/ml resveratrol, achieved a level of 28.4 μ M in the plasma following 2 weeks of oral administration¹⁶³.

Therefore, in this study a lower dose of 1 μ M was used, to treat the cells together with a higher dose either 10 or 30 μ M (depending on the polyphenol), to examine changes to proteins abundance. As previously shown (poly)phenols can alter cytokine release by cells at both low and high concentrations, see Table 4.1. Label free, shotgun proteomics were used to identify proteins that were significantly modulated following treatment with curcumin, isorhamnetin, or resveratrol. Label-free proteomics does not use stable isotopes that chemically binds to the proteins, but quantifies proteins on precursor signal intensity. The advantages of label-free proteomics means the whole proteome can be analysed and multiple states compared (DMSO and 1 and 30 μ M polyphenols)^{164,165}.

Treatment		IL2		IL8		TNF α	
		-PMA	+PMA	-PMA	+PMA	-PMA	+PMA
Cur	1 μ M	-2 \pm 6%	-43 \pm 14% *	-7 \pm 5%	-30 \pm 7% *	-	-21 \pm 4%
	30 μ M	-99 \pm 1% *	-98 \pm 0% *	242 \pm 25% *	-62 \pm 4% *	-	-98 \pm 0% *
Iso	1 μ M	-36 \pm 9% *	-50 \pm 4% *	-47 \pm 3%	-58 \pm 6% *	-	-63 \pm 7% *
	30 μ M	-61 \pm 5% *	-58 \pm 5% *	-66 \pm 4%	-59 \pm 8% *	-	-85 \pm 3% *
Res	1 μ M	-42 \pm 7% *	-34 \pm 10% *	-32 \pm 8%	-15 \pm 5%	-	-18 \pm 2% *
	30 μ M	-70 \pm 6% *	-54 \pm 9% *	-55 \pm 5%	-4 \pm 6%	-	-77 \pm 3% *

Table 4.1 - Cytokine release following 48h treatment with polyphenols curcumin (Cur), isorhamnetin (Iso) and resveratrol (Res) by Jurkat T-lymphocytes. Percentage change of interleukin 2 (IL2), interleukin 8 (IL8), and tumour necrosis factor alpha (TNF α) release with 1 and 30 μ M polyphenol treatment with (+PMA) and without (-PMA) PMA/PHA stimulation. Significant changes from DMSO treated control are highlighted in bold (*). [Data summarised from Chapter 3, figure 3.3 – 3.9, mean percentage change from DMSO treated control (0%) \pm SEM, n=6] .

4.1.2 Proteomics analysis: Label-free mass spectrometry technique.

Previous proteomics studies evaluating changes to protein abundance due to polyphenols have tended to use two-dimensional gel electrophoresis to separate proteins and identify changes to protein expression following treatments. This technique has its benefits, but is limited by reproducibility and detection of larger or less soluble proteins. More recently liquid-chromatography tandem mass spectrometry (LC-MS/MS) has become a more widely used technique, increasing protein detection rate and greater reproducibility compared with 2D gel electrophoresis. LC-MS/MS was used in this study to observe global changes in protein expression due to the (poly)phenol interventions in Jurkat T-lymphocytes. Using this quantitative proteomics technique, changes compared with DMSO treated control can be used to detect changes to protein expression following the polyphenol treatments. This allows detailed network analysis to be performed to understand the mechanisms responsible for the change in inflammatory markers.

4.1.3 Protein network analysis.

In order to understand the significance behind changes to protein expression following polyphenol treatment, software can be used to identify the processes and pathways modulated by the treatments. Being able to link individual changes in proteins with mechanisms and pathways, will give a greater insight into how (poly)phenols are modulating processes in the cells, in particular those proteins associated with inflammation. Databases such as STRING, DAVID bioinformatics and

software such as Ingenuity[®] were used to cluster the proteins into functional groups and investigate potential mechanisms linking the effects due to the (poly)phenol treatments.

4.2 AIMS.

Following the initial screening process describe in Chapter 3, which investigated the effect of (poly)phenols on inflammatory markers, potential candidates were identified for further investigation. The aim of this study was to use a proteomic approach to investigate the overall changes to the levels of individual protein components following treatment with these chosen polyphenols (curcumin, isorhamnetin and resveratrol). In addition network analysis was used to evaluate changes in signalling pathways and identify a potential mechanism of action for the polyphenols.

4.3 RESULTS.

4.3.1 Proteomics analysis: number of proteins modulated following polyphenols treatments for 48 h in Jurkat T lymphocytes.

Previous work has shown that (poly)phenols can modulate cytokine release by Jurkat T lymphocytes, and this led to investigation of the effects of the

(poly)phenols on modulating all proteins using shotgun LC-MS/MS proteomics (Methods section 2.2.18). A low (1 μ M) and a high (10 or 30 μ M) dose of curcumin, isorhamnetin, and resveratrol were used to identify numerous changes to proteins, to allow network analysis and evaluate changes to signalling pathways and processes.

Table 4.2, shows the number of proteins that were significantly modulated following the treatments with polyphenols compared to the DMSO treated control. The lower dose of 1 μ M showed fewer proteins modulated when compared with the higher dose. The low dose isorhamnetin showed the greatest number of protein changes (83) and resveratrol showed the greatest number at the higher dose (434) ($p < 0.05$). Further analysis between the number of induced and repressed proteins, categorised into function groups can be found in Appendix 5. Proteins were initial screened based on a p -value < 0.05 to show significant difference from DMSO control, however due to low fold changes observed the q -value has also been shown but was not used as an initial screening factor. The q -value is a false discovery rate (FDR) adjusted p -value, a q -value of 0.05 implies that 5% of significant tests will result in false positives, whereas a p -value of 0.05 implies that 5% of all tests will result in false positives. Q -value are more restrictive but more accuracy when evaluating small fold changes and give more confidences that the changes we have observed are actually significant.

Number of proteins significantly modulated by (poly)phenol treatments by Jurkat T-cells			
	All	Reduced	Increased
1 μ M curcumin	21	7	14
1 μ M resveratrol	42	2	40
1 μ M Isorhamnetin	83	54	29
10 μ M curcumin	187	134	53
30 μ M resveratrol	434	265	169
30 μ M Isorhamnetin	403	227	176

Table 4.2 - Number of proteins found to have significant fold changes following 48h treatment with the three different (poly)phenols curcumin, resveratrol and isorhamnetin at a low (1 μ M) and high(10 or 30 μ M) concentration compared with DMSO control. Identified by label-free shotgun proteomics, $n = 5$, $p < 0.05$.

4.3.2 Proteins modified by all three (poly)phenol treatments at either one or both doses.

Identifying proteins that were common to all three compounds will give an insight into the main proteins vital for the mechanism of action of (poly)phenols. There were 21 proteins common to all of the treatments, mainly observed at the higher doses (table 4.3). These were then split into those that had either induced or repressed expression (top half of the table) and those that had opposing effects

(bottom half). 12/21 proteins had the same effects with 8 proteins being repressed and 4 induced. Proteins such as cyclin-dependent kinase 1 which is important for cell cycle regulation were down regulated with all three treatments. Importin subunit alpha-1 (KPNA2) was also down regulated; importins transport proteins from the cytoplasm to the nucleus via nuclear localisation signal (NLS). Up regulated proteins include glutathione reductase (GSR), a key enzyme in maintaining redox homeostasis and also D-3-phosphoglycerate dehydrogenase (PHGDH) an enzyme which catalyses the formation of NADPH, was also significantly upregulated with all three treatments ($p < 0.03$). 30 μ M isorhamnetin significantly decreased hydroxymethylglutaryl-CoA synthase 1.91 fold and ribonucleoside-diphosphate reductase large subunit 1.3 fold with both p- and q- values < 0.05 . Glutathione reductase was increased 1.2 fold and phosphoserine aminotransferase 1.3 fold increase with 30 μ M isorhamnetin with both p- and q- values < 0.05 .

For all proteins significantly modified by the treatments curcumin, isorhamnetin and resveratrol see Appendix 4.

Common proteins identified by LC-MSMS following treatment with curcumin, isorhamnetin and resveratrol, all significant altered compared with DMSO control.					
Protein name	GENE accession	Protein accession	Fold change curcumin	Fold change resveratrol	Fold change Isorhamnetin
Thymidylate synthase	TYMS	P04818	1.2 (10µM) ↓	1.2 (30µM) ↓	1.1 (30µM) ↓
	p-value / q-value		0.007 / 0.353	0.002 / 0.038	0.023 / 0.139
Cyclin-dependent kinase 1	CDK1	P06493	1.1 (10µM) ↓	1.1 (30µM) ↓	1.1 (1µM) ↓
	p-value / q-value		0.035 / 0.494	0.014 / 0.076	0.009 / 0.106
Lamina-associated polypeptide 2	TMPO	P42166	1.1 (10µM) ↓	1.1 (30µM) ↓	1.1 (1µM) ↓
	p-value / q-value		0.002 / 0.257	0.008 / 0.063	0.039 / 0.987
Importin subunit alpha-1	KPNA2	P52292	1.1 (10µM) ↓	1.3 (30µM) ↓	1.2 (30µM) ↓
	p-value / q-value		0.038 / 0.494	0.000 / 0.008	0.019 / 0.129
40S ribosomal protein S18	RPS18	P62269	1.1 (10µM) ↓	1.1 (30µM) ↓	1.1 (30µM) ↓
	p-value / q-value		0.016 / 0.405	0.030 / 0.109	0.005 / 0.083
Hydroxymethylglutaryl-CoA synthase	HMGCS1	Q01581	1.3 (10µM) ↓	1.2 (30µM) ↓	1.1 (1µM) ↓ 1.91 (30µM) ↓
	p-value / q-value		0.001 / 0.232	0.000 / 0.003	0.039 / 0.987 0.000 / 0.000
Guanine nucleotide-binding protein subunit beta-2-like 1	GNB2L1	P63244	1.1 (10µM) ↓	1.1 (30µM) ↓	1.1 (30µM) ↓
	p-value / q-value		0.031 / 0.75	0.010 / 0.068	0.009 / 0.102
RNA-binding protein with serine-rich domain 1	RNPS1	Q15287	1.1 (10µM) ↓	1.1 (30µM) ↓	1.1 (30µM) ↓
	p-value / q-value		0.028 / 0.460	0.005 / 0.048	0.047 / 0.182
Alanine--tRNA ligase	AARS	P49588	1.1 (10µM) ↑	1.2 (30µM) ↑	1.1 (30µM) ↑
	p-value / q-value		0.026 / 0.443	0.000 / 0.003	0.018 / 0.125
D-3-phosphoglycerate dehydrogenase	PHGDH	O43175	1.1 (10µM) ↑	1.1 (30µM) ↑	1.1 (30µM) ↑
	p-value / q-value		0.006 / 0.353	0.002 / 0.038	0.027 / 0.144
Glutathione reductase	GSR	P00390	1.2 (10µM) ↑	1.1 (30µM) ↑	1.2 (30µM) ↑
	p-value / q-value		0.000 / 0.232	0.003 / 0.040	0.001 / 0.043
Phosphoserine aminotransferase	PSAT1	Q9Y617	1.1 (10µM) ↑	1.2 (30µM) ↑	1.3 (30µM) ↑
	p-value / q-value		0.017 / 0.405	0.001 / 0.028	0.000 / 0.018
Calnexin	CANX	P27824	1.1 (10µM) ↑	1.1 (30µM) ↑	1.1(30µM) ↓
	p-value / q-value		0.029 / 0.432	0.001 / 0.022	0.021 / 0.133
Carnitine O-palmitoyltransferase 1	CPT1A	P50416	1.1 (10µM) ↑	1.1 (30µM) ↑	1.1(1µM) ↓ 1.1(30µM) ↓

	p-value / q-value		0.004 / 0.353	0.003 / 0.040	0.025 / 0.987 0.002 / 0.053
Ribonucleoside-diphosphate reductase large subunit	RRM1	P23921	1.1 (10µM) ↓	1.2 (30µM) ↑	1.3 (30µM) ↓
	p-value / q-value		0.001 / 0.232	0.000 / 0.003	0.000 / 0.022
U1 small nuclear ribonucleoprotein A	SNRPA	P09012	1.1 (10µM) ↓	1.2 (30µM) ↓	1.1 (30µM) ↑
	p-value / q-value		0.022 / 0.428	0.006 / 0.052	0.007 / 0.090
Ribonucleoside-diphosphate reductase subunit M2	RRM2	P31350	1.3 (10µM) ↓	1.6 (30µM) ↓	1.6 (30µM) ↑
	p-value / q-value		0.002 / 0.257	0.000 / 0.003	0.018 / 0.125
Ena/VASP-like protein	EVL	Q9UI08	1.1 (10µM) ↓	1.1 (30µM) ↓	1.2 (30µM) ↑
	p-value / q-value		0.025 / 0.433	0.020 / 0.091	0.014 / 0.121
Lymphoid enhancer-binding factor 1	LEF1	Q9UJU2	1.1 (10µM) ↓	1.3 (30µM) ↓	1.1 (30µM) ↑
	p-value / q-value		0.040 / 0.494	0.000 / 0.006	0.007 / 0.090
Hematological and neurological expressed 1 protein	HN1	Q9UK76	1.09 (10µM) ↓	1.3 (30µM) ↓	1.08 (30µM) ↑
	p-value / q-value		0.038 / 0.494	0.000 / 0.003	0.035 / 0.160

Table 4.3 - Quantitative proteomics identified proteins which are common to all three (poly)phenol treatments curcumin, isorhamnetin and resveratrol, at either one or both treatment doses. Green highlights proteins repressed and blue proteins induced by (poly)phenol treatment. All proteins significant altered compared with DMSO control, $n = 5$, $p < 0.05$.

4.3.3 Redox-active centres and oxidoreductase activity.

In addition to the increase in glutathione reductase with all three treatments, other proteins containing redox-active centres were also significantly modulated by the polyphenol treatments (Table 4.4). Peroxiredoxin 1 was induced by both isorhamnetin (1.1 fold) and curcumin (1.1 fold), peroxiredoxin 6 was induced by isorhamnetin (1.1 fold) and repressed by resveratrol (1.1 fold). Isorhamnetin also

induced peroxiredoxin 2 (1.1 fold), thioredoxin (1.2 fold), and thioredoxin reductase 1 (1.2 fold). All these proteins are responsible in maintain redox homeostasis in the cell, suggesting polyphenols may be modulating redox as part of their mechanism of action.

Table 4.4 – Proteins containing redox-active centres or oxidoreductase activity that were significantly modified by the polyphenol treatments.

Gene Name	Full name	Fold change	Treatment	p-value / q-value
DHCR24	Delta(24)-sterol reductase	↓ 1.2	1µM Isorhamnetin	0.013/0.987
DHCR24	Delta(24)-sterol reductase	↓ 1.2	30µM Isorhamnetin	0.004/0.0072
DHRC7	7-dehydrocholesterol reductase	↑ 1.1	30µM Resveratrol	0.005/0.051
DHRC8	7-dehydrocholesterol reductase	↓ 1.2	30µM Isorhamnetin	0.001/0.047
MT-CO2	Cytochrome c oxidase subunit 2	↓ 1.1	30µM Isorhamnetin	0.001/0.038
MT-ATP6	ATP synthase subunit a	↓ 1.1	1µM Isorhamnetin	0.037/0.987
MT-ATP6	ATP synthase subunit a	↓ 1.1	30µM Isorhamnetin	0.004/0.072
IMPDH2	Inosine-5'-monophosphate dehydrogenase 2	↓ 1.1	10µM Curcumin	0.022/0.428
IMPDH2	Inosine-5'-monophosphate dehydrogenase 3	↓ 1.1	30µM Isorhamnetin	0.033/0.155
NDUFA9	NADH dehydrogenase [ubiquinone] 1 alpha subcomplex subunit 9	↓ 1.2	30µM Resveratrol	0.036/0.120
NDUFS3	NADH dehydrogenase [ubiquinone] iron-sulfur protein 3	↓ 1.1	30µM Isorhamnetin	0.008/0.098
NDUFS8	NADH dehydrogenase [ubiquinone] iron-sulfur protein 8	↓ 1.1	30µM Isorhamnetin	0.046/0.182
NDUFV2	NADH dehydrogenase [ubiquinone] flavoprotein 2	↓ 1.2	30µM Isorhamnetin	0.025/0.142
MT-ND4	NADH-ubiquinone oxidoreductase chain 4	↓ 1.2	30µM Isorhamnetin	0.034/0.158
ACAD9	Acyl-CoA dehydrogenase family member 9	↓ 1.1	30µM Resveratrol	0.033/0.115

ACADS	Short-chain specific acyl-CoA dehydrogenase	↑	1.1	30μM Resveratrol	0.027/0.103
ACADM	Medium-chain specific acyl-CoA dehydrogenase	↑	1.1	30μM Resveratrol	0.007/0.055
ACADM	Medium-chain specific acyl-CoA dehydrogenase	↓	1.2	30μM Isorhamnetin	0.003/0.071
ACADVL	Very long-chain specific acyl-CoA dehydrogenase	↑	1.3	30μM Resveratrol	0.000/0.003
ALDH18A1	Delta-1-pyrroline-5-carboxylate synthase	↓	1.1	10μM Curcumin	0.001/0.238
ALDH18A1	Delta-1-pyrroline-5-carboxylate synthase	↓	1.1	30μM Resveratrol	0.004/0.048
AKR1A1	Alcohol dehydrogenase [NADP(+)]	↑	1.1	30μM Isorhamnetin	0.042/0.173
AKR1B1	Aldose reductase	↑	1.2	30μM Isorhamnetin	0.007/0.090
AKR7A2	Aflatoxin B1 aldehyde reductase member 2	↑	1.0	30μM Resveratrol	0.030/0.109
AKR7A2	Aflatoxin B1 aldehyde reductase member 2	↑	1.1	30μM Isorhamnetin	0.018/0.125
TXNDC12	Thioredoxin domain-containing protein 12	↓	1.1	30μM Isorhamnetin	0.022/0.133
BLVRB	Flavin reductase (NADPH)	↑	1.2	30μM Resveratrol	0.018/0.089
CAT	Catalase	↑	1.1	30μM Resveratrol	0.003/0.046
COX4I1	Cytochrome c oxidase subunit 4 isoform 1	↓	1.1	10μM Curcumin	0.006/0.353
COX4I1	Cytochrome c oxidase subunit 4 isoform 1	↓	1.1	30μM Resveratrol	0.049/0.138
COX5B	Cytochrome c oxidase subunit 5B	↓	1.1	30μM Isorhamnetin	0.007/0.090
GLYR1	Putative oxidoreductase GLYR1	↑	1.1	1μM Isorhamnetin	0.026/0.987
DHRS7	Dehydrogenase/reductase SDR family member 7	↑	1.1	30μM Resveratrol	0.008/0.063
FDFT1	Squalene synthase	↓	1.2	30μM Resveratrol	0.001/0.022
FDFT1	Squalene synthase	↓	1.8	30μM Isorhamnetin	0.000/0.000
FASN	Fatty acid synthase	↓	1.1	30μM Resveratrol	0.000/0.018
FASN	Fatty acid synthase	↓	1.2	30μM Isorhamnetin	0.004/0.071
G6PD	Glucose-6-phosphate 1-dehydrogenase	↑	1.1	30μM Isorhamnetin	0.012/0.117
GLUD1	Glutamate dehydrogenase 1 / 2, mitochondrial	↓	1.1	30μM Isorhamnetin	0.021/0.133
GSR	Glutathione reductase	↑	1.2	10μM Curcumin	0.000/0.232
GSR	Glutathione reductase	↑	1.1	30μM Resveratrol	0.003/0.040
GSR	Glutathione reductase	↑	1.2	30μM Isorhamnetin	0.001/0.043
GAPDH	Glyceraldehyde-3-phosphate dehydrogenase	↓	1.0	30μM Resveratrol	0.011/0.069
HADH	Hydroxyacyl-coenzyme A dehydrogenase	↓	1.1	30μM Resveratrol	0.042/0.127

HADHA	Trifunctional enzyme subunit alpha, mitochondrial	↑	1.1	30µM Isorhamnetin	0.028/0.145
HSD17B4	Peroxisomal multifunctional enzyme type 2	↓	1.1	30µM Resveratrol	0.009/0.064
HSD17B4	Peroxisomal multifunctional enzyme type 2	↑	1.1	30µM Isorhamnetin	0.010/0.110
IDH1	Isocitrate dehydrogenase [NADP] cytoplasmic	↓	1.5	1µM Curcumin	0.016/0.997
IDH2	Isocitrate dehydrogenase [NADP], mitochondrial	↑	1.1	30µM Isorhamnetin	0.022/0.133
IDH3B	Isocitrate dehydrogenase [NAD] subunit beta, mitochondrial	↑	1.1	30µM Isorhamnetin	0.009/0.182
IVD	Isovaleryl-CoA dehydrogenase, mitochondria	↑	1.2	30µM Resveratrol	0.050/0.139
LDHB	L-lactate dehydrogenase B chain	↓	1.1	30µM Resveratrol	0.013/0.075
LDHB	L-lactate dehydrogenase B chain	↑	1.2	30µM Isorhamnetin	0.029/0.146
MDH1	Malate dehydrogenase, cytoplasmic	↑	1.1	30µM Isorhamnetin	0.018/0.125
ME2	NAD-dependent malic enzyme, mitochondrial	↑	1.1	10µM Curcumin	0.030/0.470
ME2	NAD-dependent malic enzyme, mitochondrial	↑	1.1	30µM Resveratrol	0.037/0.122
MTHFD2	Bifunctional methylenetetrahydrofolate dehydrogenase/cyclohydrolase, mitochondrial	↑	1.2	30µM Resveratrol	0.022/0.097
OGDH	2-oxoglutarate dehydrogenase, mitochondrial	↓	1.2	1µM Isorhamnetin	0.014/0.987
OGDH	2-oxoglutarate dehydrogenase, mitochondrial	↑	1.2	30µM Resveratrol	0.026/0.102
PRDX1	Peroxiredoxin-1	↑	1.1	10µM Curcumin	0.016/0.405
PRDX1	Peroxiredoxin-1	↑	1.1	30µM Isorhamnetin	0.041/0.171
PRDX2	Peroxiredoxin-2	↑	1.1	30µM Isorhamnetin	0.024/0.140
PRDX6	Peroxiredoxin-6	↓	1.1	30µM Resveratrol	0.006/0.053
PRDX6	Peroxiredoxin-6	↑	1.1	30µM Isorhamnetin	0.009/0.127
PGD	6-phosphogluconate dehydrogenase, decarboxylating	↑	1.1	30µM Isorhamnetin	0.016/0.125
PHGDH	D-3-phosphoglycerate dehydrogenase	↑	1.1	10µM Curcumin	0.006/0.353
PHGDH	D-3-phosphoglycerate dehydrogenase	↑	1.1	30µM Resveratrol	0.002/0.038
PHGDH	D-3-phosphoglycerate dehydrogenase	↑	1.1	30µM Isorhamnetin	0.016/0.125
PCYOX1	Prenylcysteine oxidase 1	↑	1.1	10µM Curcumin	0.012/0.386
PCYOX1	Prenylcysteine oxidase 1	↑	1.3	30µM Resveratrol	0.001/0.025
PCYOX1L	Prenylcysteine oxidase-like	↑	1.4	30µM Resveratrol	0.013/0.074

P4HA1	Prolyl 4-hydroxylase subunit alpha-1	↓	1.2	30μM Resveratrol	0.041/0.125
P4HA1	Prolyl 4-hydroxylase subunit alpha-1	↓	1.3	30μM Isorhamnetin	0.004/0.071
PDHA1	Pyruvate dehydrogenase E1 component subunit alpha, somatic form, mitochondrial	↓	1.1	30μM Resveratrol	0.030/0.109
RDH11	Retinol dehydrogenase 11	↑	1.2	30μM Resveratrol	0.026/0.102
RRM1	Ribonucleoside-diphosphate reductase large subunit	↓	1.1	10μM Curcumin	0.001/0.232
RRM1	Ribonucleoside-diphosphate reductase large subunit	↑	1.2	30μM Resveratrol	0.000/0.003
RRM1	Ribonucleoside-diphosphate reductase large subunit	↓	1.3	30μM Isorhamnetin	0.000/0.022
RRM2	Ribonucleoside-diphosphate reductase subunit M2	↓	1.3	10μM Curcumin	0.002/0.257
RRM2	Ribonucleoside-diphosphate reductase subunit M2	↑	1.6	30μM Resveratrol	0.000/0.003
RRM2	Ribonucleoside-diphosphate reductase subunit M2	↓	1.2	30μM Isorhamnetin	0.018/0.125
SCCPDH	Saccharopine dehydrogenase-like oxidoreductase	↑	1.2	30μM Resveratrol	0.006/0.051
SORD	Sorbitol dehydrogenase	↑	1.2	1μM Curcumin	0.040/0.997
SDHA	Succinate dehydrogenase [ubiquinone] flavoprotein subunit, mitochondrial	↑	1.1	30μM Resveratrol	0.006/0.054
TXNDC12	Thioredoxin domain-containing protein 12	↓	1.1	30μM Isorhamnetin	0.022/0.122
TXNRD1	Thioredoxin reductase 1, cytoplasmic	↑	1.1	1μM Isorhamnetin	0.028/0.987
TXNRD1	Thioredoxin reductase 1, cytoplasmic	↑	1.2	30μM Isorhamnetin	0.000/0.022
UQCRFS1	Cytochrome b-c1 complex subunit Rieske, mitochondrial	↓	1.1	30μM Isorhamnetin	0.030/0.148

Table 4.4 - Redox-related proteins (classified by David Bioinformatics) identified by LC-MS/MS proteomics. Significant fold changes occurring following treatment with the polyphenols compared with DMSO treated control. ($n = 5$, $p < 0.05$).

4.3.4 Oxidative phosphorylation

Other pathways modified by the treatments were oxidative phosphorylation, with 27 proteins being identified. ATPase synthase, cytochrome c oxidase, NADH dehydrogenase, and cytochrome b-c1 complex subunits are examples of some of the proteins significantly repressed by the treatments ($p < 0.05$) (see Appendix 4).

4.3.5 Ribosome modification by the three polyphenol treatments.

A number of ribosomal proteins were identified by proteomics screening with all three polyphenol treatments with both the 60S and 40S being repressed (table 4.5). Ribosomal proteins catalyse the synthesis of new proteins, suggesting a down regulation of protein synthesis. Interestingly, all three treatments had the same effect lowering the ribosomal proteins (unlike the proteins identified with redox activity, in which some compounds had opposing effects), suggesting that effects in protein synthesis may be a general polyphenol effect, whereas redox-related changes were more compound specific.

Table 4.5 – Significant modulation to ribosomal proteins with all three polyphenol treatments.

Gene name	Full name	Fold change	Treatment	p-value / q-value
RPL3	60S ribosomal protein L3	↓ 1.1	30µM Isorhamnetin	0.012 / 0.118
RPL4	60S ribosomal protein L4	↓ 1.0	10µM Curcumin	0.009 / 0.365
RPL4	60S ribosomal protein L4	↓ 1.1	30µM Isorhamnetin	0.001 / 0.047
RPL6	60S ribosomal protein L6	↓ 1.1	30µM Isorhamnetin	0.017 / 0.125
RPL7	60S ribosomal protein L7	↓ 1.0	10µM Curcumin	0.017/0.405
RPL7	60S ribosomal protein L7	↓ 1.0	30µM Resveratrol	0.031/ 0.110
RPL7A	60S ribosomal protein L7a	↓ 1.1	30µM Isorhamnetin	0.050 / 0.186
RPL9	60S ribosomal protein L9	↓ 1.1	1µM Isorhamnetin	0.046 / 0.987
RPL10	60S ribosomal protein L10	↓ 1.1	30µM Resveratrol	0.044 / 0.130
RPL10A	60S ribosomal protein L10a	↓ 1.1	30µM Resveratrol	0.014 / 0.076
RPL11	60S ribosomal protein L11	↓ 1.1	30µM Isorhamnetin	0.032 / 0.153
RPL12	60S ribosomal protein L12	↓ 1.1	10µM Curcumin	0.007 / 0.353
RPL12	60S ribosomal protein L12	↓ 1.1	30µM Resveratrol	0.009 / 0.063
RPL13	60S ribosomal protein L13	↓ 1.0	10µM Curcumin	0.039 / 0.494
RPL13	60S ribosomal protein L13	↓ 1.1	30µM Resveratrol	0.004 / 0.048
RPL13A	60S ribosomal protein L13a	↓ 1.1	30µM Isorhamnetin	0.012 / 0.112
RPL14	60S ribosomal protein L14	↓ 1.2	30µM Isorhamnetin	0.018 / 0.125
RPL15	60S ribosomal protein L15	↓ 1.1	30µM Isorhamnetin	0.001 / 0.051
RPL17	60S ribosomal protein L17	↓ 1.1	30µM Isorhamnetin	0.028 / 0.146
RPL18A	60S ribosomal protein L18a	↓ 1.1	30µM Isorhamnetin	0.047 / 0.184
RPL24	60S ribosomal protein L24	↓ 1.1	30µM Isorhamnetin	0.049 / 0.186
RPL27	60S ribosomal protein L27	↓ 1.1	30µM Isorhamnetin	0.022 / 0.186
RPL27A	60S ribosomal protein L27a	↓ 1.1	30µM Isorhamnetin	0.013 / 0.120
RPL28	60S ribosomal protein L28	↓ 1.1	30µM Resveratrol	0.025 / 0.101
RPL30	60S ribosomal protein L30	↓ 1.1	30µM Isorhamnetin	0.014 / 0.120
RPL36AL	60S ribosomal protein L36a-like	↓ 1.1	30µM Resveratrol	0.033/0.114
RPL38	60S ribosomal protein L38	↓ 1.1	30µM Isorhamnetin	0.035 / 0.186
RPLP1	60S acidic ribosomal protein P1	↓ 1.1	30µM Resveratrol	0.005/0.048
RPSA	40S ribosomal protein SA	↓ 1.1	30µM Resveratrol	0.005/0.048
RPS2	40S ribosomal protein S2	↓ 1.1	30µM Resveratrol	0.045/0.131
RPS21	40S ribosomal protein S21	↓ 1.1	30µM Resveratrol	0.026/0.102
RPS23	40S ribosomal protein S23	↓ 1.0	30µM Resveratrol	0.026/0.102
RPS23	40S ribosomal protein S23	↓ 1.1	30µM Isorhamnetin	0.002 / 0.058
RPS27	40S ribosomal protein S27	↓ 1.1	30µM Isorhamnetin	0.023 / 0.128

RPS27A	Ubiquitin-40S ribosomal protein S27a	↓	1.1	30μM Isorhamnetin	0.010 / 0.107
RPS3	40S ribosomal protein S3	↓	1.1	30μM Isorhamnetin	0.010 / 0.109
RPS3A	40S ribosomal protein S3a	↓	1.1	30μM Resveratrol	0.006/0.054
RPS3A	40S ribosomal protein S3a	↓	1.1	30μM Isorhamnetin	0.019 / 0.128
RPS5	40S ribosomal protein S5	↓	1.1	30μM Isorhamnetin	0.032 / 0.153
RPS6	40S ribosomal protein S6	↓	1.1	30μM Isorhamnetin	0.003 / 0.192
RPS8	40S ribosomal protein S8	↓	1.1	30μM Isorhamnetin	0.003 / 0.071
RPS9	40S ribosomal protein S9	↓	1.0	30μM Resveratrol	0.049/0.138
RPS9	40S ribosomal protein S9	↓	1.1	1μM Isorhamnetin	0.004 / 0.987
RPS9	40S ribosomal protein S9	↓	1.2	30μM Isorhamnetin	0.001 / 0.038
RPS28	40S ribosomal protein S28	↑	1.1	1uM Isorhamnetin	0.030 / 0.987

Ribosomal proteins (classified by David Bioinformatics) identified by proteomics. Significant fold changes occurring following treatment with the polyphenols compared with DMSO treated control. ($n = 5, p < 0.05$)

4.3.6 RESVERATROL: proteins modulated following treatment with resveratrol.

Progenesis analysis of the proteomics data identified 21 significant changes to protein abundance (7 proteins repressed and 14 induced), following treatment with 1μM resveratrol (see appendix 4 or figure 4.2). Midasin, a nuclear chaperone showed the greatest induction with a fold change of 2.7 ($p < 0.04$). Midasin is important for the maturation and nuclear export of pre-60S ribosome subunits. Other proteins of interest include ADRBK1 (GRK2), a G-protein coupled receptor kinase, which is activated by PKA and targets beta adrenergic receptor. GRK2 expression is dependent on NF-κB transcriptional activity and has been shown to be

elevated in inflammation¹⁶⁶. GRK2 was significantly repressed with the 1 μ M resveratrol treatment, but also with 30 μ M resveratrol and 10 μ M curcumin. Another protein of interest was transketolase, an enzyme part of the pentose phosphate pathway, which has also been linked to antioxidant defence pathways¹⁶⁷, which was induced with all 1 μ M treatments (1.1 fold) and repressed with the 30 μ M treatment (1.1 fold). Along with these proteins there was a significant increase in serine/threonine-protein phosphatase PGAM5 by 1.3 fold. PGAM5 is a substrate for a KEAP1-dependent ubiquitin ligase complex, contributing to the repression of Nrf2 gene expression¹⁶⁸, and also acts as a mediator for programmed necrosis¹⁶⁹.

434 proteins were modulated following treatment with the higher dose of resveratrol, 265 proteins were significantly repressed and 169 induced. Four proteins also showed the increases with 1 μ M resveratrol treatment, these included beta-adrenergic receptor kinase 1 (1.3 fold), Transketolase (1.1 fold), Ran GTPase-activating protein 1 (1.1 fold), and annexin A7 (1.1 fold). Annexin A7 regulates calcium and phospholipid binding and also involved in exocytosis. This protein is thought to have a role in cancer, since in some tissue type annexin A7 acts as a tumour suppressor such as prostate cancer but in other tissues such as the liver and breast cancer, annexin A7 promotes tumour development¹⁷⁰.

Ingenuity software was used to identify proteins that were connected to each other, linking mechanisms and pathways altered by the 30 μ M resveratrol treatment. Figure 4.1, shows one of network generated from the software, identifying two clusters of up-regulated proteins (red) feeding into NF- κ B complex and down-

regulated proteins forming around alpha- and beta- tubulin. Another network that was identified as being significantly modified was phospholipase c signalling (Fig. 4.2). Phospholipase c signalling is important for hydrolysing phosphatidylinositoldiphosphate into diacylglycerol and inositoltriphosphate, leading to the release of intracellular calcium. And a number of proteins were down-regulated in this signalling pathway, including integrin beta 1, RhoGEF and GRB2.

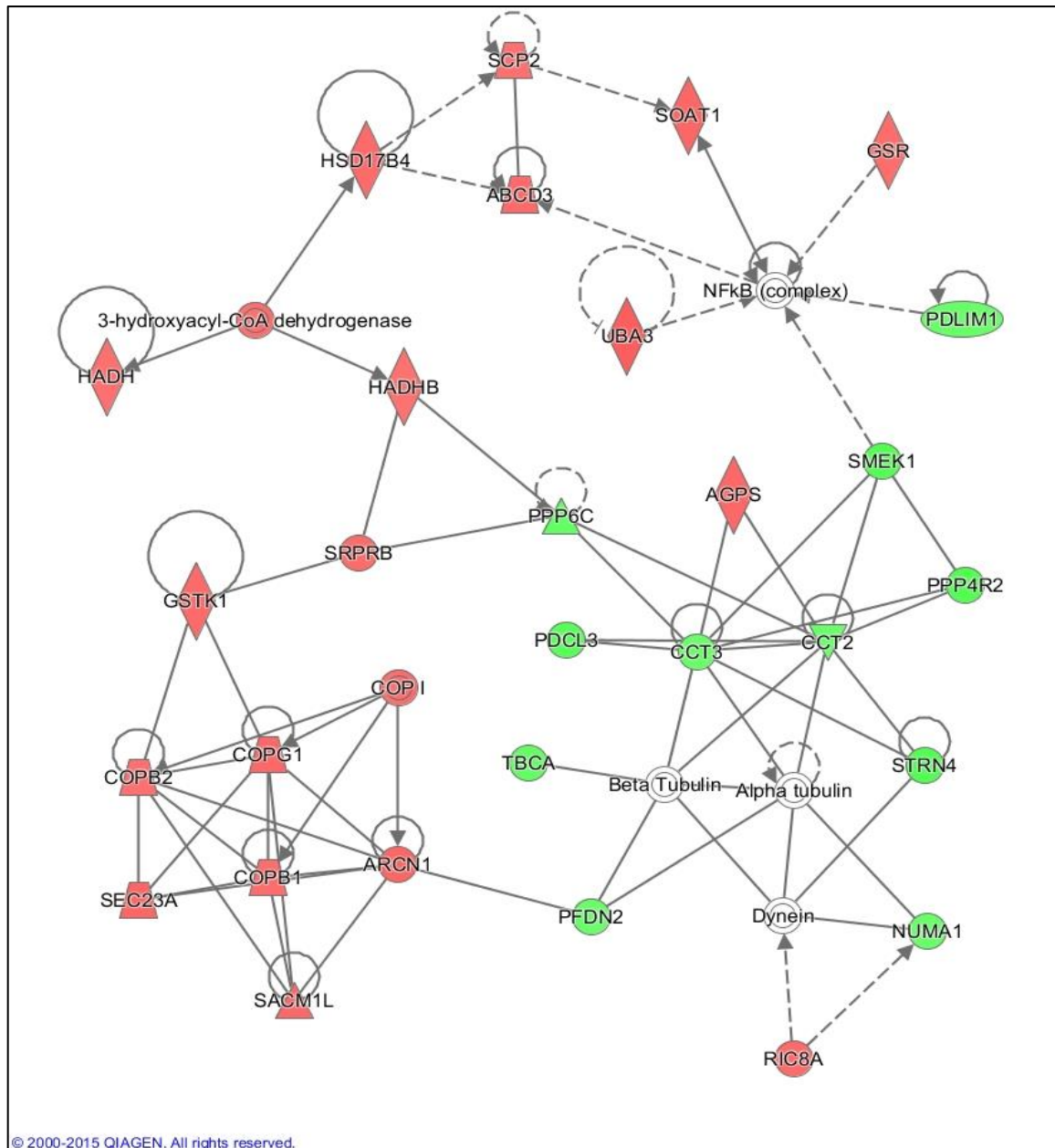


Figure 4.1 – Network analysis of proteins modulated following treatment of 30 μ M resveratrol by Jurkat T-lymphocytes. Ingenuity network analysis obtained using 30 μ M resveratrol data set. Red = induced proteins, green = repressed proteins, solid lines = direct interactions, and dashed lines = indirect interactions (full key details can be found in Appendix 5).

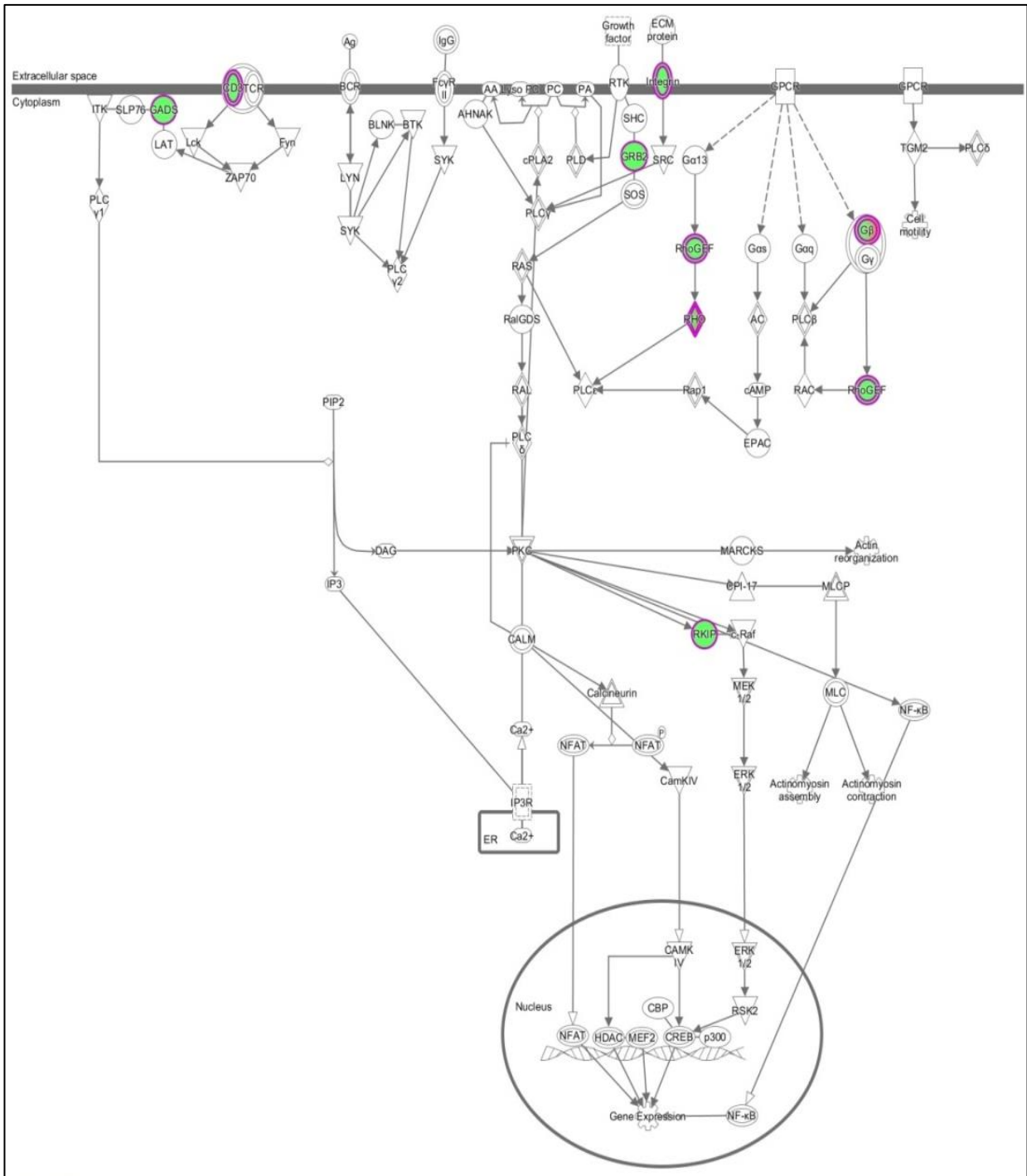


Figure 4.2 - Ingenuity network analysis obtained using the 30μM resveratrol data set, identified phospholipase c signalling as a modified pathway. Red = induced proteins, green = repressed proteins, solid lines = direct interactions, and dashed lines = indirect interactions (full key details can be found in Appendix 5).

4.3.7 CURCUMIN: proteins modulated following treatment with curcumin.

Following treatment of cells with the low dose of curcumin, 42 proteins were significant modulated, with 2 proteins significantly repressed and 40 induced. Unconventional myosin-1a (MYO1A) had the greatest fold change with a 3.6 reduction ($p < 0.05$). This protein functions as an actin-based molecular motor directing the movement of organelles along the actin filaments.

10 μ M curcumin significantly modulated changes in 187 proteins, 53 of these were induced and 134 repressed (Table 4.2, Appendix 4). None of these proteins were reproduced from the treatment with 1 μ M curcumin. However, beta-adrenergic receptor kinase 1 was suppressed with 10 μ M curcumin and this protein was also suppressed with 1 and 30 μ M resveratrol.

Beta-adrenergic receptor kinase 1 (ADRBK1 or GRK2) was suppressed with 10 μ M curcumin (1.2 fold), and 1 μ M (1.2 fold) and 30 μ M (1.3 fold) resveratrol ($p < 0.05$). Ingenuity analysis also identified NF- κ B as being associated with network modulation following 10 μ M curcumin treatment (Figure 4.3). This network centres around NF- κ B and also the 20S proteasome, similar to resveratrol being clustered into induced and repressed groups.

As mentioned previously, the glutathione pathway was modulated by all three treatments. Glutathione reductase feeds directly into the NF- κ B pathway showing in

the network analysis (Fig 4.1). For curcumin in particular, other redox proteins were identified including glutathione S-transferase P that was induced 1.1 fold ($p < 0.02$). Peroxiredoxin-1, another redox protein was induced 1.1 fold ($p < 0.02$). Ingenuity analysis also highlighted the Nrf2 pathway to be modulated following the curcumin treatment (Figure 4.4).

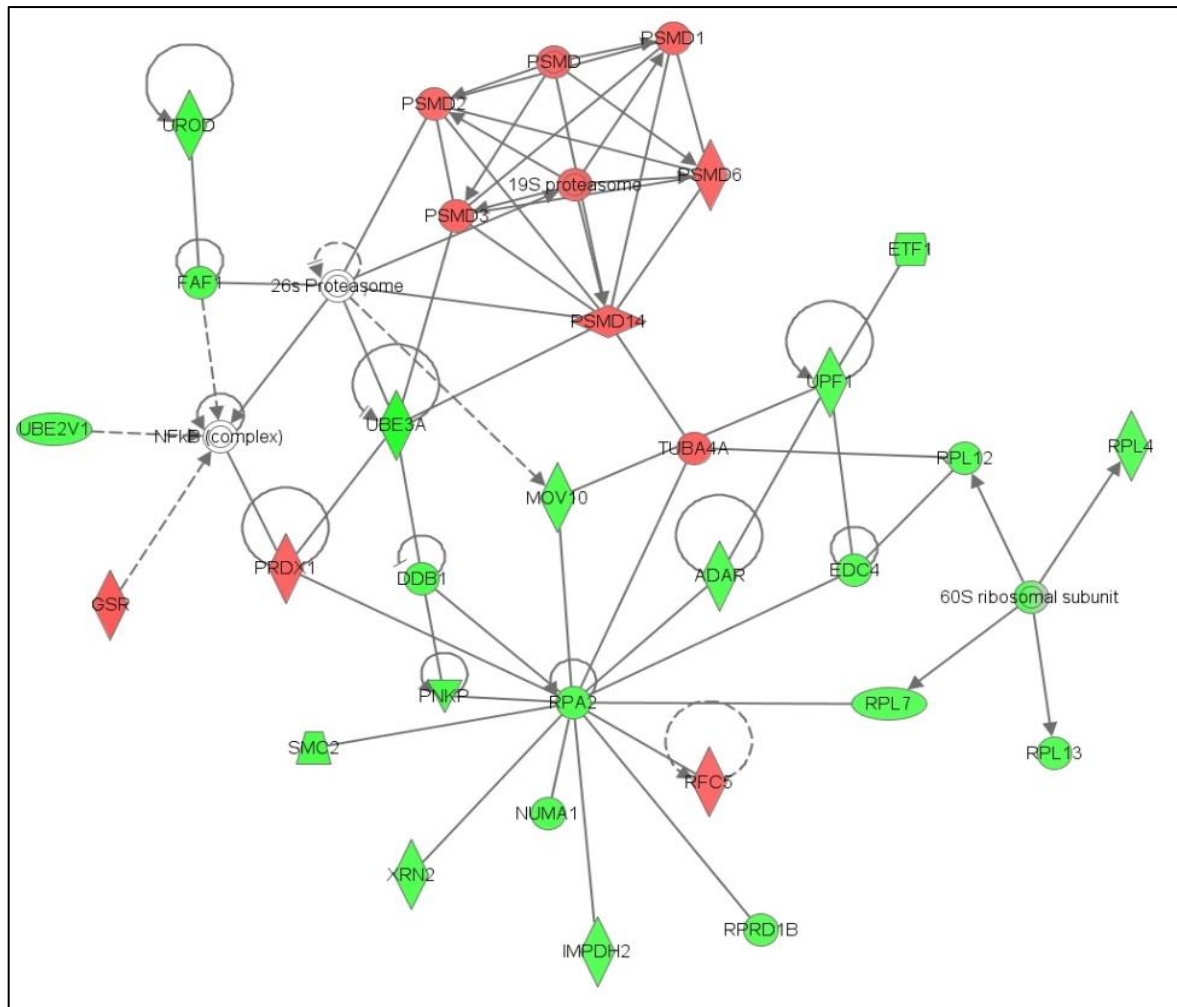


Figure 4.3 – network analysis of proteins modulated following 10 μ M treatment of curcumin. Ingenuity network analysis obtained using the 10 μ M curcumin data set. Red = induced proteins, green = repressed proteins, solid lines = direct interactions, and dashed lines = indirect interactions (full key details can be found in Appendix 5).

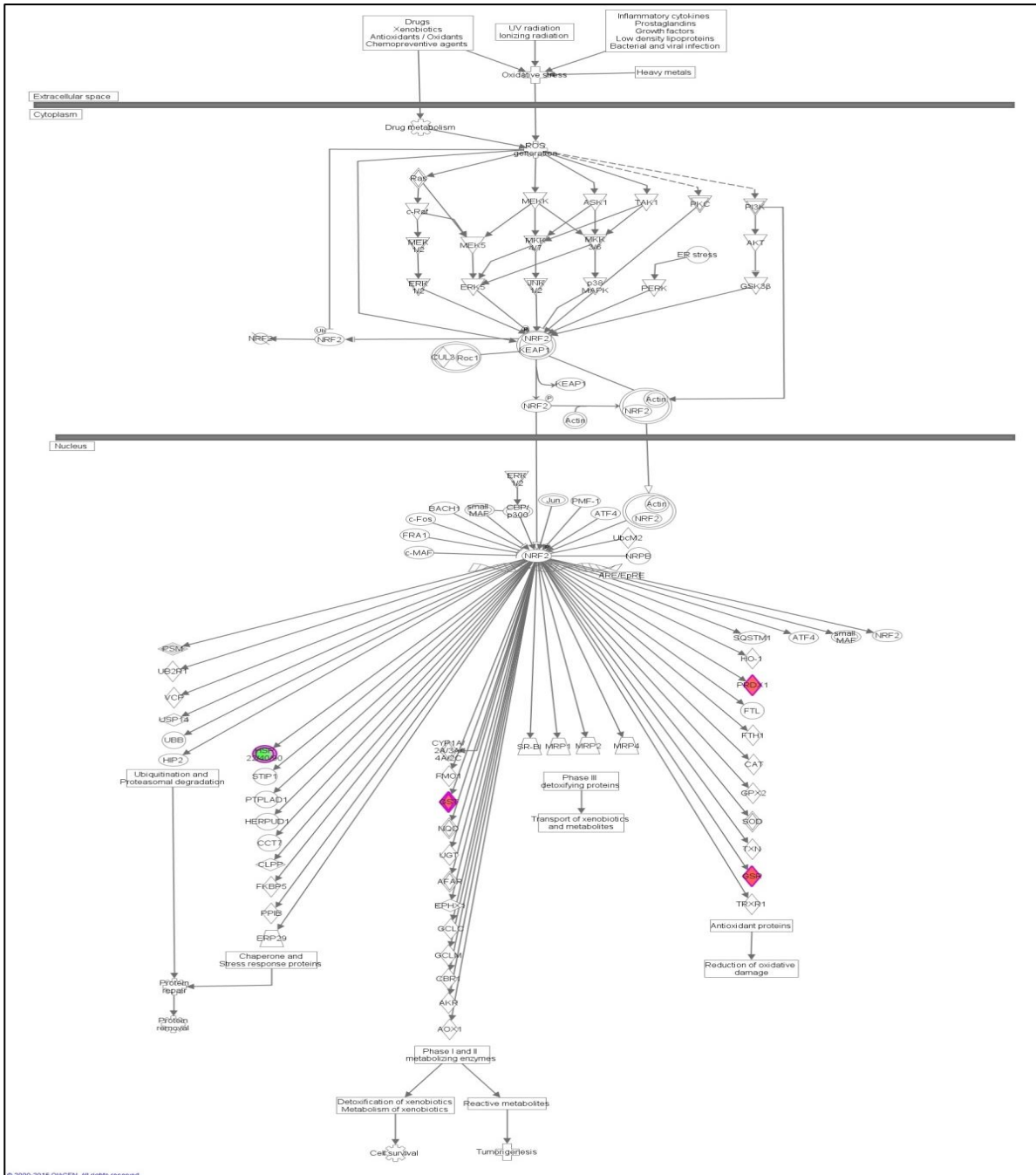


Figure 4.4 – network analysis of proteins modulated following 10µM treatment of curcumin Ingenuity network analysis obtained using the 10µM curcumin data set identified Nrf2 signalling as a modified pathway. Red = induced proteins, green = repressed proteins, solid lines = direct interactions, and dashed lines = indirect interactions (full key details and zoomed in version can be found in Appendix 5).

4.3.8 ISORHAMNETIN: proteins modulated following treatment with isorhamnetin.

83 proteins were modulated by the low dose of isorhamnetin, with 54 repressed and 29 induced. Reactive oxygen species modulator 1 (ROMO) was repressed by isorhamnetin (1.1 fold); ROMO induces ROS production, which is important for cell proliferation but is thought to play a role in oxidative DNA damage. There was also a reduction in Glutathione S-transferase Mu 3 (GSTM3) which was also observed with the higher dose of isorhamnetin, this enzyme is involved in detoxification, but may also play a role in cell signalling¹⁷¹.

Following treatment with 30µM isorhamnetin, 403 proteins were significantly modulated, 227 repressed and 176 induced (table 4.2, appendix 4). There were a number of proteins dose dependently affected, with 35 appearing in both the 1 and 30µM treatment. This included proteins such as hydroxymethylglutaryl-CoA synthase (HMCS2) which decreased from 1.1 fold with 1µM to 1.9 fold with 30µM isorhamnetin ($p < 0.04$). HMCS2 is an enzyme which combines acetyl-CoA with acetoacetyl-CoA to form HMG-CoA, an important transferase for cholesterol biosynthesis. Like the other two polyphenols network analysis isorhamnetin showed proteins clustering around the NF-κB transcription factor (Figure 4.5), showing modulation to the NF-κB signalling pathway to be a common mechanism for all three treatments. There was no direct interaction linked between all the polyphenols

treatments, however glutathione reductase was shown to have indirect links to NF- κ B between all the treatments. Suggesting redox regulation may be central to the changes in NF- κ B signalling.

A number of other redox proteins were also modulated following isorhamnetin treatment included thioredoxin (1.2 fold), thioredoxin reductase 1 (1.2 fold), peroxiredoxin 1 (1.1 fold), peroxiredoxin 2 (1.1 fold), and peroxiredoxin 6 (1.1 fold) ($p < 0.05$). Ingenuity analysis also identified the Nrf2 signalling pathway to be modulated, similar to that of curcumin (Figure 4.6). Thus it appears that all three polyphenol treatments were modulating redox proteins and for curcumin and isorhamnetin the Nrf2 signalling pathway appears to be central to that.

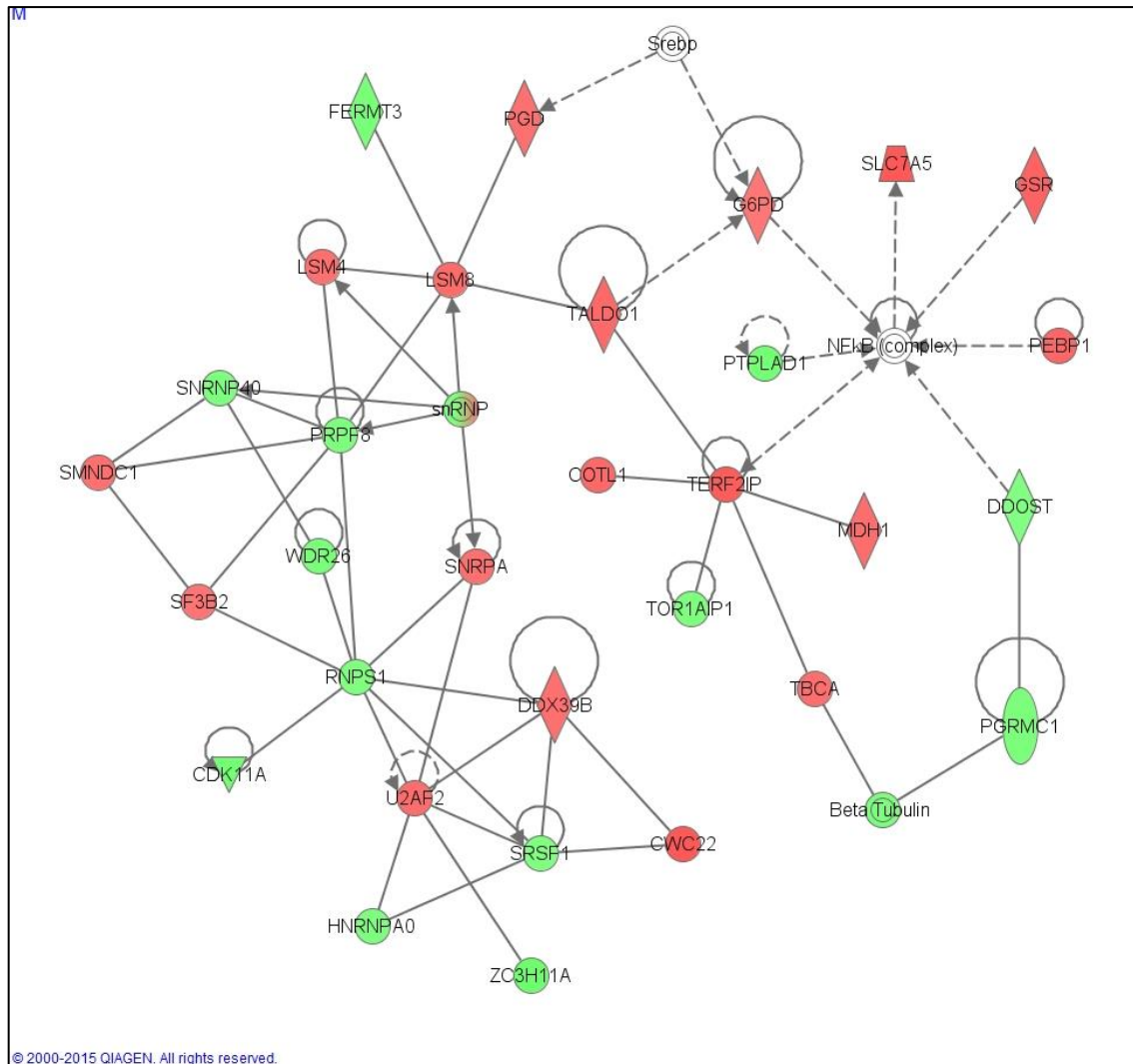


Figure 4.5 – network analysis of proteins modulated following 30µM treatment of isorhamnetin. Ingenuity network analysis obtained using the 30µM isorhamnetin data set. Red = induced proteins, green = repressed proteins, solid lines = direct interactions, and dashed lines = indirect interactions (full key details can be found in Appendix 5).

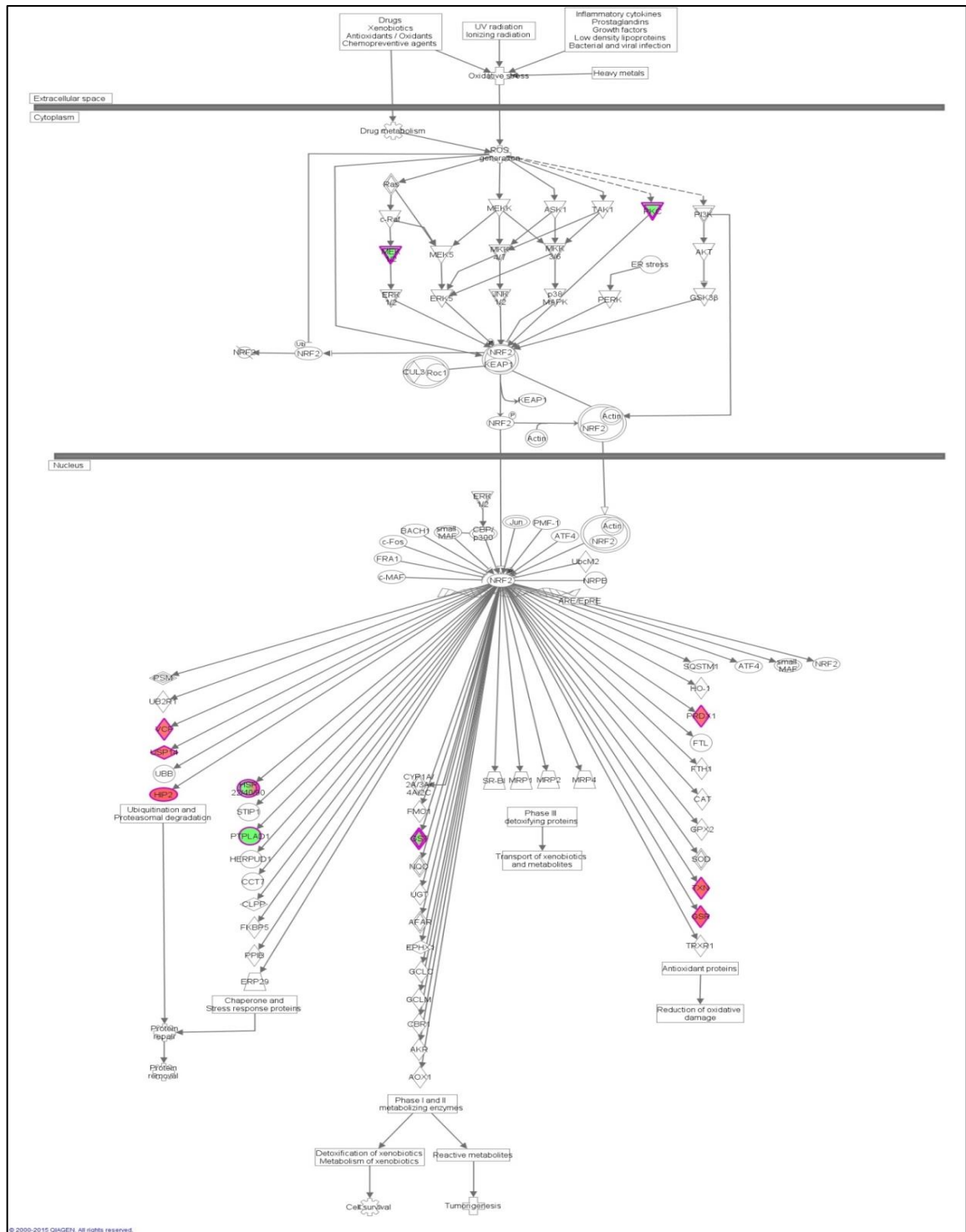


Figure 4.6 – network analysis of proteins modulated following 30µM treatment of isorhamnetin Ingenuity network analysis using 30µM isorhamnetin data set, identifying Nrf2 signalling as a modified pathway. Red = induced proteins, green = repressed proteins, solid lines = direct interactions, and dashed lines = indirect interactions (full key details and zoomed in version can be found in Appendix 5).

4.5 DISCUSSION.

From the screening study conducted in Chapter 3, investigating the anti-inflammatory effects of numerous (poly)phenols, curcumin, isorhamnetin and resveratrol were identified as having the greatest effects modulating inflammatory markers. These compounds were chosen to investigate further using a proteomic approach, treated the Jurkat cells with a low dose (1 μ M) and a high (10 or 30 μ M) of the chosen (poly)phenols (10 μ M was used for the curcumin treatment, as 30 μ M caused significant cell death in the Jurkat cells). By using quantitative proteomics, a number of proteins were found to be significantly modulated following treatments with curcumin, isorhamnetin and resveratrol. Analysis was conducted to identify common proteins and pathways between all the polyphenol treatments. Some of the pathways modulated by the treatments included glutathione homeostasis, oxidative phosphorylation and ribosomal protein expression.

4.5.1 Network analysis of polyphenol proteomics identified NF- κ B to be a central modulated factor.

Though Ingenuity network analysis, the transcription factor NF- κ B was found to be central to all three polyphenol treatments. NF- κ B is a well-defined transcription factor for regulating the expression of cytokines, in Jurkat cells NF- κ B along with AP-1 are mainly responsible for T-cell activation and the induction of pro-inflammatory

cytokines such as TNF α and IL6¹⁷². Other proteins were also identified that interact with NF- κ B, such as GRK2. GRK2 is a G-coupled receptor kinase central in signal transduction cascades; its roles include endocytosis and chemokine signalling, modulating inflammation through the NF- κ B pathway (Fig. 4.7). GRK2 was repressed by 1 and 30 μ M resveratrol and 10 μ M curcumin treatments, which would result in an inhibition of inflammation through NF- κ B. GRK2 is upregulated in patients with chronic heart failure^{173, 174}, along with elevated levels of GRK2 detected in the lymphocytes of patients suffering with heart failure¹⁷⁵. Research is being conducted with GRK2 inhibitors as potential therapeutic treatments¹⁷⁶.

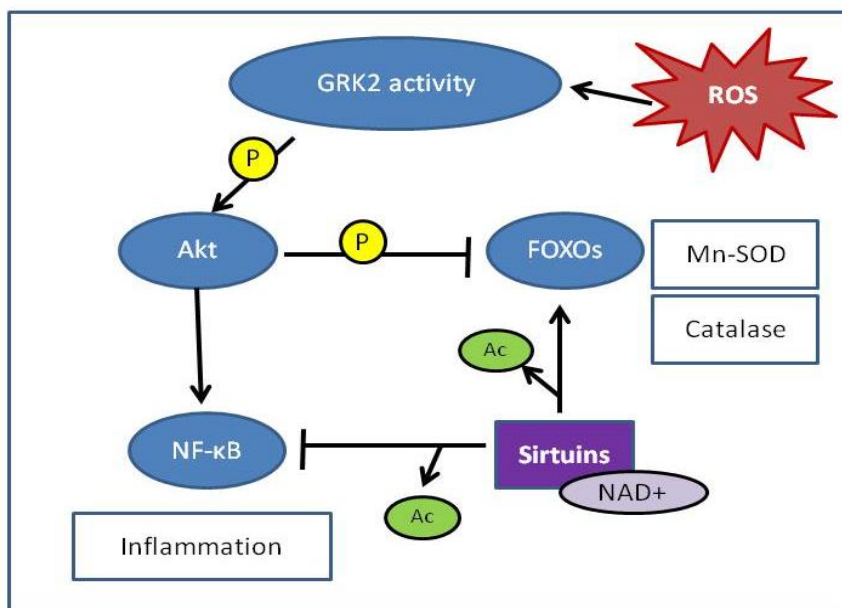


Figure 4.7 – GRK2 signalling in response to ROS leading to activation of NF- κ B, leading to the induction of inflammatory markers. (Modified from Corbi, G *et al* 2013¹⁷⁷).

4.5.2 Unconventional Myosin -1a reduction with curcumin.

Unconventional myosin-1a (MYO1A) had the greatest fold change out of all the three treatments with a 3.6 reduction ($p < 0.05$). This protein functions as an actin-based molecular motor directing the movement of organelles along the actin filaments. However there isn't much literature regarding the role of unconventional myosin and T-lymphocytes, abundance of MYO1A has been demonstrated in CD4 and CD8 T-cells, and has been shown to play a role in nuclear transcription, exocytosis, and vesicular trafficking¹⁷⁸. Other unconventional myosin's have been shown to participate in immune cells functions such as positioning of receptors on the membrane, activation following binding with MHC molecules, directing the secretion of molecules via vesicles (Figure 4.8). MYO1C is involved in transcriptional regulation, it has been shown to associate with RNA polymerase I holoenzyme and ribosomal genes¹⁷⁹. It is unclear what the role is of MYO1A in Jurkat cells, but possible lines of investigation is the reduction in MYO1A is associated with the reduction of cytokine release of IL2 observed with the curcumin, either through the release or possible transcriptional regulation.

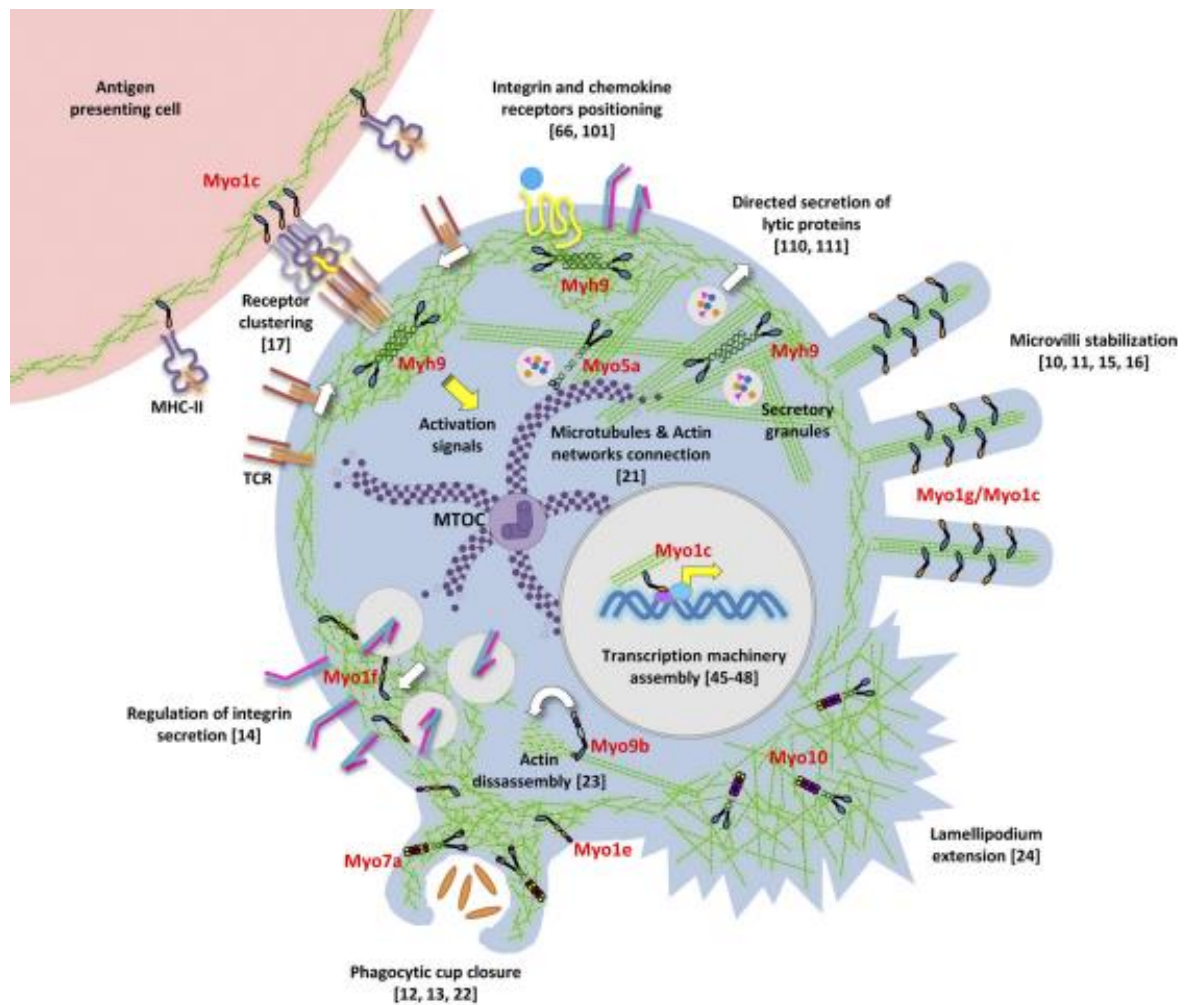


Figure 4.8 – Roles of myosins in immune cells, functions and interactions with structures (Maravillas-Montero et al, 2011)¹⁷⁸.

4.5.3 Polyphenols and oxidative phosphorylation.

As noted previously, a number of oxidative phosphorylation proteins were modulated, including ATPase synthase, cytochrome c oxidase, NADH dehydrogenase, and cytochrome b-c1 complex subunits. A recent paper by van Dijk S J *et al*¹⁸⁰

showed the expression of genes involved in oxidative phosphorylation were down-regulated in subjects with a Mediterranean diet (low in saturated fats and high in fruits and vegetables) and for some of the proteins identified in this study, the gene expression was also found to be altered in the Mediterranean diet study. These proteins included V-type proton ATPase subunit H, and subunit A, NADH dehydrogenase [ubiquinone] iron-sulfur protein 8, cytochrome c oxidase subunit 4 isoform 1, and cytochrome b-c1 complex subunit 7. This shows the potential for these dietary polyphenols to lower levels of oxidative phosphorylation.

4.5.4 Modulation of redox homeostasis with the polyphenol treatments.

Glutathione reductase was a common protein modulated by all three polyphenol treatments and is an important regulator of redox homeostasis in the cell. Glutathione reductase maintains the levels of reduced glutathione in the cytosol and was induced by the treatments. Glutathione reductase catalyses the reduction of oxidised glutathione (GSSG) to reduced glutathione (GSH), and is therefore vital in maintaining the redox homeostasis of the cell, responding to oxidative stress. Previous research has shown increases in glutathione reductase with polyphenols, for example mice fed a diet containing 2% (v/v) curcumin for 30 days showed increased glutathione reductase activity by 179% in the liver and 134% in the kidneys¹⁸¹, along with increased activity in other redox-related proteins including

glutathione peroxidase, glucose-6-phosphate dehydrogenase and catalase. Proteomics analysis also identified some of these redox-related proteins in this study.

These redox-related proteins identified including glutathione transferases, thioredoxin, and peroxiredoxins. Network analysis revealed a number of proteins involved in glutathione metabolism pathway (Table 4.6). Isorhamnetin had the greatest effect on this pathway compared with the other treatments, with at least 6 other redox proteins being identified (Figure 4.8, Table 4.6). This included 6-phosphogluconate dehydrogenase (PGD) and Glucose-6-phosphate 1-dehydrogenase (G6PD) which were both increased by 30 μ M isorhamnetin and have reducing capabilities to convert NADP^+ to NADPH. For glutathione reductase to be able to convert GSSG to GSH, NADPH is required for this reaction. Isocitrate dehydrogenase also converts NADP^+ to NADPH; this enzyme was increased by the 1 μ M curcumin treatment although a reduction was observed with the 30 μ M isorhamnetin treatment. This may be explained by the fact that isorhamnetin has already increased NADPH production via PGD or G6PD, therefore IDH1 was not stimulated, or another possibility may be the location of these enzymes. IDH1 is found in the cytoplasm as well as in peroxisomes, an organelle specialising in oxidative reactions. It could be that this protein is localising in different regions of the cell upon stimulation with the treatments, accounting for the opposing effects observed with the different treatments. Studies have shown that curcumin can activate mitochondrial isocitrate dehydrogenase in colon cancer cell line, possibly by modifying the sulphhydryl groups on the enzyme¹⁸².

Glutathione S-transferases were also modulated following the polyphenol treatments; these proteins catalyse the conjugation of GSH with various exogenous and endogenous hydrophobic electrophiles. Glutathione S-transferases serve to detoxify the cellular environment, but also have signalling capabilities. Glutathione S-transferase P (GSTP1) was induced by both 10 μ M curcumin and 30 μ M isorhamnetin, this category of glutathione S-transferases seem to have a number of signalling properties. GSTPs can bind to JNK, preventing its activation, which would lead to apoptosis; it also acts as a negative regulator of I- κ B kinase/NF- κ B signalling, stress – activated MAPK cascade and TNF α production. Curcumin has been shown to increase the gene expression of GSTP1 in humans liver cells following treatment with 20 μ M for 8h¹⁸³. Quercetin which is structurally similar to isorhamnetin has also been shown to increase the GST activity in rat liver, when fed a 2g/kg diet enriched with quercetin and catechin¹⁸⁴.

Finally, another protein feeding into the glutathione metabolism pathway is spermidine synthase, which contributes to the biosynthesis of spermidine. Spermidine is a polyamine which aids in the survival of the cell by maintaining membrane potential and regulating gene expression through chromatin regulation. This protein was induced by the 30 μ M isorhamnetin treatment; Isorhamnetin had a number of effects on this pathway, predominantly having a positive effect on the increase in reduced glutathione, protecting the cell from oxidative stress.

GSR	Glutathione reductase	↑ cur, iso, res
TXNDC12	Thioredoxin domain-containing protein 12	↓ iso
IDH1	Isocitrate dehydrogenase [NADP]	↓ iso ↑ cur
PGD	6-phosphogluconate dehydrogenase, decarboxylating	↑ iso
G6PD	Glucose-6-phosphate 1-dehydrogenase	↑ iso
GSTK1	Glutathione S-transferase kappa 1	↑ res
GSTM3	Glutathione S-transferase Mu 3	↓ iso
GSTP1	Glutathione S-transferase P	↑ cur, iso
SRM	Spermidine synthase	↑ iso

Table 4.6 – Key for glutathione metabolism pathway diagram on following page and a summary of treatment effects. Cur = curcumin, Iso = isorhamnetin, and Res = resveratrol.

The network analysis also identified the Nrf2 signalling pathway to be modulated with both curcumin and isorhamnetin (Figures 4.4 and 4.6). Nrf2 is a key regulator of the glutathione antioxidant pathway and feeds into the changes observed in the other redox proteins. As Nrf2 is a transcription factor which is responsible for the activation of antioxidant gene expression such as glutathione reductase, glutathione peroxidase, glutathione transferase, thioredoxin, peroxiredoxin, glucose-6-phosphate dehydrogenase and NAD(P)H quinone oxidoreductase 1¹⁸⁵. Polyphenols have previously been shown to modulate Nrf2 activation and for example, isorhamnetin protects against oxidative stress by activating Nrf2 in liver cells¹⁸⁶. With all these changes in redox proteins, investigating Nrf2 activation by these compounds is the next step in understanding the mechanisms of action of polyphenols and to explore in detail the changes to glutathione pathways (Figure 4.9, Table 4.6).

Due to the small fold changes observed and some high q-values with a number of the proteins identified; these statistical changes with the treatments should be taken with caution. Therefore further analysis into the changes in glutathione proteins will be examined more in-depth with other methods.

CHAPTER 5

ANALYSIS OF GLUTATHIONE MODIFICATION BY POLYPHENOL TREATMENT OF JURKAT T-LYMPHOCYTES.

5.1 INTRODUCTION

5.1.1 Ageing and elevated levels of oxidative stress.

Ageing has been associated with dysregulation of the immune system characterised by chronic inflammation¹⁸⁷, increases in baseline oxidative stress, and elevated levels of reactive oxygen species¹⁸⁸. The main source of ROS generation is in the mitochondria, as part of the electron transport chain¹⁸⁹. These molecules are important for cellular signalling¹⁹⁰, however, aberrant ROS production has been observed with ageing, results in the accumulation of oxidative damage to vital cellular components like DNA, proteins and lipids¹⁹¹, molecules important for cell survival. A number of proteins are responsible for maintaining the redox homeostasis of the cell, using antioxidant enzymes such as superoxide dismutase (O_2^- to H_2O_2), catalase and glutathione peroxidase (H_2O_2 to H_2O)¹⁹². Imbalances between antioxidant capabilities and oxidant production of the cell will lead to oxidative stress and in the elderly may aid the progression of age-related diseases such as arthritis¹⁹³, diabetes¹⁹⁴ and Alzheimer's¹⁹⁵.

5.1.2 Antioxidant proteins maintaining redox homeostasis in the cell.

Antioxidant proteins and enzymes are the major cellular protection against oxidants, maintaining the redox status of the cell. These antioxidant proteins help remove harmful oxidants by converting them into molecules such as H_2O . The major antioxidant enzymes include superoxide dismutase (SOD), catalase, glutathione peroxidase, thioredoxin and peroxiredoxins. In Chapter 4, proteomics identified a

number of these redox proteins induced by the polyphenol treatments. Catalase was induced by the 30 μ M resveratrol treatment, 10 μ M curcumin increased peroxiredoxin-1 and 30 μ M increased thioredoxin in the Jurkat T lymphocytes compared with DMSO treated control. Glutathione reductase was a common redox protein induced by all three polyphenol treatments. Suggesting that glutathione homeostasis is a central to component to the polyphenols mechanism of action.

5.1.3 Polyphenols regulating cellular redox mechanisms.

(Poly)phenols have been shown to regulate cellular redox mechanisms, in particular the glutathione system in previous studies. Resveratrol has been shown to significantly increase the glutathione content of rat astrocytes treated for 24 h with 25 and 50 μ M resveratrol compared with untreated controls¹⁹⁶. Resveratrol has also been shown to increase the protein expression of glutamate cysteine ligase, glutathione peroxidase-1 and glutathione reductase in human coronary artery endothelial cells¹⁹⁷. Supplementing the diet of mice with curcumin (2%, w/v) for 30 days significantly increased the activity of glutathione reductase, glutathione peroxidase, glucose-6-phosphate dehydrogenase and catalase in both the liver and the kidneys¹⁹⁸. In cerebellar granule neurons (CGNs) from rats, curcumin also significantly increased the activity of glutathione reductase (1.4 fold), glutathione S-transferase (2.3 fold), and superoxide dismutase (5.2 fold) with 24h treatments with curcumin and additionally observed a significant increase in the levels of GSH by 14.3 fold, with 30 μ M curcumin¹⁹⁹. This study also noted that curcumin could activate

nuclear factor (erythroid-derived 2)-like 2 (Nrf2) translocation to the nucleus of the CGNs cells, allowing the activation of antioxidant gene expression.

In this chapter, the ability of polyphenols to modulate antioxidant proteins such as glutathione reductase, along with the gene expression of glutathione peroxidase, glutathione synthetase and glutamate-cysteine ligase will be assessed. Intracellular levels of GSH will also be measured and changes to Nrf2 transcriptional activation will be studied.

5.2 AIMS

The aim was to investigate the changes to the glutathione pathway previously identified by proteomics to be modulated by all three treatments (Chapter 4) and to validate the data produced by quantitative proteomics by other methods of protein and gene expression analysis. It was also intended to explore the signalling pathway regulating antioxidant gene expression by evaluating changes to the transcription factor Nrf2.

5.3 RESULTS.

5.3.1 Glutathione reductase protein expression with polyphenol treatments over time.

Glutathione reductase was one of the proteins identified through proteomics to be significantly modulated by all three of the (poly)phenols, with curcumin increased by

1.2 fold, resveratrol by 1.1 fold and isorhamnetin by 1.2 fold ($p < 0.05$). Western blot analyses were used to examine changes to glutathione reductase following 48 h treatment with 10 μ M curcumin, 30 μ M isorhamnetin and 30 μ M resveratrol (Table 4.3). No significant changes were observed with the three treatments at 48 h following treatment (Fig. 5.1A).

The initial western blot analysis showed no significant differences between the three (poly)phenol treatments with 3 replicates. This experiment was repeated, focusing on the isorhamnetin treatment and increasing the number of replicates to 6, but again no significant changes were observed with isorhamnetin treatment (Fig. 5.1B). Therefore, further investigations at other time-points were trailed to see if significant increases could be observed with the polyphenol treatments. A significant increase in glutathione reductase following treatment with isorhamnetin, curcumin and resveratrol (Fig. 5.2) at the 24 h time-point was observed using western blot analysis.

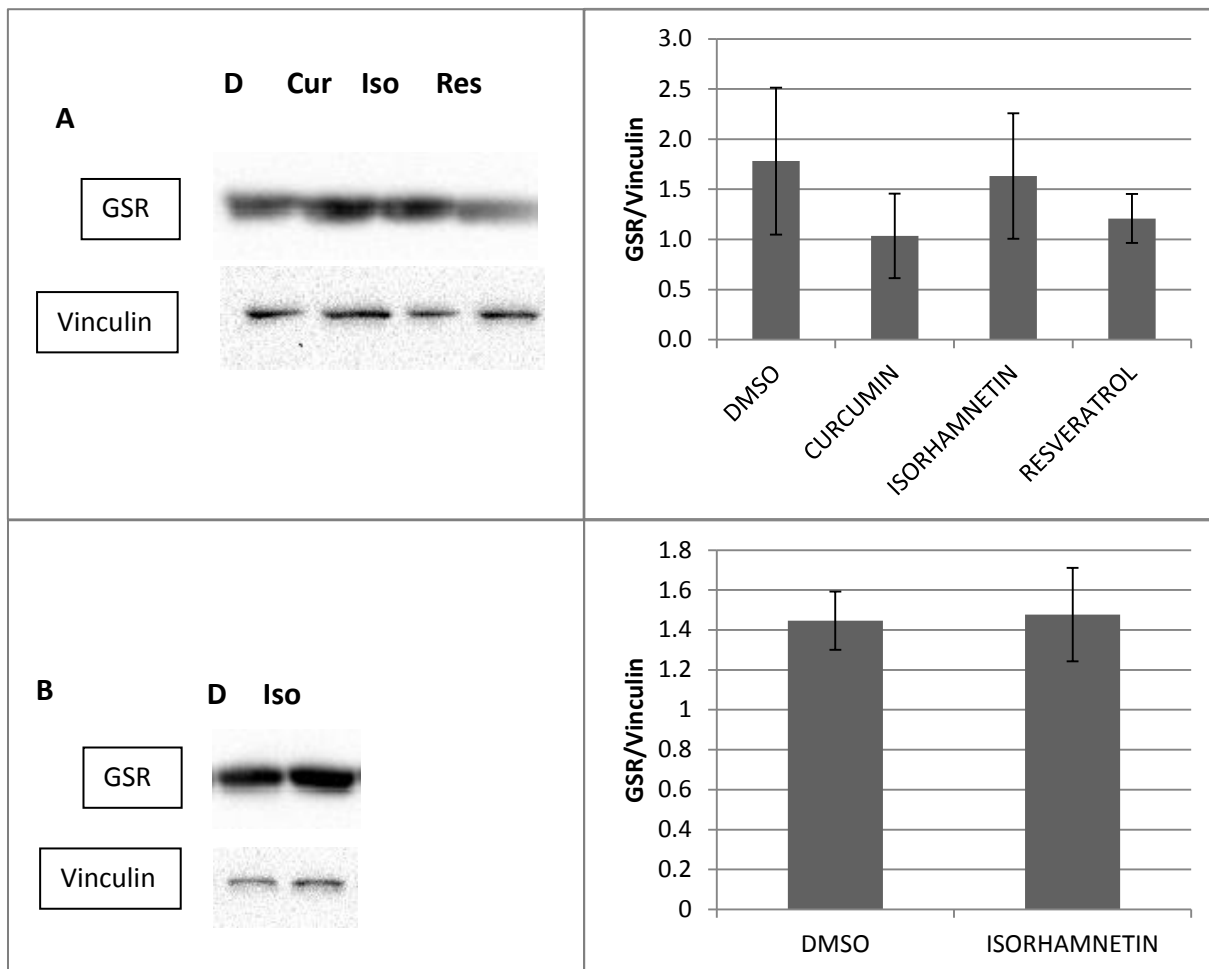


Figure 5.1 – Glutathione reductase protein expression after 48 h treatment with curcumin, isorhamnetin and resveratrol (representative blots). A) Changes in glutathione reductase (GSR) in Jurkat cells following 48 h treatment with 10 μ M curcumin (Cur) and 30 μ M isorhamnetin (Iso) and resveratrol (Res) using anti-GSR (58kDa) compared with DMSO (D) treated control. Data normalised to vinculin ($n=3$). B) Changes in glutathione reductase (GSR) in Jurkat cells following 48 h treatment with 30 μ M isorhamnetin (Iso) using anti-GSR (58kDa) compared with DMSO (D) treated control. Data normalised to vinculin ($n=6$).

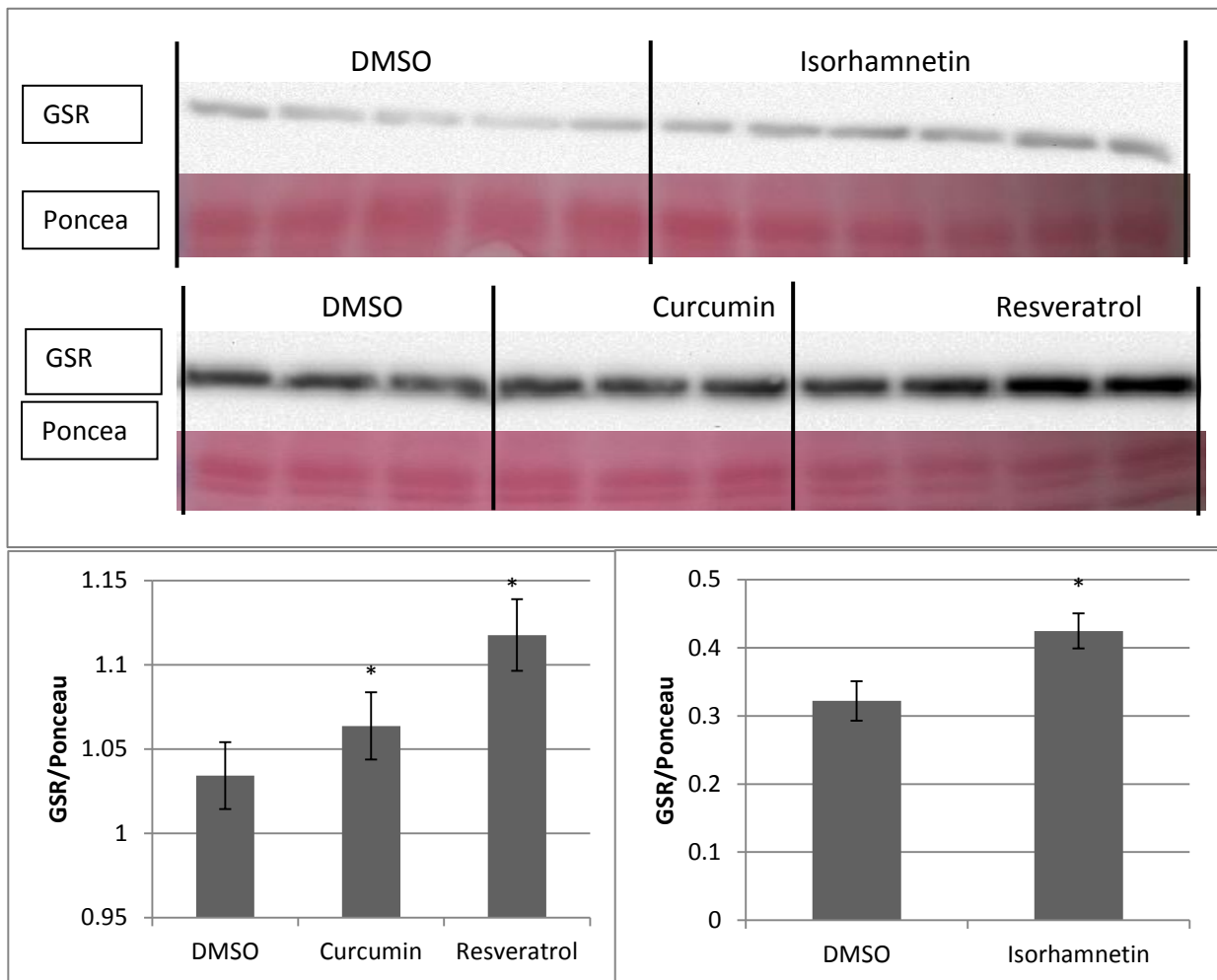
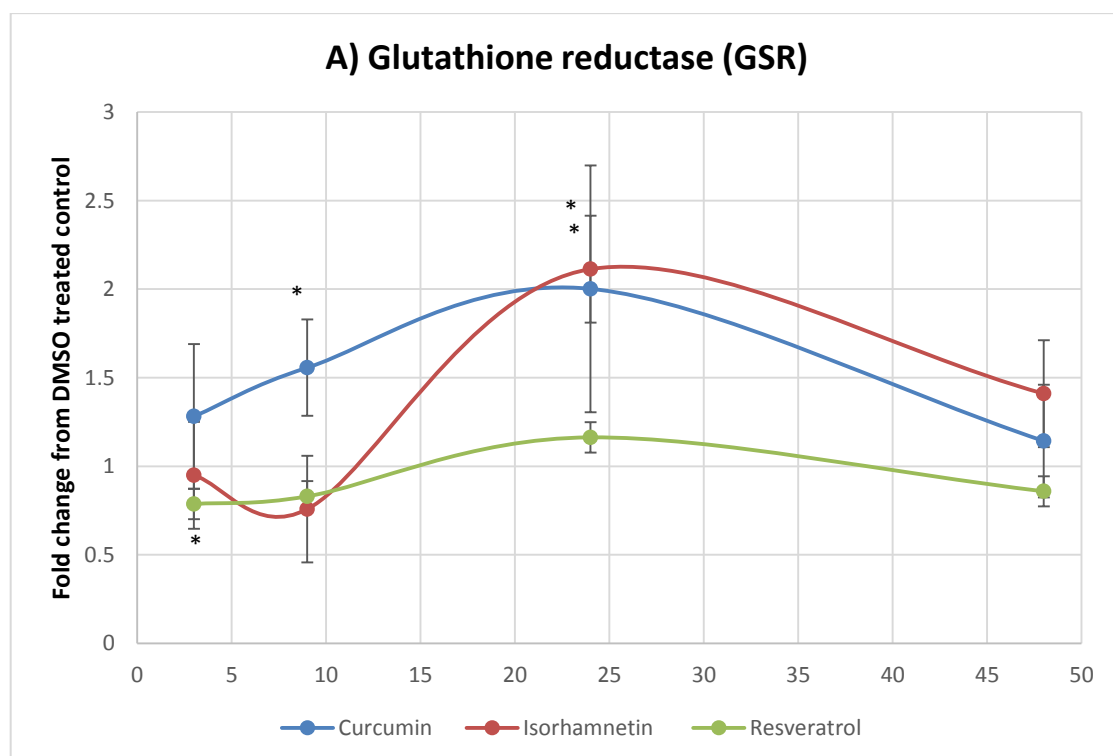


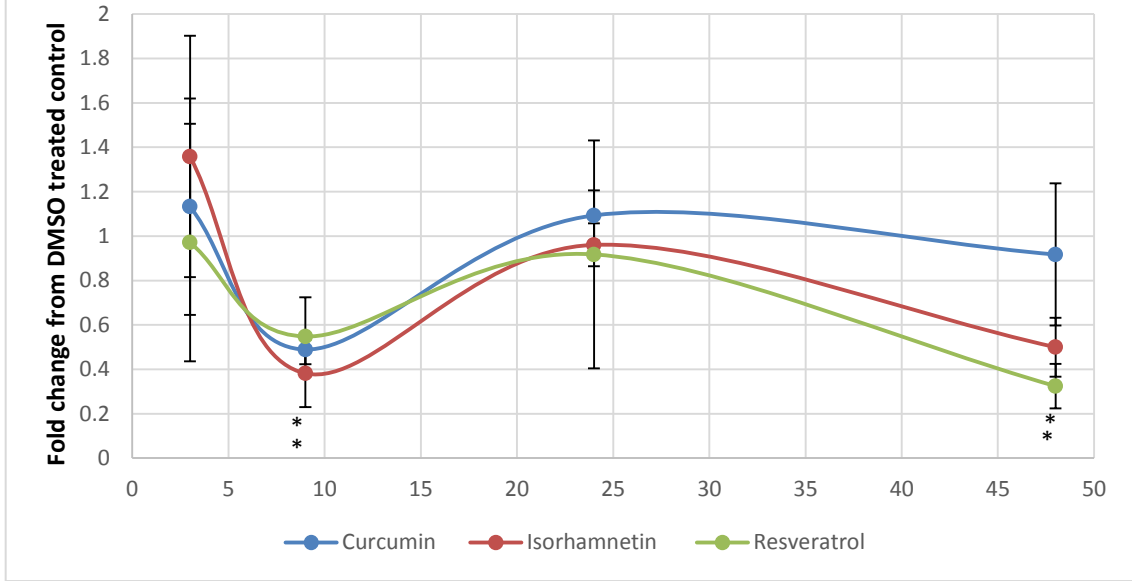
Figure 5.2 – Glutathione reductase protein content following 24 h treatment with isorhamnetin, curcumin and resveratrol (representative blots). Western blot analysis of changes in GSR in Jurkat cells following 24 h treatment with 10 μ M curcumin and 30 μ M isorhamnetin and resveratrol compared with DMSO treated control. Data normalised to Ponceau stain ($n=3$, * $p < 0.05$).

5.4.2 Analysis of glutathione reductase, glutathione synthetase, glutathione peroxidase, and glutamate—cysteine ligase gene expression.

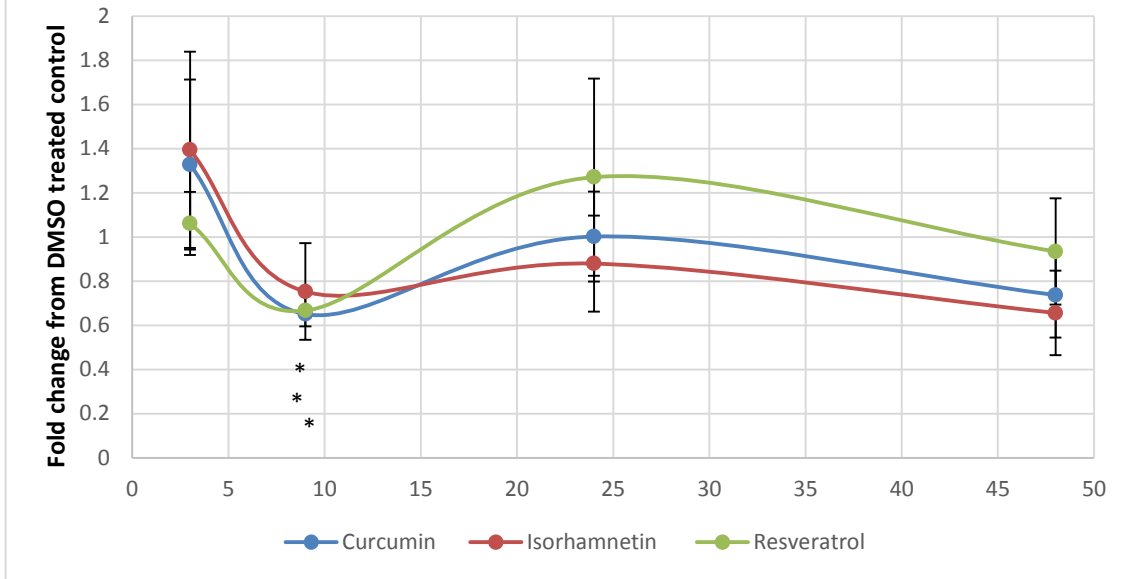
Since changes to protein levels of glutathione reductase were not seen at the 48 h time-point but were detected at the 24 h time-point, a time-course experiment was conducted, this evaluated the gene expression of glutathione reductase, along with the other glutathione homeostasis proteins, glutathione synthetase and glutamate—cysteine ligase (that are enzymes involved in the biosynthesis of glutathione, and also glutathione peroxidase, which catalyses the reaction of GSH with hydrogen peroxide).



B) Glutathione peroxidase (GPx1)



C) Glutathione synthetase (GSS)



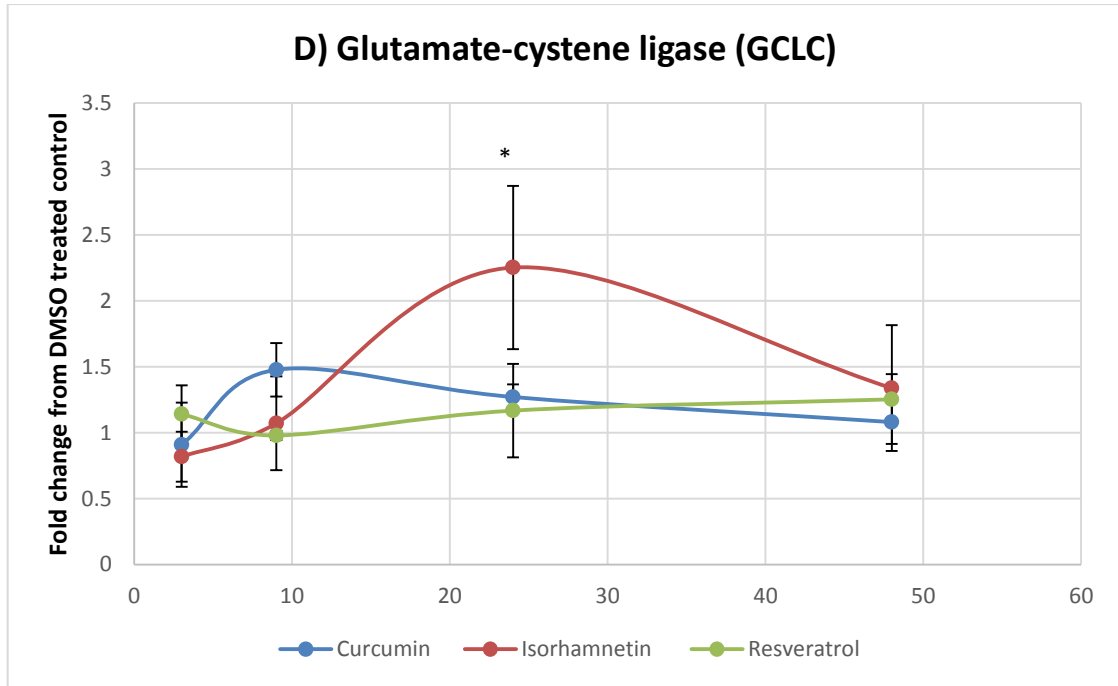


Figure 5.3 – Time-course of treatments with curcumin, isorhamnetin and resveratrol on the gene expression of GSR, GPx1, GSS, and GCLC. Analysis of gene expression of glutathione reductase (GSR), glutathione peroxidase 1 (GPx1), glutathione synthetase (GSS) and glutamate-cysteine ligase (GCLC) following treatment with 10 μ M curcumin, 30 μ M isorhamnetin and resveratrol treatment over a time-course of 3, 9, 24, and 48 h in Jurkat T-lymphocytes. Data are expressed as fold change from DMSO treated control (1), data normalised to TATA binding protein (TBP). [Mean \pm SEM, $n = 3$, * p -value < 0.05]

Significant increases in glutathione reductase mRNA were observed following isorhamnetin and curcumin treatment showed a doubling at 24h time-point (Fig. 5.3A). Significant increases in GCLC mRNA (Fig. 5.3D) were also observed at the 24h time-point with isorhamnetin and significant decreases in GSS mRNA (Fig. 5.3C) were observed at the 9h time-point following all the polyphenols treatments. Significant reductions in GPx1 mRNA (Fig. 5.3B) were observed at the 9h time-point with isorhamnetin and curcumin and again at 48h with resveratrol and isorhamnetin.

5.4.3 Glutathione modulation by (poly)phenols.

The significant increase in glutathione reductase protein concentration and gene expression, together with increases in glutamate-cysteine ligase mRNA with isorhamnetin treatment, suggested an effect of the polyphenols on cellular glutathione at the 24h time point. Jurkat T-lymphocytes were treated with various concentrations of the (poly)phenols for 48 h and intracellular levels of glutathione were measured using a spectrophotometric kinetic assay, as described in Methods section 2.2.10.

Figure 5.4A, shows a significant increase in the intracellular concentration of reduced glutathione following treatment with 10 μ M curcumin. This effect was not observed with the 30 μ M isorhamnetin or 30 μ M resveratrol treatments and both significantly reduced the cellular concentration of reduced glutathione (Fig 5.4B and C). Figure 5.5, shows levels of oxidised glutathione following 48h polyphenol treatment, a significant increase in GSSG was observed with 10 μ M curcumin and no significant changes were observed with 30 μ M isorhamnetin and resveratrol treatments. Levels of oxidised glutathione made up a maximum of 4.85% of the total glutathione present.

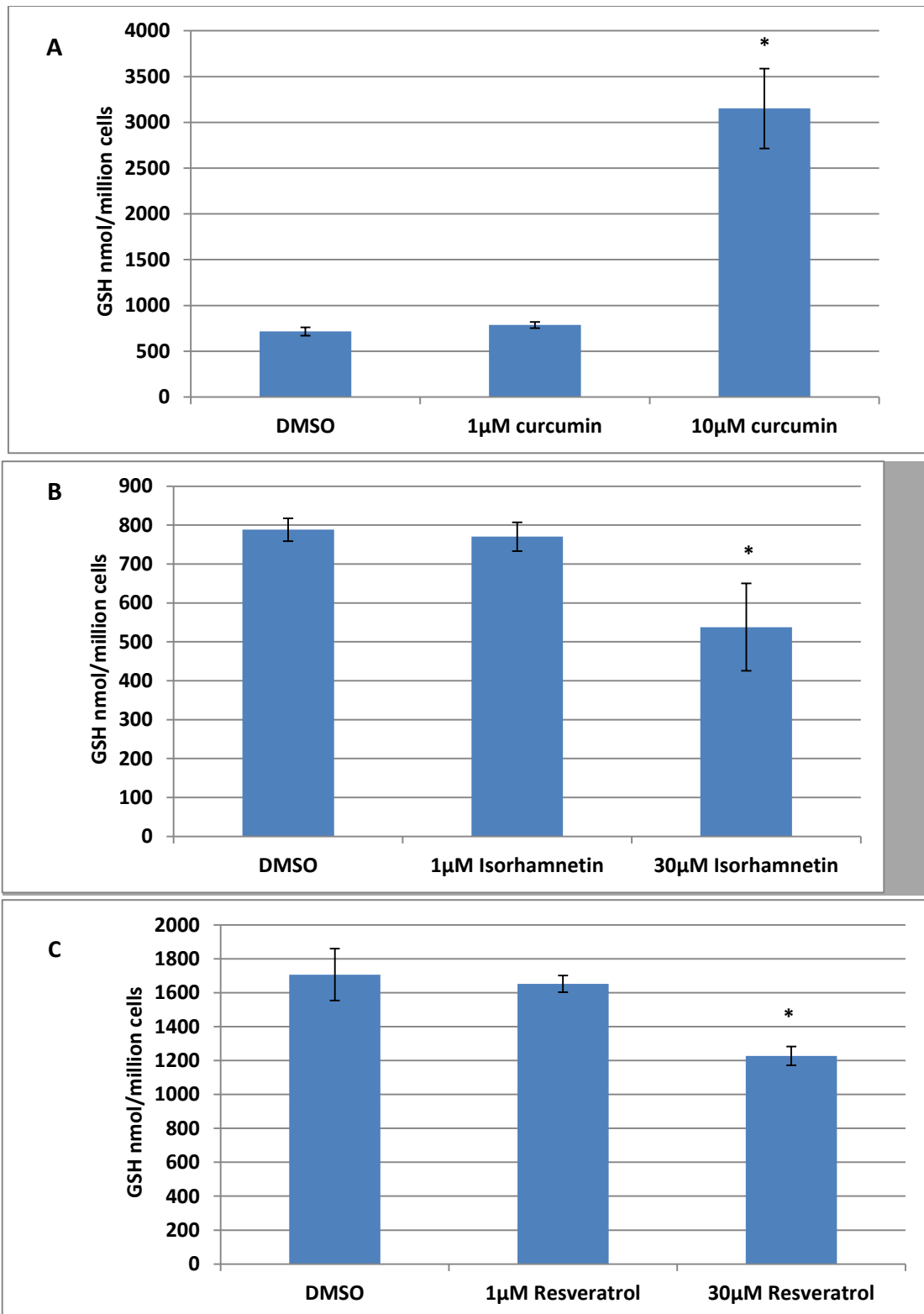


Figure 5.4 – Concentrations of intracellular reduced glutathione (GSH) in nmol/million cells from Jurkat cells treated with A) 1 and 10µM curcumin, B) 1 and 30µM isorhamnetin and C) 1 and 30µM resveratrol for 48 h, compared with DMSO treated control, [Mean ± SEM, $n = 4$, T-test * $p < 0.05$].

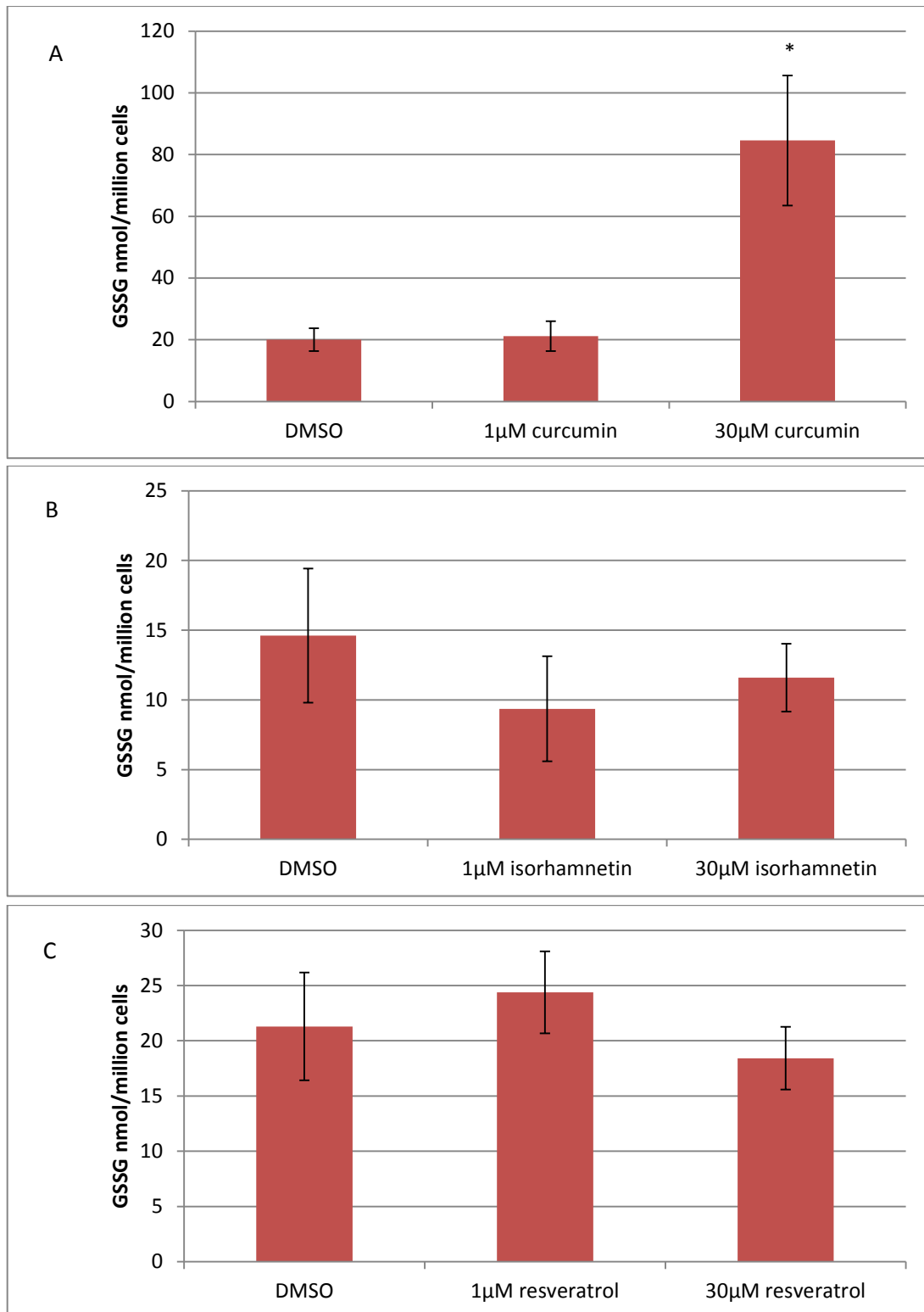


Figure 5.5 – Concentrations of intracellular oxidised glutathione (GSSG) in nmol/million cells from Jurkat cells treated with A) 1 and 10μM curcumin, B) 1 and 30μM isorhamnetin and C) 1 and 30μM resveratrol for 48 h, compared with DMSO treated control, [Mean ± SEM, $n = 4$, T-test * $p < 0.05$].

5.4.4 Curcumin and isorhamnetin increase Nrf2 activation.

A DNA binding assay was used to directly measure *in vitro* protein-DNA interaction, using dsDNA able to bind the transcription factor Nrf2 (Methods 2.2.15). Jurkat cells were treated for 48 h with a low or high doses of (poly)phenols and a positive control of tert-butylhydroquinone (t-BHQ). Both curcumin and isorhamnetin significantly increased Nrf2 activation compared with DMSO vehicle control (Fig. 5.6). There is a steady increase in Nrf2 activation with isorhamnetin, whereas 1 and 10 μ M curcumin increase Nrf2 activation to the same degree. Resveratrol had no significant effects on Nrf2 activation.

A time-course experiment of Nrf2 activation showed significant Nrf2 activation from 3h to 48h with isorhamnetin. Curcumin also showed a significant fold change in Nrf2 activation at both 9h and 48 h compared with the DMSO treated control (Fig. 5.7).

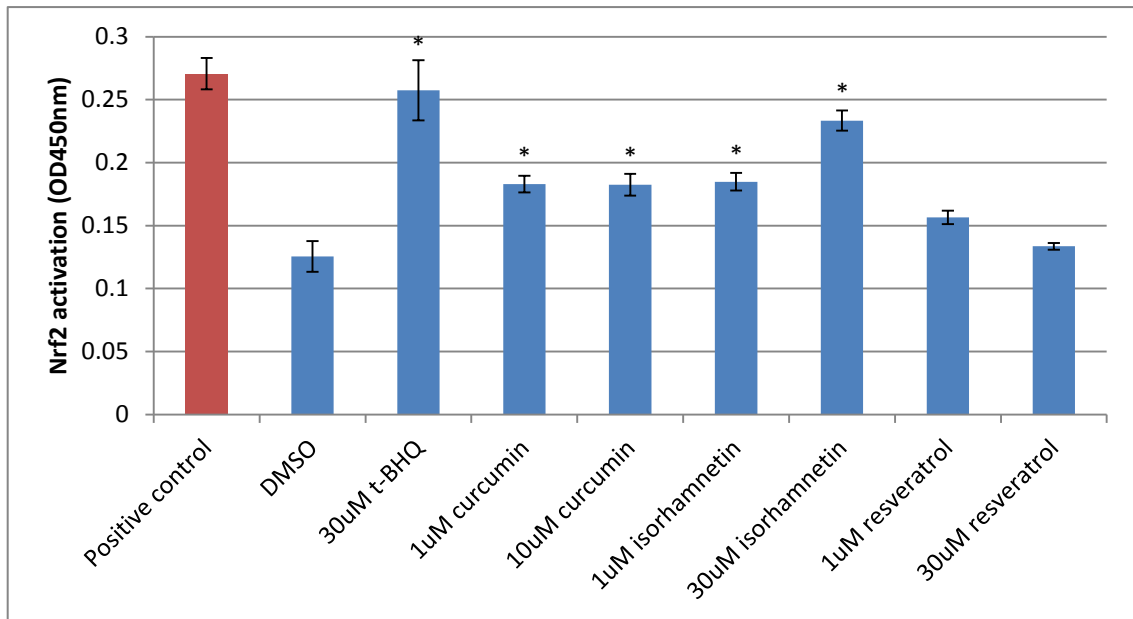


Figure 5.6 – DNA binding assay for Nrf2 activation in Jurkat cell samples following treatment with curcumin, resveratrol, and isorhamnetin for 48 hr. Positive control – Nrf2 protein provided by kit, DMSO vehicle control, tert-butylhydroquinone (t-BHQ) positive control added to cell in culture. (Mean \pm SEM, $n=5$, * $p < 0.05$).

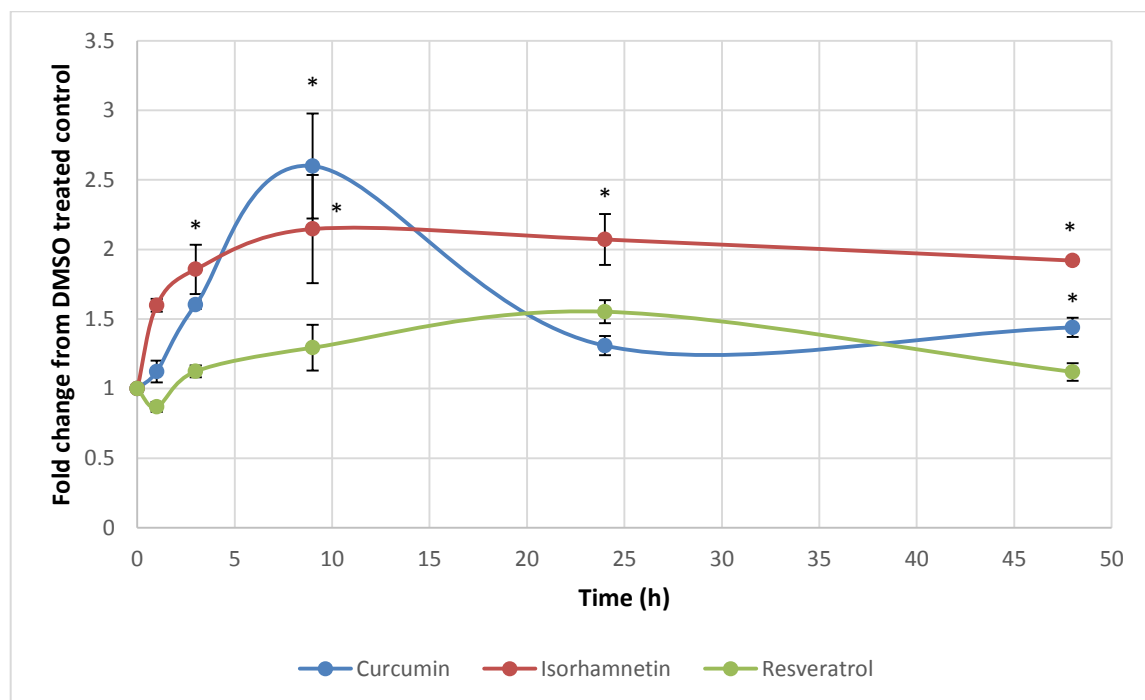


Figure 5.7 – DNA binding assay for Nrf2 activation in Jurkat cell samples following treatment with 10µM curcumin, 30µM resveratrol, and 30µM isorhamnetin for 1, 3, 9, 24, and 48 h. Data presented as a fold change from DMSO treated control valued at 1. (Mean \pm SEM, $n=5$, * $p < 0.05$).

5.3.5 Immunoblotting for Nrf2, and phosphorylated Nrf2 with isorhamnetin treatment.

Isorhamnetin had the greatest effects in Nrf2 activation assessed using the DNA binding assay. Figure 5.8A, shows an increase in protein expression of both Nrf2 and phosphorylated Nrf2. Significant increases were noted at the 24h time-point for Nrf2 following treatment with isorhamnetin compared with DMSO treated control (Fig. 5.8B). The ratio of phosphorylated Nrf2 to Nrf2 is 1.3:1 (1h), 0.9:1 (3h), 1:1 (9h) and 0.6:1 (48h).

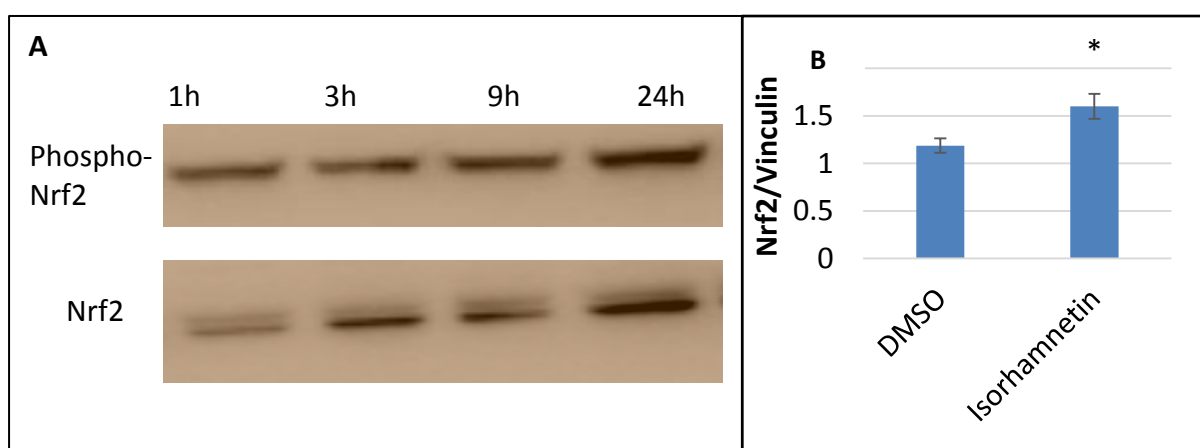


Figure 5.8 – A) Western blot for Phosphorylated- Nrf2 and Nrf2 following treatment with isorhamnetin for 1, 3, 9, and 24h in Jurkat T-lymphocytes. B) Densitometry analysis of Nrf2 following 24h treatment with isorhamnetin normalised to vinculin and compared with DMSO treated control. ($n=3$, * $p < 0.05$).

5.3.6 Inhibition of nuclear translocation of Nrf2 by the use of Ochratoxin A.

To determine how these changes to redox proteins might be linked to the changes in cytokine release already observed in Chapter 3. Experiments were

undertaken to inhibit Nrf2 and measure cytokine release following treatment with isorhamnetin. Ochratoxin A (OTA) was used to inhibit the translocation of Nrf2 into the nucleus²⁰⁰. Figure 5.9, shows Jurkat cell viability with time following increasing doses of OTA from 1 to 30 μ M.

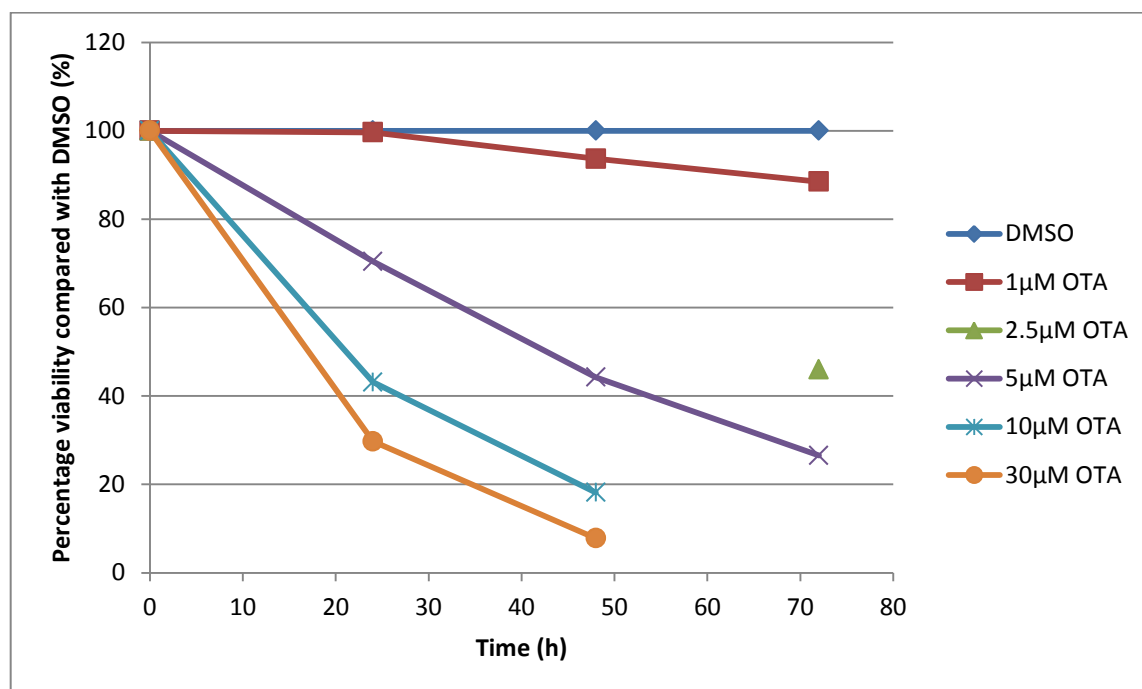


Figure 5.9 – Jurkat cell viability following treatment with 1, 2.5, 5, 10 and 30 μ M Ochratoxin A over a 72h time period. ($n=3$).

Nuclear and cytoplasmic extracts were also taken at the 72h time-point and western blotting used to measure the abundance of Nrf2. Figure 5.10A, shows western blot analysis of experiment using 1 and 2.5 μ M OTA at 72h. There was a trend to an increase in Nrf2 in the cytoplasm and decrease in the nucleus with 2.5 μ M OTA treatment (Fig. 5.10B and C). Further studies were undertaken at shorter time-point (24h, 30min pre-treatment and addition OTA at 12h time-point) and showed

significant inhibitions of Nrf2 translocation to the nucleus with 5 μ M OTA (Fig. 5.11A). Figure 5.11B, shows a slight reduction in the Nrf2 content in the nucleus with 5 μ M OTA treatment after 30min, although this inhibition was not statistically significant compared with the DMSO treated control.

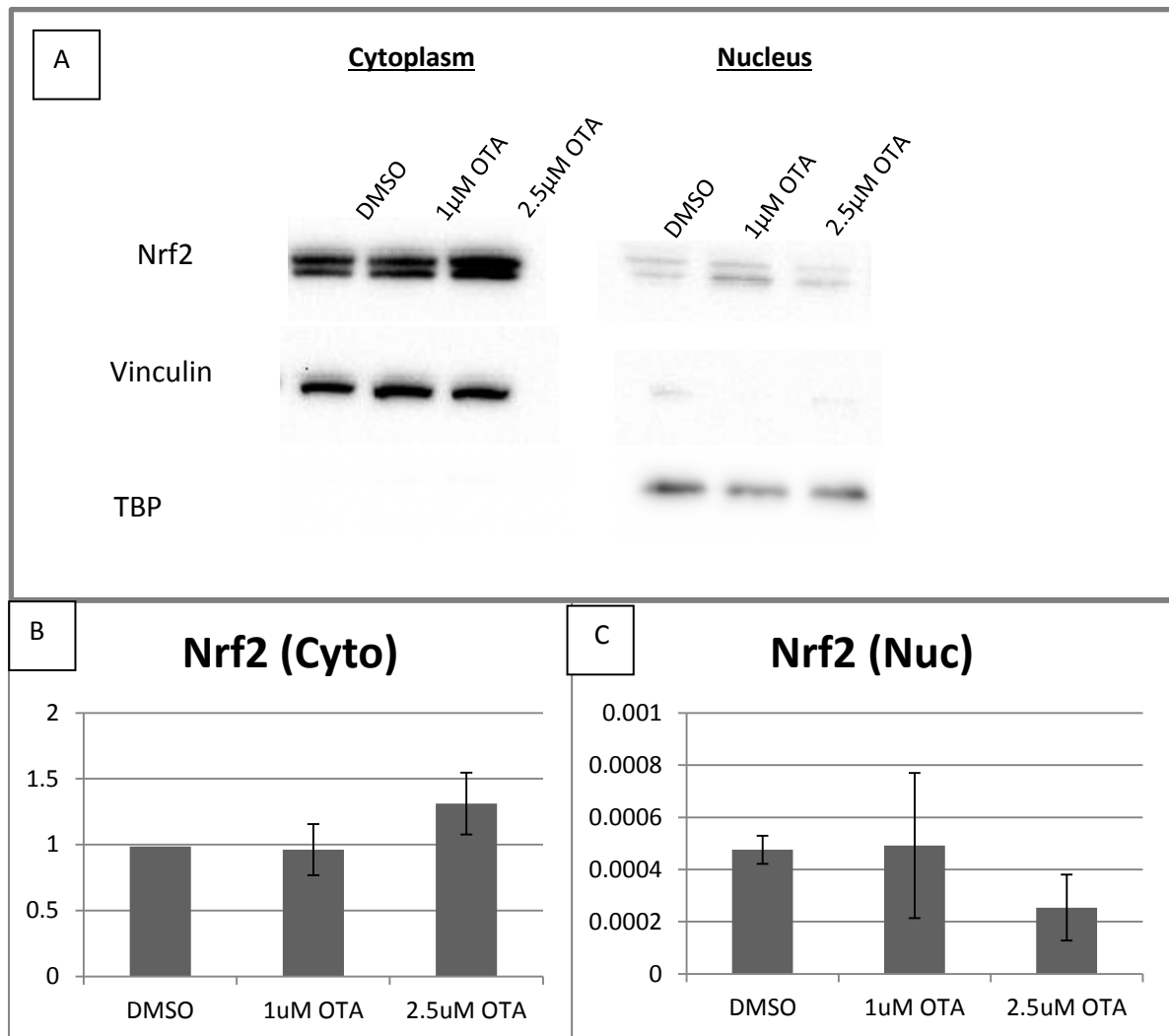


Figure 5.10 – Jurkat treatment with 1 and 2.5 μ M Ochratoxin A for 72 h, nuclear and cytoplasmic extracts taken for western blot analysis. A) Nrf2 concentration in nuclear and cytoplasmic extracts, vinculin content with cytoplasm protein control and TBP as the nuclear protein control in comparison with DMSO treated control (n=2). B) Densitometry of Nrf2 in the cytoplasm normalized to vinculin. C) Densitometry of Nrf2 in the nucleus normalized to TBP.

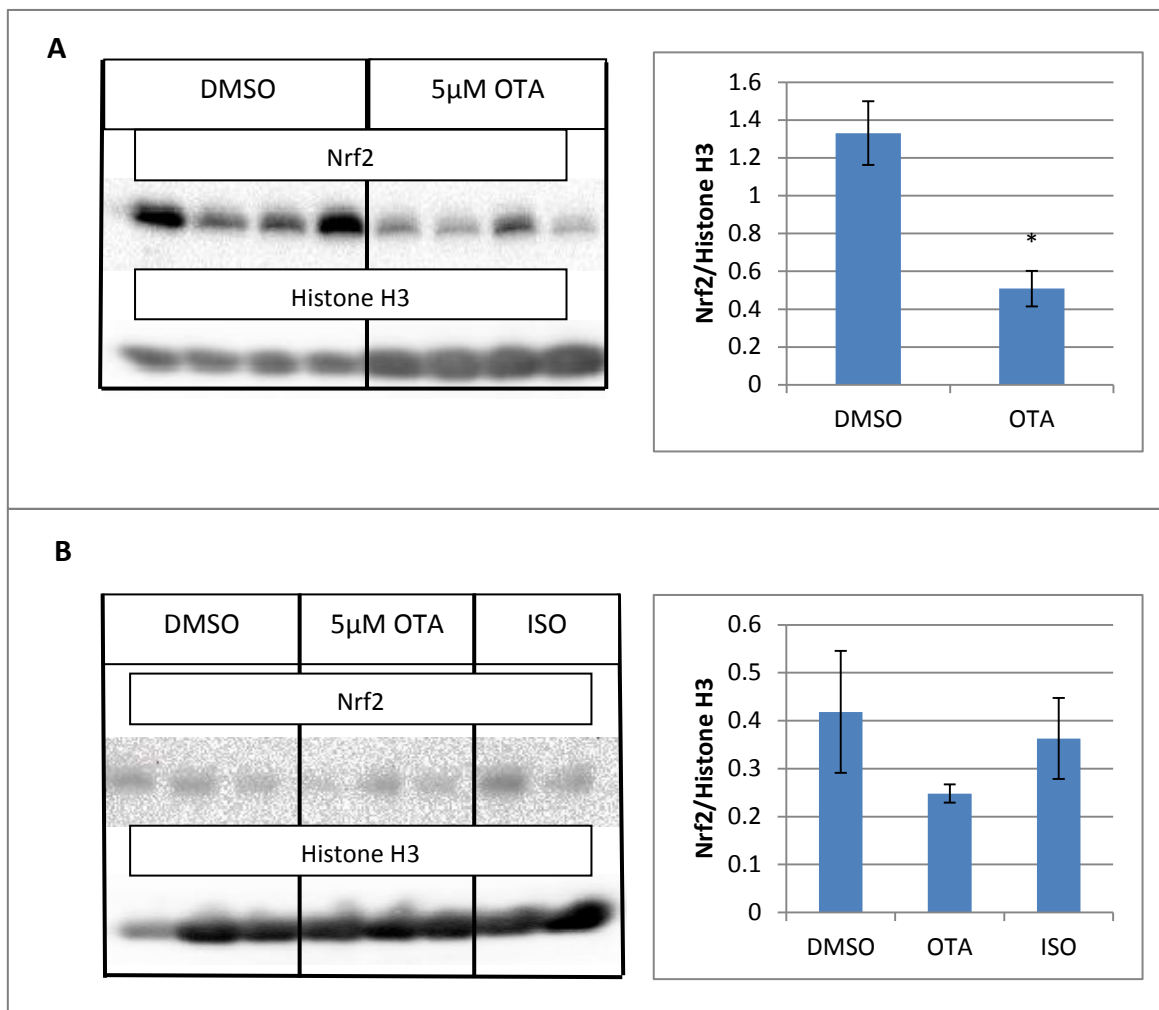


Figure 5.11 – Inhibition of Nrf2 translocation into the nucleus by 5 μ M OTA treatment in Jurkat T lymphocytes. A) Nrf2 protein concentration in nuclear extracts following 24 h treatment with 5 μ M OTA (Pre-treatment with 5 μ M OTA for 30 min and at the 12h time-point) [15 μ g protein loaded, n = 4, data normalised to nuclear control histone H3, * $p < 0.05$]. B) Nrf2 protein concentration in nuclear extracts following 30 min treatment with 5 μ M OTA [30 μ g protein loaded, n = 3, data normalised to nuclear control histone H3].

5.5 DISCUSSION.

From the previous work reported in Chapter 4 using quantitative proteomics, glutathione reductase was identified as a protein significantly induced by all three

polyphenols treatments. Curcumin increased glutathione reductase by 1.2 fold, isorhamnetin by 1.2 fold and resveratrol by 1.1 fold. Even though the increases were statistically significant the fold changes were relatively low and therefore confirmation of these changes in glutathione reductase were required using other methods.

5.4.1 Polyphenols significantly increased the gene expression and protein levels of glutathione reductase in Jurkat T lymphocytes.

Western blot analysis revealed no significant changes in glutathione reductase protein expression following 48h treatment with any of the polyphenols. Since the fold changes in glutathione reductase (identified by proteomics) were small either western blot analysis was not sensitive enough to detect these changes, or the two methods are measuring different aspects of GSR. Proteomics methods detect peptides rather than the whole protein as is the case with western blot analysis. Therefore, this may account for the lack of significant changes observed with the polyphenol treatments at 48h. However, further analysis at the 24h time-point did show increases in glutathione reductase protein content for all three treatments, isorhamnetin induced the greatest increase with 1.3 fold induction; resveratrol had a 1.1 fold and curcumin a 1.03 fold increase. These data suggest that even though proteomics identified glutathione reductase to be induced at the 48h time-point, there was a greater induction at the 24 h time-point. A further time-course

experiment would help evaluate when the peak changes in glutathione reductase occurs with the three different polyphenol treatments.

5.4.2 Increases in expression of genes involved in glutathione production.

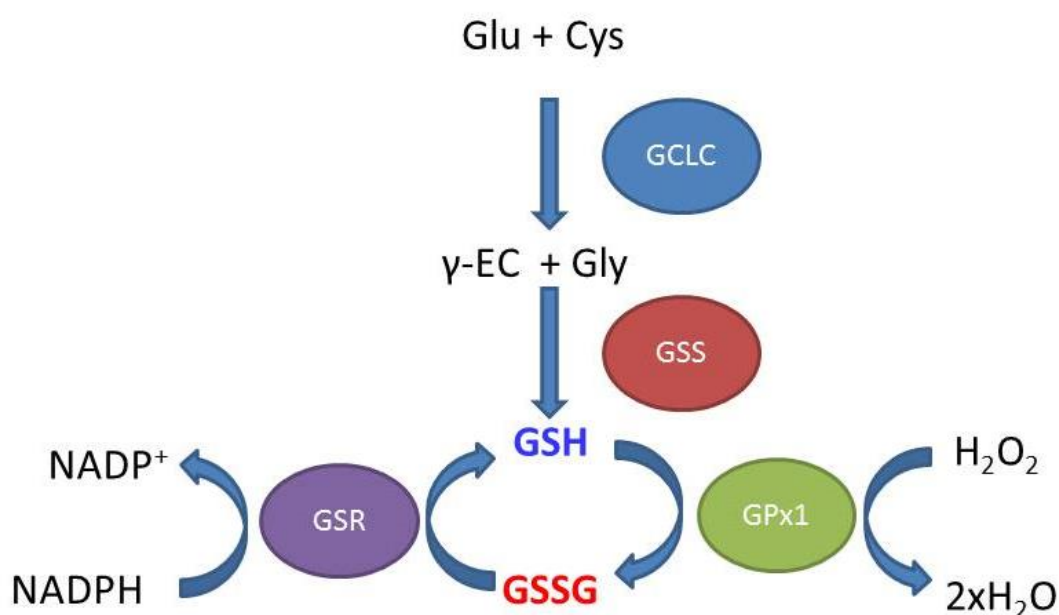


Figure 5.12 – Glutathione synthesis and regulation pathway. Reduced glutathione is generated by two enzymes glutamate-cysteine ligase (GCLC) and glutathione synthase (GSS). GCLC is the first, rate limiting enzyme in the synthesis of glutathione, it utilises L-glutamate (Glu) and L-cysteine (Cys) to produce gamma-L-glutamyl-L-cysteine (γ -EC). Glutathione synthetase combines γ -EC and glycine (Gly) to make reduced glutathione (GSH). Reduced glutathione is vital in maintaining redox homeostasis by the removal of oxidants such as hydrogen peroxide (H_2O_2) by glutathione peroxidase (GPx1). Two GSH molecules are required for the conversion of H_2O_2 into water (H_2O), glutathione is oxidised in the process (GSSG). For glutathione recycling to occur, glutathione reductase (GSR) converts GSSG back to GSH with the use of nicotinamide adenine dinucleotide phosphate (NADPH). (Figure modified from Liu *et al*, 2015)²⁰¹

A time-course experiment was conducted to evaluate the gene expression of enzymes involved in glutathione synthesis and glutathione recycling. Figure 5.12, illustrates the enzymes involved in glutathione recycling, with glutathione peroxidase (GPx1) acting to neutralise oxidants which would potentially be damaging to the cell, causing reduced glutathione (GSH) to be oxidised during the process to GSSG. Glutathione reductase then converts GSSG back to GSH with the use of NADPH. Glutathione reductase protein concentration was shown to be increase by all three treatments at 48h with proteomics and 24h using western blot analysis. Significant increases were also observed in GSR gene expression with both curcumin and isorhamnetin, with a doubling in mRNA content at the 24h time-point compared with the DMSO treated control. With gene expression peaking at the 24h time-point, this suggests that GSR protein expression maybe peaking between the 24 and 48 h time-points, thus the analysis conducted may have missed the greatest increase.

The reported relationship between glutathione reductase and polyphenols is confused, with numerous studies showing that polyphenols induce protein or gene expression of GSR^{197, 198, 199}; however there is also evidence to support polyphenols inhibiting GSR activity. Elliott *et al* in 1992 investigated the inhibition of GSR with 14 different chemically related flavonoids²⁰². For example, quercetin had an I_{50} value of 280, of which is much greater than the levels used in this study. Adding to the complexity, slight changes in polyphenol structure have been reported to dramatically affect the level of inhibition and addition of antioxidant enzymes such as superoxide dismutase and catalase have been reported to reverse the inhibition.

Isorhamnetin (structurally similar to quercetin) has not been studied for inhibitory effects on GSR, and this would be an important experiment to perform, to understand how the increases in GSR gene and protein expression and relate to GSR activity.

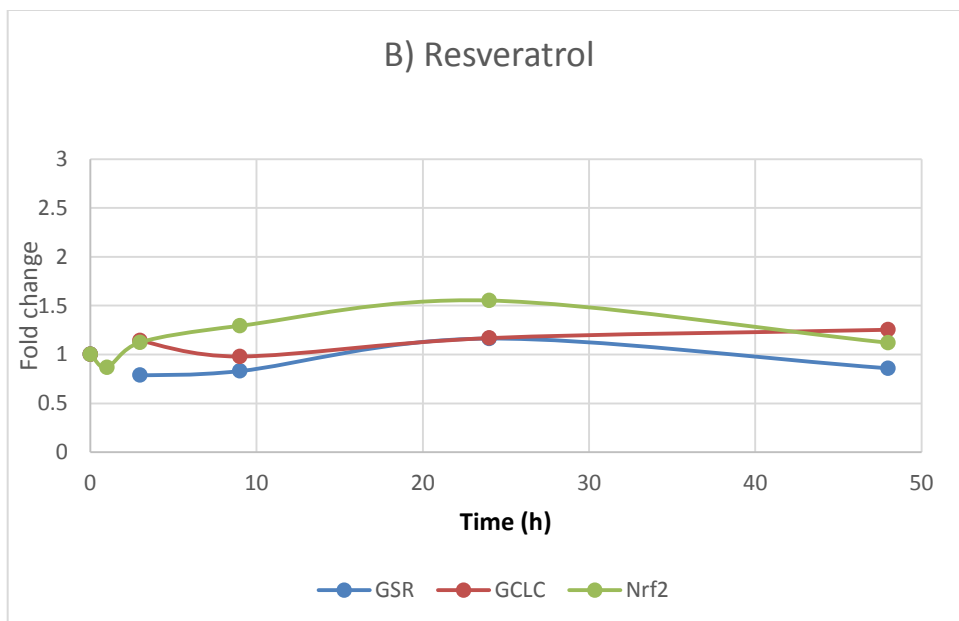
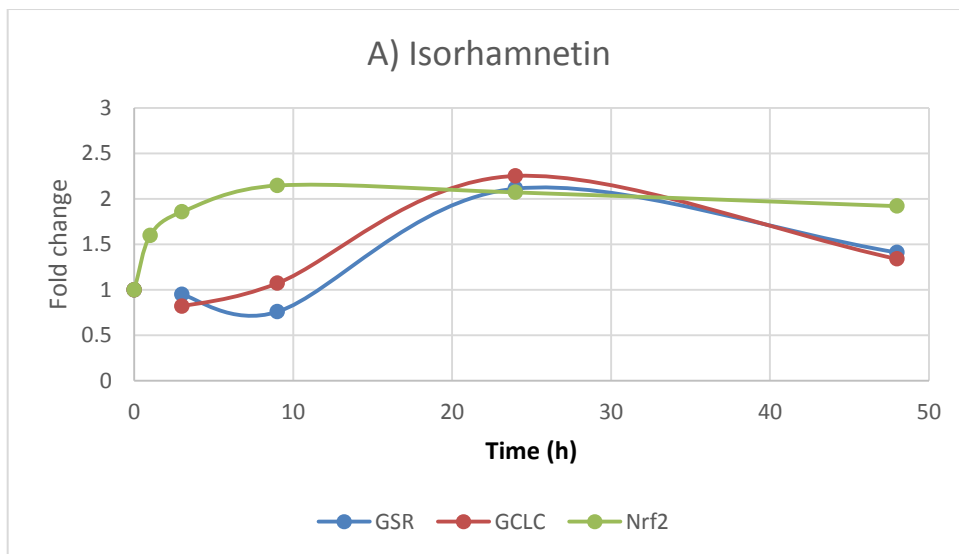
Along with the increases in GSR, significant increases in GCLC gene expression were also observed with isorhamnetin treatment at the 24h time-point; this is the rate-limiting enzyme in the formation of glutathione and was associated with a decrease in glutathione peroxidase gene expression at the 9 h time-point. For isorhamnetin, an increase in GCLC would predict an increase in GSH, an increase in GSR converting GSSG back to GSH and a lowering in GPx1 potentially generating less GSSG, would suggest an overall increase in the intracellular concentration of GSH should occur. However, when measuring GSH levels, curcumin was the only compound that induced a significant increase in GSH, with an increase from 716 to 3151 nmol/million cells compared with the DMSO treated control, there was also a significant increase in GSSG with curcumin, increasing from 20 to 85 nmol/million cells. However, this increase was less than 5% of the total glutathione measured. Isorhamnetin and resveratrol both caused a significant reduction in the levels of GSH produced, compared with DMSO treated control. There may be a number of explanations why levels of glutathione were lowered with the resveratrol and isorhamnetin treatments. It could be related to the time in which the measurements were taken since by 48h any changes in glutathione may be reversed or other redox proteins identified through the proteomics, to be increased with the isorhamnetin

treatment (Glutathione transferases²⁰³ and peroxiredoxins⁶²⁰⁴) may have used the increased amounts of glutathione.

5.4.3 Nrf2 activation induced by curcumin and isorhamnetin.

Increases in redox-proteins are regulated by the transcription factor, nuclear factor erythroid 2-related factor 2 (Nrf2). Nrf2 is a master regulator of a number of different antioxidant genes, such as thioredoxin, NADPH production and glutathione production and regeneration²⁰⁵. In this study Nrf2 activation was significantly increased by isorhamnetin at 3, 9, 24 and 48h after treatment and with 1 and 10 μ M curcumin at 48h treatment compared with the DMSO treated control. Figure 5.13, shows the fold change in Nrf2 over time, along with the changes in two antioxidant genes (glutathione reductase (GSR) and glutamate-cysteine ligase (GCLC)) known to be regulated by Nrf2 for each individual polyphenol treatment. For resveratrol, no changes were observed in Nrf2 activation and this was mirrored in the level of changes in expression of GSR and GCLC. Curcumin and isorhamnetin both increase Nrf2 activation but the patterns of activation over time were different. Curcumin increased Nrf2 by 2.5 fold at 9 h, with a lag in GSR gene expression until 24h. For isorhamnetin there was an increase in Nrf2 activation, starting at 1h, increasing till 9h and again there was a lag in GSR gene expression until an increase at 24h. In contrast to the pattern seen with curcumin; both GSR and GCLC showed the same expression pattern with isorhamnetin treatment. The two compounds that activated

Nrf2 both caused an ~doubling of activation at the 9h time-point, but had different response times and effects on gene expression of 2 antioxidant proteins. This suggests even though they both activate Nrf2, other factors affect antioxidant gene expression differ between the two compounds.



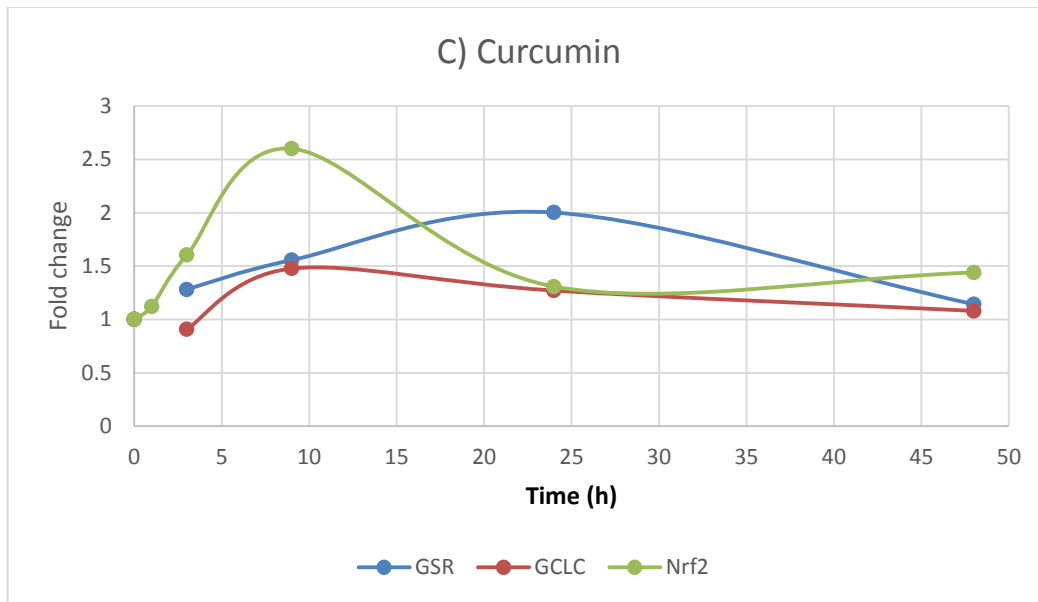


Figure 5.13 – Summary of fold changes for Nrf2, GSR and GCLC. Fold changes in Nrf2, glutathione reductase (GSR) and glutamate-cysteine ligase (GCLC) over time with the three different polyphenol treatments A) isorhamnetin B) resveratrol and C) Curcumin compared with DMSO treated control (1). (Data represented from fig. 5.3A, 5.3D and 5.6).

Preliminary work was undertaken to attempt to inhibit Nrf2 activation in Jurkat T lymphocytes, in order to determine if the activation in Nrf2 is driving the changes observed in cytokine release, as shown by polyphenols. Ochratoxin A (OTA), is a toxin produced by fungi and has been shown to inhibit Nrf2 translocation^{200, 200, 206}. This study has shown that 5µM OTA can significantly inhibit the translocation of Nrf2 into the nucleus for 24h (30 min pre-treatment and again at 12h time-point). However, even though the study showed OTA to inhibit Nrf2, the process is not ideal with the toxicity of OTA. Future work could experiment with siRNA which may prove less toxic, which could be used together with isorhamnetin for 24h to measure the

resulting cytokine release. This will identify if the reduction in cytokine release observed with isorhamnetin is mediated by activation of Nrf2 or the two are acting through different pathways. This work will bridge the findings in Chapter 3 on inflammation, with the observation in this Chapter on changes to redox proteins by polyphenols. To fully appreciate these changes, further work was conducted in another cell type, investigating if isorhamnetin could modify redox and inflammation mechanisms in THP-1 monocytes.

CHAPTER 6

VALIDATION OF THE EFFECTS OF ISORHAMNETIN ON CYTOKINES AND GLUTATHIONE IN AN ALTERNATIVE CELL TYPE, THP-1 CELLS.

6.1 INTRODUCTION.

The study conducted in Chapter 3 identified polyphenol compounds that significantly lowered markers of inflammation in Jurkat T lymphocytes. The compounds identified which had the greatest effects on lowering cytokine release in these cells were curcumin, isorhamnetin and resveratrol. Proteomic analysis was then used to investigate overall changes in protein abundance following 48h treatment with these polyphenols, as shown in Chapter 4. This revealed that the polyphenol treatment was significantly modulating redox proteins content, in particular glutathione reductase, which was induced by all three polyphenols. Treatment of cells with isorhamnetin also significantly increased thioredoxin, thioredoxin reductase, peroxiredoxin 1, 2, and 6, content in the Jurkat T lymphocytes. These redox modulations with isorhamnetin were investigated further in Chapter 5, where significant increases to Nrf2 activation were observed. Together with increases in glutamate—cysteine ligase gene expression and increases in glutathione reductase protein and gene expression compared with the DMSO treated control.

It was observed that isorhamnetin (structure shown in Figure 6.1) showed the greatest number of modulations in both redox proteins and cytokine release in Jurkat T lymphocytes; therefore this compound was used to determine if the effects could be replicated in other cell types. Another immune cell line was chosen, a human monocyte cell line (THP-1), as these are also cytokine producing cells and thus providing the investigation of inflammatory markers following treatment with

isorhamnetin. THP-1 cells are able to produce a variety of cytokines, including IL8 and TNF α , both of which are also detectable in the Jurkat T lymphocytes^{207,208}. Other cytokine markers include IL1 β , IL6, IL10²⁰⁹ and MCP-1²¹⁰ which are detectable following stimulation of THP-1 cells with lipopolysaccharide (LPS). PMA/PHA which was used previously to induce cytokine release in the Jurkat cells in Chapter 3, could not be used in these circumstances due to PMA inducing THP-1 monocyte differentiation into macrophages, therefore LPS was used to stimulate the THP-1 cells. It has been well studied in the induction of cytokines in the THP-1 cell line, there are differences in the treatment times and the pathways they induce, however there is a cross over in the cytokines that are induced by the two treatments, allowing the comparisons between the two cell lines.

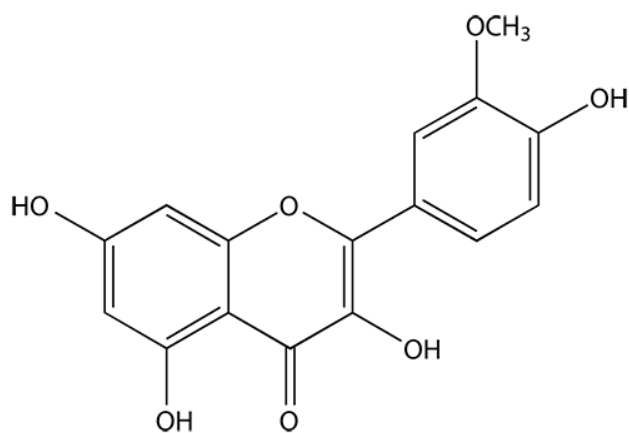


Figure 6.1 – Structure of isorhamnetin, an O-methylated flavonol.

Due to the different cell line being used, more cytokines were expressed than in the Jurkat cell line. Notably MCP-1, IL1 β , IL6 and IL10 could be detected in THP-1,

along with IL8 and TNF α in the Jurkat cells. MCP-1 is a member of the C-C chemokine family and is a chemotactic factor for monocytes and is induced by oxidative stress, cytokines or growth factors. Elevated MCP-1 and its receptors have been shown to play a role in the development of atherosclerosis²¹¹. EGCG has been shown to suppress TNF α induced MCP-1 gene expression in HUVEC cells in a dose-dependent manner²¹². IL6 is a interleukin which can act as both anti- and pro- inflammatory cytokine, secreted by both T- cells and macrophages. It plays an important role in fighting infection and tissue damage. Its anti-inflammatory effects are mediated through its inhibitory effects on TNF α and IL-1 activation of IL-10. IL6 has been shown to contribute to a number of age-related diseases such as atherosclerosis, Alzheimer's and rheumatoid arthritis²¹³. IL10 is an anti-inflammatory cytokine, it works by down regulating the expression of h1 cytokines, MHC class II antigens and co-stimulatory molecules on macrophages. IL-10 can also block NF- κ B activity, which is the main transcription factor of pro-inflammatory cytokine expression. Resveratrol has been shown to increase IL-10, and a down regulation of pro-inflammatory cytokines IL-1 β , TNF α and IL6 following induction by LPS in brain cells²¹⁴.

THP-1 cells have previously been used to investigate the anti-inflammatory effects of dietary polyphenols. Drummond *et al* in 2013 demonstrated that 25 μ M quercetin (an analogue of isorhamnetin) significantly reduced TNF α release in THP-1 macrophages following 48h treatment with LPS stimulation at the 24 h time-point²¹⁵. Other studies have shown that polyphenols lower cytokine release in this cell type, both resveratrol (2.5, 5, 10 μ M) and curcumin (10, 20 μ M) significantly inhibited steric

acid-mediated induction of the pro-inflammatory mediators TNF α and IL1 β in the THP-1 cells²¹⁶. Treatment of cells with isorhamnetin has been shown to significantly increase nuclear translocation of Nrf2 and increased heme oxygenase 1 (HO-1) protein expression in the presence of oxidized low-density lipoprotein ox-LDL which induced cell apoptosis in THP-1 macrophages²¹⁷.

6.2 AIMS.

Following the identification of polyphenols that reduced markers of inflammation in Chapter 3, and further analysis with proteomics in Chapter 4, isorhamnetin was identified to modulate to both redox proteins and inflammatory markers. The aim of the work in this Chapter was to determine if isorhamnetin had the same effect in another cell type, human monocytes THP-1. This will allow the comparison between the two cell models, and hence the more general applicability of the data.

6.3 RESULTS.

6.3.1 Optimisation of THP-1 monocytes culture with the addition of isorhamnetin.

A significant increase in cell number was observed with 10 μ M isorhamnetin in unstimulated THP-1 cells (Fig. 6.2A). Cells that were stimulated with LPS showed

no significant changes to cell number following treatment with isorhamnetin (Fig. 6.2B).

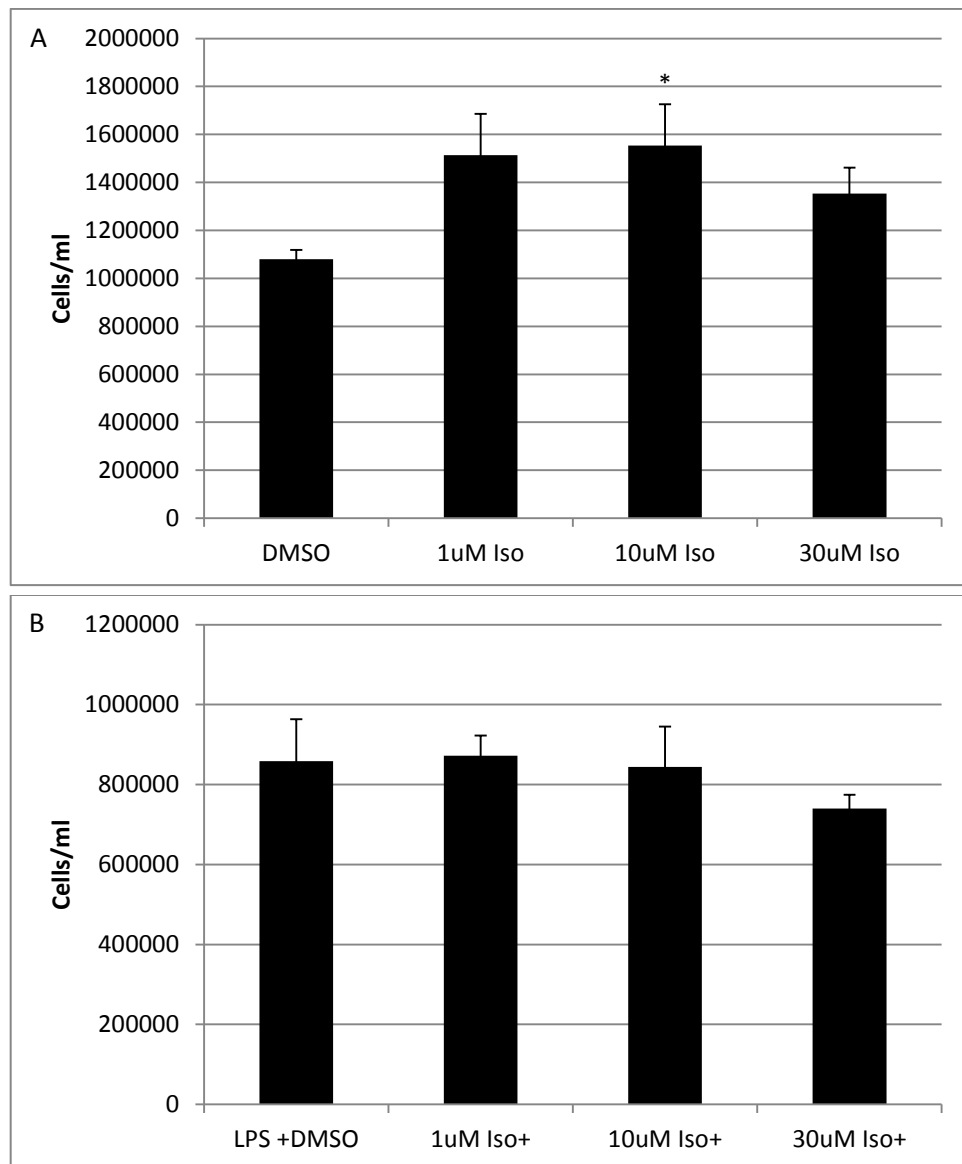


Figure 6.2. A) THP-1 cell number following treatment with 1, 10, and 30 μ M isorhamnetin for 48 h (unstimulated cells). B) THP-1 cell number following treatment with 1, 10, and 30 μ M isorhamnetin for 48 h, with a 4 h 1 μ g/ml LPS (+DMSO) stimulation at the end [Mean \pm SEM, $n = 6$, * $p < 0.05$].

6.3.2 Multiplex analysis of cytokine release in stimulated and unstimulated THP-1 cells.

The cytokines investigated were chosen as they related to the previous data from the Jurkat cells (Chapter 3), along with additional cytokines known to be produced by these cells. The 11 cytokines used were G-CSF, GM-CSF, GRO, IL1 β , IL6, IL8, IL10, IL12(p40), IL12(p70), MCP-1, and TNF α . The cells were either unstimulated to measure the effect of isorhamnetin alone or stimulated with lipopolysaccharides (LPS) to induce cytokine release. This method was similar to that used with the Jurkat T-lymphocyte experiment; however the same stimulus could not be used, since PMA/PHA does not have the same effect on THP-1 cells. LPS was chosen since it is extensively studied to induce cytokine release in this cell type.

Three out of the eleven cytokine measured had levels which were undetectable by the multiplex analysis; G-CSF, GM-CSF and IL12p40. Only two of the cytokines could be measured in both the unstimulated and stimulated cells, these were MCP-1 and TNF α . A significant dose dependant reduction was observed with MCP-1 in unstimulated cells (Fig. 6.3A); this effect was also replicated in the LPS stimulated cells following treatment with 10 and 30 μ M isorhamnetin. Both unstimulated and LPS stimulated THP-1 cells significantly reduced MCP-1 release compared with DMSO or LPS treated control (Fig. 6.3B). A reduction from 135 ± 4 pg/ml with DMSO to 67 ± 2 pg/ml with 30 μ M isorhamnetin in unstimulated cells and 265 ± 6 pg/ml (DMSO) lowered to 182 ± 5 pg/ml (30 μ M Isorhamnetin) in LPS stimulated cells. No significant effects was observed on TNF α in unstimulated cells

(Fig. 6.3C), however a significant reduction was observed in the LPS stimulated cells with the 30 μ M treatment of isorhamnetin (10223 ± 51 pg/ml), compared with LPS treated control (10428 ± 70 pg/ml) (Fig. 6.3D).

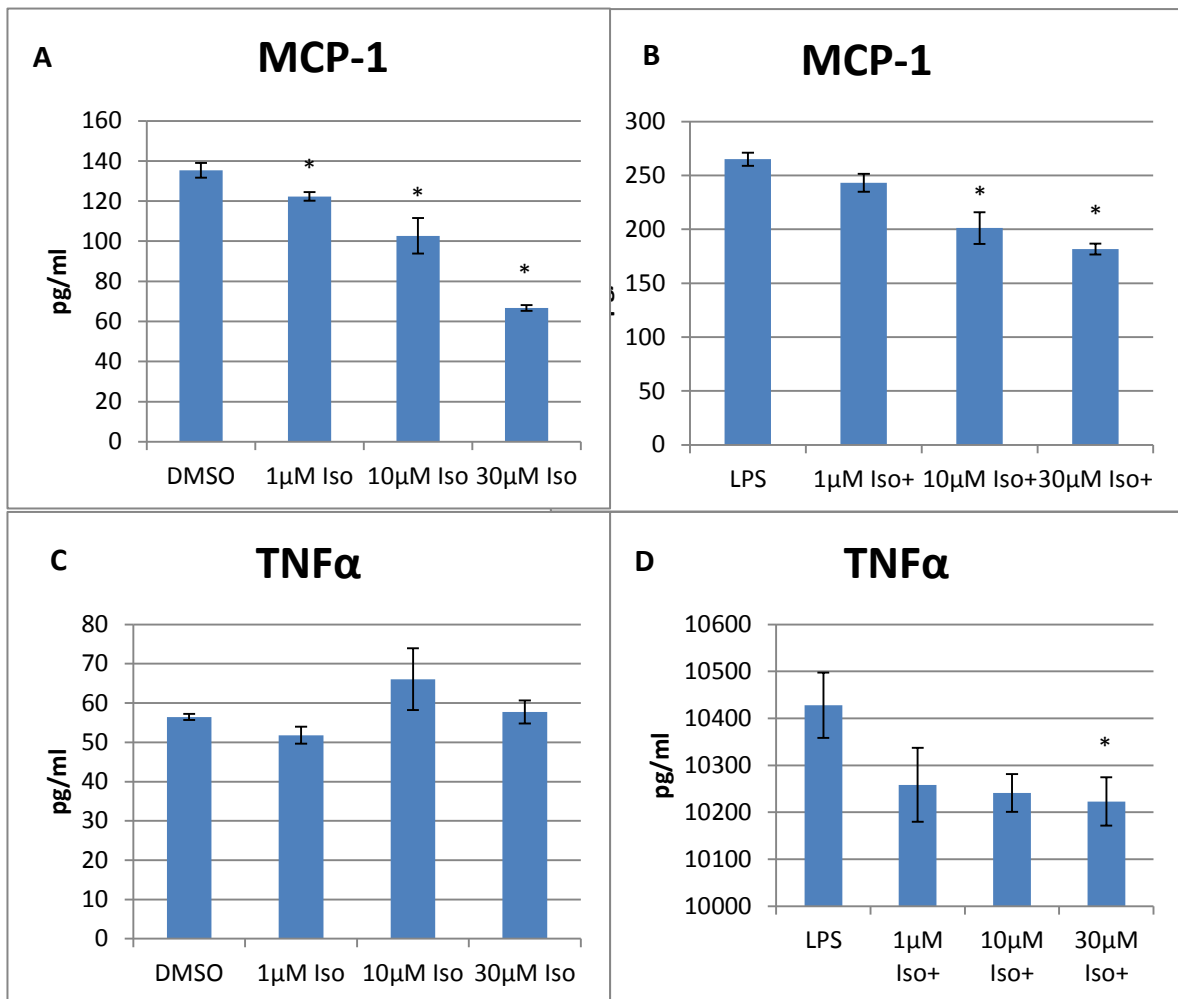


Figure 6.3 – Multiplex analysis of MCP-1 and TNF α following treatment of THP-1 cells with 1, 10, and 30 μ M isorhamnetin for 48 h. A) MCP-1 release following treatment with isorhamnetin in unstimulated cells. B) MCP-1 release following treatment with isorhamnetin in unstimulated cells. C) TNF α release following treatment with isorhamnetin for 48 h with 4 h stimulation by LPS [Mean \pm SEM, $n = 5$, * $p < 0.05$].

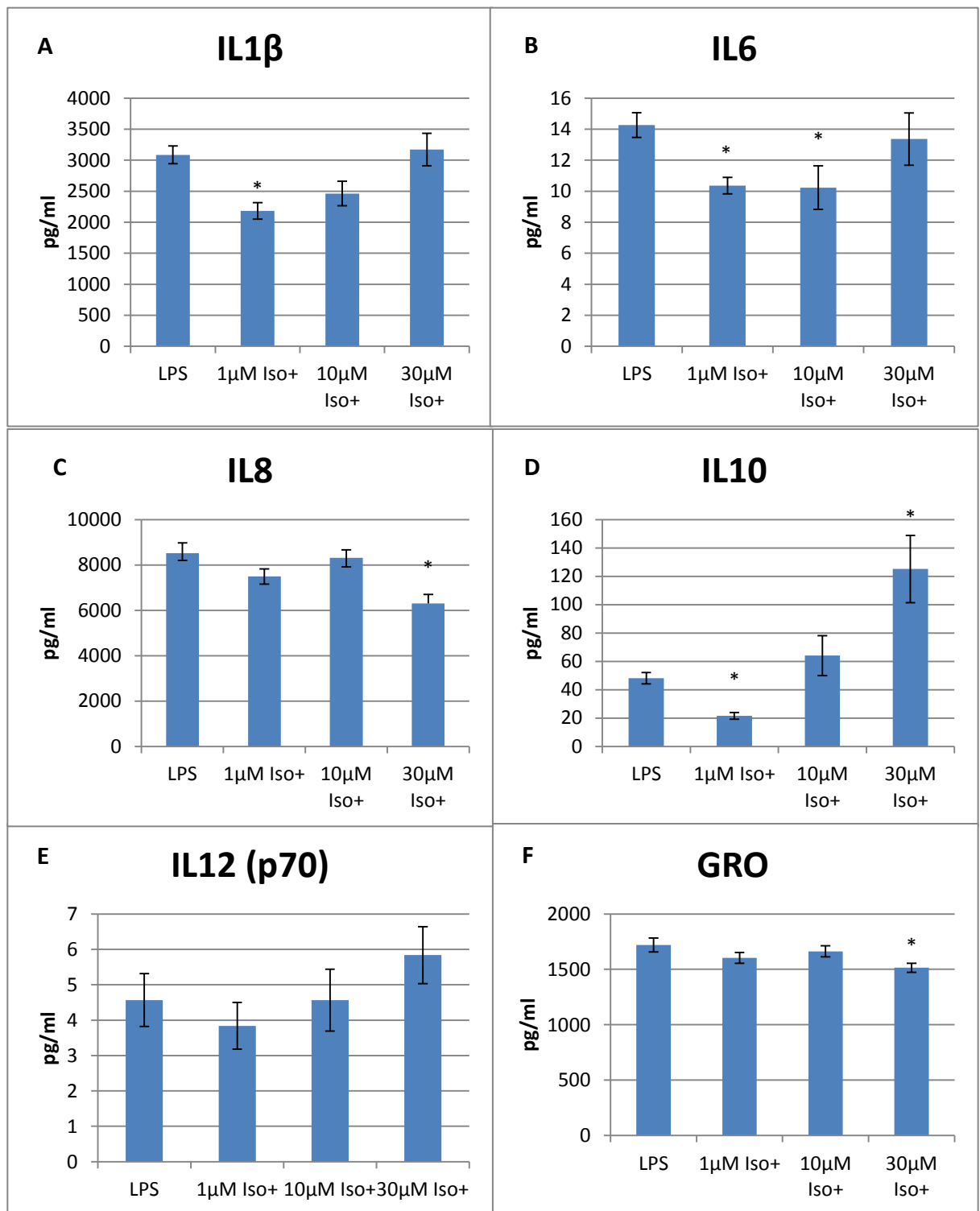


Figure 6.4 – Multiplex analysis of IL1 β , IL6, IL8, IL10, IL12(p70) and GRO following treatment with 1, 10, and 30 μ M isorhamnetin for 48 h with 4 h stimulation with LPS in THP-1 monocytes. A) IL1 β B) IL6 C) IL8 D) IL10 E) IL12(p70) F) GRO [Mean \pm SEM, $n = 5$, * $p < 0.05$].

Significant changes were observed in IL1 β , IL6, IL8, IL10 and GRO release in the cells stimulated with LPS compared with the LPS treated control. Figure 6.4(A, B, and D) shows a significant reductions in IL1 β , IL6, and IL10 with the 1 μ M isorhamnetin treatment, figures 6.4 (C and F) also significant reductions in IL8 (8521 \pm 449 LPS to 6309 \pm 395 pg/ml isorhamnetin) and GRO (1720 \pm 64 LPS to 1514 \pm 41 pg/ml isorhamnetin) with the 30 μ M isorhamnetin treatment compared with the LPS treated control. There was also a significant increase in IL10 with the 30 μ M isorhamnetin treatment, an increase from the LPS treated cells from 48 \pm 4 pg/ml to 125 \pm 24 pg/ml with isorhamnetin, a 2.5 fold increase (Fig. 6.4D). No significant effects were observed with IL12 (p70) (Fig. 6.4F).

6.3.3 Gene expression analysis of glutathione reductase, glutathione synthase, glutathione peroxidase and glutamate—cysteine ligase.

A significant increase in glutathione peroxidase 1 (GPx1) mRNA was observed at the 3 hour time-point, however no other significant changes were observed in glutathione reductase (GSR), glutathione synthase (GSS) or glutamate-cysteine ligase (GCLC) over the time-course of treatment with 30 μ M isorhamnetin, compared with DMSO treated control (Fig. 6.5).

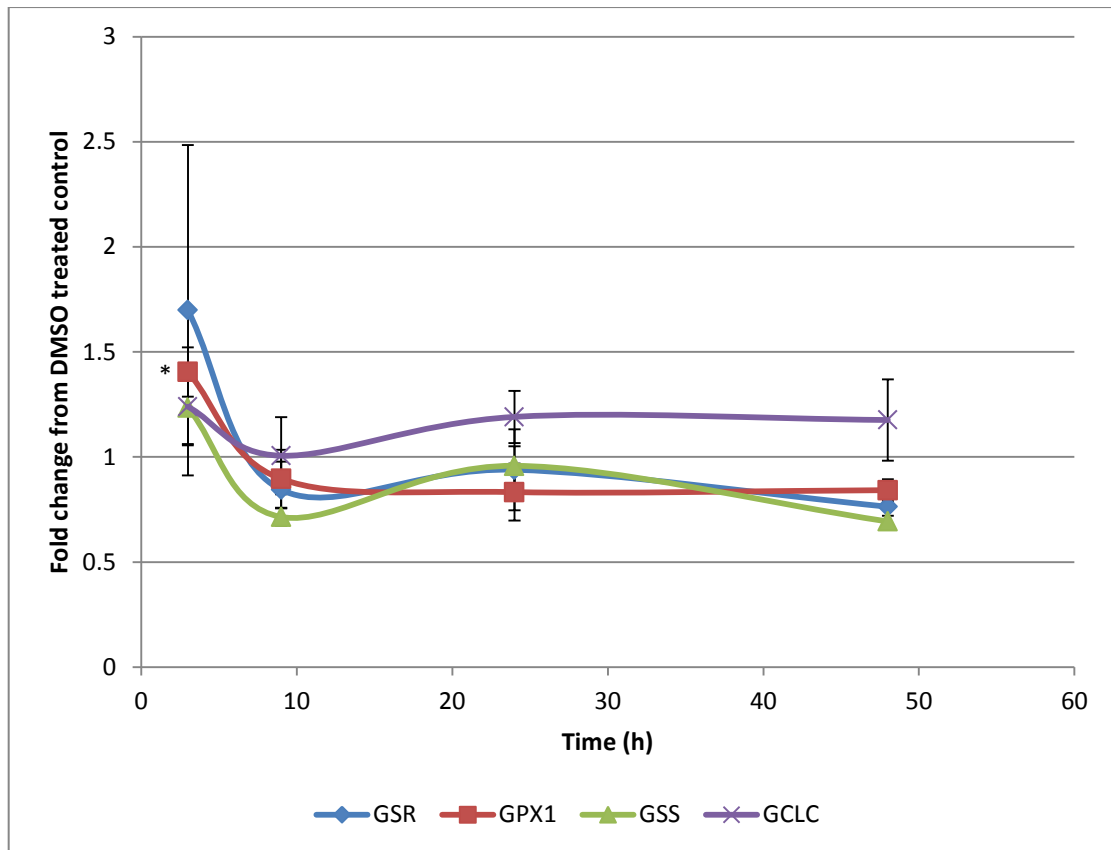


Figure 6.5 – qPCR using primers for glutathione reductase (GSR), glutathione synthase (GSS), glutathione peroxidase (GPX1) and glutamate—cysteine ligase (GCLC) following 30 μ M isorhamnetin treatment over a time-course of 3, 9, 24, and 48 h in THP-1 cells. [Mean \pm SEM, $n = 3$, * $p < 0.05$]

6.3.4 Nrf2 activation with isorhamnetin treatment in unstimulated and stimulated THP-1 cells.

A significant increase in Nrf2 activation was observed in unstimulated cells following treatment with 30 μ M isorhamnetin treatment compared with DMSO treated control (Fig. 6.6A) and also in LPS stimulated cells (Fig. 6.6B), compared with

LPS treated control. 10 μ M had no effect on Nrf2 DNA binding; however, 1 μ M isorhamnetin showed a significant lowering of Nrf2 activation in unstimulated cells.

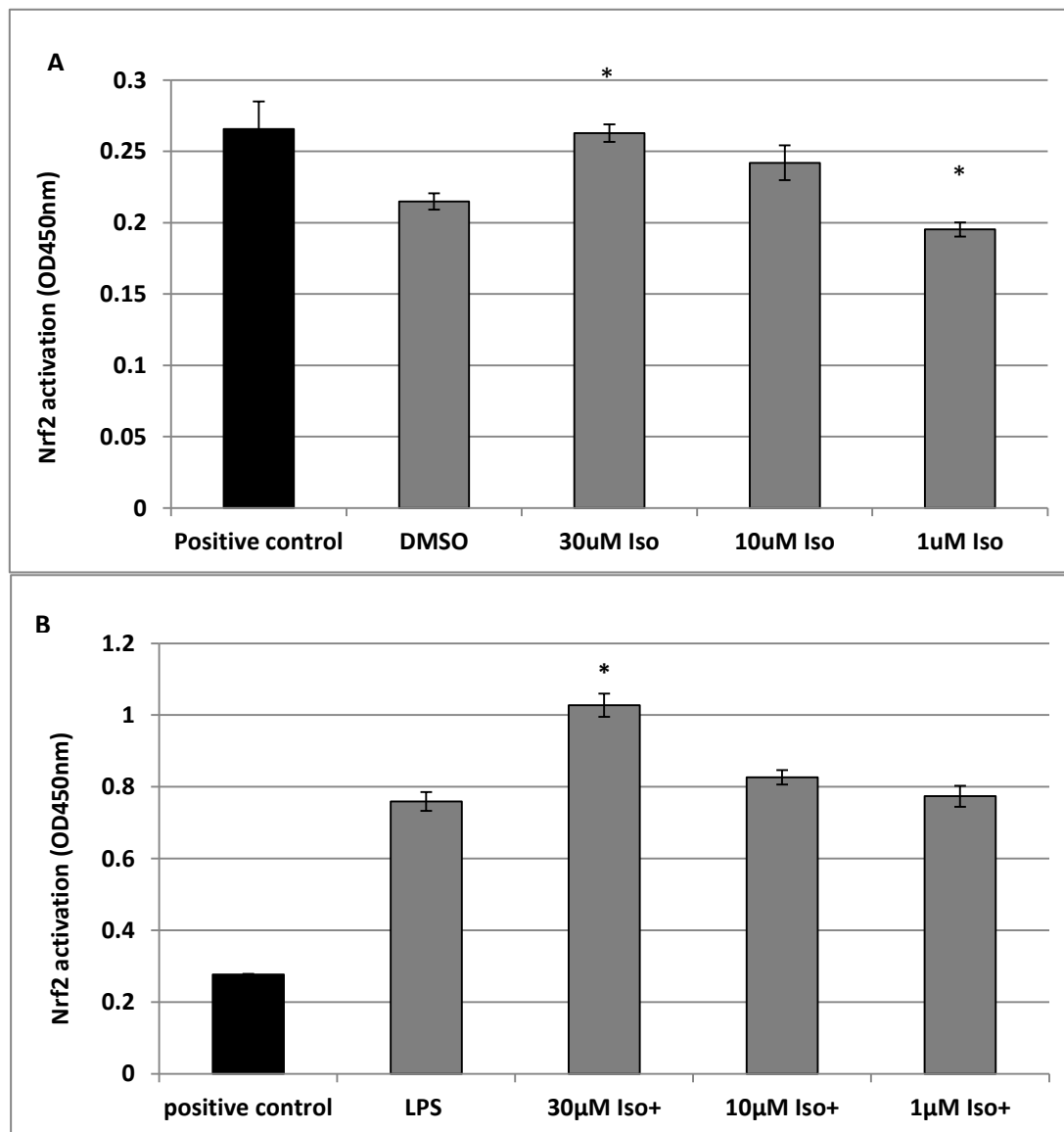


Figure 6.6 – DNA binding assay measuring Nrf2 activation in THP-1 monocyte cell samples following treatment with 1, 10, 30 μ M isorhamnetin for 48 h, without LPS treatment (A) and with 1 μ g/ml LPS stimulation for 4h (B). Positive control, Nrf2 protein provided by kit. (Mean \pm SEM, $n=5$, * $p < 0.05$).

The time course effects of 1 and 30 μ M isorhamnetin showed a significantly increase starting at 3h and peaking at 48h, with 30 μ M isorhamnetin treatment, compared with DMSO treated control. Treatment of cells with 1 μ M isorhamnetin only showed a significant increase in Nrf2 activation at the 48h time-point (Fig. 6.7).

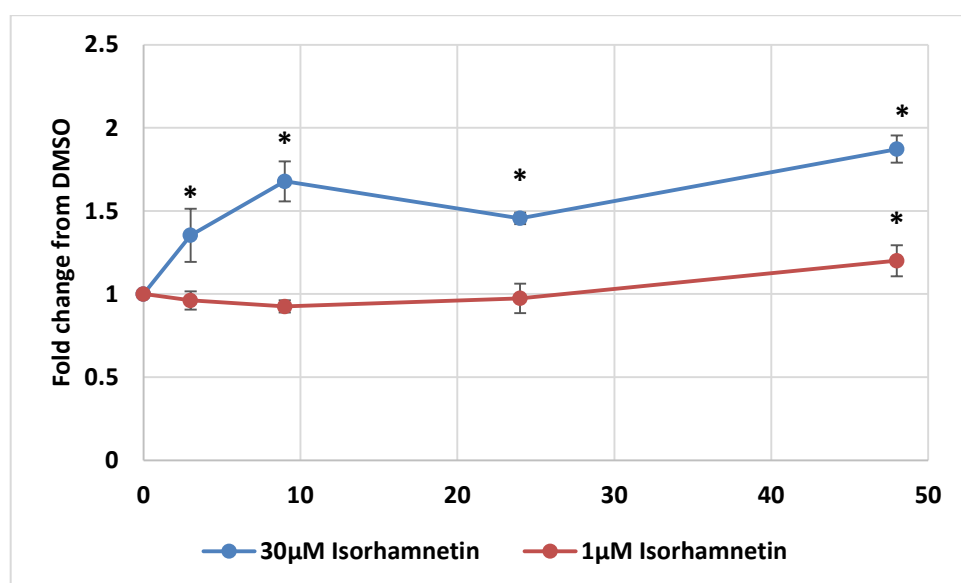


Figure 6.7 – DNA binding assay measuring Nrf2 activation in THP-1 monocyte cell samples following treatment with 1 and 30 μ M isorhamnetin for 3, 9, 24, and 48 h. (Mean \pm SEM, $n=5$, * $p < 0.05$).

6.4 DISCUSSION.

To evaluate the general applicability of the changes in isorhamnetin treatment had on markers of inflammation and redox modulation which were

previously reported in the Jurkat cell (Chapters 3, 4 and 5), the experiments were repeated using human monocytes THP-1 cells.

6.4.1 Modulations to cytokine release following treatment of THP-1 cells with isorhamnetin for 48h.

A significant reduction in IL8 and TNF α (Fig. 6.4C and 6.3D) were observed in the THP-1 cells following 48h treatment with isorhamnetin compared with LPS treated controls, which correlates with the reduction observed previously in the Jurkat cells (Chapter 3, fig. 3.8 and 3.9). Other studies have shown that other polyphenols can lower IL8 release in LPS stimulated THP-1 cells, for example resveratrol dose dependently inhibited LPS-induced IL8 production and release in THP-1 cells²¹⁸. Data showed that there were other reductions in cytokines release included MCP-1, IL1 β , IL6, and GRO, with a significant increase in IL10 also observed with 30 μ M isorhamnetin. IL10 is an anti-inflammatory cytokine, its main role is in repressing excessive immune responses and protecting against tissue damage. Dysregulation, lowers the levels of IL10 and contributes to inflammatory diseases such as inflammatory bowel disease, liver inflammation and psoriasis²¹⁹. Studies have shown that other polyphenols can increase the expression of IL10, Wong *et al* in 2010, showed a significant increases in IL10 gene expression at physiologically relevant doses of 2 and 10 μ M EGCG following 72h treatment in Jurkat T

lymphocytes²²⁰. Polyphenols that can increase anti-inflammatory cytokines and lower pro-inflammatory cytokines, have the potential ability to restore the imbalance observed in ageing, were there is a greater proportion of circulating pro-inflammatory cytokines in the system.

Mapping the cytokine interactions using Ingenuity software allowed a visual representation of the connections made between the cytokines identified (Figure 6.8). This diagram shows theoretical interactions between the treatments used, protein expression and signalling based on data found in literature research. The data base holds a number of different chemicals and molecules, which can be used to predict the interactions this has on proteins or in this case cytokine expression. However there was no literature based references that connected the compound isorhamnetin with the cytokines; but there were connections for the LPS used to stimulate the cells. This allowed the mapping of LPS stimulus and cytokine interactions with THP-1 cells. 7 out of the 8 cytokines detected using the multiplex analysis, were identified as having indirect links LPS stimulation in the software. As previous Ingenuity analysis identified NF- κ B to be a central factor in the mechanism of action of polyphenols in the Jurkat cells, LPS and NF- κ B were added to the scheme. By adding these factors, the interactions with the cytokines can be observed within the scheme. Direct interactions were identified for IL6, IL8 (CXCL8) and TNF α with NF- κ B, all three cytokines showed a reduction in cytokine release, as was also shown in the Jurkat T lymphocytes. This diagram was used to give an overall picture of the

cytokine interactions and how these cytokines are affected by LPS and isorhamnetin and their involvement with the transcription factor NF- κ B.

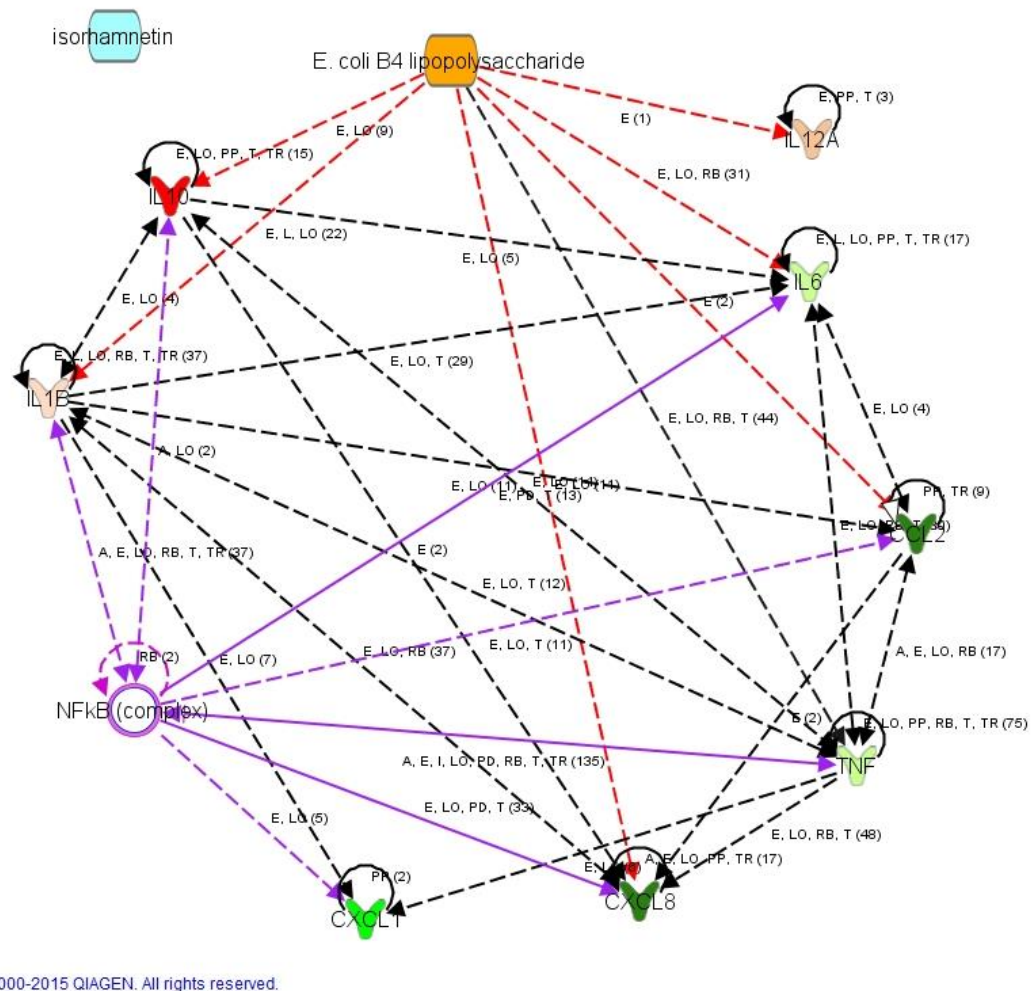


Figure 6.8. IPA cytokine network analysis, modulation occurred with isorhamnetin treatment (blue). Connections made between LPS (orange) and also connections to NF- κ B (purple) with the cytokines, which is a possible mechanism of action of isorhamnetin. Red (induction) and green (reduction) in cytokine release following 48h treatment with isorhamnetin. The eight cytokines which had detectable changes following the isorhamnetin (Blue) and LPS treatment (orange).

6.4.2 Activation of Nrf2 with isorhamnetin, but not induction of glutathione genes.

As with the Jurkat cells, a significant activation of Nrf2 was observed with isorhamnetin treatment. This increased over time from 3 to 48 h, but this activation of Nrf2 had no effect on the expression of the antioxidant genes. Quantitative PCR showed no significant changes to the mRNA for glutathione reductase, glutathione synthase and glutamate cysteine ligase following isorhamnetin treatment. There was a significant increase in the glutathione peroxidase mRNA at the 3 h time-point. This is unlike data from Jurkat T lymphocytes where a significant increase in glutathione reductase and glutamate-cysteine ligase gene expression was observed at the 24 h time-point.

These data show some overlapping areas where isorhamnetin had the same effect in both the Jurkat and THP-1 cell lines in terms of inflammation and cytokine release, but differing effects in terms of the redox-related protein expression. Further work investigating glutathione reductase protein expression and concentrations of intracellular glutathione is needed to evaluate comparisons between the Jurkat T lymphocytes and THP-1 monocytes connecting redox modulations and what functional effect these changes have in cells.

CHAPTER 7

OVERALL DISCUSSION.

7.1 SUMMARY OF MAIN FINDINGS.

The initial aims of this work described in this thesis were:

- To screen a variety of dietary (poly)phenols for their effects on cell viability and changes to cytokine release in Jurkat T-lymphocytes. These compounds included complex polyphenols and smaller metabolites phenolic acids. The aim was to determine a treatment dose and evaluate the anti-inflammatory properties of the compounds.
- (Poly)phenols identified from the screening to have the greatest anti-inflammatory effect, will be examine further with quantitative proteomics. This will allow changes in protein concentrations to be observed following treatment with the chosen (poly)phenols (curcumin, isorhamnetin and resveratrol). Network analysis will be conducted to evaluate changes to signalling pathways.
- Evaluation of changes to glutathione reductase, which was previously identified through proteomics to be modulated by all three treatments. Validation of these changes through protein and gene expression analysis and further analysis of the antioxidant signalling pathway by the transcription factor Nrf2.
- Further analysis of these changes to inflammatory cytokine release and modulations to redox homeostasis observed with Jurkat T-lymphocytes, were evaluated in another cell type (THP-1 monocytes) with the polyphenol which showed the greatest changes, which was isorhamnetin.

The data obtained have shown:

- Sixteen of the twenty-nine polyphenol treatments screened produced statistically significant reductions in the release of cytokines by Jurkat T-lymphocytes following 48h of treatment. The most anti-inflammatory polyphenols screened were curcumin, resveratrol and isorhamnetin. At 1 μ M, a physiologically relevant dose for polyphenols, resveratrol decreased IL2 by 42% \pm 7% and IL8 by 32% \pm 8% compared with vehicle control ($p < 0.05$). For cells stimulated with PMA/PHA to induce cytokine release, 1 μ M isorhamnetin reduced IL2 by 50% \pm 4%, IL8 by 58% \pm 6% and TNF α by 63% \pm 7%, and curcumin reduced IL2 by 43% \pm 14%, IL8 by 30% \pm 7% and TNF α by 22% \pm 5 ($p < 0.05$).
- Proteomics identified several proteins in the glutathione metabolism pathway that were modified by polyphenol the polyphenol treatments. Significant increases in the enzyme glutathione reductase were observed with curcumin (1.2 fold), isorhamnetin (1.2 fold) and resveratrol (1.1 fold) ($p < 0.003$) following 48 h of treatment. Isorhamnetin in particular also showed significant increases in other redox related proteins including thioredoxin and peroxiredoxins; these were confirmed with protein and gene expression analysis. A DNA-binding assay showed increases in Nrf2 activation, a transcription factor for antioxidant proteins, curcumin increased this by 1.5 fold and isorhamnetin 1.9 fold.
- While evaluating the anti-inflammatory and redox modulating effect of isorhamnetin in an alternative cell type (THP-1 monocytes), significant decreases in cytokine release were observed for IL8, MCP-1 and TNF α in LPS

stimulated cells. Increases in Nrf2 activation were also observed but no significant changes to antioxidant gene expression were seen.

7.2 Experimental set-up and limitations.

29 (poly)phenol compounds were chosen to examine the anti-inflammatory effects in Jurkat T-cells. Jurkat cells were chosen as T-lymphocytes are one of a number of cells which are greatly affected by ageing and are a large source of cytokine production. Jurkat cells are an immortalised T-lymphocyte cell line, which was chosen over a primary cell line due to the number of comparisons wanted for the screening of the (poly)phenols. This would not have been possible in primary lines, as secondary cell lines provide continual cell growth and the numbers needed for the treatments required. THP-1 monocytes were also chosen to complement the work seen in the Jurkat cells, another immune cell line which also produces large quantities of cytokines. Another area of interest may be with muscle cell or endothelial cells which also produce cytokines but are not as closely related as the lymphocytes and monocytes, it would be interesting to see if the same effects are observed in these cell lines as well.

The 29 compounds were picked to include complex polyphenols with multiple phenol rings and functional groups, along with smaller phenolic acids which would correlate with metabolic breakdown products of the larger complex polyphenols. With a wide range of (poly)phenols to choose from and a limited

number of compounds can be evaluated at any one time. One area of (poly)phenol metabolism which wasn't cover in this study was evaluating the anti-inflammatory effects was to look at those compounds that are conjugation to phenolic groups via glucuronidation and/or sulfation. This would be an interesting area to study as a number of these polyphenols are conjugated with these groups. Another limitation of the study was measuring the cell number following treatment with the (poly)phenols using the MTS assay, as previously discussed in Chapter 3, the MTS measures cell viability based on the metabolic activity of the cell, and this may vary with the treatments. Later experiments, narrowing down the (poly)phenol field to just 3 compounds meant more accurate forms of cell viability could be conducted via Trypan Blue exclusion.

Cells were treated for 48 hrs with the chosen (poly)phenols, which was chosen to allow time for gene and protein expression. Significant reductions in cytokine release were observed at the 48h time-point and this format was carried forward when investigating proteomic changes. For future work it may be interesting to look at earlier time-points as (poly)phenols can have instant effects of proteins and other proteins have quicker expression times. In this study, shorted time frames were used such as 1, 3, 9, 24 and 48h for transcription factor activation but this could have been used on a number of different proteins that were shown to have been modulated following the treatments, as significant increase in mRNA expression occurred at the 24h time-point. Also the two stimulations used were PMA/PHA and LPS, the stimulations used were to induce a cytokine response in the

cells. PMA/PHA was added at the 24h time-point and LPS at 4h time-point (prior to end); the difference in time was due to the activations pathways and toxicity of the two treatments. The time-points allowed for a protective effect of the (poly)phenols prior to the stimulation being added. The need for two different stimuli was based on the fact that PMA/PHA, which was used in the original Jurkat cell treatments couldn't be used in the THP-1 cells. As PMA in THP-1 cells had a different effect of differentiating THP-1 monocytes into macrophages.

Label-free proteomics was chosen over other proteomic methods, as it wasn't know what proteins to expect, therefore evaluating all changes to proteins would give an insight into the pathways being modulated by the treatments. Future work using label proteomics would give greater accuracy into certain pathways, such as changes to oxidations. 1 and 30 μ M treatments were used in the proteomics in unstimulated cells. Due to the cost and time these were the only experiments conducted, however future work to include more doses would give a better dose-dependent response to protein modulation, also to include the stimulus, as this might have provided large fold changes and given more confidence to the changes observed in the unstimulated experiments.

Other limitations to the study include culturing the cells at 20% O₂, this is common practise in *in vitro* studies, however no necessarily appropriate. Incubators are normally supplemented with 20% O₂ and 5% CO₂, atmospheric levels; however, very few cells actually encounter that concentration. *In vivo* the arterial blood experiences levels > 12% and tissue cells between 3-5% O₂²²¹. It has been shown that

culturing primary T-cells at atmospheric oxygen significantly alters intracellular redox states by decreasing intracellular glutathione and increasing oxidised glutathione²²². This effect was observed in this study, with increases in GSH with isorhamnetin and resveratrol treatments, when changes to glutathione reductase and other redox proteins would suggest an increase in GSH. Therefore conducting these experiments again at a lower oxygen concentration would be interesting to see if the levels of GSH increase with the polyphenol treatments.

7.3 Cytokine release from Jurkat T lymphocytes was significantly repressed by the treatment with polyphenols.

Ageing has been shown to be associated with chronic inflammation with increases in interleukin 6 (IL6)^{223,224} and tumour necrosis factor alpha (TNF α) observed being observed^{225,226}. Lowering cytokine release could be beneficial in age related disease such as atherosclerosis, type 2 diabetes, and Alzheimer's, and increased levels of TNF α have been shown to be associated with the pathogenesis of these diseases²²⁷.

It is believed that dietary interventions could have a potential benefit in overcoming age-related degeneration of the immune system and aid healthy ageing. Human's diets were once high in plant based food and humans arguably may have evolved to rely on the intake of an optimal high level of polyphenol/ antioxidants. However modern diets tend to contain less polyphenols/antioxidants, which may be

insufficient to maintain an optimal oxidation/antioxidant balance. With increases in baseline oxidative stress associated with ageing and with the number of people 60 years or over doubling since 1980²²⁸ (World Health Organisation), it appears to be important to increase dietary antioxidant intake. As dietary antioxidants can reduce oxidation and slow the progression of age-related diseases, it may potentially be possible to tailor a diet to contain foods with the greatest anti-inflammatory and antioxidant benefits. The aim of this work was to determine potential phenolic compounds that will reduce the pro-inflammatory and oxidative state observed with ageing.

The most anti-inflammatory polyphenols screened were curcumin, resveratrol and isorhamnetin. Curcumin was the most anti-inflammatory polyphenol screened, with 30 μ M treatments lowering cytokine release in unstimulated cells. For cells stimulated with PMA/PHA, 30 μ M curcumin decreased IL2 from 6802 \pm 698 pg/ml (DMSO) to 145 \pm 16.6 pg/ml, IL8 from 1133 \pm 160 pg/ml (DMSO) to 433 \pm 41 pg/ml and TNF α from 188 \pm 31 pg/ml (DMSO) to 3.2 \pm 0.2 pg/ml. Curcumin is a component of the dietary spice turmeric and traditionally has been used in herbal remedies. It has a number of beneficial properties and been shown to influence many signalling pathways. Curcumin has been reported to blocks Ca²⁺ mobilization in T cells, this prevents the activation of nuclear factor of activated T cells (NFAT) along with nuclear factor kappaB (NF- κ B) via T cell receptor²²⁹. This may explain the significant decreases in both IL2 (expression regulated by NFAT) and IL8 release (expression regulated by NF- κ B) observed with the curcumin treatment²³⁰.

Other anti-inflammatory compounds identified were quercetin and its metabolite isorhamnetin which significantly lowered cytokine release compared with DMSO treated control. 30 μ M quercetin decreased TNF α by 89% \pm 2% and 30 μ M isorhamnetin decreased IL2 from 6802 \pm 698 pg/ml (DMSO) to 2854 \pm 366 pg/ml, IL8 from 1133 \pm 160 pg/ml (DMSO) to 468 \pm 90 pg/ml and TNF α from 188 \pm 31 pg/ml (DMSO) to 29 \pm 6 pg/ml in stimulated cells. Boesch-Saadatmandi *et al* 2007 showed that 10 μ M quercetin and isorhamnetin significantly decreased mRNA and protein levels of TNF α in mouse macrophage-like cell line following stimulation with lipopolysaccharide²³¹. They also showed a significantly lowering of plasma levels of TNF α from mice fed a quercetin supplement for 6 weeks. Another compound that significantly decreased cytokine release was resveratrol, with both 1 and 30 μ M resveratrol reducing IL2 release from 14.4 \pm 1 pg/ml (DMSO) to 8.3 \pm 1 pg/ml from 1 μ M resveratrol and 9 \pm 0.8 pg/ml (DMSO) to 2.7 \pm 0.6 pg/ml with 30 μ M resveratrol in unstimulated cells. Resveratrol is commonly found in the skin of grapes and has already been reported to have effects at lowering inflammation²³². In other studies using Jurkat T lymphocyte cells, 5 μ M resveratrol was shown to suppress NF- κ B activation induced by TNF α ²³³.

Not all the phenolic compounds screened had an anti-inflammatory effects. Both 1 and 30 μ M pyrogallol increased IL8 release from 34 \pm 2 pg/ml (DMSO) to 149 \pm 19 pg/ml with 1 μ M pyrogallol and 10 \pm 0.7 pg/ml (DMSO) to 176 \pm 7 pg/ml with 30 μ M pyroallol in unstimulated cells. Pyrogallol is a metabolite of the green tea polyphenol epigallocatechin gallate (EGCG), in this study 30 μ M EGCG caused a slight

increase IL2 release from 37 ± 4 pg/ml (DMSO) to 41 ± 3 pg/ml in unstimulated cells although this was not statistically significant. Pyrogallol has been shown to be a ROS generator and this may be cause of the dramatic increases in cytokines produced. When investigating pyrogallol's effect on glutathione, it was shown to increase total and reduced glutathione and reduced the redox potential from -237.6 mV \pm 2 mV with DMSO to -241.2 mV \pm 2 mV with 30 μ M pyrogallol (data not shown). In agreement with the results shown here, Han *et al.* observed GSH levels to be increased in calf pulmonary artery endothelial cells treated with lower doses of pyrogallol (10-50 μ M)²³⁶. Pyrogallol has been shown to be a ROS generator and induces cell death in a number of cell lines including As4.1 juxtaglomerular cells²³⁴ and HeLa cells²³⁵. This could explain why high doses of pyrogallol deplete GSH, due to increased ROS whereas lower doses do not²³⁶. In this experiment pyrogallol did not significantly alter cell number in the Jurkat cells. At lower concentrations of pyrogallol, the observed increases in total and reduced glutathione may be a protective effect against the increase in ROS production.

7.4 Significant increases in the abundance of redox proteins with polyphenol treatments that were identified through quantitative proteomics.

Proteomics was used to identify changes to protein abundance following treatment with the three chosen polyphenols, curcumin, isorhamnetin and

resveratrol. 30 μ M resveratrol showed the greatest number of changes with 434 proteins being modulated. This study aimed to identify common mechanism and pathways modulated by the polyphenols treatments. Network analysis identified proteins involved in redox regulation, oxidative phosphorylation and ribosomal modifications as pathways significantly modified by all three treatments. Ribosomal proteins (60S and 40S) were significantly suppressed by the polyphenols; ribosomal proteins catalyse the synthesis of new proteins, suggesting a down regulation of protein synthesis. Cocoa polyphenols have been shown to block p90 kDa ribosomal protein S6 kinase (RSK), which directly activates the S6 component of the 40S ribosomal subunit in JB6 mice²³⁷. 40S ribosomal protein S6 was significantly repressed 1.1 fold by 30 μ M isorhamnetin. This ribosomal protein S6 becomes phosphorylated on several serine residues by RSK proteins and it is thought activation of individual ribosomal proteins regulates translation (Figure 7.1)²³⁸. In the case of the cocoa polyphenols suppressing RSK, TNF α -induced NF- κ B and AP-1 activation was reduced along with inhibiting the TNF α -induced VEGF expression and this was proposed to contribute to the chemo-protective ability of these compounds.

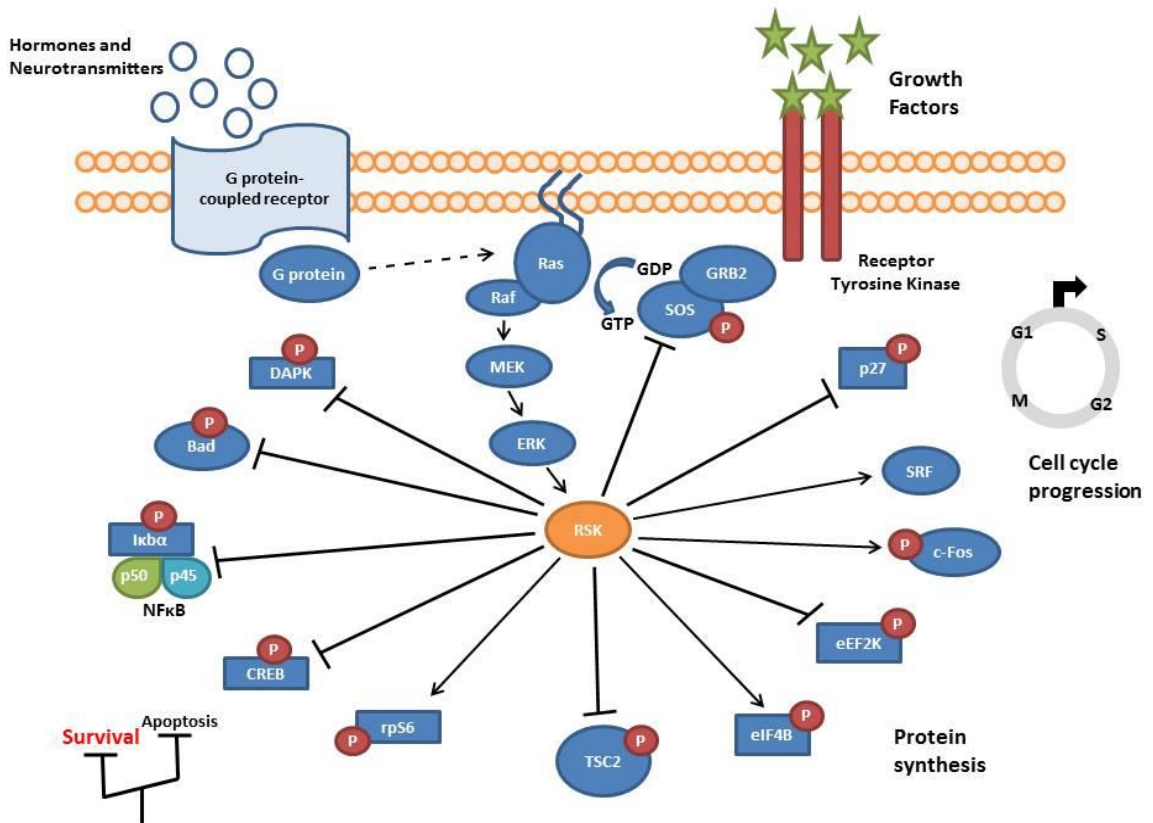


Figure 7.1 - RSK (p70 kDa ribosomal protein S6 kinase) a mediator for cell survival, protecting the cell from apoptosis. RSK is a modulator of ribosomal proteins, effecting protein synthesis, along with cell cycle progression and survival²³⁹.

Other pathways modulated by the polyphenols included oxidative phosphorylation which was significantly repressed. These included proteins such as cytochrome c oxidase, NADH dehydrogenase and ATPase synthase, in which studies have shown that suppression as these proteins, is beneficial to reduce the build-up

of free radicals associated with age. In patients with Alzheimer's disease (AD) differential expression has been observed with oxidative phosphorylation genes overexpression of 8-hydroxyguanosine and cytochrome oxidase, leading to oxidative damage and defects to mitochondrial DNA²⁴⁰.

Ingenuity network analysis examined common mechanism of action via network analysis of the proteomics data. No inflammatory networks were specifically identified, but the top networks identified using Ingenuity software all centred around the NF- κ B pathway, a major transcription factor in the regulation of inflammation^{241,242}. Investigations into polyphenols and the NF- κ B pathway have reported that certain polyphenols can inhibit the phosphorylation or ubiquitination of I κ B preventing degradation and the sub-sequential translocation of NF- κ B into the nucleus²⁴³. Also, polyphenols can inhibit the interactions NF- κ B has with its target DNA, therefore preventing the gene expression of pro-inflammatory cytokines^{243, 243,}²⁴⁴. Interestingly, glutathione reductase was a common interaction linking the NF- κ B pathway to the observed effects of all three polyphenol treatments. Glutathione reductase is as an enzyme important in maintaining the redox homeostasis of the cell by converting oxidised glutathione (GSSG) to reduced glutathione (GSH). The link between inflammation and redox is well studied and polyphenols have been show to modulate both. Curcumin for example has been shown to inhibit both hydrogen peroxide and TNF α induced activation of NF- κ B, AP-1 and the release of IL8, along with increases in levels of GSH and gene expression of GCLC in alveolar epithelial

cells²⁴⁵. With glutathione reductase being found as a common protein modulated by all three treatments, the next step was to validate the changes observed with the proteomics and investigate further the changes to glutathione reaeration and regulation.

7.5 Induction of redox proteins confirmed using protein and gene analysis, together with induction of the antioxidant transcription factor Nrf2.

To confirm the increases in glutathione reductase (GSR) observed with quantitative proteomics in Chapter 4, western blot analysis was performed. Significant increases in GSR were confirmed at the 24h time-point with all treatments, curcumin with a 1.03 fold increase, resveratrol with 1.1 fold and isorhamnetin had the greatest increase with 1.3 fold induction compared with the DMSO treated control. A time-course experiment was conducted to evaluate the gene expression of GSR, along with other genes involved in glutathione production and regeneration. This included glutathione peroxidase (GPx1), an enzyme that scavenges and inactivates hydrogen and lipid peroxidases, protecting the cells from oxidative damage, glutathione synthetase (GSS) and glutamate-cysteine ligase (GCLC), both enzymes involved in the formation of glutathione, with GCLC being the

rate-limiting enzyme. Significant increases in GSR mRNA expression were observed with both curcumin and isorhamnetin, with a doubling of gene expression at the 24h time-point. No increase was observed with resveratrol treatment compared with DMSO treated control. Both GPx1 and GSS showed a decrease in mRNA expression at the 9h time-point with the polyphenols. Only isorhamnetin showed a significant (2.3 fold) increase in GCLC gene expression at the 24 h time-point compared with DMSO treated control. With increases in GSR, converting GSSG back to GSH, GCLC generating more GSH and GPx1 decreased, this suggests an increase in the intracellular concentration of GSH may occur. This was the case for curcumin where GSH levels increased from 716 ± 45 (DMSO) to 3151 ± 436 nmol/million cells with 10 μ M curcumin, but was not seen with isorhamnetin and resveratrol, where both observed a significant reduction in GSH. An explanation may arise from the time-course experiment which showed different expression patterns. For isorhamnetin GSR mRNA expression steadily increased between 9 and 24h, whereas curcumin was increased at 9h but sharply increased at the 24h time-point, and resveratrol showed no significant changes to GSR over the time-points studied. It could be that for resveratrol and isorhamnetin 48h was not a time-point when GSH was most abundant. Further time-points would need to be investigated to determine this. Another explanation is that GSH is utilised by other redox proteins for example glutathione transferase²⁴⁶ and certain peroxiredoxins^{247, 248}, which were both significantly upregulated by the isorhamnetin treatment.

To evaluate the mechanisms underlying these increases in activation of the transcription factor, nuclear factor (erythroid-derived 2)-like 2 (Nrf2) was measured. Nrf2 is a master regulator of antioxidant responses, activating the gene expression of genes such as glutathione reductase (GSR), glutathione transferases (GSTs), Thioredoxin (TXN), thioredoxin reductase (TXNRD), Peroxiredoxins (PRDXs), Glucose-6-phosphate 1-dehydrogenase (G6PD), heme-oxygenase 1 (HO-1) and many others²⁴⁹. These genes regulate processes such as glutathione synthesis, NADPH production and quinone detoxification. The data showed that Nrf2 was significantly activated by both curcumin and isorhamnetin at the 48h time point, compared with DMSO treated control using a Nrf2 DNA binding assay. No significant increase was observed with resveratrol at the 48h time-point. These data are consistent with the changes observed with GSR and GCLC gene expression, as these genes were upregulated by curcumin and isorhamnetin, but not by resveratrol. A time course of Nrf2 activation was conducted and isorhamnetin showed significant activation, initiating at 3h and continued at, 9, 24 and 48h, curcumin was significantly induced at the 9 and 48h time-points. This shows differential activation of Nrf2 with the two compounds. Isorhamnetin appears to be having the greatest effects on Nrf2 activation and also antioxidant gene expression, with increases in glutathione reductase gene and protein expression, along with increases in other redox proteins. Pathway analysis was conducted to link all the changes observed with isorhamnetin contributes to this compound's antioxidant and anti-inflammatory properties.

7.6 Proposed mechanism of the antioxidant action of isorhamnetin.

Isorhamnetin was found to have had the greatest effect on modulation proteins in the Jurkat cell model system, with 403 proteins identified through proteomics. A number of proteins identified contribute to maintaining the redox homeostasis of the cell. These include glutathione reductase, thioredoxin and peroxiredoxins. Further analysis confirmed changes to glutathione reductase, along with the induction of antioxidant gene expression and Nrf2 activation. A proposed mechanism of action was generated, linking together these proteins which were modulated by 30 μ M isorhamnetin treatment (Fig. 7.2).

This mechanism centres on Nrf2 activation, which was demonstrated to be increased following the isorhamnetin treatment, not only at the 48h but also at 3, 9, and 24 h. This contributes to the upregulation of antioxidant genes such as glutathione reductase and glutamate-cysteine ligase which was also shown to be upregulated with isorhamnetin. Nrf2 is also responsible for the regulation of other antioxidant genes such as glutathione transferase, thioredoxin, thioredoxin reductase, peroxiredoxins 1, and for NADPH production, iron sequestration and quinone detoxification²⁵⁶.

Along with Nrf2 there are other cellular components involved in the regulation of antioxidant genes, they are Kelch-like ECH-associated protein 1 (Keap1), and also the antioxidant response elements (ARE). Keap1 is responsible for retaining Nrf2 in the cytoplasm and targets Nrf2 for degradation. Polyphenols have

been shown to inhibit Keap1 and allow nuclear translocation of Nrf2; quercetin has been shown to increase the mRNA expression of Nrf2 and protein and also reduce levels of Keap1 in human HepG2 cells²⁵⁰. Dietary polyphenols may also modulate antioxidant gene expression through the signalling pathways ERK, p38 and JNK^{251, 260}. These pathways are complex, depending on the cell type and activator; the responses can vary from cell proliferation, differentiation, gene expression and apoptosis. Preliminary additional data have shown phosphorylated ERK1/2 is significantly induced at the 24h time-point with isorhamnetin treatment using western blot analysis (data not shown).

The quantitative protein analysis identified a number of redox proteins that were induced following treatment with isorhamnetin, including glutathione reductase, thioredoxin, peroxiredoxins 1, 2, and 6, Glucose-6-phosphate 1-dehydrogenase, Prostaglandin-H2 D-isomerase, and glutathione transferases. Due to the relatively small changes observed western blot was used to confirm the data, GSR induction was observed at the 24h time-point but not at 48h and induction of GSR mRNA was observed. Induction of thioredoxin and peroxiredoxins 2 were also confirmed at the 48h time-point using western blot analysis (data not shown).

Thioredoxin (TRX) is a small, 12 kDa protein acting as an oxoreductase enzyme containing a dithiol-disulfide active site and facilitates the reduction of proteins by cysteine thiol-disulfide exchange. Thioredoxin reductase (TRDX1) regenerates oxidized TRX to its reduced form utilising NADPH²⁵². Both thioredoxin and thioredoxin reductase 1 were both induced by isorhamnetin treatment.

Peroxiredoxins (PRDX) work closely with thioredoxin, as PRDX uses TRX as a reductant after reducing hydrogen peroxide²⁵³. PRDX 1, 2, 3, and 6 were modulated by treatment with isorhamnetin. PRDX1 and 2 reduce peroxidases with reducing agents provided by the thioredoxin system, unlike PRDX6 which has glutathione peroxidase activity²⁵⁴. PRDX3 was the only peroxiredoxin reduced by the isorhamnetin treatment, and has been shown to act synergistically with MAP3K13 to regulate the activation of NF- κ B; inhibition of NF- κ B would correlate with the reduction in cytokine release observed²⁵⁵. Another important redox protein is catalase, which reduces hydrogen peroxide to water and oxygen using Fe in the catalytic site, overexpression of this protein in the mitochondria of mice has been shown to increase lifespan²⁵⁶. Although changes in catalase were not identified by proteomics for isorhamnetin treatment, it was identified for resveratrol treatment. Subsequent data of western blotting analysis has shown showed a significant increase in catalase with all three polyphenol treatments at the 48 h time-point (data not shown).

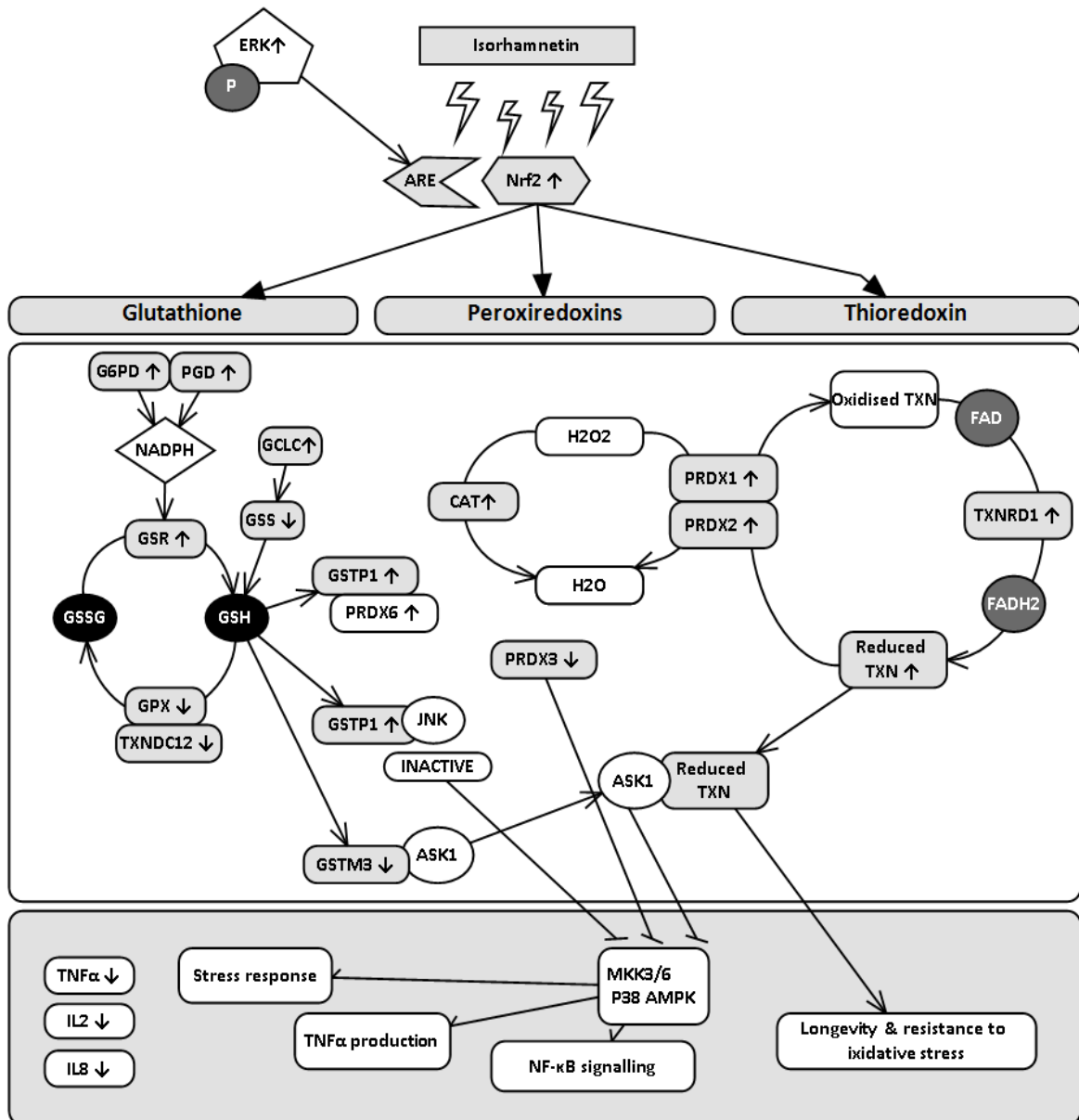


Figure 7.2 – Proposed mechanism of action for the antioxidant and anti-inflammatory effects of Isorhamnetin.

Key – Nrf2 (nuclear factor (erythroid-derived 2)-like 2), ERK (Extracellular signal-regulated kinases 1/2), PRDX (peroxiredoxin), TXN (Thioredoxin), TXNRD1 (thioredoxin reductase 1), FAD (flavin adenine dinucleotide), GSR (glutathione reductase), GPX (glutathione peroxidase), TXNDC12 (Thioredoxin domain-containing protein 12), G6PD (Glucose-6-phosphate 1-dehydrogenase), PGD (Prostaglandin-H2 D-isomerase), NADPH (Nicotinamide adenine dinucleotide phosphate reduced), GSH (reduced glutathione), GSSG (oxidised glutathione), GSTM3 (Glutathione S-transferase M3), GSTP1 (Glutathione S-transferase P), CAT

(Catalase), ASK1 (Apoptosis signal-regulating kinase 1), JNK (c-Jun N-terminal kinases), MKK (Mitogen-activated protein kinase kinase), p38 MAPK (p38 mitogen-activated protein kinase), NF- κ B (nuclear factor kappa B), IL2 (interleukin 2), IL8 (interleukin 8), TNF α (Tumour necrosis factor alpha). Arrows indicate activation whereas flat-headed arrows denote inhibitor effects. [Initial pathway was generated by KEGG pathway database²⁵⁷, additions were added from literature searches^{258,259,260,261,262}].

As discussed previously there were a number of changes to glutathione production and regulation. Increases in GCLC (the rate limiting enzyme in glutathione production) and a decrease in glutathione peroxidases (generating oxidised glutathione) were observed with isorhamnetin. Proteomics also identified proteins involved in NADPH production, G6PD (Glucose-6-phosphate 1-dehydrogenase), PGD (Prostaglandin-H2 D-isomerase), which provide the NADPH molecules required for the enzymatic activity of glutathione reductase and also the thioredoxin²⁶³ and peroxiredoxin 6 system²⁶⁴.

This mechanism proposed (Fig. 7.2) indicated that isorhamnetin treatment leads to the induction of Nrf2 activation, activation of antioxidant genes and altered redox regulation. This is thought to contribute to NF- κ B inhibition, inhibition of pro-inflammatory cytokines and results in the lowering in cytokine release observed with isorhamnetin. To fully evaluate this hypothesis, experimental inhibition of Nrf2 will be required followed by measurements of the effects on cytokine release. Preliminary work has been conducting using the mycotoxin Ochratoxin A to inhibit Nrf2 in the Jurkat T lymphocyte cells but this was inconclusive. It has been previously shown that Nrf2 knockout mice are more sensitive to inflammatory disease²⁶⁵ and carcinogenesis²⁶⁶. It therefore appears that this pathway plays a major role in health and modulations to the pathway may be beneficial in health and disease.

7.7 Cytokine release was significantly reduced by isorhamnetin in THP-1 cells, but changes to glutathione homeostasis were not.

To evaluate these changes to inflammation and redox modulation in the Jurkat cell with isorhamnetin, the experiments conducted were repeated in an alternative cell type, human monocytes THP-1 cells. A significant reduction in IL8 and TNF α , correlates with the Jurkat cells results, other cytokines also lowered included MCP-1, IL1 β , IL6, and GRO. IL10 was also induced with 30 μ M isorhamnetin treatment in THP-1 cells, IL10 is an anti-inflammatory cytokine and is a positive effect on the cell.

Significant activation of Nrf2 was observed, increasing over time from 3h to 48 h; but this activation of Nrf2 didn't result in an increase in antioxidant genes. Quantitative PCR showed no significant changes to the gene expression of glutathione reductase, glutathione peroxidase, glutathione synthase and glutamate cysteine ligase following isorhamnetin treatment. This shows that there are some overlapping areas with where isorhamnetin is having the same effect in both the Jurkat and THP-1 cell lines, but differences in terms of the redox related protein expression.

7.8 Summary.

Ageing has been associated with increases in baseline oxidative stress along with chronic inflammation. This study has shown that dietary polyphenols have the potential to modulate pathways involved in inflammation and redox homeostasis, which could benefit the elderly and could potentially prevent age-related diseases. Isorhamnetin, a compound found in onions significantly lowered the release of inflammatory markers by over 50%, for cytokines IL2, IL8 and TNF in stimulated cells. Isorhamnetin also induced activation of the antioxidant transcription factor Nrf2, which was followed by an induction of antioxidant proteins including glutathione reductase, catalase, peroxiredoxins and thioredoxin. These modulations support the potential use of isorhamnetin and other compounds evaluated in this study, in enhancing cellular antioxidant potential. The incorporation of these types of compounds into a healthy ageing diet could help prevent disease and maintain a healthy lifestyle.

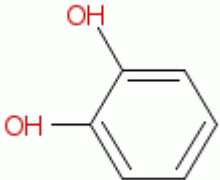
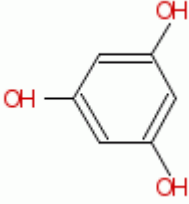
CHAPTER 8

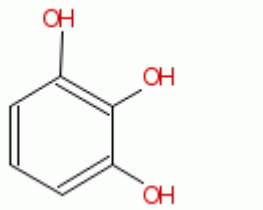
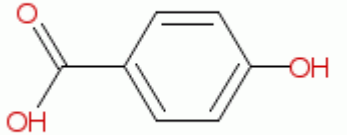
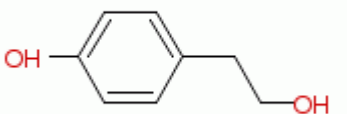
APPENDIX

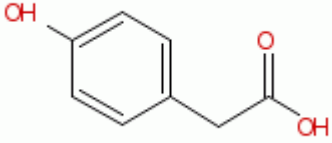
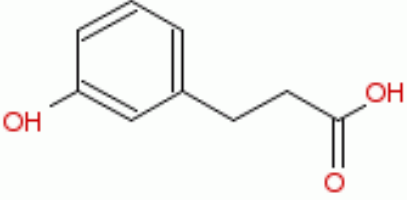
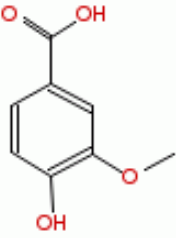
8.1 APPENDIX 1

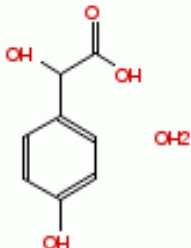
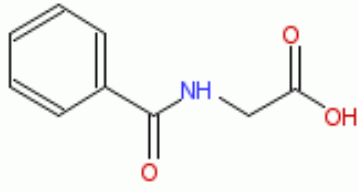
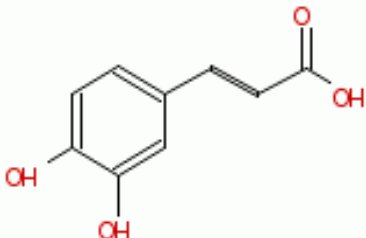
(Poly)phenol data sheets including chemical name, abbreviation, chemical formula, molar mass, structure, food sources of the (poly)phenol and concentrations found in blood plasma (where data available). Data obtained from Phenol Explorer unless otherwise stated.

Table 8.1 Polyphenol data: name, structure, molecular weight, food sources and concentrations in plasma.

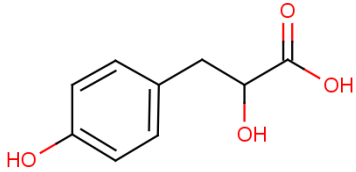
CATECHOL (CAT)		
	<p>Food sources:</p> <p>Food: Cocoa. Drink: Beers, coffee, Green tea (metabolite)</p>	<p>Concentration in plasma:</p> <p>0.262 ± 0.107 µg/ml 5 day treatment of 100mg/m² i.v. for 1h each day in humans.²⁶⁷</p>
<p>Formula: C₆H₆O₂ Molar mass: 110.1 g/mol Log Kow = 0.88</p>		
PHLOROGLUCINOL (PHL)		
	<p>Food sources:</p>	<p>Concentration in plasma:</p> <p>~700 ng/ml was detected in human plasma, 0.33h after administration of a single oral dose of 160mg of phloroglucinol²⁶⁸.</p>
<p>Formula: C₆H₆ O₃ Molar mass: 126.11 g/mol Log Kow = 0.55</p>		

PYROGALLOL (PYR)		
	<p>Food sources:</p> <p>Drinks: Beers, cocoa, green tea (metabolite), coffee, tea</p>	<p>Concentration in plasma:</p>
<p>Formula: C₆H₆O₃ Molar mass: 126.11 g/mol Log Kow = 0.97</p>		
4-HYDROXYBENZOIC ACID (HBA)		
	<p>Food sources:</p> <p>Food: Cereals (Maize, oat, rice), fruit (Berries, grapefruit, dates), carrots, olives, olive oil Drink: Beers, Wines.</p>	<p>Concentration in plasma:</p> <p>9.73 μmol/L after 24h (human – 40 g/day for 4 weeks, cocoa powder in skimmed milk)²⁶⁹</p>
<p>Formula: C₇H₆O₃ Molar mass: 138.12 g/mol Log Kow = 1.58</p>		
TYROSOL (TYR)		
	<p>Food sources:</p> <p>Food: Olives, olive oil, vinegar Drink: Beers, Wines, champagne.</p>	<p>Concentration in plasma:</p> <p>31.710 ± 0.412 μg/ml purified from olive oil by-product in (rat) plasma²⁷⁰.</p>
<p>Formula: C₈H₁₀O₂ Molar mass: 138.16 g/mol Log Kow =</p>		

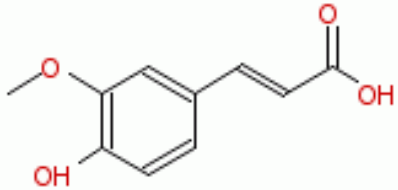
4'-HYDROXYPHENYLACETIC ACID (HPA)		
	<p>Food sources:</p> <p>Food: Cereals (Maize, oats), Olives, Olive oil Drinks: Beers, wine.</p>	<p>Concentration in plasma:</p> <p>0.11 µmol/L after 24h (human – 40 g/day for 4 weeks, cocoa powder in skimmed milk)²⁶⁹²</p>
<p>Formula: C₈H₈O₃ Molar mass: 152.15 g/mol Log Kow = 0.09</p>		
3-(3'-HYDROXYPHENYL)PROPIONIC ACID (HPP)		
	<p>Food sources:</p> <p>Drinks: Red wine and red grape extract capsules Foods: Cocoa</p>	<p>Concentration in plasma:</p> <p>0.23 µmol/L after 24h (human – 40 g/day for 4 weeks, cocoa powder in skimmed milk)²⁶⁹²</p>
<p>Formula: C₉H₁₀O₃ Molar mass: 166.17 g/mol Log Kow = 0.77</p>		
VANILLIC ACID (VAN)		
	<p>Food sources:</p> <p>Food: Cereal (rye, wheat, maize, oat, rice), fruit (dates, berries, grapefruit) Olives, olive oil, soy oil, Herbs (sage, thyme, rosemary, basil, oregano), almonds Drink: Beers, wine (red), rum, cognac, whisky, sherry</p>	<p>Concentration in plasma:</p> <p>2.71 µmol/L after 24h (human – 40 g/day for 4 weeks, cocoa powder in skimmed milk)²⁶⁹²</p>
<p>Formula: C₈H₈O₄ Molar mass: 168.15 g/mol Log Kow = 1.22</p>		

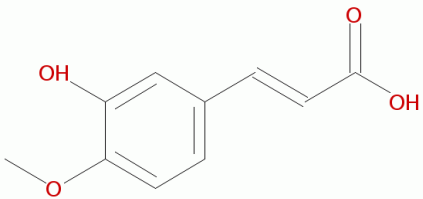
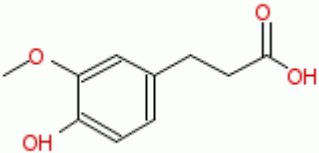
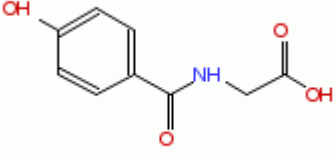
4-HYDROXYMANDELIC ACID (HMA)		
	<p>Food sources:</p> <p>Drinks: Red wine and red grape extract capsules</p>	<p>Concentration in plasma:</p>
<p>Formula: C₈H₈O₄ Molar mass: 168.15 g/mol Log Kow =</p>		
HIPPURIC ACID (HIP)		
	<p>Food sources:</p> <p>Foods: Cocoa, grapes Drinks: Black tea (metabolite), wine (red)</p>	<p>Concentration in plasma:</p> <p>11 nmol/ml in plasma from house painters²⁷¹.</p>
<p>Formula: C₉H₉NO₃ Molar mass: 179.17 g/mol Log Kow = 0.46</p>		
CAFFEIC ACID (CAF)		
	<p>Food sources:</p> <p>Foods: Cereal, dates, lingonberry, blueberries, apples, oil, herbs, olives. Drinks: Beers, cider, wine (red), prune juice, coffee²⁷²</p>	<p>Concentration in plasma:</p> <p>41.3 μmol/L after 8 days (rats 250μmol/day)²⁷³</p>
<p>Formula: C₉H₈O₄ Molar mass: 180.16 g/mol Log Kow = 1.15</p>		

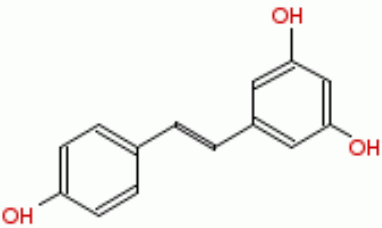
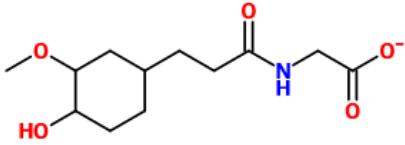
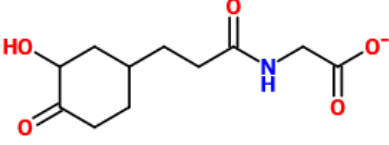
3-(4'-HYDROXYPHENYL)LACTIC ACID (HPL)

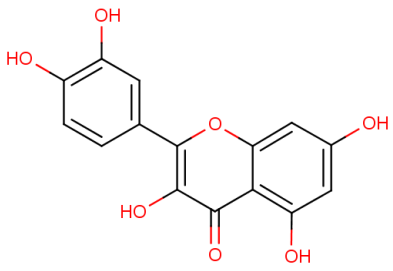
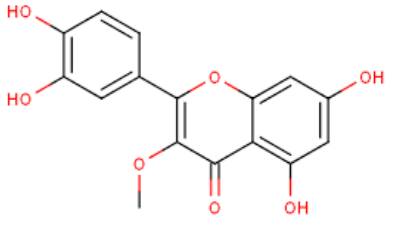
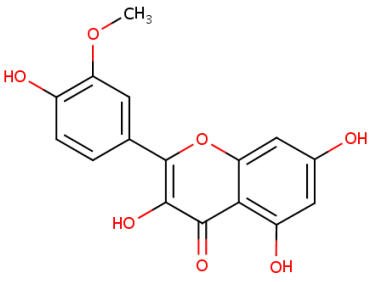
	Food sources:	Concentration in plasma: 118 +/- 45 ng/ml in the plasma of normal humans ²⁷⁴ .
Formula: C ₉ H ₁₀ O ₄ Molar mass: 182.17 g/mol Log Kow = 0.67		

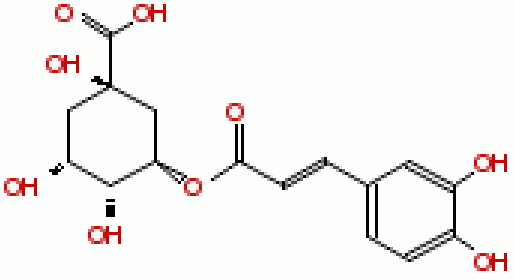
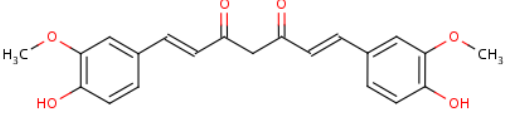
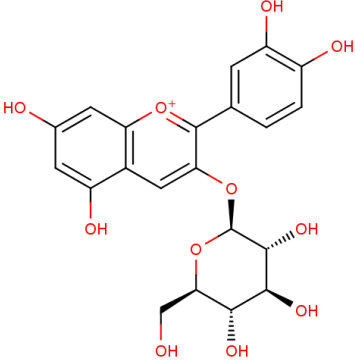
FERULIC ACID (FER)

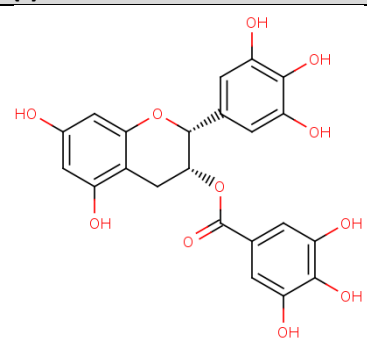
	Food sources: Foods: Cereal (rye, wheat, maize, oat, rice), chocolate, tomatoes, cabbage dried fruit, fruit (berries, grapefruit, apples), olives, olive oil, soy oil, walnuts, herbs (sage, oregano, rosemary), turmeric (metabolite). Drink: Beers, wine, sherry, champagne, coffee, citrus juices ²⁷²⁵ .	Concentration in plasma: 0.21 μmol/L after 24h (human – 40 g/day for 4 weeks, cocoa powder in skimmed milk). ²⁶⁹ 1.68 μmol/L after 30 min (rat – single dose 5.15 mg/kg body weight).
Formula: C ₁₀ H ₁₀ O ₄ Molar mass: 194.18 g/mol Log Kow = 1.51		

ISOFERULIC ACID (IFA)		
	<p>Food sources:</p> <p>Foods: Vinegar.</p>	<p>Concentration in plasma:</p> <p>4.5 $\mu\text{mol/L}$ after 8 days (rat – 250 $\mu\text{mol/day}$ 5-caffeoylquinic acid)</p>
<p>Formula: C₁₀H₁₀O₄ Molar mass: 194.18 g/mol Log Kow = 1.42</p>		
DIHYDROFERULIC ACID (FER)		
	<p>Food sources:</p> <p>Food: turmeric (metabolite). Drink: coffee.</p>	<p>Concentration in plasma:</p>
<p>Formula: C₁₀H₁₂O₄ Molar mass: 196.07 g/mol Log Kow = 1.63</p>		
4'-HYDROXYHIPPURIC ACID (HHA)		
	<p>Food sources:</p> <p>Food: Cocoa</p>	<p>Concentration in plasma:</p> <p>0.11 $\mu\text{mol/L}$ after 24h (human – 40 g/day for 4 weeks, cocoa powder in skimmed milk)²⁶⁹²</p>
<p>Formula: C₉H₉NO₄ Molar mass: 195.0 g/mol Log Kow = 0.67</p>		

RESVERATROL (RES)		
	<p>Food sources:</p> <p>Food: Chocolate, lingonberry, redcurrent, cranberry, oil, pistachio.</p> <p>Drinks: Wine (red).</p>	<p>Concentration in plasma:</p> <p>28.4µM following 2 weeks of oral administration of 75 mg/ml resveratrol in mice²⁷⁵.</p>
<p>Formula: C₁₄H₁₂O₃ Molar mass: 228.0 g/mol Log Kow = 3.1</p>		
FERULOYLGLYCINE (FLG)		
	<p>Food sources:</p> <p>Drinks: Coffee, juice drinks</p>	<p>Concentration in plasma:</p>
<p>Formula: C₁₂H₁₃NO₅ Molar mass: 251.0 g/mol Log Kow = 0.31</p>		
ISOFERULOYLGLYCINE (IFG)		
	<p>Food sources:</p> <p>Drinks: coffee</p>	<p>Concentration in plasma:</p>
<p>Formula: C₁₄H₁₂O₃ Molar mass: 228.0 g/mol Log Kow =</p>		

QUERCETIN (QUE)		
	<p>Food sources:</p> <p>Foods: Cereal, chocolate, apple, tomatoes, onions.</p> <p>Drinks: Beers, wine (red), black tea</p>	<p>Concentration in plasma:</p> <p>3.95 $\mu\text{mol/L}$ 3h after oral consumption of dry shallots (onions) in humans²⁷⁶.</p>
<p>Formula: C₁₅H₁₀O₇ Molar mass: 302.0 g/mol Log Kow = 1.48</p>		
3-O-METHYLQUERCETIN (3MQ)		
	<p>Food sources:</p> <p>Foods: Apples, onions</p>	<p>Concentration in plasma:</p> <p>$\sim 1\mu\text{M}$ after 2h following ingestion of 200mg quercetin in humans²⁷⁷.</p>
<p>Formula: C₁₆H₁₂O₇ Molar mass: 316.26 g/mol Log Kow = 1.65</p>		
ISORHAMNETIN (ISO)		
	<p>Food sources:</p> <p>Foods: Onions (red/yellow)</p> <p>Drinks: Wine (red)</p>	<p>Concentration in plasma:</p> <p>75ng/ml after 72h oral dose in rats²⁷⁸.</p> <p>(isorhamnetin/tamarixetin) 183 ng/ml after 600mg/kg body weight in rats, increased 10 fold after 8 days of Ginkgo extract (Chinese non-flowering plant)²⁷⁹.</p>
<p>Formula: C₁₆H₁₂O₇ Molar mass: 316.26 g/mol Log Kow = 1.78</p>		

CHLOROGENIC ACID (CGA)		
	<p>Food sources:</p> <p>Foods: Dried fruit, carrots, broccoli, blueberries, apples.</p> <p>Drinks: Wine (rosé), tea (green/black), coffee, cider²⁷²⁵.</p>	<p>Concentration in plasma:</p> <p>14.8 ± 11.7 μmol/L after 3h following the consumption of 0.2g decaffeinated green coffee in humans²⁸⁰.</p>
<p>Formula: C₁₆H₁₈O₉ Molar mass: 354.31 g/mol Log Kow = -1.01</p>		
CURCUMIN (CUR)		
	<p>Food sources:</p> <p>Foods: Turmeric, curry powder</p>	<p>Concentration in plasma:</p> <p>11ng/L after 1h consumption of 3.6g curcumin daily for 29 days in humans²⁸¹.</p> <p>2.3 μg/ml (10g) and 1.7μg/ml (12g) after 72h consumption of curcumin in humans²⁸².</p>
<p>Formula: C₂₁H₂₀O₆ Molar mass: 368.38 g/mol Log Kow = 3.29</p>		
CYANIDIN-3-O-GLUCOSIDE (CYA)		
	<p>Food sources:</p> <p>Foods: Olives, lettuce, marionberry</p> <p>Drinks: Wine (red), black grape, raspberry, strawberry, blackcurrent, blackberry, pomegranate juice</p>	<p>Concentration in plasma:</p> <p>0.31 μmol/L after single dose of 0.9mmol/kg body weight in rats.</p> <p>43nmol/L oral consumption of marionberries in pigs²⁸³.</p>
<p>Formula: C₂₁H₂₁O₁₁ Molar mass: 449.0 g/mol Log Kow = 0.77</p>		

(-)-EPIGALLOCATECHIN-3-O-GALLATE (EGCGI)

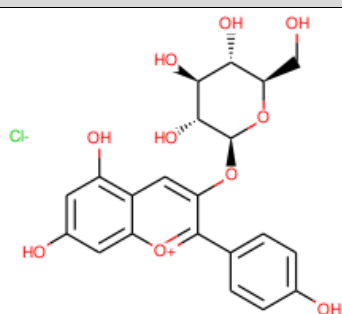
Formula: C₂₂H₁₈O₁₁
Molar mass: 458.37 g/mol
Log Kow = 2.56

Food sources:

Foods: Kiwi,
pecan, hazelnut,
avocado
Drinks: Tea
(green, black,
camomile,
oolong)

Concentration in plasma:

~4μM 90 min after oral
ingestion of green tea
extract in humans. ~8μM
30min post injection of
EGCG

PERARGONIDIN-3-O-GLUCOSIDE (PEL)

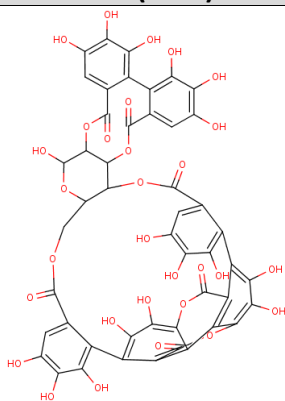
Formula: C₂₁H₂₁O₁₀
Molar mass: 468.84 g/mol
Log Kow = 1.25

Food sources:

Food:
strawberries²⁸⁴

Concentration in plasma:

274 nmol/L after 1h
consumption
of
strawberries in humans²⁸⁴.

PUNICALAGIN (PUN)

Formula: C₄₈H₂₈O₃₀
Molar mass: 1084.0 g/mol
Log Kow = -2.33

Food sources:

Drinks:
Pomegranate
juice

Concentration in plasma:

30μg/ml following
consumption of 1.2g
punicalagin for 37 days in
rats²⁸⁵.

Structures and data from EMBL-EBI (www.ebi.ac.uk, accessed 14.8.13) or Phenol-Explorer (www.phenol-explorer.eu, accessed June 2015)

8.2 APPENDIX 2

Due to the number of (poly)phenols used in the study, experiments were conducted on different days. Graphs were plotted with individual cell numbers or cytokine data both on the same day and also between days to assess the variability between experiments.

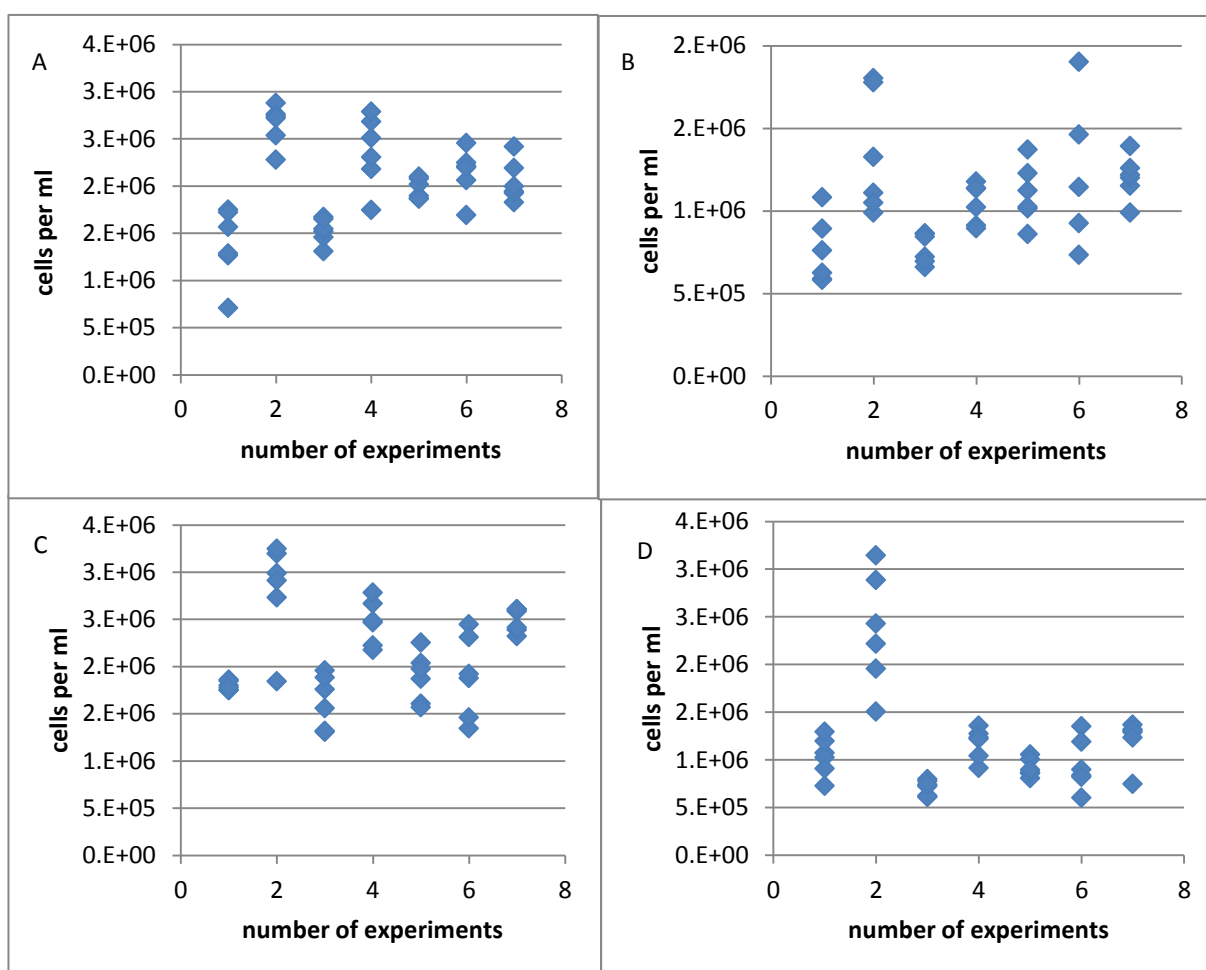


Figure 8.1 – Variability between cell number both within an experiment and also between experiments conducted on different days. Cell viability with 1µM DMSO in A) unstimulated B) stimulated cells and with 30µM DMSO C) unstimulated and D) stimulated cells.

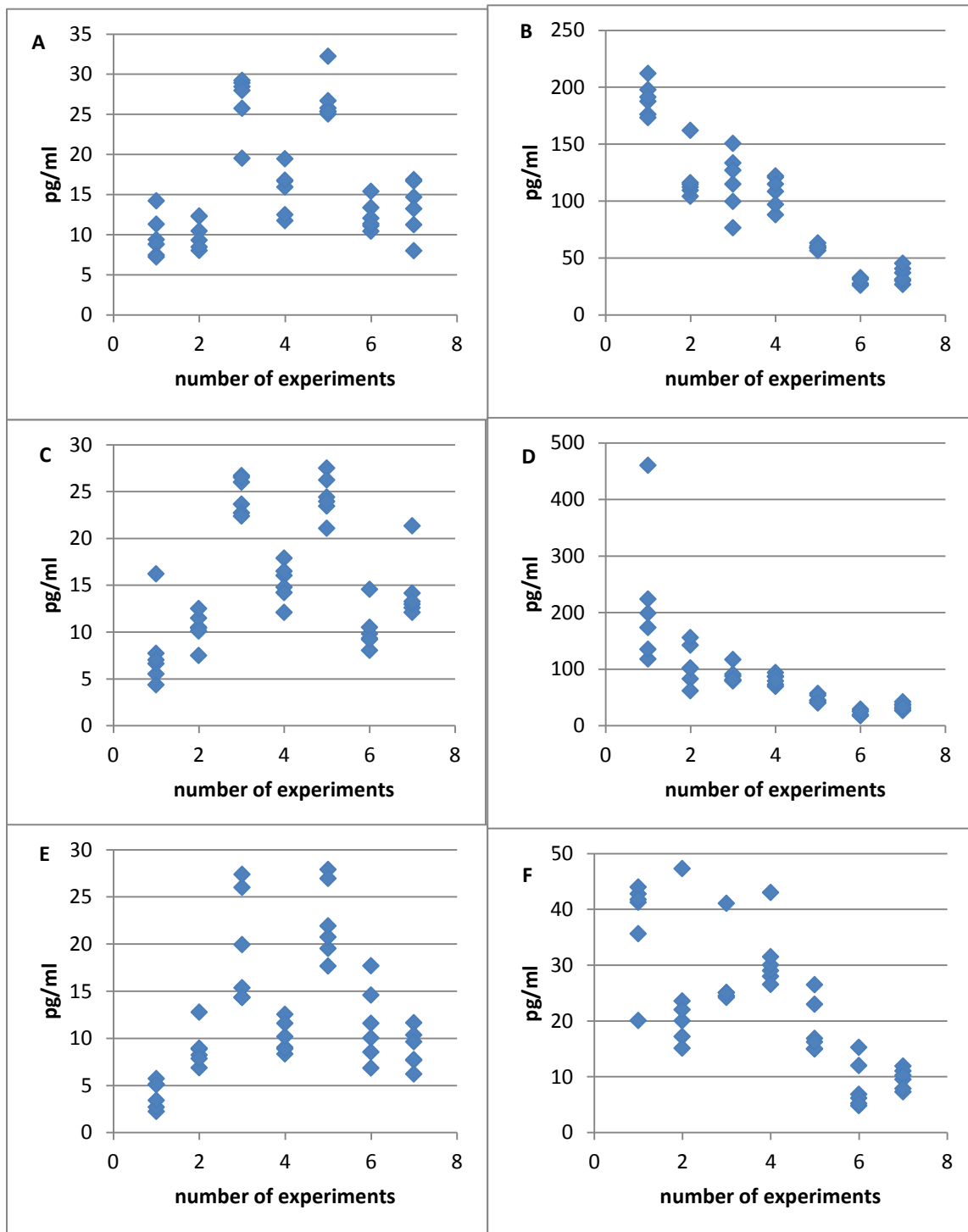


Figure 8.2 – Variability between IL2 and IL8 in unstimulated cells both within an experiment and also between experiments conducted on different days. Variability in untreated cells A) IL2 B) IL8 release, in 1 μ M DMSO treated cells C) IL2 D) IL8 and in 30 μ M DMSO treated cells E) IL2 and F) IL8.

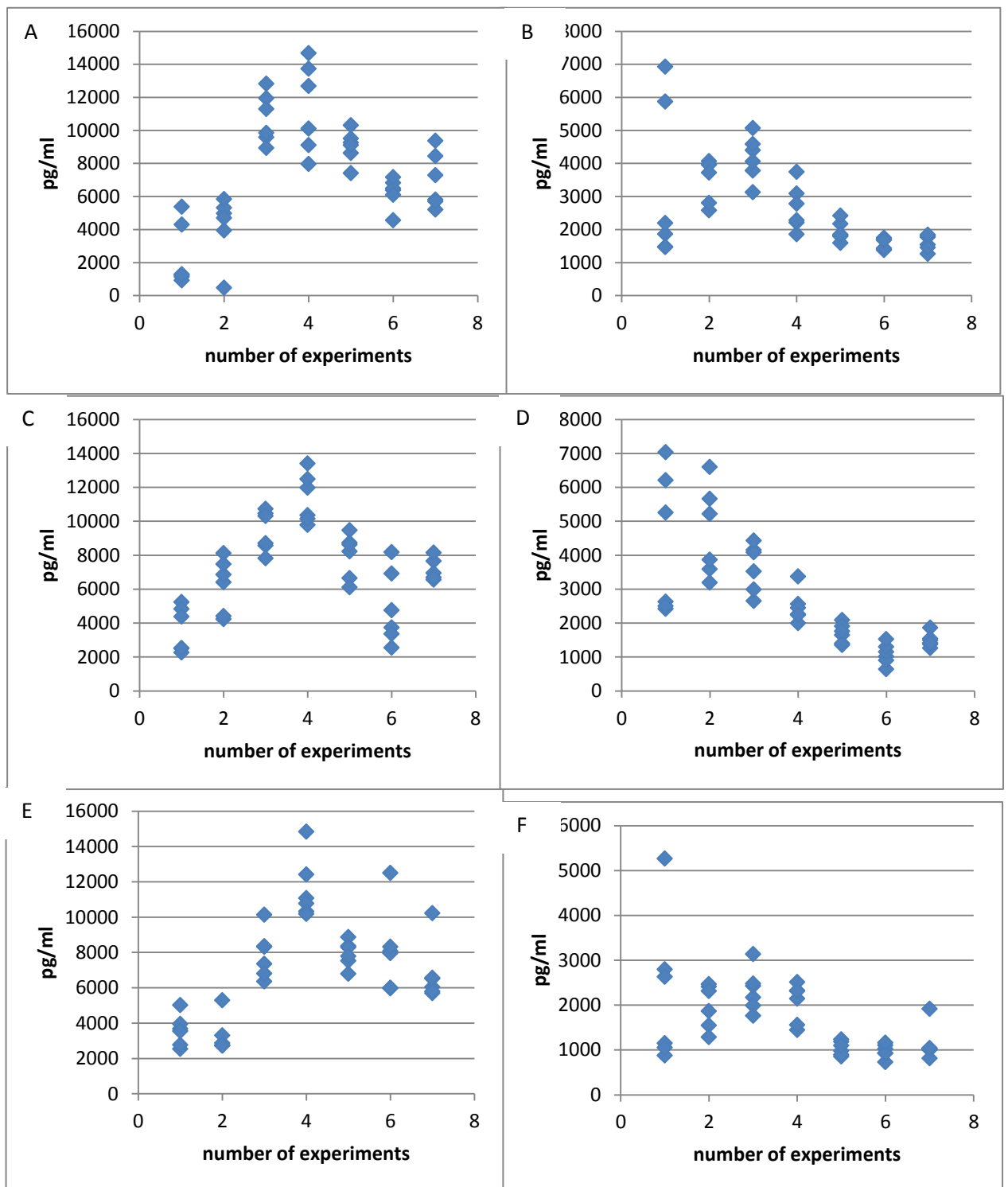


Figure 8.3 – Variability between IL2 and IL8 in PMA/PHA stimulated cells both within an experiment and also between experiments conducted on different days. Variability in untreated cells A) IL2 B) IL8 release, in 1µM DMSO treated cells C) IL2 D) IL8 and in 30µM DMSO treated cells E) IL2 and F) IL8.

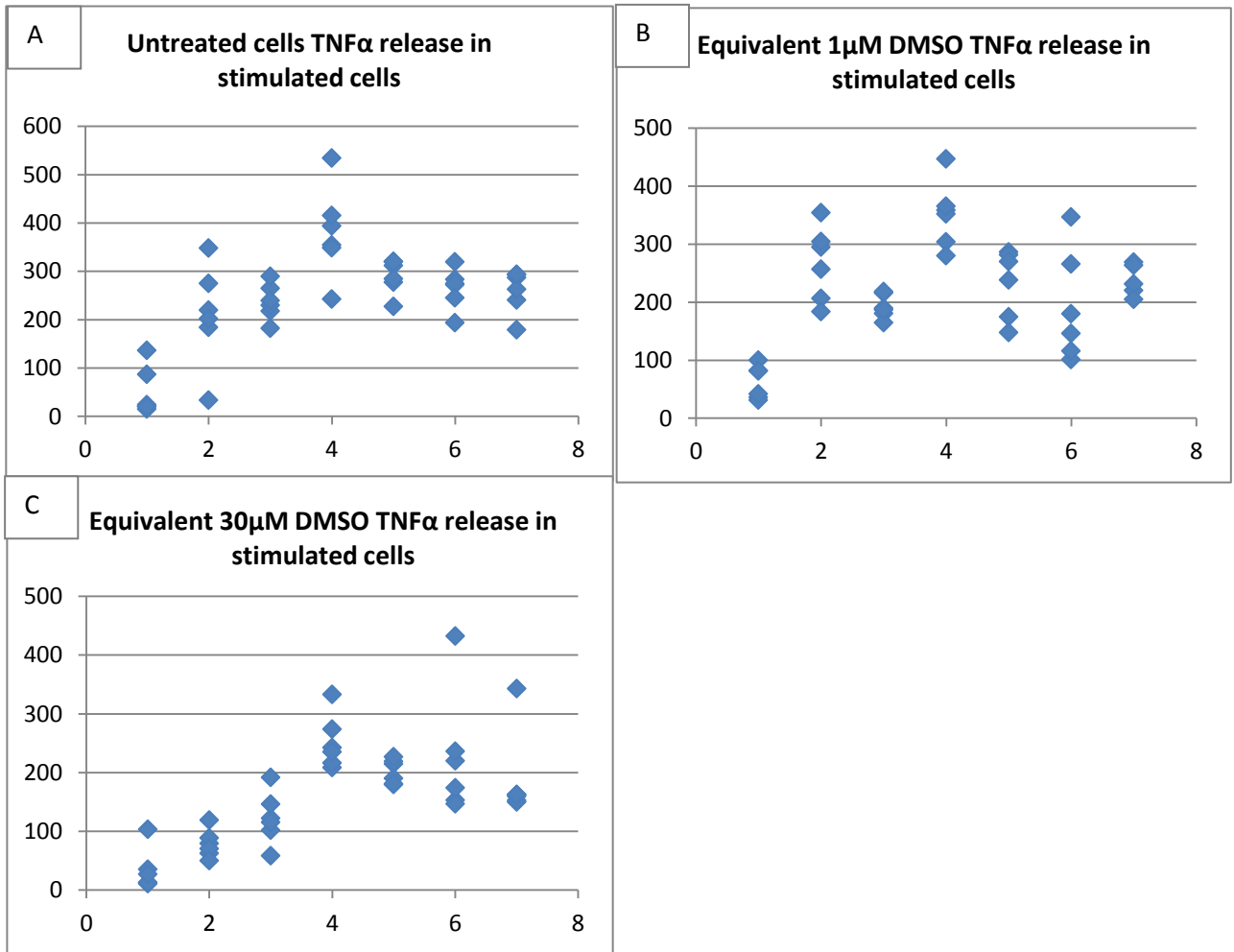


Figure 8.4 – Variability between TNF α in PMA/PHA stimulated cells both within an experiment and also between experiments conducted on different days. Variability in A) untreated cells B) 1 μ M DMSO treated cells C) 30 μ M DMSO treated cells.

Polyphenol cytokine raw data.

Table 8.2. Luminex data for cells treated with 29 different polyphenols at both 1 and 30µM for 48h (unstimulated cells). Mean of the raw data minus DMSO treated control (pg/ml) along with standard error of the mean (SEM).

	IL2 (pg/ml)	SEM	IL8 (pg/ml)	SEM
1µM Catechol	2.4	2.0	23.9	31.0
30µM Catechol	-42.8	8.1	19.1	4.0
1µM Phloroglcinol	-2.4	0.8	-22.4	8.8
30µM Phloroglcinol	-18.2	4.0	4.3	1.4
1µM Pyrogallol	1.4	1.1	114.3	17.2
30µM Pyrogallol	-1.6	0.6	166.1	7.1
1µM Hippuric acid	-0.4	1.2	-1.5	3.1
30µM Hippuric acid	-0.7	1.1	-1.9	0.9
1µM 4'hydroxybenzoic acid	-0.8	0.9	-3.3	14.7
30µM 4'hydroxybenzoic acid	-10.5	11.1	2.4	6.0
1µM Protocatechuic acid	-1.0	1.3	4.0	22.4
30µM Protocatechuic acid	-3.7	14.8	5.5	5.8
1µM 4'Hydroxyphenyllacetic acid	-3.3	1.0	-14.2	5.8
30µM 4'Hydroxyphenyllacetic acid	-3.2	1.2	0.0	1.5
1µM Vanillic acid	-6.5	0.5	-14.4	1.9
30µM Vanillic acid	-2.9	0.5	-4.5	1.7
1µM 4'Hydroxymandelic acid	-6.7	1.7	-28.1	5.2
30µM 4'Hydroxymandelic acid	-3.4	1.1	-8.3	1.7
1µM 3-(3'-hydroxyphenyl)propionic acid	-6.5	1.0	-17.4	4.5
30µM 3-(3'-hydroxyphenyl)propionic acid	-2.3	0.6	-5.6	2.2
1µM 3-(4'-hydroxyphenyl)lactic acid	-4.4	2.0	-23.3	4.8
30µM 3-(4'-hydroxyphenyl)lactic acid	-4.2	1.4	0.8	1.6
1µM Caffeic acid	-1.5	1.9	-2.6	4.2
30µM Caffeic acid	-0.3	1.0	-2.2	2.1
1µM Ferulic acid	-2.1	0.6	-51.5	2.0
30µM Ferulic acid	-1.7	0.5	37.4	2.5
1µM Isoferulic acid	-3.3	0.5	-11.7	4.4
30µM Isoferulic acid	-0.5	0.5	-5.0	1.5
1µM Trysol	-4.1	1.0	-9.7	1.7
30µM Trysol	-6.7	1.0	-7.5	0.6
1µM Dihydroferulic acid	-1.4	0.3	-2.9	1.0
30µM Dihydroferulic acid	-4.4	0.2	-2.1	0.5
1µM 4'-hydroxyhippuric acid	-2.6	0.8	-13.6	2.3

30µM 4'-hydroxyhippuric acid	-2.8	1.0	-3.3	0.7
1µM Feruloglycine	-1.8	0.4	-3.4	1.3
30µM Feruloglycine	-4.6	0.6	-1.8	0.9
1µM Isoferuloylglycine	-2.4	1.1	-55.6	1.7
30µM Isoferuloylglycine	-2.0	0.3	39.3	4.7
1µM Resveratrol	-6.1	1.0	-10.9	2.6
30µM Resveratrol	-6.2	0.6	-5.3	0.5
1µM 5-O-caffeoylquinic acid	-4.0	1.0	-11.6	0.6
30µM 5-O-caffeoylquinic acid	-5.8	0.7	-7.5	0.9
1µM Curcumin	-0.3	0.8	-2.3	1.7
30µM Curcumin	-8.8	0.1	23.4	2.4
1µM Quercetin	-2.1	0.5	-3.9	0.9
30µM Quercetin	-6.1	0.6	-2.4	0.9
1µM 3-O-methylquercetin	4.8	0.8	-1.3	0.9
30µM 3-O-methylquercetin	-5.0	0.6	-3.6	0.6
1µM Isohamnetin	-5.2	1.3	-15.9	0.9
30µM Isohamnetin	-5.4	0.5	-6.4	0.4
1µM EGCG	-0.8	0.3	-100.8	20.4
30µM EGCG	-3.9	0.5	3.8	2.8
1µM Kuromanin	-3.6	0.2	-70.1	23.9
30µM Kuromanin	-5.1	0.3	5.1	8.0
1µM Callistephin chloride	-3.5	0.6	-105.9	6.7
30µM Callistephin chloride	-4.1	0.6	7.5	5.2
1µM Punicalagin	-1.0	1.1	-94.1	10.5
30µM Punicalagin	0.3	0.7	-15.3	2.3

Table 8.3. Luminex data for cells treated with mixtures of 4 different polyphenol compounds at both 1 and 30µM for 48h (unstimulated cells). Mean of the raw data minus DMSO treated control (pg/ml) along with standard error of the mean (SEM).

	IL2 (pg/ml)	SEM	IL8 (pg/ml)	SEM
1µM Mix EGCG, Pun, Call, Kur	-4.7	0.3	-99.9	16.2
30µM Mix EGCG, Pun, Call, Kur	-2.8	0.5	-8.3	4.3
1µM Mix Phlor, Cat, Proto,4-HBA	-0.4	0.7	5.4	16.0
30µM Mix Phlor, Cat, Proto,4-HBA	-20.9	11.3	16.0	9.5
1µM Mix 4-HPLA, 4-HMA, 3HPPA, 3HPLA	-7.5	1.1	-28.5	5.5
30µM Mix 4-HPLA, 4-HMA, 3HPPA, 3HPLA	-7.7	0.6	-9.7	0.7
1µM Mix (Caff, Fer, IF, IFG)	-4.4	0.9	-16.2	4.3
30µM Mix (Caff, Fer, IF, IFG)	-2.0	0.5	-5.3	1.2
1µM Mix (Hipp, 4HHA, Try, 5OCQA)	-3.0	0.8	-6.9	1.9
30µM Mix (Hipp, 4HHA, Try, 5OCQA)	-6.0	0.9	-4.8	1.4
1µM Mix(DHFA, FG, Q, 3OMQ)	-3.6	0.7	-6.5	0.9
30µM Mix(DHFA, FG, Q, 3OMQ)	-5.2	0.6	-4.3	0.5

Mix 1 = Epigallocatechin gallate (EGCG), kuromanin, callistephin chloride, and punicalagin.

Mix 2 = Phloroglucinol, catechol, protocatechuic acid and 4-hydroxybenzoic acid.

Mix 3 = 4'-Hydroxyphenyllacetic acid, 4'-hydroxymandelic acid, 3-(3'-hydroxyphenyl)propionic acid and 3-(4'-hydroxyphenyl)lactic acid.

Mix 4 = Caffeic acid, Ferulic acid, Isoferulic acid and isoferuloylglycine.

Mix 5= Hippuric acid, 4'-hydroxyhippuric acid, tyrosol and chlorogenic acid.

Mix 6 = Dihydroferulic acid, feruloylglycine, quercetin and 3-O-methylquercetin.

Table 8.4. Luminex data for cells treated with 29 different polyphenols at both 1 and 30 μ M for 48h with PMA/PHA stimulation at the 24h time-point (stimulated cells). Mean of the raw data minus DMSO treated control (pg/ml) along with standard error of the mean (SEM).

	IL2 (pg/ml)	SEM	IL8 (pg/ml)	SEM	TNF α (pg/ml)	SEM
1 μ M Catechol	-2056.5	1152.9	229.5	1005.2	-93.6	48.4
30 μ M Catechol	-2495.3	83.3	5015.3	211.9	-52.7	3.0
1 μ M Phloroglucinol	-1400.1	923.2	-1677.2	344.6	-20.1	7.1
30 μ M Phloroglucinol	4106.7	489.3	4336.4	655.9	206.5	22.7
1 μ M Pyrogallol	-716.1	410.8	-199.5	115.6	-62.6	23.0
30 μ M Pyrogallol	-2601.4	467.6	337.2	74.4	-77.5	19.4
1 μ M Hippuric acid	1580.9	596.8	-48.2	91.1	129.3	26.5
30 μ M Hippuric acid	228.6	393.7	82.3	52.0	0.3	11.3
1 μ M 4'hydroxybenzoic acid	5248.1	1111.1	1587.0	841.8	282.5	67.4
30 μ M 4'hydroxybenzoic acid	6328.4	346.8	2667.6	162.1	187.8	25.3
1 μ M Protocatechuic acid	-1674.7	627.0	-280.5	696.0	-21.2	43.4
30 μ M Protocatechuic acid	1823.3	283.6	1750.6	155.4	39.0	5.5
1 μ M 4'Hydroxyphenyllacetic acid	-1184.9	245.6	-347.0	238.0	8.5	14.3
30 μ M 4'Hydroxyphenyllacetic acid	1030.2	629.5	822.4	276.0	22.9	11.6
1 μ M Vanillic acid	-1511.6	451.0	-417.8	128.7	-34.4	23.7
30 μ M Vanillic acid	-1769.4	210.2	-456.8	54.4	-85.6	9.4
1 μ M 4'Hydroxymandelic acid	229.8	212.6	-8.3	265.6	8.8	6.4
30 μ M 4'Hydroxymandelic acid	1071.5	532.9	110.0	155.1	10.3	10.6
1 μ M 3-(3'-hydroxyphenyl)propionic acid	-389.4	415.2	-278.1	290.9	-3.2	3.9
30 μ M 3-(3'-hydroxyphenyl)propionic acid	1519.8	407.8	-3.9	180.7	16.8	5.5
1 μ M 3-(4'-hydroxyphenyl)lactic acid	-917.8	463.3	-959.8	226.0	-15.4	12.9
30 μ M 3-(4'-hydroxyphenyl)lactic acid	-352.7	378.3	-356.1	249.3	-15.5	9.8
1 μ M Caffeic acid	-2617.5	401.0	-701.5	155.5	-50.4	15.1
30 μ M Caffeic acid	-1901.4	518.7	-365.3	139.1	-42.0	11.7
1 μ M Ferulic acid	-1366.5	281.6	-458.6	89.1	-34.0	18.8
30 μ M Ferulic acid	-1394.2	546.1	-571.4	144.4	-51.8	23.2
1 μ M Isoferulic acid	-13.6	581.9	-281.2	151.7	-2.0	21.8
30 μ M Isoferulic acid	-1677.9	468.6	-507.6	94.4	-59.5	14.1
1 μ M Trysol	-141.1	284.3	141.0	120.1	75.7	26.7

30µM Trysol	-920.3	381.8	-23.5	77.0	21.5	22.0
1µM Dihydroferulic acid	-730.0	592.4	-353.6	105.3	-30.8	22.4
30µM Dihydroferulic acid	-3263.8	500.2	-433.9	41.3	-126.8	11.2
1µM 4'-hydroxyhippuric acid	-751.4	237.9	-192.8	90.7	34.8	16.5
30µM 4'-hydroxyhippuric acid	-687.1	381.5	92.9	79.0	12.2	13.1
1µM Feruloglycine	8322.7	1500.0	825.1	279.0	265.6	50.4
30µM Feruloglycine	-296.1	939.5	56.2	147.8	-54.0	14.4
1µM Isoferuloylglycine	-2065.0	517.1	-606.6	144.0	-56.6	27.0
30µM Isoferuloylglycine	-3393.3	554.3	-918.7	98.4	-78.8	18.3
1µM Resveratrol	-1311.0	77.5	-216.5	75.6	-96.5	34.2
30µM Resveratrol	-4260.4	177.6	-50.7	68.0	-144.3	5.7
1µM 5-O-caffeoylquinic acid	-222.3	356.1	-94.3	112.7	43.3	16.6
30µM 5-O-caffeoylquinic acid	-1162.0	337.0	-189.6	79.4	-19.3	12.4
1µM Curcumin	-2169.0	404.3	-567.2	159.8	-81.2	31.3
30µM Curcumin	-6656.7	16.6	-699.9	40.8	-185.2	0.2
1µM Quercetin	8268.4	1001.0	290.1	171.3	70.4	36.8
30µM Quercetin	-6844.8	238.1	-84.4	138.2	-202.6	3.3
1µM 3-O-methylquercetin	24240.9	2178.8	1904.4	178.9	185.2	27.7
30µM 3-O-methylquercetin	-6820.9	123.8	-314.4	75.5	-208.8	1.9
1µM Isohamnetin	-3608.9	290.9	-860.7	90.4	-150.4	17.2
30µM Isohamnetin	-3947.5	365.8	-665.1	89.9	-159.4	5.1
1µM EGCG	-420.5	254.1	1014.2	490.7	22.3	6.6
30µM EGCG	-821.2	268.7	1459.4	251.2	16.7	8.2
1µM Kuromanin	-804.2	488.6	-428.8	588.3	31.2	6.2
30µM Kuromanin	-928.3	215.6	354.1	273.2	-1.6	2.7
1µM Callistephin chloride	-636.6	304.2	572.0	244.4	22.8	8.7
30µM Callistephin chloride	-884.2	132.5	221.7	93.7	-2.9	2.1
1µM Punicalagin	595.6	231.3	1774.6	398.1	148.5	8.8
30µM Punicalagin	-456.5	275.9	147.2	226.5	170.9	6.2

Table 8.4. Luminex data for cells treated with mixtures of 4 different polyphenol compounds at both 1 and 30µM for 48h with PMA/PHA stimulation at the 24h time-point (stimulated cells). Mean of the raw data minus DMSO treated control (pg/ml) along with standard error of the mean (SEM).

	IL2 (pg/ml)	SEM	IL8 (pg/ml)	SEM	TNFα (pg/ml)	SEM
1µM Mix 1(EGCG, Pun, Call, Kur)	-1121.3	681.0	107.5	1284.8	10.8	19.6
30µM Mix 1 (EGCG, Pun, Call, Kur)	-2518.5	202.0	-1630.5	122.2	6.5	1.6
1µM Mix 2(Phlor, Cat, Proto,4-HBA)	1397.3	683.3	2208.6	531.1	73.2	35.9
30µM Mix 2 (Phlor, Cat, Proto,4-HBA)	1180.9	428.5	4990.8	493.4	-5.2	6.6
1µM Mix 3 (4-HPLA, 4-HMA, 3HPPA, 3HPLA)	-1065.5	328.0	-692.1	225.2	-22.2	10.7
30µM Mix 3 (4-HPLA, 4-HMA, 3HPPA, 3HPLA)	602.6	387.5	217.2	223.6	-4.5	2.4
1µM Mix 4 (Caff, Fer, IF, IFG)	-2181.5	438.4	-633.0	100.9	-64.7	11.4
30µM Mix 4 (Caff, Fer, IF, IFG)	-980.4	498.3	-725.5	120.9	-37.6	12.9
1µM Mix 5 (Hipp, 4HHA, Try, 5OCQA)	-666.9	385.5	-408.9	98.2	-55.1	20.6
30µM Mix 5 (Hipp, 4HHA, Try, 5OCQA)	-1345.8	75.7	-330.6	52.5	-104.0	13.3
1µM Mix 6 (DHFA, FG, Q, 3OMQ)	2689.1	673.0	-291.1	150.6	-60.3	12.9
30µM Mix 6 (DHFA, FG, Q, 3OMQ)	-4120.4	633.1	-215.1	140.9	-174.5	6.8

Mix 1 = Epigallocatechin gallate (EGCG), kuromanin, callistephin chloride, and punicalagin.

Mix 2 = Phloroglucinol, catechol, protocatechuic acid and 4-hydroxybenzoic acid.

Mix 3 = 4'-Hydroxyphenyllactic acid, 4'-hydroxymandelic acid, 3-(3'-hydroxyphenyl)propionic acid and 3-(4'-hydroxyphenyl)lactic acid.

Mix 4 = Caffeic acid, Ferulic acid, Isoferulic acid and isoferuloylglycine.

Mix 5= Hippuric acid, 4'-hydroxyhippuric acid, tyrosol and chlorogenic acid.

Mix 6 = Dihydroferulic acid, feruloylglycine, quercetin and 3-O-methylquercetin.

8.3 APPENDIX 3

Principal component analysis (PCA): PCA plots are used to determine how well the proteomics data has separated between control and treatment groups.

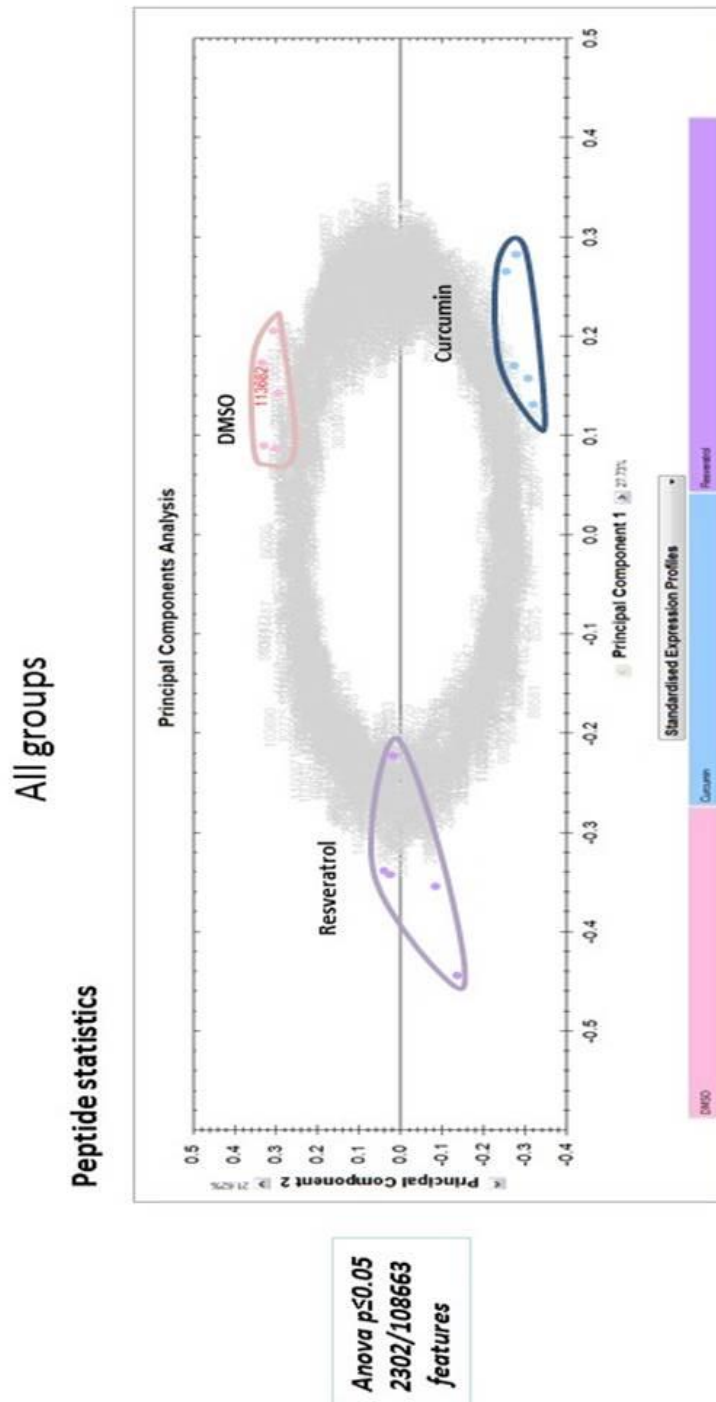


Figure 8.5 - PCA Plots for peptide data generated from proteomics using 1 μ M treatments of curcumin and resveratrol compared to DMSO treated control.

Protein statistics

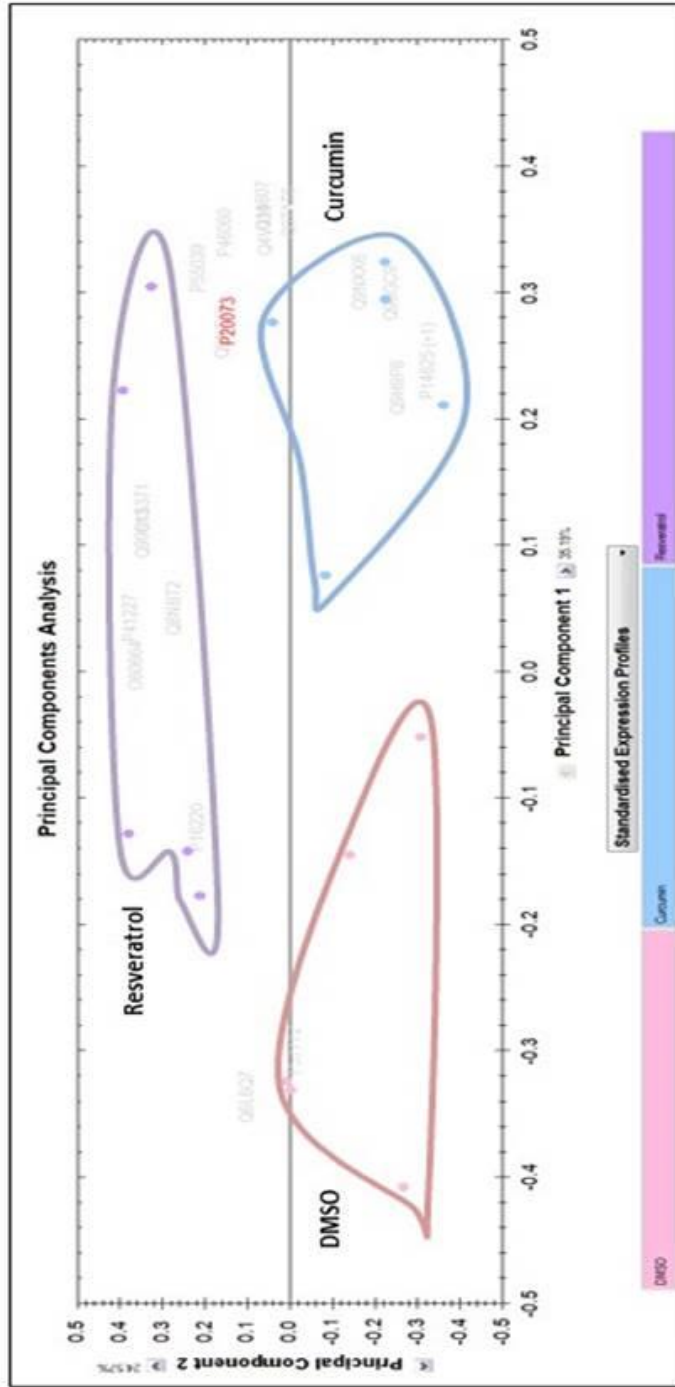


Figure 8.6 - PCA Plots for protein data generated from proteomics using 1µM treatments of curcumin and resveratrol compared to DMSO treated control.

Peptide statistics

DMSO vs Curcumin

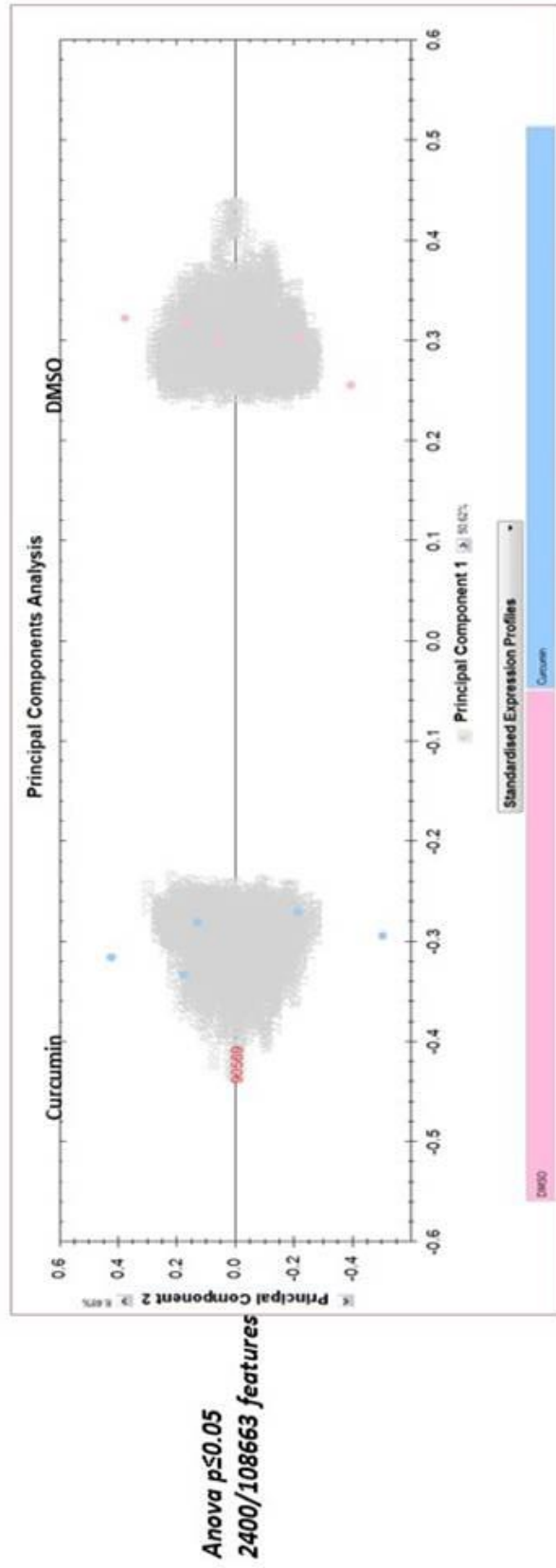
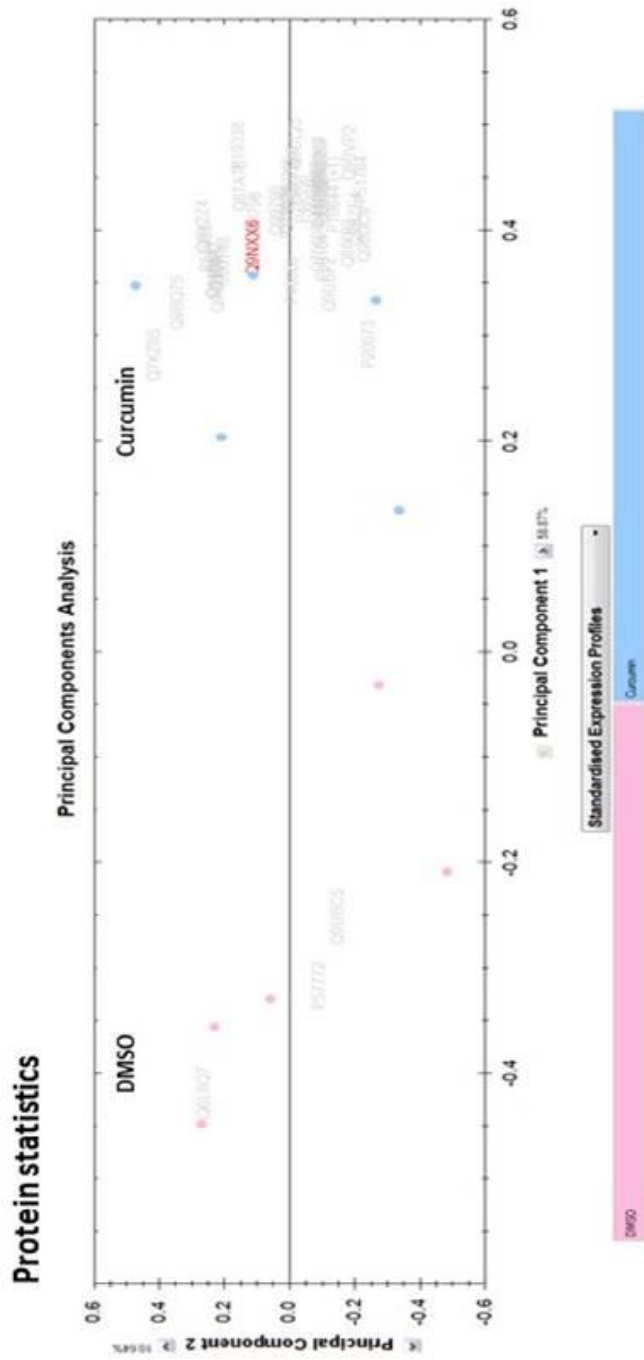


Figure 8.7 - PCA Plots for peptide data generated from proteomics using 1 μ M treatments of curcumin compared to DMSO treated control.



Anova $p \leq 0.05$
 42/2048 proteins

Figure 8.8 - PCA Plots for protein data generated from proteomics using 1 μ M treatments of curcumin compared to DMSO treated control.

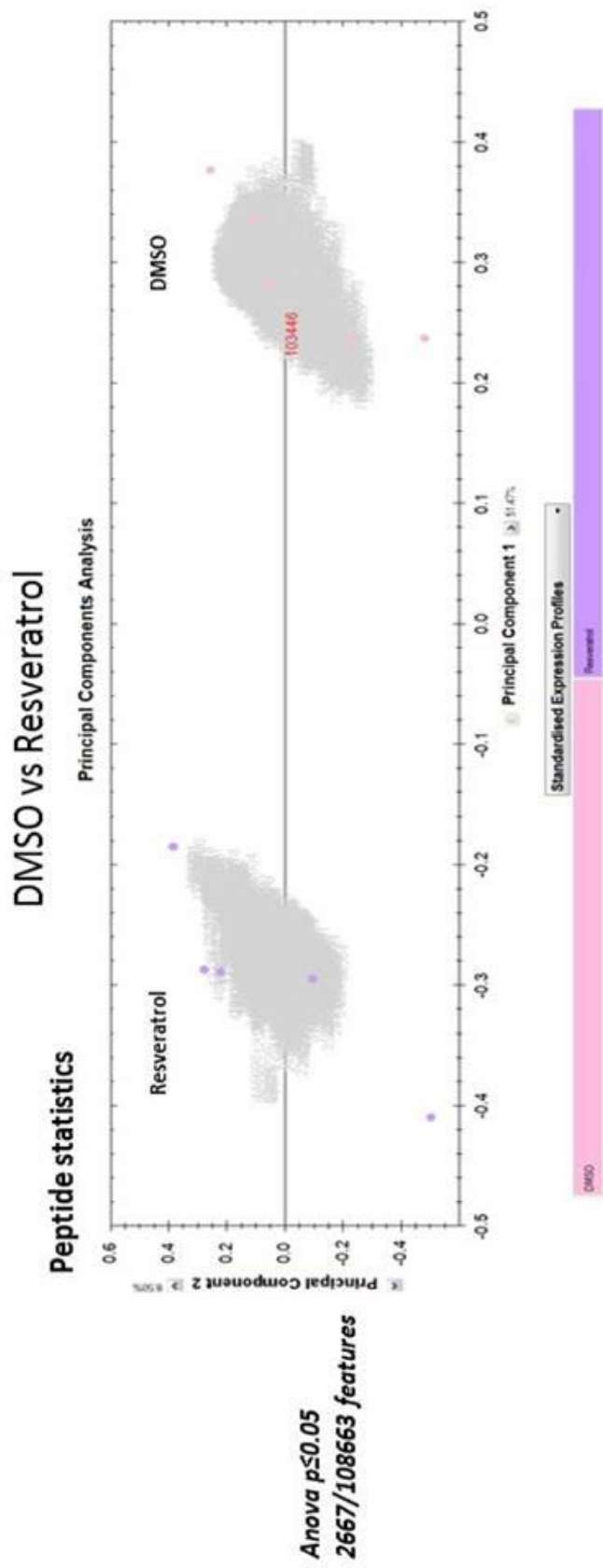
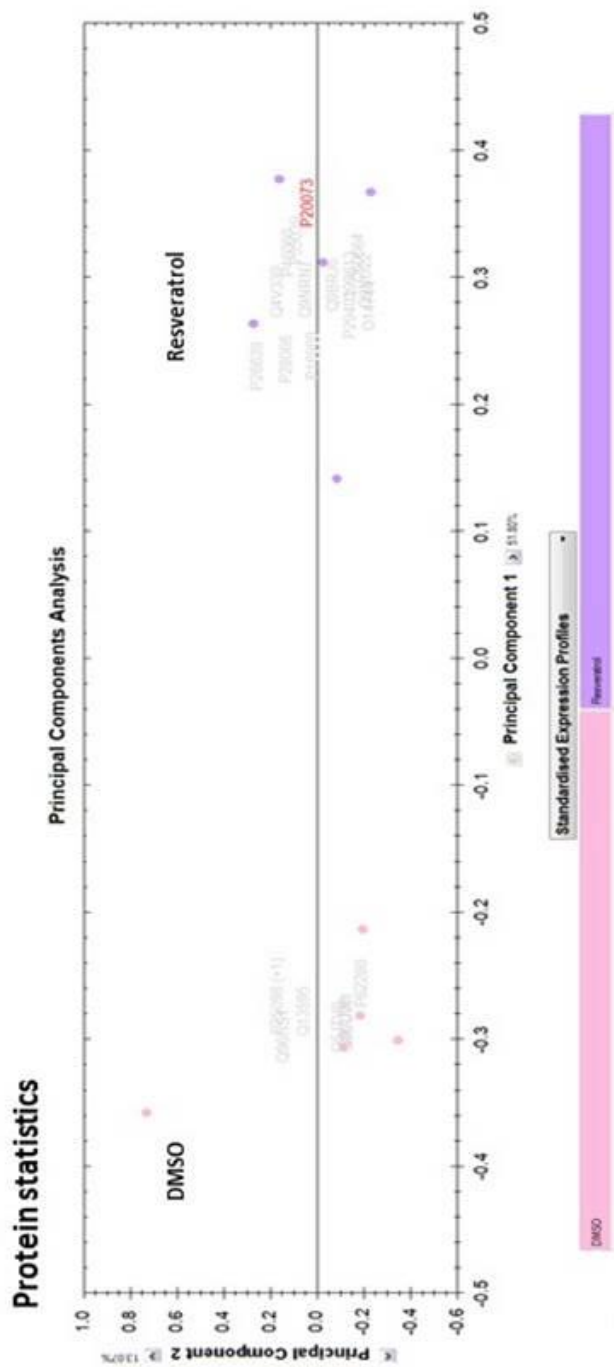


Figure 8.9 - PCA Plots for peptide data generated from proteomics using 1 μ M treatments of resveratrol compared to DMSO treated control.



Anova $p < 0.05$
21/2048 proteins

Figure 8.10 - PCA Plots for protein data generated from proteomics using 1µM treatments of resveratrol compared to DMSO treated control.

Peptide statistics

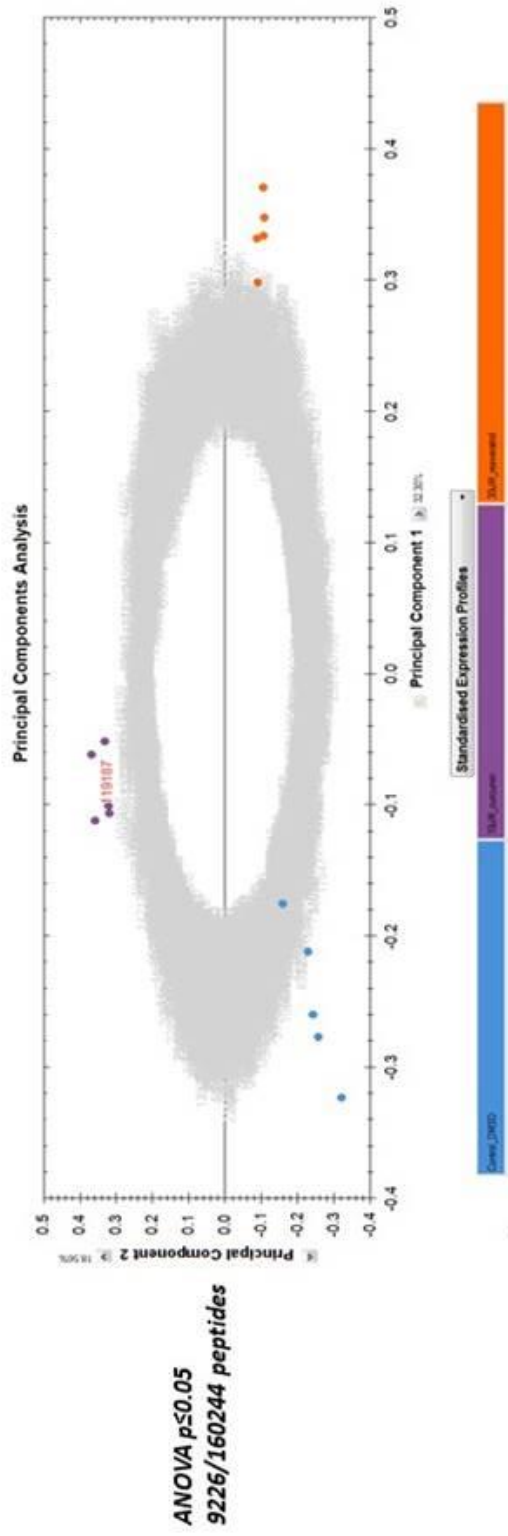


Figure 8.11 - PCA Plots for peptide data generated from proteomics using 10µM treatments of curcumin and 30µM resveratrol compared to DMSO treated control.

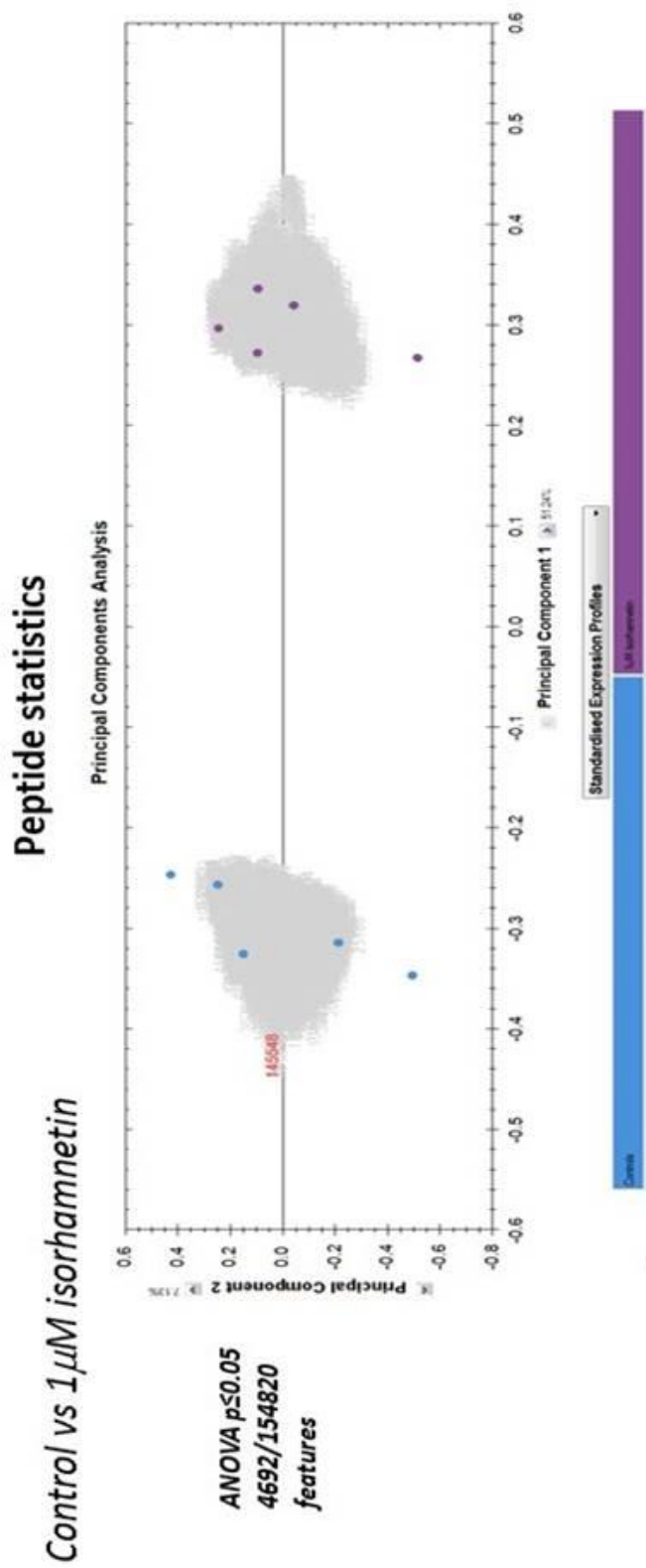


Figure 8.13 - PCA Plots for peptide data generated from proteomics using 1µM treatments of isorhamnetin compared to DMSO treated control.

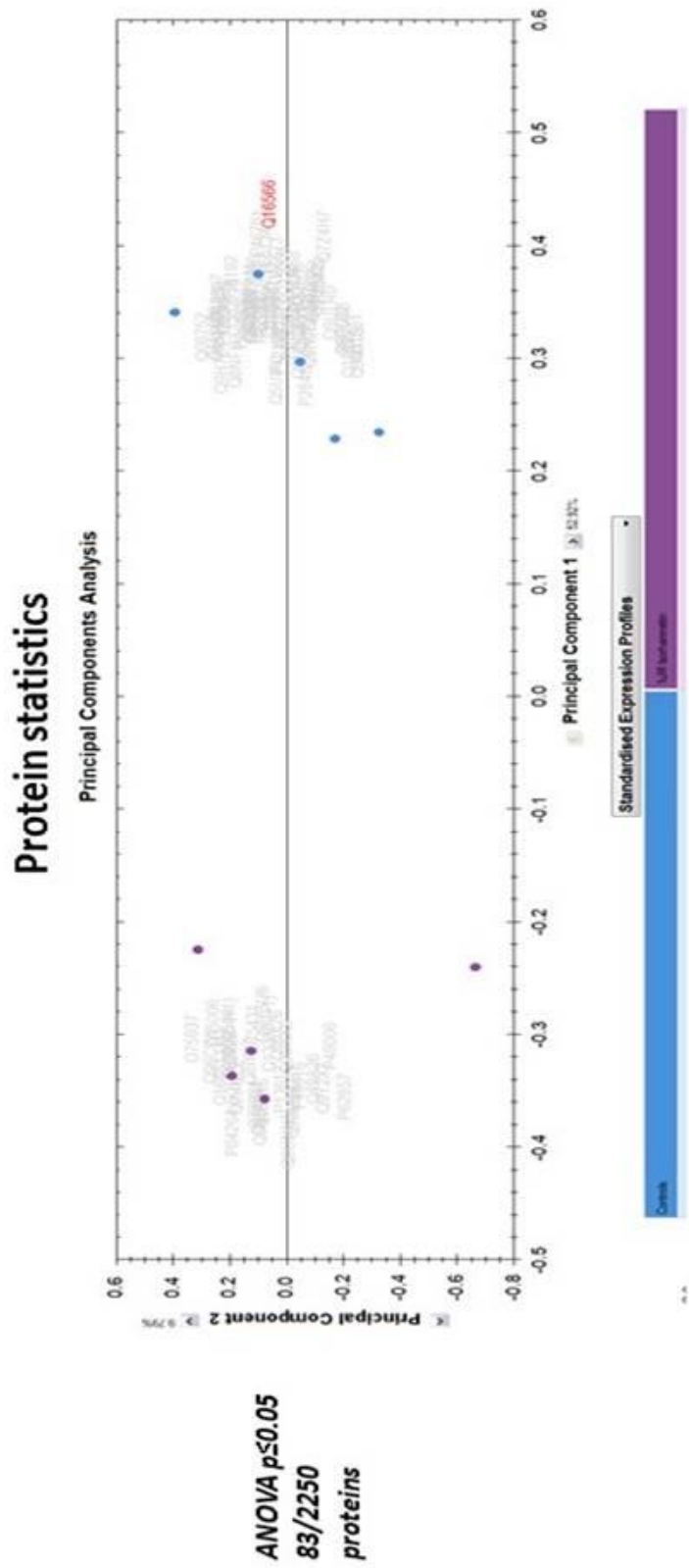


Figure 8.14 - PCA Plots for protein data generated from proteomics using 1µM treatments of isorhamnetin compared to DMSO treated control.

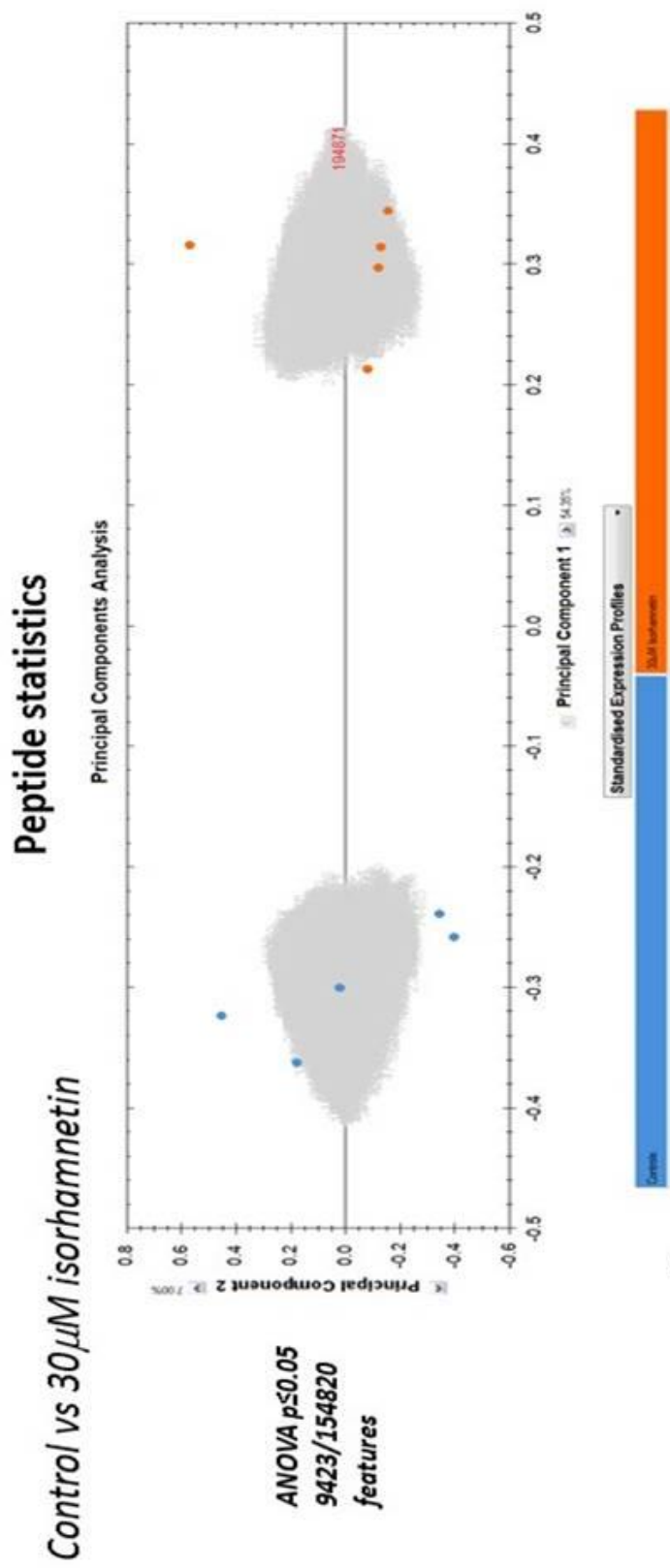
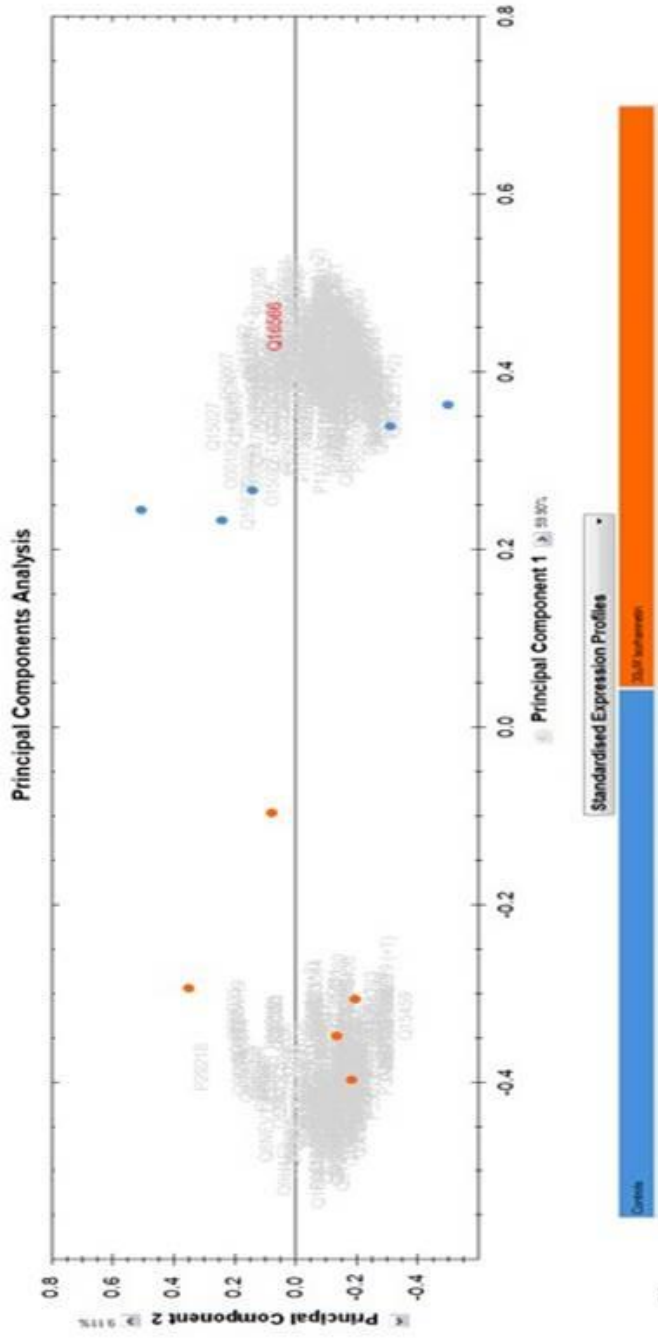


Figure 8.15 - PCA Plots for peptide data generated from proteomics using 30µM treatments of isorhamnetin compared to DMSO treated control.

Protein statistics



ANOVA $p \leq 0.05$
403/2250
proteins

Figure 8.16 - PCA Plots for protein data generated from proteomics using 30µM treatments of isorhamnetin compared to DMSO treated control.

8.4 APPENDIX 4

Table 8.6 – Significantly modulated proteins in Jurkat T lymphocytes after 1 μ M resveratrol identified by label-free LC-MS.

Accession ^a	Description ^b	Confidence score ^c	Fold change	p-value	q-value
Q96HS1	Serine/threonine-protein phosphatase PGAM5, mitochondrial, PGAM5	91.21	1.32	0.040	0.999
Q86U38	Nucleolar protein 9, NOP9	136.99	1.27	0.006	0.999
P25098	Beta-adrenergic receptor kinase 1, ADRBK1	187.92	1.22	0.046	0.999
Q9UDW1	Cytochrome b-c1 complex subunit 9, UQCR10	113.05	1.20	0.013	0.999
P62280	40S ribosomal protein S1, RPS11	492.97	1.14	0.028	0.999
Q5JTV8	Torsin-1A-interacting protein 1, TOR1AIP1	140.77	1.14	0.032	0.999
P29401	Transketolase, TKT	1231.04	1.10	0.041	0.999
Q13595	Transformer-2 protein homolog alpha, TRA2A	151.78	1.10	0.037	0.999
P28066	Proteasome subunit alpha type-5, PSMA5	252	1.10	0.041	0.999
P26639	Threonine--tRNA ligase, cytoplasmic, TARS	431.43	1.12	0.046	0.999
P46060	Ran GTPase-activating protein 1, RANGAP1*	486.43	1.17	0.024	0.999
Q99613	Eukaryotic translation initiation factor 3 subunit C, EIF3C	639.11	1.19	0.039	0.999
O14744	Protein arginine N-methyltransferase 5, PRMT5	252.84	1.19	0.021	0.999
Q9BRJ6	Uncharacterized protein,	54.59	1.21	0.018	0.999

	C7orf50				
P20073	Annexin A7, ANXA7*	141.91	1.23	0.000	0.300
P16989	Y-box-binding protein 3, CSDA	268.94	1.28	0.039	0.999
P55039	Developmentally-regulated GTP-binding protein 2, DRG2*	70.26	1.29	0.010	0.999
O60664	Perilipin-3, PLIN3	241.46	1.31	0.017	0.999
Q9NRN7	L-aminoadipate-semialdehyde dehydrogenase - phosphopantetheinyl transferase, AASDHPPT	74.55	1.38	0.048	0.999
Q4V339	COBW domain-containing protein 6, CBWD6*	35.08	1.85	0.028	0.999
Q9NU22	Midasin, MDN1	67.54	2.65	0.036	0.999

^a Accession number according to UniProt database. ^b Protein description with relative symbol. ^c Confidence score generated by Progenesis. * Proteins shared between both treatments (resveratrol and curcumin). Green reduction, red induction.

1.0 – 1.49		
1.5 – 1.99		
2 – 2.49		
2.5 – 2.99		
3 – 3.49		
3.5 +		
* Protein common between resveratrol and curcumin treatment.		

Table 8.7 – Significantly modulated proteins in Jurkat T lymphocytes after 1 μ M curcumin identified by label-free LC-MS.

Accession ^a	Description ^b	Confidence score ^c	Fold change	p-value	q-value
Q9UBC5	Unconventional myosin-1a, MYO1A	55.74	3.63	0.048	0.997
Q6L8Q7	2',5'-phosphodiesterase 12, HNRPD1	53.82	1.33	0.019	0.997
P57772	Selenocysteine-specific elongation factor, EEFSEC	31.69	1.29	0.013	0.997
O75608	Acyl-protein thioesterase 1, LYPLA1	124.72	1.11	0.043	0.997
P19338	Nucleolin, NCL	2004.18	1.12	0.003	0.997
P36954	DNA-directed RNA polymerase II subunit RPB9, POLR2I	83.56	1.12	0.33	0.997
Q9UBF2	Coatomer subunit gamma-2, COPG2	282.00	1.13	0.024	0.997
O14979	Heterogeneous nuclear ribonucleoprotein D-like, HNRPD1	374.30	1.13	0.021	0.997
Q99798	Aconitate hydratase, mitochondrial, ACO2	697.28	1.14	0.037	0.997
Q9Y3D6	Mitochondrial fission 1 protein, FIS1	27.44	1.15	0.010	0.997
Q14257	Reticulocalbin-2, RCN2	235.41	1.16	0.039	0.997
Q10567	AP-1 complex subunit beta-1, Ap1B1	360.9	1.17	0.031	0.997
Q07960	Rho GTPase-activating protein 1, ARHGAP1	160.70	1.17	0.005	0.997
P46060	Ran GTPase-activating protein 1, RANGAP1*	486.43	1.17	0.016	0.997
P48556	26S proteasome non-ATPase regulatory subunit 8, PSMD8	149.62	1.18	0.041	0.997
O00148	ATP-dependent RNA helicase, DDX39A	879.06	1.18	0.045	0.997

P20073	Annexin A7, ANXA7*	141.91	1.19	0.035	0.997
Q9BQ75	Protein CMSS1, C3orf26	73.7	1.19	0.045	0.997
Q00796	Sorbitol dehydrogenase, SORD	199.37	1.20	0.040	0.997
P10644	cAMP-dependent protein kinase type I-alpha regulatory subunit, PRKAR1A	185.21	1.21	0.037	0.997
Q16851	UTP--glucose-1-phosphate uridylyltransferase, UGP2	181.55	1.23	0.030	0.997
P51784	Ubiquitin carboxyl-terminal hydrolase 11, USP11	153.8	1.23	0.041	0.997
P09104	Gamma-enolase, ENO2	1052.23	1.24	0.046	0.997
Q15363	Transmembrane emp24 domain-containing protein 2, TMED2	165.36	1.25	0.003	0.997
Q9UL25	Ras-related protein Rab-21, RAB21	116.79	1.26	0.008	0.997
Q9BVP2	Guanine nucleotide-binding protein-like 3, GNL3	176.98	1.27	0.008	0.997
P55039	Developmentally-regulated GTP-binding protein, DRG2*	70.26	1.28	0.043	0.997
Q7KZ85	Transcription elongation factor SPT6, EEFSEC	136.36	1.31	0.036	0.997
Q14807	Kinesin-like protein KIF22	34.55	1.31	0.035	0.997
Q8IYB3	Serine/arginine repetitive matrix protein 1, SRRM1	114.74	1.31	0.041	0.997
Q8IZ69	tRNA (uracil-5-)-methyltransferase homolog A, TRMT2A	40.54	1.32	0.042	0.997
Q9NTX5	Ethylmalonyl-CoA decarboxylase, ECHDC1	61.11	1.34	0.045	0.997
Q14011	Cold-inducible RNA-binding protein, CIRPDL	48.91	1.34	0.018	0.997
Q9Y4P1	Cysteine protease ATG4B	64.94	1.40	0.042	0.997

Q96GC9	Vacuole membrane protein 1, VMP1	32.02	1.47	0.039	0.997
Q9Y2Z4	Tyrosine--tRNA ligase, mitochondrial, YARS2	29.61	1.51	0.003	0.997
O75874	Isocitrate dehydrogenase [NADP] cytoplasmic, IDH1	124.87	1.51	0.016	0.997
Q9NXX6	Non-structural maintenance of chromosomes element 4 homolog A, NSMCE4A	32.05	1.59	0.001	0.997
Q9BZE4	Nucleolar GTP-binding protein , GTPBP4	92.43	1.74	0.014	0.997
Q9C0C9	Ubiquitin-conjugating enzyme E2 O, UBE20	55.05	1.74	0.032	0.997
Q8TAT6	Nuclear protein localization protein 4 homolog, NPLOC4	91.12	1.76	0.002	0.997
Q4V339	COBW domain-containing protein 6 (Cobalamin synthase W domain containing protein 6. Colbalamin = vitamin B12), CBWD6*	35.08	1.99	0.010	0.997

^a Accession number according to UniProt database. ^b Protein description with relative symbol. ^c Confidence score generated by Progenesis. * Proteins shared between both treatments (resveratrol and curcumin). Green reduction, red induction.

1.0 – 1.49		
1.5 – 1.99		
2 – 2.49		
2.5 – 2.99		
3 – 3.49		
3.5 +		
* Protein common between resveratrol and curcumin treatment.		

Table 8.8 – Significantly modulated proteins in Jurkat T lymphocytes after 30 μ M resveratrol identified by label-free LC-MS.

Accession	Description	Confidence score	Fold change	p value	q-value
Q9Y5K8	V-type proton ATPase subunit D	34.03	1.91	0.031	0.111
Q92917	G patch domain and KOW motifs-containing protein	34.95	1.60	0.028	0.106
P16402	Histone H1.3	664.87	1.56	0.025	0.101
Q01581	Hydroxymethylglutaryl-CoA synthase, cytoplasmic	137.6	1.53	0.000	0.003
P18065	Insulin-like growth factor-binding protein 2	109.7	1.50	0.011	0.069
Q9UG63	ATP-binding cassette sub-family F member 2	93.35	1.47	0.012	0.070
P16403; P22492; Q02539	Histone H1.2	768.82	1.44	0.002	0.035
P04264; P19013; Q6KB66; Q7Z794	Keratin, type II cytoskeletal 1	517.39	1.43	0.019	0.090
Q9P2K5	Myelin expression factor 2	41.24	1.41	0.036	0.120
Q05086	Ubiquitin-protein ligase E3A	36.49	1.39	0.007	0.060
P41567;	Eukaryotic translation initiation factor	254.95	1.34	0.001	0.022

O60739	1				
P62633	Cellular nucleic acid-binding protein	204.08	1.34	0.004	0.048
Q13422	DNA-binding protein Ikaros	99.61	1.33	0.003	0.041
A0A5B9	T-cell receptor beta-2 chain C region	48.89	1.31	0.007	0.060
Q8WW12	PEST proteolytic signal-containing nuclear protein	39.68	1.30	0.011	0.069
P20290	Transcription factor BTF3	258.04	1.29	0.000	0.003
P49366	Deoxyhypusine synthase	241.19	1.29	0.013	0.074
Q9NRX4	14 kDa phosphohistidine phosphatase	81.18	1.29	0.002	0.038
O43747	AP-1 complex subunit gamma-1	47.02	1.28	0.035	0.118
Q9UEY8	Gamma-adducin	50.56	1.28	0.015	0.083
P25098; P35626	Beta-adrenergic receptor kinase 1	379.78	1.28	0.002	0.035
Q9Y6H1; Q5T1J5	Coiled-coil-helix-coiled-coil-helix domain-containing protein 2, mitochondrial	116.57	1.27	0.003	0.046
Q9UK76	Hematological and neurological expressed 1 protein	157.04	1.27	0.000	0.003
P98179	Putative RNA-binding protein 3	57.01	1.26	0.002	0.039
P35613	Basigin	151.91	1.26	0.007	0.059
P52292	Importin subunit alpha-1	285.55	1.25	0.000	0.008
Q9UJU2; P36402	Lymphoid enhancer-binding factor 1	125.22	1.25	0.000	0.006
O60880	SH2 domain-containing protein 1A	233.37	1.25	0.000	0.006
Q86X55	Histone-arginine methyltransferase CARM1	79.86	1.25	0.047	0.135
Q9NZT2	Opioid growth factor receptor	30.45	1.24	0.036	0.120
Q14444	Caprin-1	317.74	1.24	0.000	0.006

P02786	Transferrin receptor protein 1	751.33	1.24	0.000	0.003
Q9NY27	Serine/threonine-protein phosphatase 4 regulatory subunit 2	151.06	1.23	0.002	0.035
Q9NRL3	Striatin-4	33.58	1.23	0.003	0.046
Q9UHD9	Ubiquilin-2	361.52	1.23	0.040	0.125
Q7Z5R6	Amyloid beta A4 precursor protein-binding family B member 1-interacting protein	105.04	1.23	0.002	0.035
A6NCE7; Q9H492	Microtubule-associated proteins 1A/1B light chain 3 beta 2	32.86	1.23	0.000	0.015
Q6IN85	Serine/threonine-protein phosphatase 4 regulatory subunit 3A	50.12	1.22	0.024	0.101
O95671	N-acetylserotonin O-methyltransferase-like protein	49.68	1.22	0.014	0.076
O15117	FYN-binding protein	194.45	1.22	0.005	0.048
E9PAV3; Q9BZK3	Nascent polypeptide-associated complex subunit alpha, muscle-specific form	357.92	1.22	0.000	0.011
Q15397	Pumilio domain-containing protein KIAA0020	73.06	1.22	0.005	0.051
P62805	Histone H4	730.01	1.22	0.001	0.025
P37268	Squalene synthase	570.67	1.22	0.001	0.022
P30520	Adenylosuccinate synthetase isozyme 2	224.65	1.21	0.002	0.035
Q9BZX2	Uridine-cytidine kinase 2	34.33	1.21	0.040	0.125
Q86Y56	HEAT repeat-containing protein 2	35.29	1.21	0.023	0.098
A8MWD9	Small nuclear ribonucleoprotein G-like protein	62.19	1.20	0.034	0.116
Q9NR30	Nucleolar RNA helicase 2	554.67	1.20	0.001	0.022
Q9UBC2	Epidermal growth factor receptor substrate 15-like 1	168.36	1.20	0.008	0.063

Q32MZ4; Q9Y608	Leucine-rich repeat flightless-interacting protein 1	481.3	1.19	0.001	0.028
Q9H2J4	Phosducin-like protein 3	33.16	1.19	0.003	0.046
Q96RU3	Formin-binding protein 1	585.89	1.19	0.000	0.011
Q9BV44	THUMP domain-containing protein 3	51.83	1.19	0.046	0.132
O75940	Survival of motor neuron-related-splicing factor 30	110.3	1.19	0.007	0.060
Q9UKX7	Nuclear pore complex protein Nup50	362.63	1.19	0.001	0.031
Q8N257	Histone H2B type 3-B	793.32	1.19	0.048	0.137
Q99543	DnaJ homolog subfamily C member 2	40.25	1.19	0.041	0.126
Q9Y5A9	YTH domain-containing family protein 2	33.93	1.19	0.019	0.090
Q9UBU8	Mortality factor 4-like protein 1	95.95	1.18	0.004	0.048
P13674	Prolyl 4-hydroxylase subunit alpha-1	369.15	1.18	0.041	0.125
Q9BTE6	Alanyl-tRNA editing protein Aarsd1	145.39	1.18	0.018	0.088
O75534	Cold shock domain-containing protein E1	202.3	1.18	0.001	0.022
Q16795	NADH dehydrogenase [ubiquinone] 1 alpha subcomplex subunit 9, mitochondrial	35.16	1.18	0.036	0.120
Q14978	Nucleolar and coiled-body phosphoprotein 1	248.18	1.18	0.003	0.046
Q8ND56	Protein LSM14 homolog A	60.15	1.17	0.034	0.115
O75368	SH3 domain-binding glutamic acid-rich-like protein	316.99	1.17	0.001	0.022
P09012	U1 small nuclear ribonucleoprotein A	272.05	1.17	0.006	0.052
Q9H307	Pinin	337.09	1.17	0.017	0.087
Q86UP2	Kinectin	187.47	1.16	0.007	0.060
Q9UI30	tRNA methyltransferase 112 homolog	118.91	1.16	0.008	0.063

O43660	Pleiotropic regulator 1	175.44	1.16	0.013	0.074
P07311	Acylphosphatase-1	82.06	1.16	0.004	0.048
P49247	Ribose-5-phosphate isomerase	179.41	1.16	0.040	0.125
Q9NY12	H/ACA ribonucleoprotein complex subunit 1	133.13	1.15	0.011	0.070
P04818	Thymidylate synthase	295.42	1.15	0.002	0.038
Q8WU90	Zinc finger CCCH domain-containing protein 15	126.94	1.15	0.030	0.109
O14745	Na(+)/H(+) exchange regulatory cofactor NHE-RF1	404.93	1.15	0.030	0.109
Q9NZL9	Methionine adenosyltransferase 2 subunit beta	298.63	1.15	0.009	0.065
Q5T8P6	RNA-binding protein 26	32.64	1.15	0.006	0.053
P49006	MARCKS-related protein	367.08	1.15	0.016	0.085
Q13895	Bystin	152.67	1.15	0.045	0.131
O60869	Endothelial differentiation-related factor 1	133.9	1.15	0.033	0.115
P61077; P51668	Ubiquitin-conjugating enzyme E2 D3	124.88	1.15	0.005	0.048
Q9Y295	Developmentally-regulated GTP-binding protein 1	316.25	1.15	0.010	0.068
Q96CT7	Coiled-coil domain-containing protein 124	198.22	1.15	0.023	0.097
Q9H845	Acyl-CoA dehydrogenase family member 9, mitochondrial	49.36	1.15	0.033	0.115
Q92522	Histone H1x	515.28	1.15	0.019	0.090
Q9NX55	Huntingtin-interacting protein K	57.99	1.14	0.002	0.038
Q6YP21	Kynurenine--oxoglutarate transaminase 3	127.61	1.14	0.040	0.125
P62495	Eukaryotic peptide chain release factor subunit 1	431.99	1.14	0.000	0.016

Q9NZL4	Hsp70-binding protein 1	331.9	1.13	0.008	0.063
Q15843	NEDD8	87.62	1.13	0.004	0.048
Q9UN86	Ras GTPase-activating protein-binding protein 2	161.75	1.13	0.025	0.101
Q9H4E7	Differentially expressed in FDCP 6 homolog	151.95	1.13	0.040	0.125
Q92974	Rho guanine nucleotide exchange factor 2	980.94	1.13	0.000	0.003
Q9Y4Z0	U6 snRNA-associated Sm-like protein LSM4	75.4	1.13	0.042	0.126
Q6PKG0; Q659C4	La-related protein 1	245.38	1.12	0.009	0.065
P00813	Adenosine deaminase	562.55	1.12	0.002	0.035
Q7Z6Z7	E3 ubiquitin-protein ligase HUWE1	138.15	1.12	0.011	0.069
Q13243	Serine/arginine-rich splicing factor 5	284.11	1.12	0.009	0.065
Q13347	Eukaryotic translation initiation factor 3 subunit I	466.6	1.12	0.013	0.074
P51858	Hepatoma-derived growth factor	472.6	1.12	0.001	0.028
Q9Y3F4	Serine-threonine kinase receptor-associated protein	497.38	1.12	0.001	0.024
P06454	Prothymosin alpha	541.29	1.12	0.041	0.126
P62993	Growth factor receptor-bound protein 2	415.34	1.12	0.019	0.090
P30086	Phosphatidylethanolamine-binding protein 1	544.57	1.12	0.019	0.090
Q6FI81	Anamorsin	145.83	1.12	0.022	0.097
O00170	AH receptor-interacting protein	291.69	1.12	0.001	0.028
P13073	Cytochrome c oxidase subunit 4 isoform 1, mitochondrial	199.5	1.12	0.002	0.038
O94900	Thymocyte selection-associated high mobility group box protein TOX	92.22	1.12	0.009	0.066

Q6JBY9	CapZ-interacting protein	184.69	1.12	0.037	0.121
Q9UEE9	Craniofacial development protein 1	100.06	1.12	0.028	0.108
Q96AE4; Q6TDU7	Far upstream element-binding protein 1	768.47	1.12	0.005	0.048
Q8WZA0	Protein LZIC	39.03	1.12	0.002	0.035
Q08722	Leukocyte surface antigen CD47	81.28	1.11	0.017	0.087
P06493	Cyclin-dependent kinase 1	357.46	1.11	0.014	0.076
O00743	Serine/threonine-protein phosphatase 6 catalytic subunit	277.01	1.11	0.012	0.073
P49903	Selenide, water dikinase 1	183.03	1.11	0.007	0.060
Q969Q0	60S ribosomal protein L36a-like	133.76	1.11	0.033	0.114
Q15287	RNA-binding protein with serine-rich domain 1	104.21	1.11	0.005	0.048
P63220	40S ribosomal protein S21	153.73	1.11	0.026	0.102
Q93009	Ubiquitin carboxyl-terminal hydrolase 7	181.42	1.11	0.044	0.130
Q14008	Cytoskeleton-associated protein 5	509.07	1.11	0.029	0.109
P68402	Platelet-activating factor acetylhydrolase IB subunit beta	113.42	1.11	0.013	0.074
P68400; Q8NEV1	Casein kinase II subunit alpha	356.95	1.11	0.001	0.035
P54886	Delta-1-pyrroline-5-carboxylate synthase	306.09	1.11	0.004	0.048
O15347; P0C6E5	High mobility group protein B3	200.88	1.11	0.024	0.099
P62306	Small nuclear ribonucleoprotein F	148.54	1.11	0.038	0.122
Q9BTD8	RNA-binding protein 42	166.61	1.11	0.031	0.109
P31689	DnaJ homolog subfamily A member 1	420.34	1.11	0.006	0.055

P05556	Integrin beta-1	190.12	1.11	0.029	0.109
P12814; O94979; P35609; Q08043	Alpha-actinin-1	1730.34	1.11	0.033	0.115
O43396	Thioredoxin-like protein 1	315.19	1.11	0.005	0.051
Q9UMX0; Q9NRR5	Ubiquilin-1	560.33	1.11	0.020	0.091
O00410; O60518	Importin-5	919.06	1.11	0.021	0.095
O75821	Eukaryotic translation initiation factor 3 subunit G	347.4	1.10	0.001	0.025
O14980	Exportin-1	801.14	1.10	0.002	0.038
P07195	L-lactate dehydrogenase B chain	1171.65	1.10	0.013	0.075
O75347	Tubulin-specific chaperone A	320.88	1.10	0.038	0.124
P49327	Fatty acid synthase	945.33	1.10	0.000	0.018
O75791	GRB2-related adapter protein 2	271.69	1.10	0.030	0.109
P54725	UV excision repair protein RAD23 homolog A	285.71	1.10	0.003	0.046
P08559; P29803	Pyruvate dehydrogenase E1 component subunit alpha, somatic form, mitochondrial	87.04	1.10	0.030	0.109
P13693	Translationally-controlled tumor protein	238.44	1.10	0.017	0.087
P16401	Histone H1.5	684.91	1.10	0.033	0.115
P67936; P07951	Tropomyosin alpha-4 chain	955.83	1.10	0.017	0.088
Q9BQA1	Methylosome protein 50	255.29	1.10	0.022	0.097

Q9UBQ5	Eukaryotic translation initiation factor 3 subunit K	117.86	1.10	0.020	0.091
Q9UKV3	Apoptotic chromatin condensation inducer in the nucleus	389.29	1.10	0.010	0.068
P28062	Proteasome subunit beta type-8	377.13	1.10	0.029	0.109
Q7L1Q6	Basic leucine zipper and W2 domain-containing protein 1	342.92	1.10	0.002	0.038
O43504	Ragulator complex protein LAMTOR5	183.16	1.10	0.025	0.101
P26583	High mobility group protein B2	642.03	1.10	0.011	0.069
P34932	Heat shock 70 kDa protein 4	2122.67	1.10	0.032	0.112
P62258	14-3-3 protein epsilon	929.19	1.09	0.019	0.090
P14324	Farnesyl pyrophosphate synthase	342.1	1.09	0.005	0.051
P17844	Probable ATP-dependent RNA helicase DDX5	1180.49	1.09	0.000	0.007
O95433	Activator of 90 kDa heat shock protein ATPase homolog 1	598.35	1.09	0.002	0.035
Q9Y266	Nuclear migration protein nudC	420.29	1.09	0.044	0.130
P26196; Q8TCU6	Probable ATP-dependent RNA helicase DDX6	465.06	1.09	0.009	0.063
P61247	40S ribosomal protein S3a	903.43	1.09	0.006	0.054
P11940; Q4VXU2; Q96DU9; Q9H361	Polyadenylate-binding protein 1	1090.82	1.09	0.004	0.048
O95347	Structural maintenance of chromosomes protein 2	252.71	1.09	0.008	0.063
P07766	T-cell surface glycoprotein CD3 epsilon chain	135.04	1.09	0.016	0.085
P15880	40S ribosomal protein S2	627.29	1.09	0.045	0.131

Q14847	LIM and SH3 domain protein 1	406.09	1.09	0.045	0.131
Q9UNX4	WD repeat-containing protein 3	236.19	1.09	0.018	0.088
Q53GS9	U4/U6.U5 tri-snRNP-associated protein 2	221.7	1.09	0.023	0.098
Q15269	Periodic tryptophan protein 2 homolog	301.88	1.09	0.011	0.069
P08865	40S ribosomal protein SA	631.66	1.09	0.005	0.048
Q14019	Coactosin-like protein	468.22	1.09	0.043	0.129
Q14318	Peptidyl-prolyl cis-trans isomerase FKBP8	361.26	1.09	0.019	0.090
Q14498; Q86U06	RNA-binding protein 39	711.79	1.09	0.012	0.072
P17174	Aspartate aminotransferase, cytoplasmic	388.1	1.09	0.002	0.038
P46060	Ran GTPase-activating protein 1	697.25	1.09	0.010	0.067
Q8NC51	Plasminogen activator inhibitor 1 RNA-binding protein	493.03	1.08	0.025	0.101
P13807	Glycogen [starch] synthase, muscle	204.91	1.08	0.003	0.045
Q15691; Q9UPY8	Microtubule-associated protein RP/EB family member 1	453.96	1.08	0.038	0.122
B5ME19; Q8ND83	Eukaryotic translation initiation factor 3 subunit C-like protein	691.44	1.08	0.036	0.120
Q9UI08	Ena/VASP-like protein	736.92	1.08	0.020	0.091
P36405	ADP-ribosylation factor-like protein 3	198.43	1.08	0.039	0.124
P04075; P05062	Fructose-bisphosphate aldolase A	1632.72	1.08	0.030	0.109
O95865	N(G),N(G)-dimethylarginine dimethylaminohydrolase 2	434.12	1.08	0.001	0.034
P62942	Peptidyl-prolyl cis-trans isomerase FKBP1A	312.02	1.08	0.047	0.134

P62269	40S ribosomal protein S18	492.85	1.08	0.030	0.109
O43684	Mitotic checkpoint protein BUB3	333.72	1.08	0.015	0.080
P62316	Small nuclear ribonucleoprotein Sm D2	256.88	1.08	0.044	0.130
Q01130; Q9BRL6	Serine/arginine-rich splicing factor 2	417.47	1.08	0.002	0.038
P22234	Multifunctional protein ADE2	1268.29	1.08	0.000	0.003
P52907	F-actin-capping protein subunit alpha-1	686.35	1.08	0.022	0.097
Q15046	Lysine--tRNA ligase	519.41	1.08	0.025	0.101
P05386	60S acidic ribosomal protein P1	293.95	1.08	0.005	0.048
Q14980	Nuclear mitotic apparatus protein 1	2382.65	1.08	0.005	0.051
Q13435	Splicing factor 3B subunit 2	914.21	1.08	0.006	0.053
P42166	Lamina-associated polypeptide 2, isoform alpha	1091.49	1.08	0.008	0.063
Q9BXJ9	N-alpha-acetyltransferase 15, NatA auxiliary subunit	411.09	1.08	0.018	0.089
P46779	60S ribosomal protein L28	268.52	1.08	0.025	0.101
Q13123	Protein Red	142.18	1.08	0.034	0.115
P36639	7,8-dihydro-8-oxoguanine triphosphatase	264.86	1.08	0.010	0.068
O43768; P56211	Alpha-endosulfine	158.37	1.07	0.036	0.119
Q70J99	Protein unc-13 homolog D	282.89	1.07	0.002	0.035
P63104	14-3-3 protein zeta/delta	1155.92	1.07	0.015	0.083
O00299	Chloride intracellular channel protein 1	729.86	1.07	0.002	0.038
P60228	Eukaryotic translation initiation factor 3 subunit E	413.98	1.07	0.037	0.122
Q13151	Heterogeneous nuclear ribonucleoprotein A0	626.79	1.07	0.011	0.069

Q14240	Eukaryotic initiation factor 4A-II	785.95	1.07	0.018	0.088
P30153; P30154	Serine/threonine-protein phosphatase 2A 65 kDa regulatory subunit A alpha isoform	916.1	1.07	0.047	0.135
P26373	60S ribosomal protein L13	440.18	1.07	0.004	0.048
O00151	PDZ and LIM domain protein 1	413.36	1.07	0.015	0.080
Q15181	Inorganic pyrophosphatase	823.4	1.07	0.008	0.062
Q9UHD8	Septin-9	671.18	1.07	0.005	0.051
Q01082; P11277	Spectrin beta chain, non-erythrocytic 1	4885.22	1.07	0.000	0.018
P62826	GTP-binding nuclear protein Ran	473.02	1.07	0.001	0.025
Q14152; Q15650	Eukaryotic translation initiation factor 3 subunit A	778.49	1.07	0.021	0.095
P31948	Stress-induced-phosphoprotein 1	1552.32	1.06	0.026	0.102
P63244	Guanine nucleotide-binding protein subunit beta-2-like 1	1251.87	1.06	0.010	0.068
O75533	Splicing factor 3B subunit 1	1447.45	1.06	0.011	0.069
O75822	Eukaryotic translation initiation factor 3 subunit J	185.59	1.06	0.042	0.126
Q16630	Cleavage and polyadenylation specificity factor subunit 6	330.28	1.06	0.011	0.069
P19338	Nucleolin	1725.72	1.06	0.018	0.088
P29401	Transketolase	1572.82	1.06	0.002	0.036
O76021	Ribosomal L1 domain-containing protein 1	493.24	1.06	0.021	0.093
O94776; Q9BTC8	Metastasis-associated protein MTA2	681.1	1.06	0.008	0.063
Q15365	Poly(rC)-binding protein 1	781.54	1.06	0.022	0.097
P30041	Peroxiredoxin-6	716.74	1.06	0.006	0.053

P37802	Transgelin-2	735.45	1.06	0.040	0.125
Q07021	Complement component 1 Q subcomponent-binding protein, mitochondrial	542.83	1.06	0.012	0.072
P49368	T-complex protein 1 subunit gamma	1646.66	1.06	0.010	0.069
P62318	Small nuclear ribonucleoprotein Sm D3	396.06	1.06	0.011	0.069
Q9UHV9	Prefoldin subunit 2	238.84	1.06	0.017	0.087
Q15019	Septin-2	572.78	1.06	0.023	0.097
O15371	Eukaryotic translation initiation factor 3 subunit D	411.23	1.06	0.022	0.096
O75083	WD repeat-containing protein 1	1553.05	1.06	0.018	0.089
O43390	Heterogeneous nuclear ribonucleoprotein R	1125.31	1.06	0.025	0.101
Q9NX58	Cell growth-regulating nucleolar protein	343.48	1.06	0.042	0.126
O60711	Leupaxin	215.86	1.06	0.042	0.126
P61978	Heterogeneous nuclear ribonucleoprotein K	1488.79	1.06	0.034	0.116
P27635; Q96L21	60S ribosomal protein L10	423.3	1.06	0.044	0.130
P62906	60S ribosomal protein L10a	217.31	1.06	0.014	0.076
P41091; Q2VIR3	Eukaryotic translation initiation factor 2 subunit 3	415.61	1.06	0.023	0.098
P78371	T-complex protein 1 subunit beta	1948.05	1.05	0.004	0.048
Q13177; O75914; Q13153	Serine/threonine-protein kinase PAK 2	797.73	1.05	0.030	0.109
P30050	60S ribosomal protein L12	505.8	1.05	0.009	0.063
Q15393	Splicing factor 3B subunit 3	1279.11	1.05	0.002	0.035

Q9P258	Protein RCC2	919.6	1.05	0.004	0.048
P51610	Host cell factor 1	497.77	1.05	0.035	0.118
P08621	U1 small nuclear ribonucleoprotein 70 kDa	455.1	1.05	0.024	0.100
O14979	Heterogeneous nuclear ribonucleoprotein D-like	416.28	1.05	0.025	0.101
Q99733	Nucleosome assembly protein 1-like 4	580.16	1.05	0.044	0.130
P55327	Tumor protein D52	382.04	1.05	0.004	0.048
P04406; O14556	Glyceraldehyde-3-phosphate dehydrogenase	1450.97	1.05	0.011	0.069
P18124	60S ribosomal protein L7	594.63	1.05	0.031	0.110
P46781	40S ribosomal protein S9	441.05	1.05	0.049	0.138
P62266	40S ribosomal protein S23	280.91	1.05	0.026	0.102
P50395	Rab GDP dissociation inhibitor beta	1487.24	1.05	0.022	0.097
Q86V81	THO complex subunit 4	503.33	1.05	0.005	0.048
P00492	Hypoxanthine-guanine phosphoribosyltransferase	408.53	1.05	0.037	0.122
P18669; P15259; Q8N0Y7	Phosphoglycerate mutase 1	1120.25	1.05	0.035	0.118
Q13813; Q15643	Spectrin alpha chain, non-erythrocytic 1	5359.81	1.03	0.020	0.091
P13639	Elongation factor 2	2127.27	1.03	0.008	0.063
Q15459	Splicing factor 3A subunit 1	535.62	1.03	0.027	0.103
Q99986	Serine/threonine-protein kinase VRK1	508.71	1.03	0.047	0.135
P49736	DNA replication licensing factor MCM2	1351.22	1.02	0.021	0.093
O43488;	Aflatoxin B1 aldehyde reductase member 2	462.63	1.03	0.030	0.109

O95154; Q8NHP1					
P21281; P15313	V-type proton ATPase subunit B, brain isoform	473.82	1.03	0.042	0.126
P13489	Ribonuclease inhibitor	1077.08	1.03	0.040	0.125
Q9Y4L1	Hypoxia up-regulated protein 1	1551.1	1.03	0.048	0.136
Q01813	6-phosphofructokinase type C	1550.41	1.04	0.029	0.109
Q9NQR4	Omega-amidase NIT2	357.97	1.04	0.040	0.125
Q52LJ0	Protein FAM98B	289.38	1.04	0.019	0.090
P49321	Nuclear autoantigenic sperm protein	1018.75	1.04	0.031	0.110
P38606			1.04	0.024	0.100
P55084	Trifunctional enzyme subunit beta, mitochondrial	420.82	1.04	0.048	0.137
Q92973	Transportin-1	411.11	1.04	0.023	0.097
P45880	Voltage-dependent anion-selective channel protein 2	658.71	1.05	0.045	0.131
Q14697	Neutral alpha-glucosidase AB	1909.17	1.05	0.030	0.109
P36871	Phosphoglucomutase-1	608.02	1.05	0.005	0.051
P27694	Replication protein A 70 kDa DNA-binding subunit	1027	1.05	0.019	0.090
Q99460	26S proteasome non-ATPase regulatory subunit 1	964.51	1.05	0.025	0.101
Q8TEM1	Nuclear pore membrane glycoprotein 210	1066.6	1.05	0.005	0.051
Q08211	ATP-dependent RNA helicase A	2489.66	1.05	0.009	0.065
P11310	Medium-chain specific acyl-CoA dehydrogenase, mitochondrial	701.71	1.05	0.007	0.055
Q9HCE1	Putative helicase MOV-10	425.86	1.05	0.019	0.090
Q8WWP7	GTPase IMAP family member 1	195.03	1.05	0.017	0.088

Q16836	Hydroxyacyl-coenzyme A dehydrogenase, mitochondrial	213.73	1.06	0.042	0.127
Q06210; O94808	Glutamine--fructose-6-phosphate aminotransferase [isomerizing] 1	890.28	1.06	0.017	0.087
P35606	Coatomer subunit beta'	1012.26	1.06	0.008	0.060
P22307	Non-specific lipid-transfer protein	487.81	1.06	0.010	0.067
P78527	DNA-dependent protein kinase catalytic subunit	4240.54	1.06	0.004	0.048
P23368	NAD-dependent malic enzyme, mitochondrial	495.38	1.06	0.037	0.122
P99999	Cytochrome c	204.25	1.06	0.049	0.138
P27797	Calreticulin	941.73	1.06	0.020	0.091
P45974	Ubiquitin carboxyl-terminal hydrolase 5	368.88	1.06	0.020	0.092
P14625; Q58FF3	Endoplasmin	1591.23	1.06	0.018	0.088
P04844	Dolichyl-diphosphooligosaccharide--protein glycosyltransferase subunit 2	1263.95	1.07	0.004	0.048
P30085	UMP-CMP kinase	368.12	1.07	0.010	0.069
Q15942	Zyxin	141.74	1.07	0.034	0.115
Q9H9B4; Q9BWM7	Sideroflexin-1	536.97	1.07	0.017	0.087
P53618	Coatomer subunit beta	678.32	1.07	0.038	0.123
P39748	Flap endonuclease 1	625.62	1.07	0.002	0.036
P39656	Dolichyl-diphosphooligosaccharide--protein glycosyltransferase 48 kDa subunit	493.31	1.07	0.004	0.048
Q99798	Aconitate hydratase, mitochondrial	1341.41	1.07	0.000	0.011
Q9BQ69	O-acetyl-ADP-ribose deacetylase MACROD1	211.59	1.07	0.008	0.063

Q6DD88; Q8NHH9	Atlastin-3	549.03	1.07	0.024	0.099
P07237	Protein disulfide-isomerase	1433.87	1.07	0.012	0.071
P11216; P06737; P11217	Glycogen phosphorylase, brain form	588.14	1.08	0.004	0.048
P11021; O95399	78 kDa glucose-regulated protein	1803.98	1.08	0.002	0.036
P00390	Glutathione reductase, mitochondrial	591.49	1.08	0.003	0.040
Q9BTV4	Transmembrane protein 43	220.02	1.08	0.025	0.101
Q9Y5B9	FACT complex subunit SPT16	1138.09	1.08	0.015	0.082
P08107; P48741	Heat shock 70 kDa protein 1A/1B	812.68	1.08	0.038	0.123
P27824	Calnexin	921.13	1.08	0.001	0.022
P46459	Vesicle-fusing ATPase	388.19	1.08	0.005	0.048
Q9H3N1	Thioredoxin-related transmembrane protein 1	207.26	1.08	0.031	0.110
Q96CS3	FAS-associated factor 2	142.79	1.08	0.040	0.125
Q8WXF1	Paraspeckle component 1	398.39	1.08	0.035	0.118
Q9H4A4	Aminopeptidase B	259.08	1.08	0.011	0.069
P12955	Xaa-Pro dipeptidase	204.66	1.08	0.040	0.125
Q9Y5M8	Signal recognition particle receptor subunit beta	188.62	1.09	0.041	0.126
P24539	ATP synthase F(0) complex subunit B1, mitochondrial	349.23	1.09	0.044	0.129
Q02978	Mitochondrial 2-oxoglutarate/malate carrier protein	417.62	1.09	0.019	0.090
O14929	Histone acetyltransferase type B	389.28	1.09	0.016	0.083

	catalytic subunit				
Q15435	Protein phosphatase 1 regulatory subunit 7	298.92	1.09	0.029	0.109
O75694	Nuclear pore complex protein Nup155	342.84	1.09	0.005	0.048
Q9NPQ8	Synembryn-A	67.84	1.09	0.004	0.048
O75915	PRA1 family protein 3	64.72	1.09	0.030	0.109
Q9NYU2	UDP-glucose:glycoprotein glucosyltransferase 1	459.23	1.09	0.028	0.106
Q9Y2Q5	Ragulator complex protein LAMTOR2	79.84	1.09	0.046	0.133
P17858	6-phosphofructokinase, liver type	762.02	1.10	0.013	0.075
Q9Y2Q3	Glutathione S-transferase kappa 1	213.37	1.10	0.027	0.104
P53007	Tricarboxylate transport protein, mitochondrial	293.76	1.10	0.045	0.131
O15173	Membrane-associated progesterone receptor component 2	223.17	1.10	0.034	0.116
Q15006	ER membrane protein complex subunit 2	160.14	1.10	0.040	0.125
P28288	ATP-binding cassette sub-family D member 3	200.35	1.10	0.009	0.065
Q9UBM7	7-dehydrocholesterol reductase	268.1	1.10	0.005	0.051
P51571	Translocon-associated protein subunit delta	152.76	1.10	0.004	0.047
P51659	Peroxisomal multifunctional enzyme type 2	635.52	1.10	0.009	0.064
Q96F07; Q7L576	Cytoplasmic FMR1-interacting protein 2	153.02	1.10	0.042	0.126
Q6NUK1	Calcium-binding mitochondrial carrier protein SCaMC-1	184.97	1.10	0.020	0.092
P31040	Succinate dehydrogenase [ubiquinone] flavoprotein subunit, mitochondrial	787.16	1.10	0.006	0.054
P20073	Annexin A7	401.75	1.11	0.008	0.060

Q9BSJ8	Extended synaptotagmin-1	1047.19	1.11	0.006	0.053
O43169	Cytochrome b5 type B	171.08	1.11	0.013	0.074
P55145	Mesencephalic astrocyte-derived neurotrophic factor	219.25	1.11	0.006	0.053
P34913	Bifunctional epoxide hydrolase 2	158.27	1.11	0.011	0.069
Q15005	Signal peptidase complex subunit 2	315.44	1.11	0.030	0.109
Q00534	Cyclin-dependent kinase 6	453.5	1.11	0.006	0.053
Q86YV0	RAS protein activator like-3	98.56	1.11	0.041	0.126
P04040	Catalase	452.67	1.11	0.003	0.046
P08134	Rho-related GTP-binding protein RhoC	400.33	1.12	0.006	0.053
Q9NVP2	Histone chaperone ASF1B	94.35	1.12	0.018	0.088
O00116	Alkyldihydroxyacetonephosphate synthase, peroxisomal	217.32	1.12	0.027	0.103
P62879	Guanine nucleotide-binding protein G(I)/G(S)/G(T) subunit beta-2	694.09	1.12	0.042	0.126
P69905; P02008	Hemoglobin subunit alpha	319.91	1.12	0.001	0.022
P53990	IST1 homolog	225.87	1.12	0.002	0.038
P61619; Q9H9S3	Protein transport protein Sec61 subunit alpha isoform 1	386.38	1.12	0.010	0.068
O43175	D-3-phosphoglycerate dehydrogenase	870.82	1.12	0.002	0.038
Q9NTJ5	Phosphatidylinositide phosphatase SAC1	512.85	1.12	0.006	0.051
Q9Y678	Coatmer subunit gamma-1	535.67	1.12	0.003	0.046
Q12769	Nuclear pore complex protein Nup160	212.95	1.12	0.047	0.134
P48444	Coatmer subunit delta	455.06	1.12	0.002	0.036
O43252	Bifunctional 3'-phosphoadenosine 5'-phosphosulfate synthase 1	332.4	1.13	0.001	0.025

P61009	Signal peptidase complex subunit 3	105.12	1.13	0.025	0.101
Q9Y394	Dehydrogenase/reductase SDR family member 7	334.92	1.13	0.008	0.063
Q14790	Caspase-8	78.87	1.13	0.013	0.074
Q13555; Q13554	Calcium/calmodulin-dependent protein kinase type II subunit gamma	142.26	1.13	0.014	0.077
P23258	Tubulin gamma-1 chain	141.13	1.13	0.040	0.125
Q9UM00	Transmembrane and coiled-coil domain-containing protein 1	90.32	1.13	0.012	0.070
P48651	Phosphatidylserine synthase 1	108.56	1.13	0.012	0.070
Q15436	Protein transport protein Sec23A	362.12	1.13	0.045	0.131
P35610	Sterol O-acyltransferase 1	41.75	1.13	0.022	0.096
P18858	DNA ligase 1	134.39	1.14	0.001	0.025
O43852	Calumenin	247.71	1.14	0.029	0.109
Q96P70	Importin-9	279.02	1.14	0.015	0.080
Q9NPF4	Probable tRNA N6-adenosine threonylcarbamoyltransferase	127.38	1.14	0.040	0.125
Q16629	Serine/arginine-rich splicing factor 7	143.28	1.14	0.008	0.063
P50416	Carnitine O-palmitoyltransferase 1, liver isoform	663.42	1.14	0.003	0.040
P40937	Replication factor C subunit 5	330.3	1.14	0.000	0.021
P16219	Short-chain specific acyl-CoA dehydrogenase, mitochondrial	136.02	1.14	0.027	0.103
P35244	Replication protein A 14 kDa subunit	241.15	1.15	0.003	0.045
P49588	Alanine--tRNA ligase, cytoplasmic	1261.62	1.15	0.000	0.003
Q9H3U1	Protein unc-45 homolog A	79.69	1.15	0.017	0.086
Q15437	Protein transport protein Sec23B	340.66	1.15	0.004	0.048
Q9Y617	Phosphoserine aminotransferase	379.25	1.16	0.001	0.028

Q99805	Transmembrane 9 superfamily member 2	50.51	1.16	0.040	0.125
Q86WV1	Src kinase-associated phosphoprotein 1	74.51	1.16	0.043	0.129
Q9NRP0	se complex subunit OSTC	58.9	1.16	0.035	0.118
A6NDJ8	Putative Rab-43-like protein ENSP00000330714	117.15	1.16	0.008	0.063
Q8WY22	BRI3-binding protein	135.37	1.16	0.004	0.048
P13995; Q9H903	Bifunctional methylenetetrahydrofolate dehydrogenase/cyclohydrolase, mitochondrial	82.82	1.16	0.022	0.097
P42765	3-ketoacyl-CoA thiolase, mitochondrial	151.54	1.16	0.033	0.114
Q02218; Q9ULD0	2-oxoglutarate dehydrogenase, mitochondrial	140.72	1.17	0.026	0.102
P20645	Cation-dependent mannose-6-phosphate receptor	119.18	1.17	0.001	0.028
Q9UNL2	Translocon-associated protein subunit gamma	102.86	1.17	0.011	0.069
Q8N766	ER membrane protein complex subunit 1	157.91	1.18	0.023	0.098
Q13464	Rho-associated protein kinase 1	88.41	1.18	0.032	0.112
Q8TC12	Retinol dehydrogenase 11	148.3	1.18	0.026	0.102
Q9H3P7	Golgi resident protein GCP60	122.57	1.19	0.021	0.094
Q8TBC4	NEDD8-activating enzyme E1 catalytic subunit	56.31	1.19	0.030	0.109
O15533	Tapasin	73.93	1.19	0.012	0.073
Q9H061	Transmembrane protein 126A	44.52	1.19	0.040	0.125
Q9Y2H1	Serine/threonine-protein kinase 38-like	75.01	1.20	0.021	0.093
Q8NBX0	Saccharopine dehydrogenase-like oxidoreductase	214.21	1.20	0.006	0.051

Q9Y2Y0	ADP-ribosylation factor-like protein 2-binding protein	50.44	1.20	0.033	0.115
P23921	Ribonucleoside-diphosphate reductase large subunit	505.12	1.21	0.000	0.003
P30043	Flavin reductase (NADPH)	62.02	1.21	0.018	0.089
Q96N66	Lysophospholipid acyltransferase 7	50.35	1.22	0.027	0.105
P00747	Plasminogen	200.49	1.22	0.010	0.068
Q8NFW8	N-acylneuraminate cytidyltransferase	297.19	1.23	0.007	0.059
O95400	CD2 antigen cytoplasmic tail-binding protein 2	50.26	1.23	0.016	0.086
P52732	Kinesin-like protein KIF11	249.33	1.23	0.003	0.044
P26440	Isovaleryl-CoA dehydrogenase, mitochondrial	45.62	1.23	0.050	0.139
Q9Y5P6	Mannose-1-phosphate guanyltransferase beta	30.85	1.24	0.019	0.090
Q9NVI1	Fanconi anemia group I protein	103.5	1.25	0.000	0.003
Q9BT22	Chitobiosyldiphosphodolichol beta-mannosyltransferase	124.21	1.25	0.004	0.048
Q9NQS7	Inner centromere protein	102.02	1.25	0.003	0.044
Q9UHG3	Prenylcysteine oxidase 1	121.58	1.25	0.001	0.025
P16278	Beta-galactosidase	63.32	1.26	0.011	0.069
Q9UM22	Mammalian ependymin-related protein 1	30.04	1.26	0.000	0.007
P10253	Lysosomal alpha-glucosidase	44.87	1.26	0.012	0.073
P49748	Very long-chain specific acyl-CoA dehydrogenase, mitochondrial	665.69	1.28	0.000	0.003
O60749	Sorting nexin-2	67.33	1.29	0.005	0.048
Q08AF3	Schlafen family member 5	42.15	1.32	0.030	0.109
Q96CM8	Acyl-CoA synthetase family member 2, mitochondrial	44.2	1.33	0.000	0.006

Q6PL18	ATPase family AAA domain-containing protein 2	31.66	1.33	0.001	0.028
Q9BQE5	Apolipoprotein L2	95.59	1.34	0.001	0.025
Q8NBM8	Prenylcysteine oxidase-like	55.45	1.40	0.013	0.074
Q9Y3B3	Transmembrane emp24 domain-containing protein 7	81.75	1.46	0.028	0.108
Q9Y4F9	Protein FAM65B	47.04	1.46	0.042	0.126
Q9Y6A5	Transforming acidic coiled-coil-containing protein 3	56.19	1.51	0.015	0.080
Q15022	Polycomb protein SUZ12	39.03	1.51	0.005	0.048
P31350; Q7LG56	Ribonucleoside-diphosphate reductase subunit M2	437.12	1.59	0.000	0.003
Q9UKR5	Probable ergosterol biosynthetic protein 28	33.42	1.72	0.001	0.022

^a Accession number according to UniProt database. ^b Protein description with relative symbol. ^c Confidence score generated by Progenesis. * Proteins shared between both treatments (resveratrol and curcumin). Green reduction, red induction.

1.0 – 1.49		
1.5 – 1.99		
2 – 2.49		
2.5 – 2.99		
3 – 3.49		
3.5 +		
* Protein common between resveratrol and curcumin treatment.		

Table 8.9 – Significantly modulated proteins in Jurkat T lymphocytes after 10 μ M curcumin identified by label-free LC-MS.

Accession ^a	Description ^b	Confidence score ^c	Fold change	p-value	q-value
Q13257	Mitotic spindle assembly checkpoint protein MAD2A	77.24	1.41	0.016	0.405
Q9NQS7	Inner centromere protein	102.02	1.40	0.001	0.232
Q9UG63	ATP-binding cassette sub-family F member 2	93.35	1.39	0.015	0.405
Q9UN37	Vacuolar protein sorting-associated protein 4A	65.05	1.36	0.039	0.494
Q14061	Cytochrome c oxidase copper chaperone	78.49	1.35	0.004	0.353
Q05086	Ubiquitin-protein ligase E3A	36.49	1.34	0.028	0.458
Q9UIL1	Short coiled-coil protein	57.87	1.32	0.021	0.421
Q9UIQ6	Leucyl-cystinyl aminopeptidase	50.35	1.30	0.007	0.353
Q96I25	Splicing factor 45	58.17	1.29	0.001	0.232
Q01581	Hydroxymethylglutaryl-CoA synthase, cytoplasmic	137.6	1.27	0.001	0.232
P31350; Q7LG56	Ribonucleoside-diphosphate reductase subunit M2	437.12	1.26	0.002	0.257
Q9Y697	Cysteine desulfurase, mitochondrial	33.68	1.25	0.035	0.494
Q96BF6	Nucleus accumbens-associated protein 2	47.73	1.25	0.024	0.433
P34896	Serine hydroxymethyltransferase, cytosolic	126.99	1.24	0.035	0.494
Q9UEY8	Gamma-adducin	50.56	1.23	0.036	0.494
Q8WW12	PEST proteolytic signal-containing nuclear protein	39.68	1.23	0.031	0.471
O14907	Tax1-binding protein 3	101.14	1.21	0.012	0.386

O95671	N-acetylserotonin O-methyltransferase-like protein	49.68	1.20	0.024	0.432
P06132	Uroporphyrinogen decarboxylase	36.47	1.19	0.007	0.353
P04818	Thymidylate synthase	295.42	1.19	0.007	0.353
Q9ULR0	Pre-mRNA-splicing factor ISY1 homolog	97.96	1.19	0.038	0.494
P98175	RNA-binding protein 10	123.1	1.19	0.043	0.517
P25098; P35626	Beta-adrenergic receptor kinase 1	379.78	1.19	0.010	0.386
O43660	Pleiotropic regulator 1	175.44	1.18	0.012	0.386
Q6FI81	Anamorsin	145.83	1.18	0.012	0.386
Q9NVI1	Fanconi anemia group I protein	103.5	1.17	0.003	0.335
Q99848	Probable rRNA-processing protein EBP2	46.52	1.17	0.048	0.534
P51570	Galactokinase	56.25	1.16	0.047	0.530
P29083	General transcription factor IIE subunit 1	42.88	1.16	0.007	0.353
Q9UHA4	Ragulator complex protein LAMTOR3	45.13	1.15	0.006	0.353
Q16576	Histone-binding protein RBBP7	314.02	1.15	0.013	0.391
Q8WU39	Marginal zone B- and B1-cell-specific protein	301.22	1.15	0.014	0.398
P14927	Cytochrome b-c1 complex subunit 7	70.82	1.15	0.025	0.433
P18858	DNA ligase 1	134.39	1.15	0.007	0.353
Q9UN86	Ras GTPase-activating protein-binding protein 2	161.75	1.15	0.037	0.494
Q96T60	Bifunctional polynucleotide phosphatase/kinase	69.68	1.15	0.029	0.468
Q13123	Protein Red	142.18	1.14	0.018	0.405
Q96CT7	Coiled-coil domain-containing protein	198.22	1.14	0.027	0.453

	124				
O95347	Structural maintenance of chromosomes protein 2	252.71	1.14	0.005	0.353
Q6JBY9	CapZ-interacting protein	184.69	1.14	0.001	0.238
P54886	Delta-1-pyrroline-5-carboxylate synthase	306.09	1.13	0.001	0.238
Q9UNN5	FAS-associated factor 1	111.24	1.13	0.049	0.541
Q96PE3	Type I inositol 3,4-bisphosphate 4-phosphatase	119.89	1.13	0.011	0.386
P09012	U1 small nuclear ribonucleoprotein A	272.05	1.13	0.022	0.428
E9PAV3; Q9BZK3	Nascent polypeptide-associated complex subunit alpha, muscle-specific form	357.92	1.13	0.016	0.405
P23921	Ribonucleoside-diphosphate reductase large subunit	505.12	1.13	0.001	0.232
P13798	Acylamino-acid-releasing enzyme	610.9	1.13	0.017	0.405
Q8NCW5	NAD(P)H-hydrate epimerase	175.02	1.12	0.022	0.428
P46013	Antigen KI-67	283.08	1.12	0.009	0.364
Q16566	Calcium/calmodulin-dependent protein kinase type IV	280.76	1.12	0.023	0.432
Q7Z6Z7	E3 ubiquitin-protein ligase HUWE1	138.15	1.12	0.012	0.386
P09497	Clathrin light chain B	134.83	1.12	0.003	0.335
O15117	FYN-binding protein	194.45	1.12	0.046	0.530
O75792	Ribonuclease H2 subunit A	122.68	1.12	0.018	0.405
P30520	Adenylosuccinate synthetase isozyme 2	224.65	1.12	0.047	0.534
P52888	Thimet oligopeptidase	224.72	1.12	0.009	0.364
Q16531	DNA damage-binding protein 1	1055.93	1.12	0.001	0.232
Q15287	RNA-binding protein with serine-rich domain 1	104.21	1.11	0.028	0.460

P17480	Nucleolar transcription factor 1	206.05	1.11	0.039	0.494
Q9UBX3	Mitochondrial dicarboxylate carrier	76.36	1.11	0.013	0.391
P07311	Acylphosphatase-1	82.06	1.11	0.044	0.530
O00410; O60518	Importin-5	919.06	1.11	0.025	0.433
O00170	AH receptor-interacting protein	291.69	1.11	0.038	0.494
O75368	SH3 domain-binding glutamic acid-rich-like protein	316.99	1.11	0.014	0.398
Q13404	Ubiquitin-conjugating enzyme E2 variant 1	259.98	1.10	0.039	0.494
P19174	1-phosphatidylinositol 4,5-bisphosphate phosphodiesterase gamma-1	356.21	1.10	0.032	0.487
Q9NR30	Nucleolar RNA helicase 2	554.67	1.10	0.031	0.471
O15067	Phosphoribosylformylglycinamide synthase	374.31	1.10	0.009	0.365
P33316	Deoxyuridine 5'-triphosphate nucleotidohydrolase, mitochondrial	588.33	1.10	0.012	0.386
P33991; Q9UJA3	DNA replication licensing factor MCM4	1496.23	1.10	0.007	0.353
P42166	Lamina-associated polypeptide 2, isoform alpha	1091.49	1.10	0.002	0.257
Q9UK76	Hematological and neurological expressed 1 protein	157.04	1.10	0.038	0.494
Q969G3	SWI/SNF-related matrix-associated actin-dependent regulator of chromatin subfamily E member 1	437.15	1.10	0.007	0.353
O43768; P56211	Alpha-endosulfine	158.37	1.10	0.009	0.364
P35611	Alpha-adducin	425.46	1.10	0.011	0.386
P11388	DNA topoisomerase 2-alpha	2184.55	1.10	0.024	0.433

Q4G176	Acyl-CoA synthetase family member 3, mitochondrial	260.7	1.09	0.016	0.405
P49915	GMP synthase [glutamine-hydrolyzing]	544.58	1.09	0.008	0.353
P06493	Cyclin-dependent kinase 1	357.46	1.09	0.035	0.494
Q9HCE1	Putative helicase MOV-10	425.86	1.09	0.009	0.364
O94874	E3 UFM1-protein ligase 1	64.48	1.09	0.026	0.443
P62310	U6 snRNA-associated Sm-like protein LSM3	32.54	1.09	0.036	0.494
P25685	DnaJ homolog subfamily B member 1	404.23	1.09	0.017	0.405
P36639	7,8-dihydro-8-oxoguanine triphosphatase	264.86	1.09	0.038	0.494
Q9Y5Z4	Heme-binding protein 2	121.02	1.09	0.001	0.257
P63208	S-phase kinase-associated protein 1	118.69	1.09	0.027	0.450
Q9UJU2; P36402	Lymphoid enhancer-binding factor 1	125.22	1.09	0.040	0.494
Q8IX12	Cell division cycle and apoptosis regulator protein 1	63.87	1.09	0.038	0.494
Q15691 Q9UPY8	Microtubule-associated protein RP/EB family member 1	453.96	1.09	0.047	0.534
P13073	Cytochrome c oxidase subunit 4 isoform 1, mitochondrial	199.5	1.09	0.006	0.353
P62495	Eukaryotic peptide chain release factor subunit 1	431.99	1.08	0.005	0.353
Q14980	Nuclear mitotic apparatus protein 1	2382.65	1.08	0.002	0.257
P62269	40S ribosomal protein S18	492.85	1.08	0.016	0.405
Q5TBB1	Ribonuclease H2 subunit B	155.52	1.08	0.041	0.505
Q9H0D6	5'-3' exoribonuclease 2	429.62	1.08	0.049	0.541
P33993	DNA replication licensing factor MCM7	760.99	1.08	0.016	0.405

P15927	Replication protein A 32 kDa subunit	159.26	1.08	0.046	0.530
Q9NVP2	Histone chaperone ASF1B	94.35	1.08	0.029	0.466
P12004	Proliferating cell nuclear antigen	598.14	1.08	0.005	0.353
P67809; P16989	Nuclease-sensitive element-binding protein 1	786.89	1.08	0.018	0.405
P45973	Chromobox protein homolog 5	378.89	1.08	0.046	0.530
P55265	Double-stranded RNA-specific adenosine deaminase	656.1	1.08	0.042	0.511
Q99986	Serine/threonine-protein kinase VRK1	508.71	1.07	0.002	0.257
O76071	Probable cytosolic iron-sulfur protein assembly protein CIAO1	123.04	1.07	0.020	0.420
Q86XP3	ATP-dependent RNA helicase DDX42	189.62	1.07	0.017	0.405
Q09028	Histone-binding protein RBBP4	484.41	1.07	0.045	0.530
Q14566	DNA replication licensing factor MCM6	1269.25	1.07	0.005	0.353
Q6P2E9	Enhancer of mRNA-decapping protein 4	640.32	1.07	0.023	0.432
Q92900	Regulator of nonsense transcripts 1	555.69	1.07	0.008	0.353
P17174	Aspartate aminotransferase, cytoplasmic	388.1	1.06	0.020	0.418
P13693	Translationally-controlled tumor protein	238.44	1.06	0.049	0.541
Q9UI08	Ena/VASP-like protein	736.92	1.06	0.025	0.433
P23193; Q15560	Transcription elongation factor A protein 1	461.31	1.06	0.036	0.494
Q9NY27	Serine/threonine-protein phosphatase 4 regulatory subunit 2	151.06	1.06	0.014	0.395
P12268	Inosine-5'-monophosphate dehydrogenase 2	912.86	1.06	0.022	0.428
Q9GZS3	WD repeat-containing protein 61	255.78	1.06	0.030	0.471

Q8WXX5	DnaJ homolog subfamily C member 9	489.02	1.06	0.024	0.432
Q15181	Inorganic pyrophosphatase	823.4	1.06	0.027	0.457
Q9NQR4	Omega-amidase NIT2	357.97	1.06	0.012	0.386
P17812; Q9NRF8	CTP synthase 1	695.16	1.06	0.048	0.538
P30050	60S ribosomal protein L12	505.8	1.06	0.007	0.353
P49736	DNA replication licensing factor MCM2	1351.22	1.06	0.003	0.335
P49321	Nuclear autoantigenic sperm protein	1018.75	1.05	0.048	0.536
P18669; P15259; Q8N0Y7	Phosphoglycerate mutase 1	1120.25	1.05	0.046	0.531
P55060	Exportin-2	1119.92	1.05	0.011	0.386
P26373	60S ribosomal protein L13	440.18	1.05	0.039	0.494
P52292	Importin subunit alpha-1	285.55	1.05	0.038	0.494
P63244	Guanine nucleotide-binding protein subunit beta-2-like 1	1251.87	1.05	0.031	0.475
Q9NQG5	Regulation of nuclear pre-mRNA domain-containing protein 1B	287.6	1.04	0.018	0.405
P41091; Q2VIR3	Eukaryotic translation initiation factor 2 subunit 3	415.61	1.04	0.049	0.541
Q15029	116 kDa U5 small nuclear ribonucleoprotein component	1121.6	1.04	0.032	0.483
P62318	Small nuclear ribonucleoprotein Sm D3	396.06	1.04	0.013	0.391
P18124	60S ribosomal protein L7	594.63	1.04	0.018	0.405
P36578	60S ribosomal protein L4	881.37	1.04	0.009	0.365
Q52LJ0	Protein FAM98B	289.38	1.03	0.043	0.517

P59998	Actin-related protein 2/3 complex subunit 4	285.45	1.04	0.008	0.353
O00571; O15523; Q9NQI0	ATP-dependent RNA helicase DDX3X	1006.7	1.04	0.039	0.494
Q92556	Engulfment and cell motility protein 1	384.64	1.05	0.020	0.418
Q13200	26S proteasome non-ATPase regulatory subunit 2	891.94	1.05	0.032	0.483
P40937	Replication factor C subunit 5	330.3	1.05	0.036	0.494
P09211	Glutathione S-transferase P	829.47	1.05	0.018	0.405
Q9NTJ5	Phosphatidylinositide phosphatase SAC1	512.85	1.06	0.042	0.511
P49588	Alanine--tRNA ligase, cytoplasmic	1261.62	1.06	0.026	0.443
P27824	Calnexin	921.13	1.06	0.023	0.432
Q04760	Lactoylglutathione lyase	242.54	1.06	0.037	0.494
P21333	Filamin-A	5864.52	1.06	0.009	0.364
P23368	NAD-dependent malic enzyme, mitochondrial	495.38	1.07	0.030	0.470
Q15008	26S proteasome non-ATPase regulatory subunit 6	531.9	1.07	0.028	0.458
P41250	Glycine--tRNA ligase	635.35	1.07	0.045	0.530
Q99460	26S proteasome non-ATPase regulatory subunit 1	964.51	1.08	0.006	0.353
O43242	26S proteasome non-ATPase regulatory subunit 3	669.32	1.08	0.022	0.432
O43175	D-3-phosphoglycerate dehydrogenase	870.82	1.08	0.006	0.353
P07339	Cathepsin D	708.95	1.08	0.017	0.405
Q92685	Dol-P-Man:Man(5)GlcNAc(2)-PP-Dol alpha-1,3-mannosyltransferase	93.69	1.09	0.028	0.457
P68366	Tubulin alpha-4A chain	1313.56	1.09	0.041	0.503

O43670	Zinc finger protein 207	74.45	1.09	0.023	0.432
Q06830	Peroxiredoxin-1	493.88	1.09	0.016	0.405
P08195	4F2 cell-surface antigen heavy chain	533.29	1.10	0.019	0.415
P30405	Peptidyl-prolyl cis-trans isomerase F, mitochondrial	128.03	1.10	0.012	0.386
O00487	26S proteasome non-ATPase regulatory subunit 14	173.62	1.10	0.004	0.353
P08754	Guanine nucleotide-binding protein G(k) subunit alpha	504.6	1.11	0.023	0.432
Q9UHG3	Prenylcysteine oxidase 1	121.58	1.11	0.012	0.386
P61009	Signal peptidase complex subunit 3	105.12	1.11	0.020	0.418
P53634	Dipeptidyl peptidase 1	305.95	1.11	0.006	0.353
Q9Y617	Phosphoserine aminotransferase	379.25	1.13	0.017	0.405
Q8N5M4	Tetratricopeptide repeat protein 9C	64.74	1.13	0.010	0.385
Q9UM00	Transmembrane and coiled-coil domain-containing protein 1	90.32	1.14	0.022	0.428
O15173	Membrane-associated progesterone receptor component 2	223.17	1.14	0.004	0.353
Q01650; Q92536	Large neutral amino acids transporter small subunit 1	142.25	1.14	0.005	0.353
Q9BQE5	Apolipoprotein L2	95.59	1.14	0.045	0.530
P50416	Carnitine O-palmitoyltransferase 1, liver isoform	663.42	1.14	0.004	0.353
P20645	Cation-dependent mannose-6-phosphate receptor	119.18	1.14	0.017	0.405
P00390	Glutathione reductase, mitochondrial	591.49	1.15	0.000	0.232
A6NDJ8	Putative Rab-43-like protein ENSP00000330714	117.15	1.16	0.003	0.335
Q9UJW0	Dynactin subunit 4	167.33	1.17	0.020	0.418

Q9NQ75	Exosome complex component RRP40	62.98	1.18	0.039	0.494
Q969V3	Nicalin	71.9	1.19	0.055	0.558
P55212	Caspase-6	73.75	1.20	0.007	0.353
P07355; A6NMY6	Annexin A2	600.64	1.23	0.002	0.257
Q7L0Y3	Mitochondrial ribonuclease P protein 1	70.74	1.24	0.033	0.493
P02795; P04731; P04732	Metallothionein-2	92.55	1.25	0.019	0.415
P00747	Plasminogen	200.49	1.25	0.014	0.395
P78559	Microtubule-associated protein 1A	58.28	1.26	0.007	0.353
Q9BT22	Chitobiosyldiphosphodolichol beta-mannosyltransferase	124.21	1.27	0.039	0.494
Q9BT09	Protein canopy homolog 3	47.93	1.31	0.035	0.494
O75569	Interferon-inducible double-stranded RNA-dependent protein kinase activator A	199.26	1.38	0.036	0.494
P12259	Coagulation factor V	77.83	1.44	0.030	0.471

^a Accession number according to UniProt database. ^b Protein description with relative symbol. ^c Confidence score generated by Progenesis. * Proteins shared between both treatments (resveratrol and curcumin). Green reduction, red induction.

1.0 – 1.49		
1.5 – 1.99		
2 – 2.49		
2.5 – 2.99		
3 – 3.49		
3.5 +		
* Protein common between resveratrol and curcumin treatment.		

Table 8.10 – Significantly modulated proteins in Jurkat T lymphocytes after 1 μ M isorhamnetin identified by label-free LC-MS.

Accession ^a	Description ^b	Confidence score ^c	Fold change	p-value	q-value
Q6UXB8	Peptidase inhibitor 16	31.35	1.27	0.036	0.987
Q86TU7	Histone-lysine N-methyltransferase setd3	34.83	1.25	0.021	0.987
Q5UIP0	Telomere-associated protein RIF1	30.91	1.25	0.039	0.987
Q02218	2-oxoglutarate dehydrogenase, mitochondrial	31.22	1.23	0.014	0.987
Q92552	28S ribosomal protein S27, mitochondrial	44.06	1.23	0.015	0.987
Q9HC07	Transmembrane protein 165	45.58	1.21	0.011	0.987
Q9NXJ5	Pyroglutamyl-peptidase 1	31.61	1.21	0.049	0.987
Q9Y5Z4	Heme-binding protein 2	48.89	1.21	0.019	0.987
O15305	Phosphomannomutase 2	33.42	1.20	0.023	0.987
Q9ULR0	Pre-mRNA-splicing factor ISY1 homolog	94.69	1.19	0.024	0.987
P60602	Reactive oxygen species modulator 1	56.72	1.17	0.031	0.987
O15160	DNA-directed RNA polymerases I and III subunit RPAC1	37.84	1.17	0.028	0.987
Q8N5M4	Tetratricopeptide repeat protein 9C	39.27	1.16	0.009	0.987
Q7Z4H7	HAUS augmin-like complex subunit 6	51.45	1.16	0.003	0.987
Q96ER3	Protein SAAL1	84.76	1.15	0.038	0.987
Q15392	Delta(24)-sterol reductase	136.11	1.15	0.013	0.987
Q9UI12	V-type proton ATPase subunit H	40.45	1.15	0.009	0.987
Q7L1Q6	Basic leucine zipper and W2 domain-containing protein 1	313.99	1.15	0.019	0.987

Q8NFH3	Nucleoporin Nup43	223.78	1.15	0.024	0.987
P43897	Elongation factor Ts, mitochondrial	149.55	1.14	0.012	0.987
Q9UQ88	Cyclin-dependent kinase 11A	124.58	1.14	0.031	0.987
Q08752	Peptidyl-prolyl cis-trans isomerase D	199.15	1.14	0.033	0.987
O95379	Tumor necrosis factor alpha-induced protein 8	161.61	1.13	0.035	0.987
Q9UBE0	SUMO-activating enzyme subunit 1	313.59	1.13	0.036	0.987
Q9Y4W6	AFG3-like protein 2	61.2	1.12	0.041	0.987
Q9UGP8	Translocation protein SEC63 homolog	162.48	1.12	0.040	0.987
P63092; P38405	Guanine nucleotide-binding protein G(s) subunit alpha isoforms short	254.28	1.12	0.017	0.987
O75396	Vesicle-trafficking protein SEC22b	364.6	1.11	0.005	0.987
Q6L8Q7	2',5'-phosphodiesterase 12	96.55	1.11	0.035	0.987
O95573	Long-chain-fatty-acid--CoA ligase 3	224.99	1.11	0.002	0.987
Q9Y4P1	Cysteine protease ATG4B	148.92	1.11	0.023	0.987
P00846	ATP synthase subunit a	44.36	1.10	0.037	0.987
Q9UBX3	Mitochondrial dicarboxylate carrier	129.56	1.10	0.025	0.987
Q16566	Calcium/calmodulin-dependent protein kinase type IV	262.66	1.10	0.000	0.188
P12236	ADP/ATP translocase 3	600.74	1.10	0.031	0.987
Q15005	Signal peptidase complex subunit 2	215.12	1.10	0.016	0.987
Q9H9B4; Q9BWM7	Sideroflexin-1	525.31	1.10	0.033	0.987
Q01581	Hydroxymethylglutaryl-CoA synthase, cytoplasmic	168.58	1.10	0.039	0.987
P21266	Glutathione S-transferase Mu 3	274.29	1.10	0.050	0.987
P60468	Protein transport protein Sec61	133.46	1.10	0.004	0.987

	subunit beta				
P46781	40S ribosomal protein S9	367.26	1.09	0.004	0.987
P48449	Lanosterol synthase	488.43	1.09	0.014	0.987
Q9H7D7	WD repeat-containing protein 26	89.11	1.09	0.044	0.987
Q92930	Ras-related protein Rab-8B	328.85	1.09	0.048	0.987
P32969	60S ribosomal protein L9	383.76	1.09	0.046	0.987
P50416	Carnitine O-palmitoyltransferase 1, liver isoform	309.47	1.08	0.025	0.987
P28482; P09619; P27361	Mitogen-activated protein kinase 1	216.29	1.08	0.031	0.987
P56192	Methionine--tRNA ligase, cytoplasmic	571.26	1.08	0.015	0.987
P56134	ATP synthase subunit f, mitochondrial	109.15	1.08	0.012	0.987
Q9UQE7	Structural maintenance of chromosomes protein 3	531.87	1.07	0.035	0.987
P06493	Cyclin-dependent kinase 1	349.99	1.07	0.038	0.987
O14980	Exportin-1	608.63	1.07	0.018	0.987
Q9NPQ8; Q9NVN3	Synembryn-A	218.4	1.07	0.018	0.987
Q15008	26S proteasome non-ATPase regulatory subunit 6	274.56	1.06	0.005	0.987
P42166	Lamina-associated polypeptide 2, isoform alpha	1157.24	1.05	0.039	0.987
P62826	GTP-binding nuclear protein Ran	374.58	1.04	0.010	0.987
Q9BXS5; Q9Y6Q5	AP-1 complex subunit mu-1	95.16	1.06	0.049	0.987
Q8NEV1	Casein kinase II subunit alpha 3	214.01	1.06	0.008	0.987
Q15006	ER membrane protein complex	185.43	1.06	0.041	0.987

	subunit 2				
Q16881; Q9NNW7	Thioredoxin reductase 1, cytoplasmic	431.42	1.07	0.028	0.987
Q49A26	Putative oxidoreductase GLYR1	53.13	1.07	0.026	0.987
Q99598	Translin-associated protein X	115.83	1.08	0.041	0.987
Q96CW1	AP-2 complex subunit mu	197.07	1.09	0.040	0.987
P49916	DNA ligase 3	240.06	1.09	0.011	0.987
O75821	Eukaryotic translation initiation factor 3 subunit G	205.44	1.09	0.006	0.987
O75937	DnaJ homolog subfamily C member 8	100.29	1.09	0.035	0.987
Q9UNZ2	NSFL1 cofactor p47	441.85	1.10	0.038	0.987
P49006	MARCKS-related protein	308.67	1.10	0.044	0.987
Q9UUK9	ADP-sugar pyrophosphatase	164.34	1.10	0.024	0.987
Q9UNN5	FAS-associated factor 1	91.91	1.11	0.008	0.987
O75431	Metaxin-2	79.14	1.12	0.034	0.987
P62857	40S ribosomal protein S28	250.78	1.12	0.030	0.987
Q86X76	Nitrilase homolog 1	130.09	1.14	0.027	0.987
Q9BV44	THUMP domain-containing protein 3	85.19	1.15	0.002	0.987
Q9HBU6	Ethanolamine kinase 1	94.98	1.15	0.024	0.987
Q13330; Q9BTC8	Metastasis-associated protein MTA1	269.09	1.17	0.013	0.987
Q96F15	GTPase IMAP family member 5	68.51	1.23	0.002	0.987
P13612	Integrin alpha-4	32.61	1.25	0.011	0.987
P55081	Microfibrillar-associated protein 1	33.84	1.29	0.017	0.987
Q9H0R4	Haloacid dehalogenase-like hydrolase domain-containing protein 2	32.38	1.31	0.013	0.987

Q8IY37	Probable ATP-dependent RNA helicase DHX37	34.64	1.35	0.039	0.987
Q9Y2X7	ARF GTPase-activating protein GIT1	33.12	1.70	0.016	0.987
P04264; P04259; P35908	Keratin, type II cytoskeletal 1	88.8	2.01	0.008	0.987

^a Accession number according to UniProt database. ^b Protein description with relative symbol. ^c Confidence score generated by Progenesis. * Proteins shared between both treatments (resveratrol and curcumin). Green reduction, red induction.

1.0 – 1.49		
1.5 – 1.99		
2 – 2.49		
2.5 – 2.99		
3 – 3.49		
3.5 +		
* Protein common between resveratrol and curcumin treatment.		

Table 8.11 – Significantly modulated proteins in Jurkat T lymphocytes after 30 μ M isorhamnetin identified by label-free LC-MS.

Accession ^a	Description ^b	Confidence score ^c	Fold change	p-value	q-value
P06396	Gelsolin	33.62	2.64	0.001	0.038
Q01581	Hydroxymethylglutaryl-CoA synthase, cytoplasmic	168.58	1.91	0.000	0.000
P37268	Squalene synthase	704.92	1.79	0.000	0.000
Q8NBT2	Kinetochose protein Spc24	141.91	1.50	0.013	0.120
Q92522	Histone H1x	401.69	1.42	0.001	0.043
Q5MIZ7	Serine/threonine-protein phosphatase 4 regulatory subunit 3B	50.04	1.40	0.028	0.146
Q9NXJ5	Pyroglutamyl-peptidase 1	31.61	1.31	0.005	0.077
P02774	Vitamin D-binding protein	57.1	1.30	0.049	0.186
Q9HBM1	Kinetochose protein Spc25	35.24	1.30	0.036	0.162
Q14790	Caspase-8	29.02	1.30	0.032	0.154
P48449	Lanosterol synthase	488.43	1.29	0.000	0.027
Q9BZF1	Oxysterol-binding protein-related protein 8	49.77	1.28	0.031	0.151
P63092; P38405	Guanine nucleotide-binding protein G(s) subunit alpha isoforms short	254.28	1.27	0.000	0.022
P23921	Ribonucleoside-diphosphate reductase large subunit	551.47	1.27	0.000	0.022
P13674	Prolyl 4-hydroxylase subunit alpha-1	416.86	1.27	0.004	0.071
Q15836	Vesicle-associated membrane protein 3	42.62	1.24	0.038	0.166
Q9UBM7	7-dehydrocholesterol reductase	222.35	1.24	0.001	0.047
O75152	Zinc finger CCCH domain-containing protein 11A	86.12	1.24	0.035	0.160

Q8NFH3	Nucleoporin Nup43	223.78	1.24	0.001	0.039
P53007	Tricarboxylate transport protein, mitochondrial	227.59	1.23	0.015	0.125
Q9NRX4	14 kDa phosphohistidine phosphatase	75.66	1.23	0.010	0.109
P10515	Dihydrolipoyllysine-residue acetyltransferase component of pyruvate dehydrogenase complex, mitochondrial	515.96	1.23	0.001	0.039
Q9BZX2	Uridine-cytidine kinase 2	56.3	1.22	0.012	0.116
Q15392	Delta(24)-sterol reductase	136.11	1.22	0.004	0.072
P31350	Ribonucleoside-diphosphate reductase subunit M2	146.64	1.22	0.018	0.125
Q7L1Q6	Basic leucine zipper and W2 domain-containing protein 1	313.99	1.22	0.000	0.027
P55212	Caspase-6	56.64	1.22	0.010	0.108
O15305	Phosphomannomutase 2	33.42	1.22	0.005	0.080
Q63HN8	E3 ubiquitin-protein ligase RNF213	94.06	1.21	0.048	0.185
Q7Z4H7	HAUS augmin-like complex subunit 6	51.45	1.20	0.000	0.027
Q9H4E7	Differentially expressed in FDCP 6 homolog	118	1.20	0.028	0.146
Q9Y6G9	Cytoplasmic dynein 1 light intermediate chain 1	53.87	1.20	0.002	0.059
Q99943	1-acyl-sn-glycerol-3-phosphate acyltransferase alpha	63.87	1.20	0.006	0.089
Q86YV0	RAS protein activator like-3	122.95	1.20	0.033	0.158
O15027	Protein transport protein Sec16A	109.7	1.20	0.037	0.165
Q86TU7	Histone-lysine N-methyltransferase setd3	34.83	1.20	0.048	0.184
Q9NSE4	Isoleucine--tRNA ligase, mitochondrial	52.94	1.20	0.037	0.165
P49327	Fatty acid synthase	879.28	1.19	0.004	0.071

P08134	Rho-related GTP-binding protein RhoC	203.16	1.19	0.003	0.063
Q9P035	Very-long-chain (3R)-3-hydroxyacyl-[acyl-carrier protein] dehydratase 3	263.43	1.19	0.042	0.172
P52292	Importin subunit alpha-1	449.61	1.19	0.019	0.129
P10155	60 kDa SS-A/Ro ribonucleoprotein	49.1	1.19	0.050	0.186
O00182; Q3B8N2	Galectin-9	161.13	1.19	0.043	0.173
Q92665	28S ribosomal protein S31, mitochondrial	50.73	1.19	0.011	0.112
P50416	Carnitine O-palmitoyltransferase 1, liver isoform	309.47	1.18	0.002	0.053
Q9UNF1	Melanoma-associated antigen D2	48.74	1.18	0.004	0.071
Q14558	Phosphoribosyl pyrophosphate synthase-associated protein 1	153.92	1.18	0.000	0.033
P53396	ATP-citrate synthase	2180.48	1.18	0.000	0.002
P22830	Ferrochelatase, mitochondrial	136.1	1.18	0.030	0.148
Q9H4M9	EH domain-containing protein 1	41.58	1.18	0.024	0.141
P03905	NADH-ubiquinone oxidoreductase chain 4	48.04	1.18	0.034	0.158
Q9UQ88	Cyclin-dependent kinase 11A	124.58	1.18	0.009	0.106
P60842	Eukaryotic initiation factor 4A-I	1242.37	1.17	0.002	0.055
Q9P003	Protein cornichon homolog 4	49.21	1.17	0.017	0.125
P12236	ADP/ATP translocase 3	600.74	1.16	0.003	0.071
Q9Y6B6	GTP-binding protein SAR1b	152.12	1.16	0.014	0.121
Q5JPE7	Nodal modulator 2	633.91	1.16	0.001	0.051
P63218	Guanine nucleotide-binding protein G(I)/G(S)/G(O) subunit gamma-5	32.15	1.16	0.043	0.173
O15258	Protein RER1	74.79	1.16	0.028	0.145

P50914	60S ribosomal protein L14	187.02	1.16	0.018	0.125
Q15027	Arf-GAP with coiled-coil, ANK repeat and PH domain-containing protein 1	379.54	1.16	0.017	0.125
Q5T4S7	E3 ubiquitin-protein ligase UBR4	384.69	1.16	0.029	0.147
P11310	Medium-chain specific acyl-CoA dehydrogenase, mitochondrial	535.89	1.16	0.003	0.071
Q9NS69	Mitochondrial import receptor subunit TOM22 homolog	219.29	1.16	0.026	0.143
Q96F07; Q7L576	Cytoplasmic FMR1-interacting protein 2	252.41	1.16	0.016	0.125
P46781	40S ribosomal protein S9	367.26	1.16	0.001	0.038
Q9NUU7; Q9UHL0; Q9UMR2	ATP-dependent RNA helicase DDX19A	259.82	1.15	0.002	0.052
Q5SRE5	Nucleoporin NUP188 homolog	78.44	1.15	0.011	0.111
P19404	NADH dehydrogenase [ubiquinone] flavoprotein 2, mitochondrial	47.32	1.15	0.025	0.142
Q16566	Calcium/calmodulin-dependent protein kinase type IV	262.66	1.15	0.002	0.054
O95573	Long-chain-fatty-acid--CoA ligase 3	224.99	1.15	0.016	0.125
P78344	Eukaryotic translation initiation factor 4 gamma 2	269.3	1.15	0.018	0.125
Q96CS3	FAS-associated factor 2	92.79	1.15	0.029	0.146
Q9BTT0	Acidic leucine-rich nuclear phosphoprotein 32 family member E	630.39	1.15	0.004	0.073
P05771	Protein kinase C beta type	345.22	1.15	0.022	0.133
O75832	26S proteasome non-ATPase regulatory subunit 10	136.94	1.15	0.019	0.126
Q96D05	Uncharacterized protein C10orf35	93.05	1.14	0.026	0.144
Q86UX7	Fermitin family homolog 3	850.38	1.14	0.004	0.071

O95571	Persulfide dioxygenase ETHE1, mitochondrial	248.41	1.14	0.006	0.086
P07305	Histone H1.0	162.04	1.14	0.001	0.048
Q8WU39	Marginal zone B- and B1-cell-specific protein	296.2	1.14	0.002	0.052
P62879	Guanine nucleotide-binding protein G(I)/G(S)/G(T) subunit beta-2	674.25	1.14	0.011	0.112
P15153	Ras-related C3 botulinum toxin substrate 2	232.08	1.14	0.009	0.106
Q9H7D7	WD repeat-containing protein 26	89.11	1.14	0.010	0.108
P19367; Q2TB90	Hexokinase-1	772.01	1.14	0.010	0.108
Q8N752	Casein kinase I isoform alpha-like	48.66	1.14	0.046	0.182
O94925	Glutaminase kidney isoform, mitochondrial	233.6	1.14	0.003	0.063
P19784	Casein kinase II subunit alpha'	208.38	1.14	0.042	0.173
P10606	Cytochrome c oxidase subunit 5B, mitochondrial	81.62	1.14	0.007	0.090
Q92974	Rho guanine nucleotide exchange factor 2	741.41	1.13	0.003	0.063
P21266	Glutathione S-transferase Mu 3	274.29	1.13	0.015	0.125
O75489	NADH dehydrogenase [ubiquinone] iron-sulfur protein 3, mitochondrial	264.83	1.13	0.008	0.098
Q16563	Synaptophysin-like protein 1	61.13	1.13	0.044	0.176
Q14157	Ubiquitin-associated protein 2-like	250.46	1.13	0.028	0.146
P62280	40S ribosomal protein S11	278.08	1.13	0.029	0.146
P62979; P0CG47	Ubiquitin-40S ribosomal protein S27a	359.63	1.13	0.010	0.107
P56134	ATP synthase subunit f, mitochondrial	109.15	1.13	0.003	0.063
P02786	Transferrin receptor protein 1	980.43	1.13	0.011	0.112

Q9BV86	N-terminal Xaa-Pro-Lys N-methyltransferase 1	131.96	1.13	0.002	0.058
Q7L014	Probable ATP-dependent RNA helicase DDX46	743.53	1.13	0.004	0.071
Q9BSJ8	Extended synaptotagmin-1	927.4	1.13	0.015	0.125
Q01813	6-phosphofructokinase type C	1504.46	1.13	0.000	0.022
Q9H9B4; Q9BWM7	Sideroflexin-1	525.31	1.13	0.007	0.090
Q13576	Ras GTPase-activating-like protein IQGAP2	628.25	1.13	0.025	0.142
Q16512	Serine/threonine-protein kinase N1	53.05	1.13	0.014	0.121
Q96T76	MMS19 nucleotide excision repair protein homolog	144.44	1.12	0.015	0.125
Q13885	Tubulin beta-2A chain	1390.54	1.12	0.038	0.166
P39023; Q92901	60S ribosomal protein L3	834.85	1.12	0.012	0.118
Q00839	Heterogeneous nuclear ribonucleoprotein U	1887.69	1.12	0.002	0.054
Q9BVK6	Transmembrane emp24 domain-containing protein 9	210.62	1.12	0.030	0.149
Q9BWD1	Acetyl-CoA acetyltransferase, cytosolic	468.41	1.12	0.006	0.089
P14868	Aspartate--tRNA ligase, cytoplasmic	861.83	1.12	0.007	0.090
O94874	E3 UFM1-protein ligase 1	157.26	1.11	0.047	0.184
P00846	ATP synthase subunit a	44.36	1.11	0.004	0.072
P51659	Peroxisomal multifunctional enzyme type 2	804.27	1.11	0.010	0.110
Q9Y5Y2	Cytosolic Fe-S cluster assembly factor NUBP2	224.62	1.11	0.031	0.152
P46782	40S ribosomal protein S5	651.39	1.11	0.032	0.153
Q9Y4W6	AFG3-like protein 2	61.2	1.11	0.047	0.182

O00264	Membrane-associated progesterone receptor component 1	258.59	1.11	0.045	0.180
P47985; P0C7P4	Cytochrome b-c1 complex subunit Rieske, mitochondrial	269.52	1.11	0.030	0.148
O00217	NADH dehydrogenase [ubiquinone] iron-sulfur protein 8, mitochondrial	85.63	1.11	0.046	0.182
Q96CN7	Isochorismatase domain-containing protein 1	81.46	1.11	0.021	0.133
O00571; O15523	ATP-dependent RNA helicase DDX3X	971.13	1.11	0.002	0.051
Q9UBX3	Mitochondrial dicarboxylate carrier	129.56	1.11	0.011	0.111
Q9NVI7; Q5T2N8; Q5T9A4	ATPase family AAA domain-containing protein 3A	483.99	1.11	0.001	0.047
P62266	40S ribosomal protein S23	349.48	1.11	0.002	0.058
Q13011	Delta(3,5)-Delta(2,4)-dienoyl-CoA isomerase, mitochondrial	660.24	1.11	0.040	0.170
P46459	Vesicle-fusing ATPase	276.05	1.11	0.048	0.186
Q6P2Q9	Pre-mRNA-processing-splicing factor 8	1795.45	1.11	0.022	0.136
P48047	ATP synthase subunit O, mitochondrial	613.99	1.11	0.016	0.125
P62753	40S ribosomal protein S6	492.29	1.11	0.003	0.192
Q15185	Prostaglandin E synthase 3	519.64	1.10	0.005	0.079
P40939	Trifunctional enzyme subunit alpha, mitochondrial	1068.05	1.10	0.028	0.145
Q13094	Lymphocyte cytosolic protein 2	75.38	1.10	0.031	0.192
P00403	Cytochrome c oxidase subunit 2	203.18	1.10	0.001	0.038
P62913	60S ribosomal protein L11	287.84	1.10	0.032	0.153
P68371;	Tubulin beta-4B chain	1935.29	1.10	0.048	0.184

Q3ZCM7					
P17252; P05129	Protein kinase C alpha type	561.07	1.10	0.018	0.125
P51665	26S proteasome non-ATPase regulatory subunit 7	310.19	1.10	0.020	0.132
Q5JTV8	Torsin-1A-interacting protein 1	136.24	1.10	0.017	0.125
P38117	Electron transfer flavoprotein subunit beta	445.82	1.10	0.006	0.086
A0AVT1	Ubiquitin-like modifier-activating enzyme 6	308.59	1.10	0.020	0.129
P13804	Electron transfer flavoprotein subunit alpha, mitochondrial	679.66	1.10	0.013	0.118
P36507	Dual specificity mitogen-activated protein kinase kinase 2	372.26	1.10	0.050	0.186
P01111; P01116	GTPase NRas	189.44	1.10	0.049	0.186
P30085	UMP-CMP kinase	212.43	1.10	0.039	0.169
P10809	60 kDa heat shock protein, mitochondrial	2904.81	1.10	0.023	0.139
O95881	Thioredoxin domain-containing protein 12	71.56	1.10	0.022	0.133
Q9BQE3; A6NHL2; Q9H853	Tubulin alpha-1C chain	1765.34	1.10	0.035	0.160
P62269	40S ribosomal protein S18	568.99	1.10	0.005	0.083
Q00610; P53675	Clathrin heavy chain 1	3109.45	1.10	0.003	0.067
P40763	Signal transducer and activator of transcription 3	272.49	1.10	0.015	0.125
P04818	Thymidylate synthase	320.63	1.10	0.023	0.139

P62241	40S ribosomal protein S8	496.38	1.09	0.003	0.071
P35998	26S protease regulatory subunit 7	1000.15	1.09	0.043	0.173
Q96DI7	U5 small nuclear ribonucleoprotein 40 kDa protein	287.22	1.09	0.011	0.112
Q13151	Heterogeneous nuclear ribonucleoprotein A0	607.45	1.09	0.014	0.121
P36578	60S ribosomal protein L4	883.13	1.09	0.001	0.047
Q02878	60S ribosomal protein L6	867.33	1.09	0.017	0.125
P16615	Sarcoplasmic/endoplasmic reticulum calcium ATPase 2	1195.67	1.09	0.019	0.126
P27824	Calnexin	1078.73	1.09	0.021	0.133
Q9UBS4	DnaJ homolog subfamily B member 11	223.96	1.09	0.020	0.129
Q15287	RNA-binding protein with serine-rich domain 1	227.89	1.09	0.047	0.182
O43837	Isocitrate dehydrogenase [NAD] subunit beta, mitochondrial	420.5	1.09	0.009	0.106
Q14498; Q86U06	RNA-binding protein 39	648.84	1.09	0.018	0.125
P62888	60S ribosomal protein L30	460.88	1.09	0.014	0.120
P50570; Q05193; Q9UQ16	Dynamin-2	462.5	1.09	0.011	0.111
O43615	Mitochondrial import inner membrane translocase subunit TIM44	290.5	1.09	0.028	0.146
Q9NSD9	Phenylalanine--tRNA ligase beta subunit	520.43	1.09	0.019	0.126
O60831	PRA1 family protein 2	88.37	1.09	0.029	0.146
P61604	10 kDa heat shock protein, mitochondrial	472.98	1.09	0.016	0.125
Q12769	Nuclear pore complex protein Nup160	159.72	1.09	0.035	0.160

P40429; Q6NVV1	60S ribosomal protein L13a	373.67	1.08	0.012	0.112
Q07960	Rho GTPase-activating protein 1	241.38	1.08	0.040	0.169
P22307	Non-specific lipid-transfer protein	493.33	1.08	0.005	0.080
Q92973	Transportin-1	505.82	1.08	0.001	0.051
P84095	Rho-related GTP-binding protein RhoG	535.95	1.08	0.041	0.171
P48735	Isocitrate dehydrogenase [NADP], mitochondrial	1330.31	1.08	0.022	0.133
P31943	Heterogeneous nuclear ribonucleoprotein H	980.42	1.08	0.014	0.120
P30048	Thioredoxin-dependent peroxide reductase, mitochondrial	428.51	1.08	0.037	0.165
P56192	Methionine--tRNA ligase, cytoplasmic	571.26	1.08	0.013	0.118
P60709; A5A3E0; P0CG38; P0CG39; Q562R1; Q6S8J3; Q9BYX7	Actin, cytoplasmic 1	2271.13	1.08	0.005	0.083
Q07955	Serine/arginine-rich splicing factor 1	555.74	1.08	0.012	0.116
P25398	40S ribosomal protein S12	390.6	1.08	0.025	0.192
Q02543	60S ribosomal protein L18a	318.67	1.08	0.047	0.184
Q08J23	tRNA (cytosine(34)-C(5))- methyltransferase	845.53	1.08	0.008	0.094
Q8WYJ6	Septin-1	512.17	1.08	0.041	0.171
Q13547; O15379	Histone deacetylase 1	520.45	1.08	0.005	0.083

P11717	Cation-independent mannose-6-phosphate receptor OS=Homo sapiens GN=IGF2R PE=1 SV=3	315.72	1.08	0.034	0.159
P31942	Heterogeneous nuclear ribonucleoprotein H3	687.57	1.08	0.027	0.145
P46776	60S ribosomal protein L27a	184.8	1.08	0.013	0.120
P42677; Q71UM5	40S ribosomal protein S27	187.14	1.08	0.023	0.138
P18621	60S ribosomal protein L17	205.73	1.08	0.028	0.146
P61313	60S ribosomal protein L15	261.41	1.08	0.001	0.051
P61247	40S ribosomal protein S3a	793.01	1.08	0.019	0.128
P62263	40S ribosomal protein S14	314.21	1.08	0.025	0.142
P62244	40S ribosomal protein S15a	209.97	1.08	0.005	0.080
P55209	Nucleosome assembly protein 1-like 1	576.82	1.08	0.025	0.142
P22102	Trifunctional purine biosynthetic protein adenosine-3	858.05	1.08	0.028	0.146
P14625; Q58FF3	Endoplasmic	2119.46	1.08	0.008	0.094
P60468	Protein transport protein Sec61 subunit beta	133.46	1.08	0.034	0.158
P23396	40S ribosomal protein S3	853.45	1.07	0.010	0.109
P00367; P49448	Glutamate dehydrogenase 1, mitochondrial	757.31	1.07	0.021	0.133
Q9UHD8	Septin-9	454.96	1.07	0.020	0.129
P62424	60S ribosomal protein L7a	690.58	1.07	0.050	0.186
P51149	Ras-related protein Rab-7a	649.34	1.07	0.049	0.186
P61353	60S ribosomal protein L27	244.37	1.07	0.022	0.136
P63244	Guanine nucleotide-binding protein subunit beta-2-like 1	1304.43	1.07	0.009	0.102

P63173	60S ribosomal protein L38	164.85	1.07	0.035	0.160
P24539	ATP synthase F(0) complex subunit B1, mitochondrial	236.1	1.07	0.035	0.160
Q14204	Cytoplasmic dynein 1 heavy chain 1	2076.8	1.07	0.013	0.118
P52272	Heterogeneous nuclear ribonucleoprotein M	2073.74	1.07	0.018	0.125
P83731	60S ribosomal protein L24	431.86	1.07	0.049	0.186
Q16629	Serine/arginine-rich splicing factor 7	228.25	1.07	0.026	0.144
Q9Y230	RuvB-like 2	616.83	1.07	0.032	0.153
Q15365	Poly(rC)-binding protein 1	845.71	1.06	0.027	0.145
P33992	DNA replication licensing factor MCM5	1066.36	1.06	0.017	0.125
Q14566	DNA replication licensing factor MCM6	1629.88	1.06	0.022	0.133
Q15008	26S proteasome non-ATPase regulatory subunit 6	274.56	1.06	0.002	0.052
P47897	Glutamine--tRNA ligase	721.93	1.06	0.001	0.051
P14324	Farnesyl pyrophosphate synthase	332.03	1.06	0.001	0.051
P07686	Beta-hexosaminidase subunit beta	143.46	1.06	0.035	0.160
P39656	Dolichyl-diphosphooligosaccharide--protein glycosyltransferase 48 kDa subunit	484.81	1.06	0.025	0.142
Q15366; P57721	Poly(rC)-binding protein 2	606.4	1.06	0.037	0.165
P11021; O95399	78 kDa glucose-regulated protein	2044.95	1.06	0.033	0.155
P12268	Inosine-5'-monophosphate dehydrogenase 2	1214.57	1.05	0.038	0.167
Q92841	Probable ATP-dependent RNA helicase DDX17	1329.48	1.05	0.018	0.125
Q9P258	Protein RCC2	670.33	1.04	0.018	0.125

P11413	Glucose-6-phosphate 1-dehydrogenase	654.38	1.06	0.012	0.117
O43765	Small glutamine-rich tetratricopeptide repeat-containing protein alpha	279.15	1.06	0.043	0.173
P62826	GTP-binding nuclear protein Ran	374.58	1.06	0.023	0.137
Q9Y2W1	Thyroid hormone receptor-associated protein 3	426.09	1.06	0.014	0.121
P26196	Probable ATP-dependent RNA helicase DDX6	491.27	1.06	0.040	0.169
P22234	Multifunctional protein ADE2	1389.4	1.06	0.041	0.171
P29144	Tripeptidyl-peptidase 2	249.74	1.07	0.045	0.179
O43175	D-3-phosphoglycerate dehydrogenase	822.26	1.07	0.027	0.144
O43776	Asparagine--tRNA ligase, cytoplasmic	514.13	1.07	0.022	0.133
P49588	Alanine--tRNA ligase, cytoplasmic	1396.95	1.07	0.018	0.125
Q16531	DNA damage-binding protein 1	755.41	1.07	0.007	0.090
Q04837	Single-stranded DNA-binding protein, mitochondrial	294.31	1.07	0.017	0.125
Q9BT78	COP9 signalosome complex subunit 4	302.1	1.07	0.024	0.140
Q13428	Treacle protein	504.02	1.07	0.039	0.169
P55072	Transitional endoplasmic reticulum ATPase	2044.99	1.07	0.007	0.090
P63010	AP-2 complex subunit beta	420.33	1.07	0.036	0.162
P06733	Alpha-enolase	2107.6	1.08	0.009	0.106
P26639	Threonine--tRNA ligase, cytoplasmic	592.55	1.08	0.008	0.097
Q06830	Peroxiredoxin-1	515.18	1.08	0.041	0.171
Q96CW1	AP-2 complex subunit mu	197.07	1.08	0.027	0.144
P00558	Phosphoglycerate kinase 1	1975.91	1.08	0.045	0.179
O43488; O95154;	Aflatoxin B1 aldehyde reductase member 2	324.91	1.08	0.018	0.125

Q8NHP1					
Q9GZL7	Ribosome biogenesis protein WDR12	224.38	1.08	0.019	0.126
Q9Y266	Nuclear migration protein nudC	509.24	1.08	0.024	0.141
Q9NQC3	Reticulon-4	240.28	1.08	0.004	0.076
P62993	Growth factor receptor-bound protein 2	289.01	1.08	0.033	0.158
Q9UK76	Hematological and neurological expressed 1 protein	235.51	1.08	0.035	0.160
Q13435	Splicing factor 3B subunit 2	500.01	1.08	0.018	0.125
P08575	Receptor-type tyrosine-protein phosphatase C	1149.04	1.08	0.018	0.125
P54578	Ubiquitin carboxyl-terminal hydrolase 14	999.86	1.08	0.002	0.061
P54577	Tyrosine--tRNA ligase, cytoplasmic	793.47	1.08	0.015	0.125
P34932	Heat shock 70 kDa protein 4	1847.08	1.09	0.021	0.133
O60880	SH2 domain-containing protein 1A	210.08	1.09	0.041	0.171
P78406	mRNA export factor	220.12	1.09	0.018	0.125
Q9NZL4	Hsp70-binding protein 1	226.91	1.09	0.018	0.125
Q16543	Hsp90 co-chaperone Cdc37	268.35	1.09	0.027	0.145
P19623	Spermidine synthase	278.54	1.09	0.039	0.168
O14818; Q8TAA3	Proteasome subunit alpha type-7	603.55	1.09	0.049	0.186
Q15459	Splicing factor 3A subunit 1	445.91	1.09	0.030	0.149
Q13617	Cullin-2	96.42	1.09	0.043	0.174
P09429; B2RPK0; P23497	High mobility group protein B1	487.64	1.09	0.016	0.125
P12814;	Alpha-actinin-1	1332.6	1.10	0.035	0.160

P35609; Q08043					
Q13283	Ras GTPase-activating protein-binding protein 1	188.15	1.10	0.031	0.153
Q13177; O75914; Q13153	Serine/threonine-protein kinase PAK 2	671.02	1.10	0.027	0.145
P63104	14-3-3 protein zeta/delta	1109.71	1.10	0.026	0.143
P11233; P11234	Ras-related protein Ral-A	155.23	1.10	0.024	0.140
O96019; O94805	Actin-like protein 6A	253.02	1.10	0.026	0.144
P14550; Q96JD6	Alcohol dehydrogenase [NADP(+)]	322.65	1.10	0.042	0.173
P39687; O43423; O95626	Acidic leucine-rich nuclear phosphoprotein 32 family member A	556.07	1.10	0.021	0.133
Q04760	Lactoylglutathione lyase	249.58	1.10	0.050	0.186
P32119	Peroxiredoxin-2	450.78	1.10	0.024	0.140
Q9Y4Z0	U6 snRNA-associated Sm-like protein LSm4	148.09	1.10	0.033	0.158
P33316	Deoxyuridine 5'-triphosphate nucleotidohydrolase, mitochondrial	413.27	1.10	0.016	0.125
O75940	Survival of motor neuron-related-splicing factor 30	67.51	1.11	0.025	0.142
P61964	WD repeat-containing protein 5	204.38	1.11	0.014	0.120
P16949; H7BZ55; Q93045;	Stathmin	704.09	1.11	0.019	0.127

Q9H169					
P30041	Peroxiredoxin-6	617.68	1.11	0.009	0.102
P28066	Proteasome subunit alpha type-5	295.16	1.11	0.018	0.125
Q8NEV1	Casein kinase II subunit alpha 3	214.01	1.11	0.002	0.058
Q93084	Sarcoplasmic/endoplasmic reticulum calcium ATPase 3	884.11	1.11	0.018	0.125
Q13838	Spliceosome RNA helicase DDX39B	1077.99	1.11	0.014	0.120
P52209	6-phosphogluconate dehydrogenase, decarboxylating	995.07	1.11	0.016	0.125
Q9UI30	tRNA methyltransferase 112 homolog	209.5	1.11	0.026	0.144
Q9UJU2; P36402	Lymphoid enhancer-binding factor 1	138.29	1.11	0.007	0.090
P54727	UV excision repair protein RAD23 homolog B	265.22	1.11	0.035	0.160
Q9BXS5; Q9Y6Q5	AP-1 complex subunit mu-1	95.16	1.12	0.025	0.142
P09012	U1 small nuclear ribonucleoprotein A	173.95	1.12	0.007	0.090
P07737	Profilin-1	782.27	1.12	0.011	0.112
P62328	Thymosin beta-4	110.74	1.12	0.017	0.125
P62820; A6NDJ8; P51153; P59190	Ras-related protein Rab-1A	508.76	1.12	0.004	0.071
Q04323	UBX domain-containing protein 1	270.27	1.12	0.041	0.171
P09211	Glutathione S-transferase P	928.54	1.12	0.042	0.172
P25788	Proteasome subunit alpha type-3	351.31	1.12	0.020	0.129
Q9UQ35	Serine/arginine repetitive matrix protein 2	370.91	1.12	0.041	0.171

O75347	Tubulin-specific chaperone A	348.71	1.12	0.006	0.089
P83916	Chromobox protein homolog 1	235.4	1.13	0.029	0.146
P00491	Purine nucleoside phosphorylase	891.19	1.13	0.039	0.169
P29218	Inositol monophosphatase 1	158.94	1.13	0.030	0.148
Q06203	Amidophosphoribosyltransferase	126.8	1.13	0.044	0.178
Q06323	Proteasome activator complex subunit 1	479.26	1.13	0.038	0.167
P40925	Malate dehydrogenase, cytoplasmic	629.68	1.13	0.018	0.125
P26368	Splicing factor U2AF 65 kDa subunit	314.83	1.13	0.036	0.162
P61225; P10114	Ras-related protein Rap-2b	96.37	1.13	0.022	0.133
P62942	Peptidyl-prolyl cis-trans isomerase FKBP1A	174.86	1.13	0.029	0.147
P99999	Cytochrome c	256.19	1.13	0.029	0.146
Q92945	Far upstream element-binding protein 2	1093.26	1.13	0.001	0.051
P27695	DNA-(apurinic or apyrimidinic site) lyase	636.27	1.13	0.006	0.085
Q01082; O15020; P11277	Spectrin beta chain, non-erythrocytic 1	4279.5	1.13	0.001	0.051
Q14978	Nucleolar and coiled-body phosphoprotein 1	357.76	1.14	0.007	0.090
Q13813	Spectrin alpha chain, non-erythrocytic 1	4310.16	1.14	0.002	0.054
Q12906; Q96SI9	Interleukin enhancer-binding factor 3	745.67	1.14	0.000	0.008
Q13330; Q9BTC8	Metastasis-associated protein MTA1	269.09	1.14	0.010	0.108

P04439; P16188; P30512	HLA class I histocompatibility antigen, A-3 alpha chain	198.82	1.14	0.039	0.168
P28072	Proteasome subunit beta type-6	126.69	1.14	0.004	0.071
Q96KP4	Cytosolic non-specific dipeptidase	422.74	1.14	0.017	0.125
O43813	LanC-like protein 1	108.5	1.14	0.025	0.142
Q9UKV3	Apoptotic chromatin condensation inducer in the nucleus	307.98	1.14	0.009	0.106
Q5T280	Uncharacterized protein C9orf114	30.72	1.14	0.048	0.185
P61923	Coatomer subunit zeta-1	108.72	1.14	0.011	0.111
O95777	N-alpha-acetyltransferase 38, NatC auxiliary subunit	179.95	1.15	0.041	0.172
O43670	Zinc finger protein 207	111.06	1.15	0.004	0.077
Q9UI08	Ena/VASP-like protein OS=Homo sapiens GN=EVL PE=1 SV=2	601.46	1.15	0.014	0.121
P28074	Proteasome subunit beta type-5	157.85	1.15	0.001	0.051
P30626	Sorcin	167.9	1.15	0.026	0.143
Q99497	Protein DJ-1	658.95	1.15	0.005	0.081
O43399	Tumor protein D54	275.09	1.15	0.035	0.160
P48444	Coatomer subunit delta	304.57	1.15	0.013	0.118
Q92769	Histone deacetylase 2	246.03	1.15	0.001	0.051
P49589	Cysteine--tRNA ligase, cytoplasmic	182.97	1.15	0.046	0.182
P23526	Adenosylhomocysteinase	617.03	1.15	0.008	0.094
P28070	Proteasome subunit beta type-4	314.75	1.15	0.027	0.144
Q04917	14-3-3 protein eta	479.74	1.16	0.042	0.172
P61289	Proteasome activator complex subunit 3	170.47	1.16	0.039	0.168

P21333	Filamin-A	4586.31	1.16	0.001	0.051
P10599	Thioredoxin	198.56	1.16	0.004	0.071
Q01105	Protein SET	423.03	1.16	0.041	0.172
P69905; P02008	Hemoglobin subunit alpha	290.61	1.17	0.007	0.090
Q9Y490; Q9Y4G6	Talin-1	3475.69	1.17	0.001	0.038
O75431	Metaxin-2	79.14	1.17	0.017	0.125
Q9UKK9	ADP-sugar pyrophosphatase	164.34	1.17	0.005	0.077
Q14019	Coactosin-like protein	305.64	1.17	0.005	0.083
O43598	2'-deoxynucleoside 5'-phosphate N-hydrolase 1	68.34	1.17	0.014	0.120
P37837	Transaldolase	520.1	1.17	0.007	0.090
P07195	L-lactate dehydrogenase B chain	1251.65	1.18	0.029	0.146
O75937	DnaJ homolog subfamily C member 8	100.29	1.18	0.001	0.039
Q86X76	Nitrilase homolog 1	130.09	1.18	0.013	0.118
Q15424; Q14151	Scaffold attachment factor B1	592.66	1.18	0.002	0.058
P49006	MARCKS-related protein	308.67	1.18	0.006	0.089
Q00534	Cyclin-dependent kinase 6	537.66	1.18	0.000	0.027
P51858	Hepatoma-derived growth factor	239.73	1.18	0.017	0.125
Q9Y6H1; Q5T1J5	Coiled-coil-helix-coiled-coil-helix domain-containing protein 2, mitochondrial	119.59	1.18	0.004	0.071
Q9UFW8	CGG triplet repeat-binding protein 1	30.44	1.18	0.000	0.033
P41250	Glycine--tRNA ligase	713.6	1.19	0.006	0.086
P30086	Phosphatidylethanolamine-binding	511.76	1.19	0.016	0.125

	protein 1				
Q9H6Z4	Ran-binding protein 3	91.88	1.19	0.023	0.138
Q13112	Chromatin assembly factor 1 subunit B	38.55	1.19	0.014	0.152
Q9Y237	Peptidyl-prolyl cis-trans isomerase NIMA-interacting 4	61.92	1.19	0.028	0.145
Q6P1J9	Parafibromin	84.57	1.19	0.011	0.112
O43768; P56211	Alpha-endosulfine	82.49	1.19	0.032	0.155
P52888	Thimet oligopeptidase	30.92	1.19	0.004	0.071
P15121; C9JRZ8	Aldose reductase	312.17	1.20	0.007	0.090
Q9BXV9	Uncharacterized protein C14orf142	47.76	1.20	0.020	0.132
P55327	Tumor protein D52	239.84	1.20	0.003	0.067
Q9BQ52	Zinc phosphodiesterase ELAC protein 2	39.99	1.21	0.009	0.106
Q16881; Q9NNW7	Thioredoxin reductase 1, cytoplasmic	431.42	1.21	0.000	0.022
Q99808	Equilibrative nucleoside transporter 1	92.77	1.21	0.049	0.186
P05556	Integrin beta-1	53.3	1.22	0.046	0.182
P00390	Glutathione reductase, mitochondrial	354.49	1.22	0.001	0.043
Q9NWH9	SAFB-like transcription modulator	83.1	1.22	0.044	0.176
P61086	Ubiquitin-conjugating enzyme E2 K	175.11	1.22	0.004	0.071
P61077	Ubiquitin-conjugating enzyme E2 D3	90.67	1.23	0.019	0.126
P39210	Protein Mpv17	69.15	1.23	0.027	0.144
P08195	4F2 cell-surface antigen heavy chain	643.73	1.23	0.000	0.016
Q9BZZ5	Apoptosis inhibitor 5	185.11	1.24	0.002	0.061
O75995	SAM and SH3 domain-containing protein 3	103.89	1.25	0.000	0.038

Q8TDQ7	Glucosamine-6-phosphate isomerase 2	30.53	1.26	0.007	0.090
P52655	Transcription initiation factor IIA subunit 1	56.2	1.26	0.006	0.088
Q9NYB0	Telomeric repeat-binding factor 2-interacting protein 1	41.98	1.27	0.000	0.029
Q15257	Serine/threonine-protein phosphatase 2A activator	74.73	1.28	0.021	0.133
Q9HB07	UPF0160 protein MYG1, mitochondrial	88.83	1.28	0.049	0.186
Q96F15	GTPase IMAP family member 5	68.51	1.28	0.006	0.088
P15374	Ubiquitin carboxyl-terminal hydrolase isozyme L3	72.94	1.28	0.034	0.159
P28062	Proteasome subunit beta type-8	131.73	1.28	0.002	0.052
P50897	Palmitoyl-protein thioesterase 1	71.64	1.29	0.038	0.167
Q01650	Large neutral amino acids transporter small subunit 1	134.83	1.30	0.002	0.056
Q9HCG8	Pre-mRNA-splicing factor CWC22 homolog	53.8	1.30	0.011	0.111
Q9Y617	Phosphoserine aminotransferase	279.9	1.30	0.000	0.018
Q8IYS1	Peptidase M20 domain-containing protein 2	42.47	1.31	0.001	0.051
Q9NWW4	UPF0587 protein C1orf123	46.85	1.34	0.032	0.153
Q9NTZ6	RNA-binding protein 12	113.39	1.42	0.026	0.144
Q5BKY9	Protein FAM133B	37.97	1.46	0.018	0.125
Q9H0R4	Haloacid dehalogenase-like hydrolase domain-containing protein 2	32.38	1.48	0.004	0.071
P82650	28S ribosomal protein S22, mitochondrial	108.96	1.56	0.010	0.110
P08243	Asparagine synthetase [glutamine-hydrolyzing]	31.56	1.60	0.013	0.118
Q9H1E3	Nuclear ubiquitous casein and cyclin-dependent kinase substrate 1	121.62	1.78	0.000	0.001

^a Accession number according to UniProt database. ^b Protein description with relative symbol. ^c Confidence score generated by Progenesis. * Proteins shared between both treatments (resveratrol and curcumin). Green reduction, red induction.

1.0 – 1.49		
1.5 – 1.99		
2 – 2.49		
2.5 – 2.99		
3 – 3.49		
3.5 +		
* Protein common between resveratrol and curcumin treatment.		

8.5 Appendix 5

Functional classification of induced vs repressed proteins observed with polyphenol treatments,

As the dose of the polyphenols increased the number of proteins modified also increased. There seemed to be a difference in the number of repressed and induced proteins with dose. The greatest number of dose dependent protein modulations was observed with the isorhamnetin treatment, with 35 proteins in common between the 1 and 30 μ M. Isorhamnetin was used to investigate the differences in repressed and induced proteins with the different doses. Fig 8.17, shows all data from 1 and 30 μ M treatments split into functional categories. These functional categories were identified using Reactome. There was an approx. 9 fold increase from the 1 μ M treatment to the 30 μ M treatment.

When examining these functional classes, to see whether induced and repressed patterns were maintained when the dose increased, at least 4 of the categories had notable differences between 1 and 30 μ M (fig. 8.18), in particular with protein classified under 'metabolism' and 'metabolism of proteins'. It was noted that the number of repressed proteins increased with the 30 μ M dose. Other changes were observed with the proteins classified under 'cell cycle' & 'DNA repair', 'cellular stress response' and 'gene expression'. Isorhamnetin had no significant effect on the

viability of the Jurkat cells, showing that the changes to cell cycle and repair proteins are not affecting the ability of the cells to replicate. This is contrary to previous research investigating isorhamnetin and cell proliferation, where 50 μ M significantly decreased cell viability in gastric cancer cells after 48h and 72h treatment²⁸⁶. Concentrations as low as 2.5 μ M significantly lowered cell proliferation in a human lung cancer cell line, following 24h treatment²⁸⁷. Since the Jurkat cell line is also a cancer cell line, it is unusual that the same effect on cell viability and apoptosis was not seen in these cells.

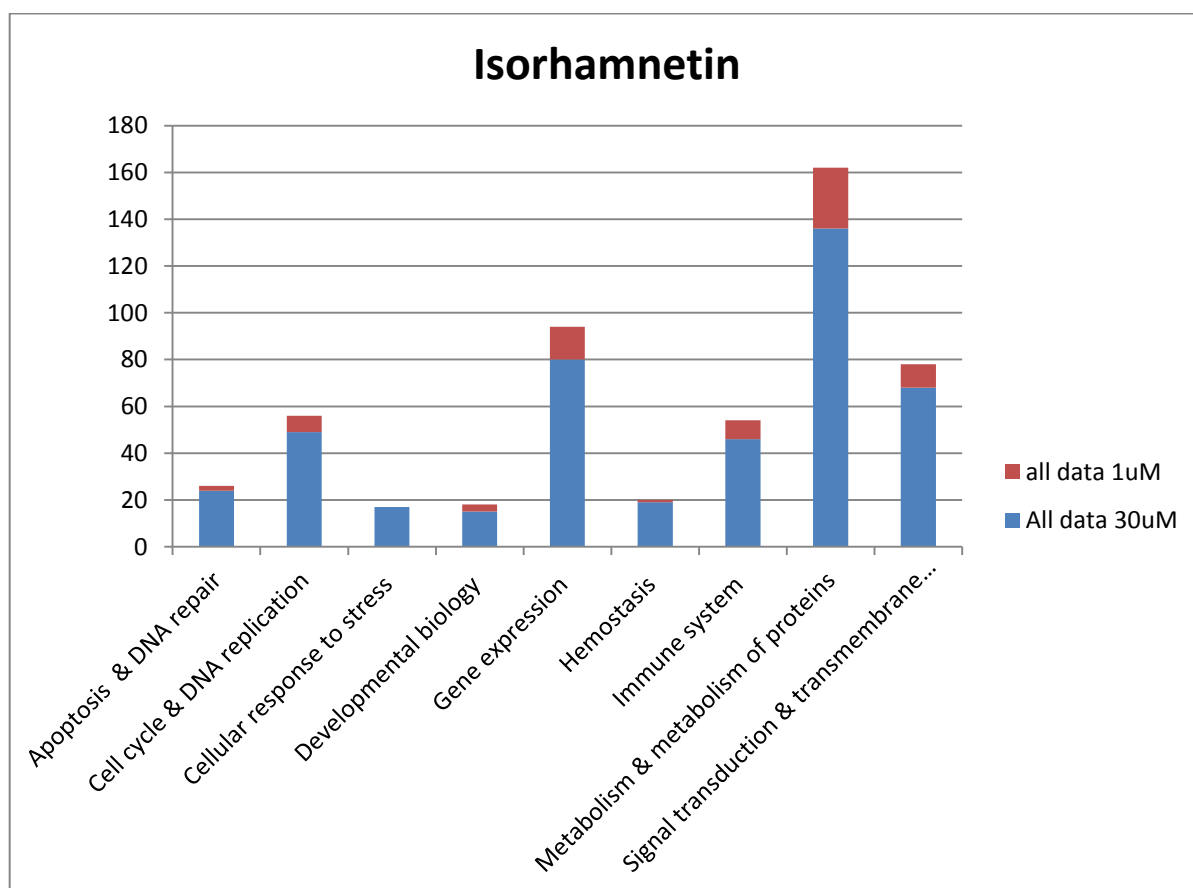


Figure 8.17 – Proteomics data from Isorhamnetin both doses (1 and 30 μ M) split into function categories. Reactome was used to categorise protein functions (<http://www.reactome.org/>) accessed 15/12/14)

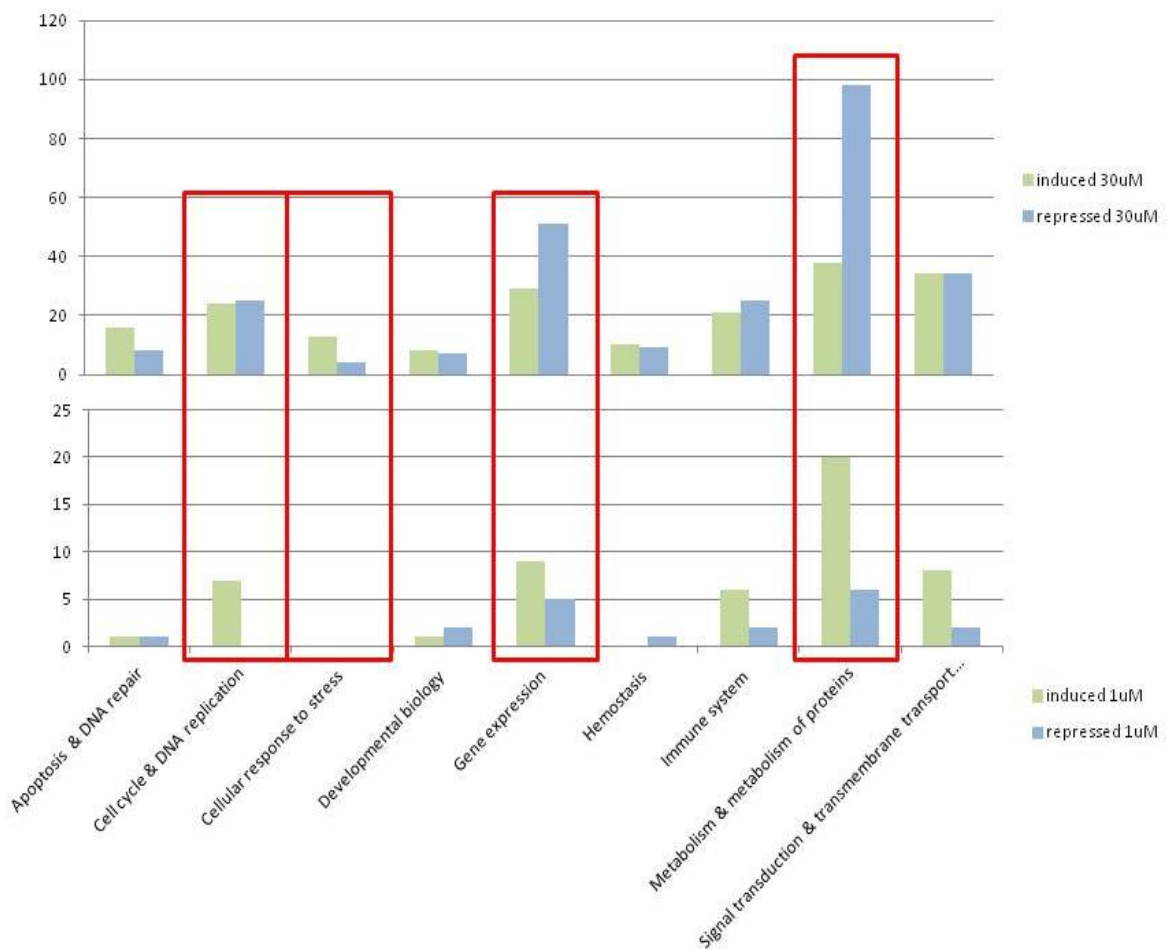
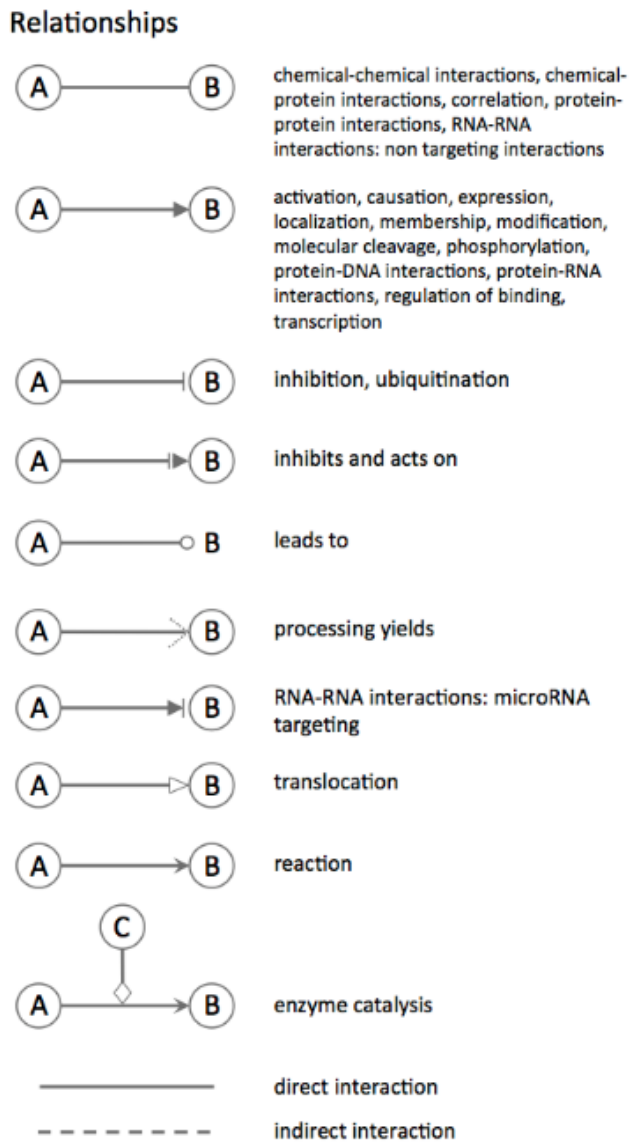


Figure 8.5 – Proteomics data characterised into function categories, Isorhamnetin 1 μM (bottom) and 30μM (top), each category is split into induced (green) and repressed (blue) proteins . Those highlighted in red are those where the induced/repressed trend is altered by dose. Reactome was used to categorise proteins functions (accessed 15/12/14)

Proteins classified under ‘Metabolism and metabolism of proteins’ were of particular interest showing the biggest difference in the number of repressed proteins. This category included translation, protein folding, post-translational

protein modifications and unfolded protein response and correlated with the decrease in the number of ribosomal proteins observed with all the treatments.

Figure 8.19 - Key for Ingenuity network analysis pathways.



A relationship with an X over it indicates that the interaction does not occur. These relationships are only in Disease pathways to indicate an interaction that would

normally happen in the absence of the disease, but does not happen in the disease context.

An arrow pointing from A to B signifies different actions for different circumstances, as described below:

For signalling pathways:

An arrow pointing from A to B signifies that A causes B to be activated (includes any direct interaction: eg binding, phosphorylation, dephosphorylation, etc).

For metabolic pathways:

An arrow pointing from A to B signifies that B is produced from A.

For ligand/receptors:

An arrow pointing from a ligand to a receptor signifies that the ligand binds the receptor and subsequently leads to activation of the receptor. The binding event does not necessarily directly activate the receptor; activation of the receptor could be caused by events secondary to the ligand/receptor binding event.

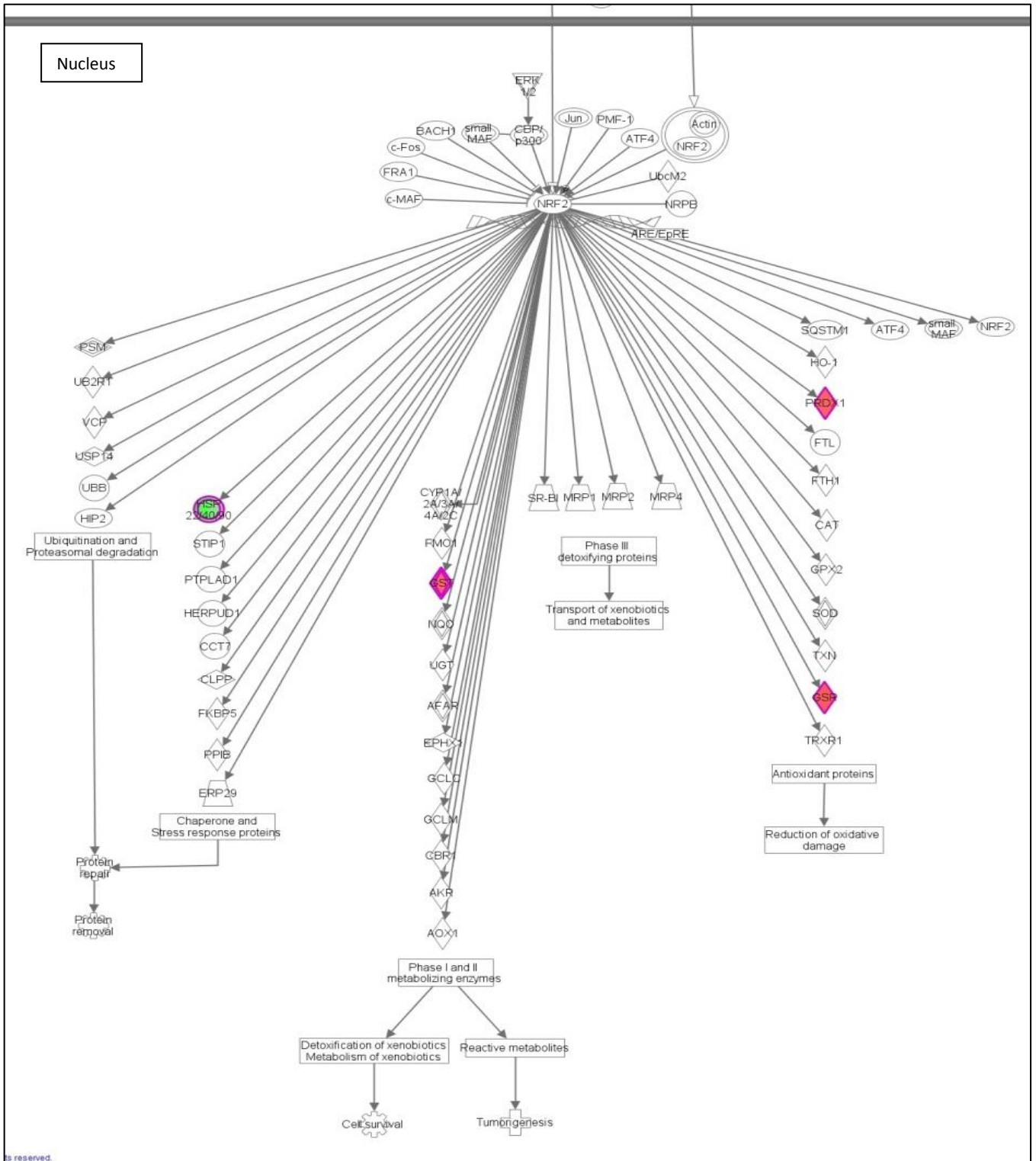
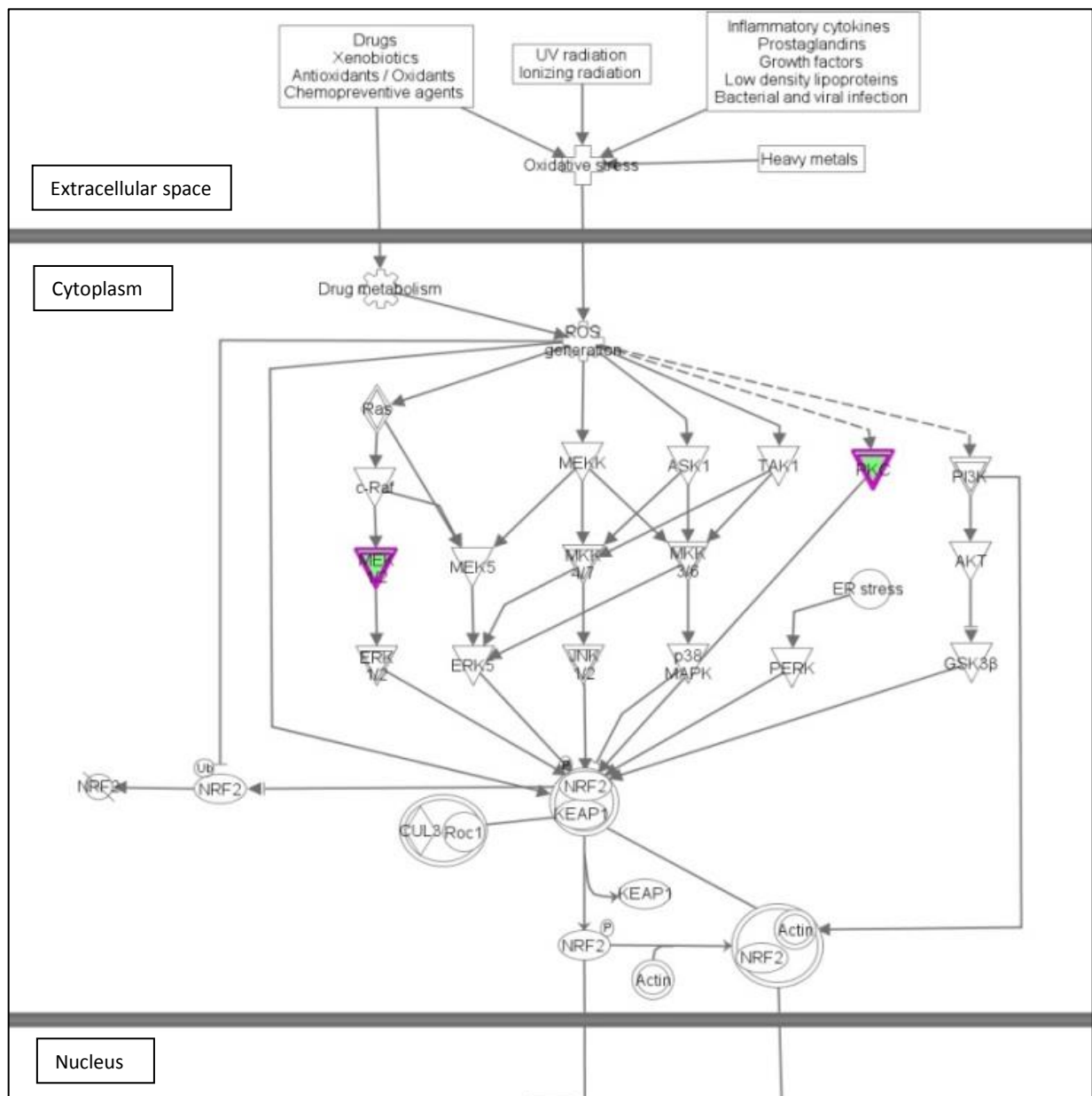
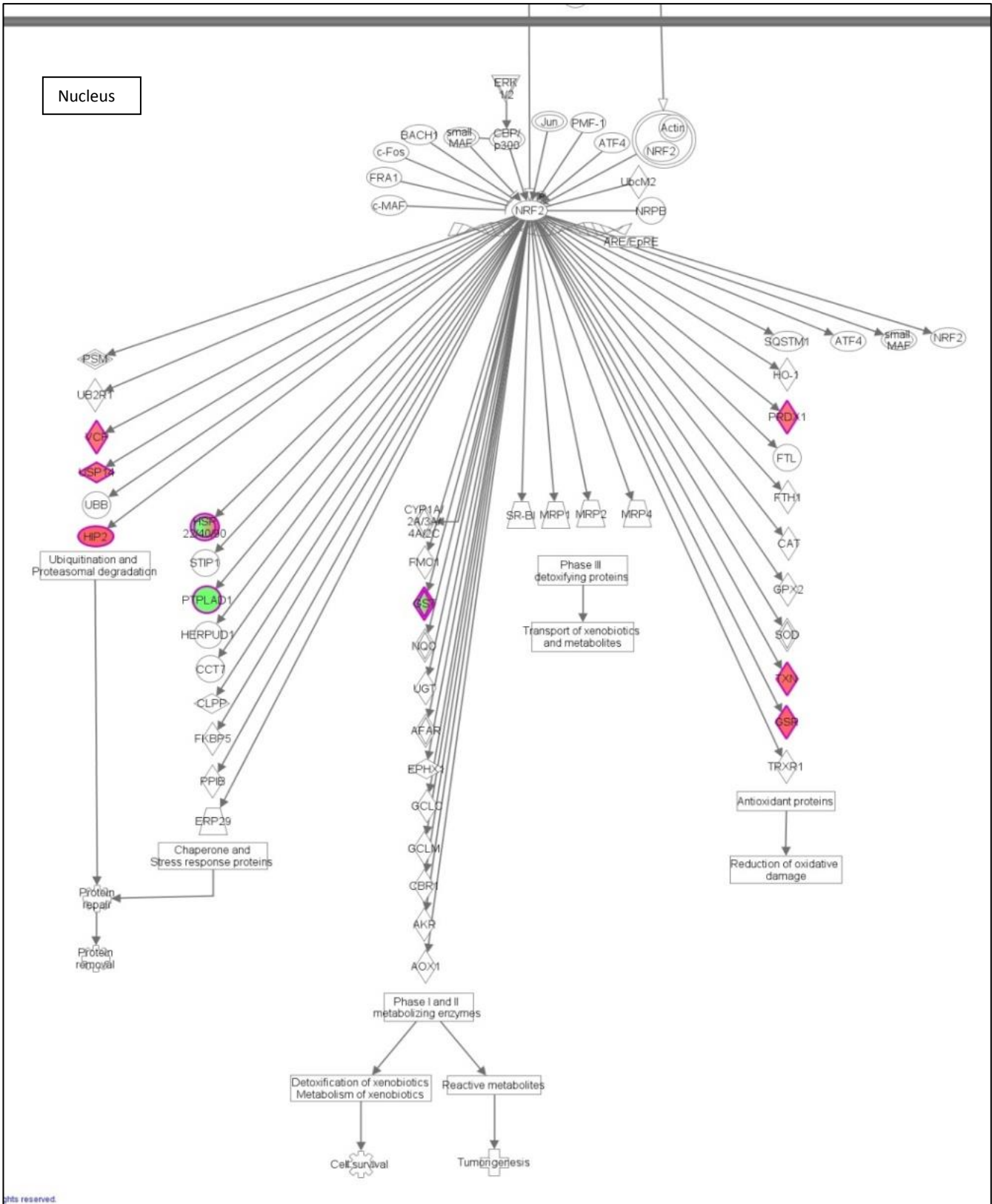


Figure 8.21 – Enlarged version of Ingenuity network analysis for 30 μ M isorhamnetin data set identified Nrf2 signalling as a modified pathway, (original figure 4.6, page 171).





8.6 Appendix 6

Outcomes

Conference attendance:

- **2015 – Healthy Ageing: From Molecules to Organisms (Wellcome Trust, Cambridge).** Poster presentation.
- **2014 – Proteomics bioinformatics workshop** held by the Wellcome trust, EBI in Cambridge. Poster presentation.
- **2014 – Experimental Biology (San Diego).** Oral and poster presentation.
- **2013 – 10th International Medical Postgraduate Conference (Czech Republic).** Oral presentations.
- **2013/14 - BBSRC PhD Studentship day at Unilever.** Poster presentation.
- **2012/13/14/15 – BBSRC DRINC (Diet and health research industry club) conference.** Bristol (2012), Nottingham (2013), Chester (2014), and Oxford (2015). Poster presentation

Publications:

- May 2016 - Identification of (poly)phenol treatments that modulate the release of pro-inflammatory cytokines by human lymphocytes. *British Journal of Nutrition*.
- Draft paper - Effects of polyphenols of glutathione metabolism in Jurkat T lymphocytes.
- Abstracts - Cytokine release by Jurkat T-lymphocytes is modulated following treatment with polyphenols or *Lactobacillus rhamnosus* probiotic extracts (1044.10) *The FASEB Journal* (April, 2014) and Dietary phenolic compounds modify glutathione redox homeostasis and cytokine release in human T lymphocytes (134.1) *The FASEB Journal* (April, 2014).

Certificates/awards:

- **2015 – Healthy Ageing: From Molecules to Organisms (Wellcome Trust, Cambridge).** Awarded a bursary to cover 50% of the cost of the conference.
- **2014 – Experimental Biology (San Diego).** Posters accepted into two poster competitions by the American society of nutrition.
- **2014 – University of Liverpool.** Awarded 2nd place at the poster day online event.

Industrial Placement:

This study was part-funded by industry which allowed me a 6 months placement based in the strategic science group at Unilever (Bedford). Whilst on my placement I

continued my work in the lab, using a different cell line and exploring the redox related biology. I also took advantages of some of the software and expertise available on site. This placement gave me a feel for working in industry, to observe areas of process development and pilot plant scale of products. This experience allowed me to become more independent with my research, gaining experience in new techniques and successfully continuing my research in a new and unfamiliar environment, whilst also understanding the rules and regulations associated with industry related work.

9.0 REFERENCES

¹ World Health Agency (WHO). [<http://www.who.int/topics/ageing/en/>] accessed July 2015.

² The King's Fund > Ideas that change health care. [<http://www.kingsfund.org.uk/>] accessed Aug 2015.

³ Institute for Fiscal Studies. [<http://www.ifs.org.uk/>] accessed Aug 2015.

⁴ Gordon, M.H. (2012). Significance of dietary antioxidants for health. In *J Mol Sci.* 13(1): 173-179.

⁵ Wilson, M.A., Shukitt-Hale, B., Kalt, W., Ingram, D.K., Joseph, J.A., and Wolkow, C.A. (2006). Blueberry polyphenols increase lifespan and thermotolerance in *Caenorhabditis elegans*. *Aging Cell.* 5(1): 59-68.

⁶ Andújar, I., Recio, M.C., Giner, R.M., and Ríos, J.L. (2012). Cocoa polyphenols and their potential benefits for human health. *Oxi Med Cell Long.* 906252.

⁷ Franceschi, C., Bonafè, M., Valensin, S., Olivieri, F., De Luca, M., Ottaviani, E., and De Benedictis, G. (2000). Inflamm-aging. An evolutionary perspective on immunosenescence. *Ann N Y Acad Sci.* 908:244-54.

⁸ Balaban, R.S., Nemoto, S., and Finkel, T. (2005). Mitochondria, Oxidants, and Ageing. *Cell.* 120 (4), 483-495.

⁹ Bruunsgaard, H., Pedersen, M., and Pedersen, B.K. (2001). Aging and proinflammatory cytokines. *Curr Opin Hematol.* 8(3): 131-136.

¹⁰ Harman, D. (1956). Aging: a theory based on free radical and radiation chemistry. *J Gerontol.* 11(3): 298-300.

¹¹ Harman, D. (1972). "A biologic clock: the mitochondria?". *J. Am Geriatrics. Soc.* 20(4): 145-147.

¹² Pawelec, G., Goldeck, D., and Derhovanessian, E. (2014). Inflammation, ageing and chronic disease. *Curr. Opin. Immuno.* 29: 23-28.

¹³ Larbi, A., Dupuis, G., Douziech, N., Khalil, A., and Fülöp Jr, T. (2006). Low-grade inflammation with aging has consequences for T-lymphocyte signalling. *Annals of the New York Academy of Sciences.* 1030(1).

-
- ¹⁴ Schindowski, K., Fröhlich, L., Maurer, K., Müller, W.E., and Eckert, A. (2002). Age-related impairment of human T lymphocytes' activation: specific differences between CD4(+) and CD8(+) subsets. *Mech. Ageing. Dev.* 123(4): 375-90.
- ¹⁵ ATCC – American type culture collection. [<http://www.lgcstandards-atcc.org/en.aspx>] assessed Aug 2015.
- ¹⁶ Khalaf, H., Jass, J., and Olsson, P. (2010). Differential cytokine regulation by NF- κ B and AP-1 in Jurkat T-cells. *BMC Immunol.* 11:26.
- ¹⁷ Boulay, J.L., O'Shea, J.J., and Paul, W.E. (2003). Molecular phylogeny within type cytokines and their cognate receptors. *Immunity.* 19: 159-163.
- ¹⁸ Tedgui, A., and Mallat, Z. (2006). Cytokines in atherosclerosis: Pathogenic and regulatory pathways. *Physiological reviews.* 86(2): 515-581.
- ¹⁹ Gereda, J.E., Leung, D.Y.M., Thatayatikom, A., Streib, J.E., Price, M.R., Klinnert, M.D., and Liu, A.H. (2000). Relation between house-dust endotoxin exposure, type 1 T cell development, and allergen sensitisation in infants at high risk of asthma. *Web Sci.* 355(9216):1680-1683.
- ²⁰ Smeets, R.L., Fleuren, W.W., He, X., Vink, P.M., Wijnands, F., Gorecka, M., Klop, H., Bauerschmidt, S., Garritsen, A., Koenen, H.J., Joosten, I., Boots, A.M. and Alkema, W. (2012). Molecular pathway profiling of T lymphocyte signal transduction pathways; Th1 and Th2 genomic fingerprints are defined by TCR and CD28-mediated signalling. *BMC Immunol.* 13:12.
- ²¹ Dobbs, R.J., Charlett, A., Purkiss, A.G., Dobbs, S.M., Weller, C., and Peterson, D.W. (1999). Association of circulating TNF-alpha and IL-6 with ageing and parkinsonism. *Acta Neurol Scand.* 100(1): 34-41.
- ²² Singh, T., and Newman, A. B. (2011). Inflammatory markers in population studies of aging. *Ageing Research Reviews.* 10 (3): 319-329.
- ²³ Álvarez-Rodríguez, L., López-Hoyos, M., Muñoz-Cacho, P., and Martínez-Taboada, M. (2012). Aging is associated with circulating cytokine dysregulation. *Cellular Immunology.* 273(2): 124-132.
- ²⁴ Marik, P.E., and Zaloga, G.P. (2001). The effect of aging on circulating levels of proinflammatory cytokines during septic shock. *J. Amer. Geriatrics Society.* 49: 5-9.

-
- ²⁵ RCSB Protein Data Bank: An information portal to 110790 biological macromolecular structures. [<http://www.rcsb.org/pdb/home/home.do>] assessed Aug 2015.
- ²⁶ Beverley, P.C.L. (2007). Primer: making sense of T cell memory. *Nature Clin. Prac. Rheum.* 4: 43-49.
- ²⁷ Gillis, S., and Watson, J. (1980). Biochemical and biological characterization of lymphocyte regulatory molecules. V. Identification of an interleukin 2-producing human leukaemia T cell line. *J. Exp. Med.* 152: 1709-1719.
- ²⁸ Manger, B., Hardy, K.J., Weiss, A., and Stobo, J.D. (1986). Differential effect of cyclosporin A on activation signaling in human T cell lines. *J Clin Invest.* 77(5): 1501-6.
- ²⁹ Roose, J.P., Diehn, M., Tominson, M.G., Lin, J., Alizadeh, A.A., Botstein, D., Brown, P.O., and Weiss, A. (2003). T cell receptor-independent basal signalling via Erk and Abl kinases suppresses RAG gene expression. *PLoS Biology.* 1(2): 271-287.
- ³⁰ Sakata-Kaneko, S., Wakatsuki, Y., Matsunaga, Y., Usui, T., and Kita, T. (2000). Altered Th1/Th2 commitment in human CD4⁺ T cells with ageing. *Clin Exp Immunol.* 120(2): 267-73.
- ³¹ Hoffmann, F., Albert, M.H., Arenz, S., Bidlingmaier, C., Berowicz, N., Sedlaczek, S., Till, H., Pawlita, I., Renner, E.D., Weiss, M., and Belohradsky, B.H. (2005). Intracellular T-cell cytokine levels are age-dependent in healthy children and adults.
- ³² Forsey, R.J., Thompson, M., Ernerudh, J., Hurst, T.L., Strindhall, J., Johansson, B., Nilsson, B.O., and Wikby, A. (2003). Plasma cytokine profiles in elderly humans. *Mech. Ageing. Devel.* 124(4): 487-493.
- ³³ Schmidt, A., Oberle, N., and Krammer, P.H. (2012). Molecular mechanisms of Treg-mediated T cells suppression. *Fron. Immuno.* 00051.
- ³⁴ Khalaf, H., Jass, J., and Olsson, P. (2010). Differential cytokine regulation by NF- κ B and AP-1 in Jurkat T cells. *BMC Immuno.* 11:26.
- ³⁵ Tedgui, A., and Mallat, Z. (2006). Cytokine in atherosclerosis: Pathogenic and regulatory pathways. *Physio. Rev.* 86(2): 515-581.
- ³⁶ Feldmann, M., and Maini, R.N. (2003). TNF defined as a therapeutic target for rheumatoid arthritis and other autoimmune diseases. *Nature medicine.* 9: 1245-1250.

-
- ³⁷ Hanauer, S., Feagan, B., Lichenstein, G., Mayer, L., Schreiber, S., Colombel, J., Rachmilewitz, D., Wolf, D., Olson, A., Bao, W., and Rutgeerts, P. (2002). Maintenance infliximab for Crohn's disease: the ACCENT I randomised trial. *Lancet*. 359(9317): 1541-9.
- ³⁸ Rutgeerts, P., Sandborn, W., Feagan, B., Reinisch, W., Olson, A., Johanns, J., Travers, S., Rachmilewitz, D., Hanauer, S., Lichtenstein, G., de Villiers, W., Present, D., Sands, B., and Colombel, J. (2005). Infliximab for induction and maintenance therapy for ulcerative colitis. *N. Engl. J. Med.* 353(23): 2462-76.
- ³⁹ Taillé, C., Poulet, C., Marchand-Adam, S., Borie, R., Dombret, M., Crestani, B., and Aubier, M. (2013). Monoclonal anti-TNF α antibodies for severe steroid-dependent asthma: a case series. *Open Resp. Med. J.* 7: 21-25.
- ⁴⁰ Nichols, B.A., Bainton, D.F., and Farquhar, M.G. (1971). Differentiation of Monocytes. Origin, Nature, and Fate of Their Azurophil Granules. *J. Cell Biol.* 50: 498-515.
- ⁴¹ Schwende, H., Fitzke, E., Ambs, P., and Dieter, P. (1996). Differences in the state of differentiation of THP-1 cells induced by phorbol ester and 1,25-dihydroxyvitamin D3. *J. Leukocyte Biol.* 59:555.
- ⁴² ATCC: The Global Bioresource center. THP-1 (ATCC[®] TIB-202[™]), Characteristics. LGC Standards, Middlesex, UK [http://www.lgcstandards-atcc.org/products/all/TIB-202.aspx?geo_country=gb#characteristics] (assessed 17.12.15).
- ⁴³ Danis, V.A., Millington, M., Hyland, V.J., and Grennan, D. (1995). Cytokine production by normal human monocytes: inter-subject variation and relationship to an IL-1 receptor antagonist (IL-1Ra) gene polymorphism. *Clin. Exp. Immunol.* 99(2):303-10.
- ⁴⁴ Rossol, M., Heine, H., Meusch, U., Quandt, D., Klein, C., Sweet, M.J., and Hauschildt, S. (2011). LPS-induced cytokine production in human monocytes and macrophages. *Crit. Rev. Immunol.* 31(5):379-446.
- ⁴⁵ Seider, S., Zimmermann, H.W., Bartneck, M., Trautwein, C., Tacke, F. (2010). Age-dependent alterations of monocyte subset and monocyte-related chemokine pathways in healthy adults. *BMC Immunol.* 11:30.
- ⁴⁶ Ashok, B.T., and Ali, R. (1999). The aging paradox: free radical theory of aging. *Exper. Gerontol.* 34(3): 293-303.
- ⁴⁷ Cadenas, E., and Davies, K.J. (2000). Mitochondrial free radical generation, oxidative stress, and aging. *Free Radic. Biol. Med.* 29(3-4):222-30.

-
- ⁴⁸ Conner, E.M., and Grisham, M.B. (1996). Inflammation, free radicals, and antioxidants. *Nutrition*. 12(4): 274-7.
- ⁴⁹ Vallyathan, V., Mega, J.F., Shi, X., and Dalal, N.S. (1992). Enhanced generation of free radicals from phagocytes induced by mineral dust. *Am. J. Respir. Cell. Mol. Biol.* 6(4): 404-13.
- ⁵⁰ Davies, K.J.A., Quintanilha, A.J., Brooks, G.A. and Packer, L. (1982). Free radicals and tissue damage produced by exercise. *Biochem. Biophys. Res. Commun.* 107: 1198-1205.
- ⁵¹ Ignarro, L.J. (2000). *Nitric Oxide: Biology and pathobiology*. Academic Press, NY.
- ⁵² Cross, C.E., Halliwell, B., Borisch, H.T., Pryor, W.A., Ames, B.N., Saul, R.L., McCord, J.M., and Harman, D. (1987). Oxygen radicals and human disease. *Ann. Intern. Med.* 107: 526-545.
- ⁵³ Boveris, A., and Cadenas, E. (1975). Mitochondria production of superoxide anions and its relationship to the antimycin-insensitive respiration. *FEBS Lett.* 54: 311-314.
- ⁵⁴ Antunes, F., and Cadenas, E. (20001). Cellular titration of apoptosis with steady state concentrations of H₂O₂ : submicromolar levels of H₂O₂ induce apoptosis through Fenton chemistry independent of cellular thiol state. *Free Radical Biol. Med.* 30: 1008-1018.
- ⁵⁵ Murphy, M.P. (2009). How mitochondria produce reactive oxygen species. *Biochem journal.* 417 (Pt 1): 1-13.
- ⁵⁶ Roberts, B.R., Tainer, J.A., Getzoff, E.D., Malencik, D.A., Anderson, S.R., Bomben, V.C., Meyers, K.R., Karplus, P.A., and Beckman, J.S. (2007). Structural characterization of zinc-deficient human superoxide dismutase and implication for ALS. *J Mol Biol.* 373(4): 877-90.4
- ⁵⁷ MacMillan-Crow, L.A., and Thompson, J.A. (1999). Tyrosine modification and inactivation of the active site manganese superoxide dismutase mutant (Y34F) by peroxynitrite. *Arch Biochem Biophys.* 366(1): 82-8.
- ⁵⁸ Lee, J.W., Roe, J.H., and Kang, S.O. (2002). Nickel-containing superoxide dismutase. *Methods Enzymol.* 349: 90-101.
- ⁵⁹ Roberts, M.B.V (1986). *Biology: A functional approach* 4th ed. Thomas Nelson and Sons Ltd. Pg 88.

-
- ⁶⁰ Takeuchi, A., Miyamoto, T., Yamaji, K., Masuho, Y., Hayashi, M., Hayashi, H., and Onozaki, K. (1995). A human erythrocyte-derived growth-promoting factor with a wide target cell spectrum: identified as catalase. *Cancer Research*. 55: 1586-1589.
- ⁶¹ Kesarwani, P., Murali, A.K., Al-Khami, A.A., and Mehrototra, S. (2013). Redox regulation of T-cell function: From molecular mechanisms to significance in human health and disease. *Antioxid Redox Signal*. 18(12): 1497-1534.
- ⁶² Kim, H.R., Lee, A., Choi, E.J., Hong, M.P., Kie, J.H., Lim, W., Lee, H.K., Moon, B.I., and Seoh, J.Y. (2014). Reactive oxygen species prevent imiquimod-induced psoriatic dermatitis through enhancing regulatory T cell function. *PLoS One*. 9(3):e91146.
- ⁶³ Yasui, K., and Baba, A. (2006). Therapeutic potential of superoxide dismutase (SOD) for resolution of inflammation. *Inflamm, Res*. 55: 359-363.
- ⁶⁴ Chen, Z., Oberley, T.D., Ho, Y., Chua, C.C., Siu, B., Hamdy, R.C., Epstein, C.J., and Chua, B.H. (2000). Overexpression of CuZnSOD in coronary vascular cells attenuates myocardial ischemia/reperfusion injury. *Free Radic. Biol. Med*. 29: 589-96.
- ⁶⁵ Papp, L.V., Lu, J., Holmgren, A., and Khana, K.K. (2007). From selenium to selenoproteins: synthesis, identity, and their role in human health. *Antioxid. Redox Signal*. 9: 775-806.
- ⁶⁶ Rotruck, J.T., Pope, A.L., Ganther, H.E., Swanson, A.B., Hafeman, D.G., and Hoekstra, W.G. (1973). Selenium: biochemical role as a component of glutathione peroxidase. *Science*. 179(73): 588-90.
- ⁶⁷ Sastre J, Pellardo FV, Vina J. Glutathione, oxidative stress and aging. *Age*. 1996;19:129–39.
- ⁶⁸ Stipanuk, M.H., Coloso, R.M., Garcia, R.A., and Banks, M.F. (1992). Cysteine concentration regulates cysteine metabolism to glutathione, sulfate and taurine in rats. *J. Nutr*. 122: 420-7.
- ⁶⁹ Lyons, J., Rah-Pfeiffer, A., Yu, Y.M., Lu, X.M., Zurakowski, D., Tompkins, R.G., Ajamin, A.M., Young, V.R., and Castillo, L. (2000). Bood glutathione synthesis rates in healthy adults receiving a sulphur amino acid-free diet. *Proc. Nat. Acad. Sci. USA*. 97: 5071-6.
- ⁷⁰ Samiec, P.S., Drews-Botsch, C., Flagg, E.W., Kurtz, J.C., Sternberg, P.Jr., Reed, R.L., and Jones, D.P. (1998). Glutathione in human plasma: decline in association with aging, age-related macular degeneration, and diabetes. *Free Radic. Bio. Med*. 24(5):699-704.

-
- ⁷¹ Sekhar, R. V., Patel, S.G., Guthikonda, A.P., Reid, M., Balasubramanyam, A., Taffet, G.E., and Jahoor, F. (2011). Deficient synthesis of glutathione underlies oxidative stress in aging and can be corrected by dietary cysteine and glycine supplementation. *American Journal of clinical nutrition*. 94(3): 847-853.
- ⁷² Beckman, K.B., and Ames, B.M. (1998). The free radical theory of ageing matures. *Physiological Reviews*. 78 (2): 547-581.
- ⁷³ Espinoza, S.E., Guo, H., Fedarko, N., DeZern, A., Fried, L.P., Xue, Q, Leng, S., Beamer, B., and Walston, J.D. (2010). Glutathione peroxidase enzyme activity in aging. *J. Gerontol. A Biol. Sci. Med. Sci*. 63(5): 505-509.
- ⁷⁴ Hayes, J.D., Flanagan, J.U., and Jowsey, I.R. (2005). Glutathione transferases. *Annu. Rev. Pharmacol. Toxicol*. 45: 51-88.
- ⁷⁵ Fisher, A.B. (2011). Peroxiredoxin 6: a biofunctional enzyme with glutathione peroxidase and phospholipase A₂ activities. *Antioxid. Redox Signal*. 15(3): 831-44.
- ⁷⁶ Tomizawa, H.H., and Varandani, P.T. (1965). Glutathione-insulin transhydrogenase of human liver. *J. Biol. Chem*. 240(7): 3191-3194.
- ⁷⁷ Lu, J., and Holmgren, A. (2014). The thioredoxin antioxidant system. *Free Radical Biol. Med*. 66(8): 75-87.
- ⁷⁸ Holmgren, A. (1985). Thioredoxin. *Annu. Rev. Biochem*. 54: 237-271.
- ⁷⁹ Haenderler, J. (2006). Thioredoxin-1 and posttranslational modifications. *Antioxid Redox Signal*. 8(9-10): 1723-8.
- ⁸⁰ Luo, S., and Levine, R. (2009). Methionine in protein defends against oxidative stress. *FASEB J*. 23(2): 464-72.
- ⁸¹ Nonn, L., Berggren, M., and Powis, G. (2003). Increased expression of mitochondrial peroxiredoxins-3 (thioredoxin peroxidase-2) protects cancer cells against hypoxia and drug-induced hydrogen peroxide-dependent apoptosis. *Mol. Cancer Res*. 1(9): 682-9.
- ⁸² Fourquet, S., Guerois, R., Biard, D, and Toledano, M.B. (2010). Activation of NRF2 by nitrosative agents and H₂O₂ involves KEAP1 disulfide formation. *J Biol. Chem*. 285: 8463-8471.

-
- ⁸³ Lee, S.R., Kwon, K.S., Kim, S.R., and Rhee, S.G. (1998). Reversible inactivation of protein-tyrosine phosphatase 1B in A431 cells stimulated with epidermal growth factor. *J. Biol. Chem.* 273: 15366-15372.
- ⁸⁴ Yoshida, T, Nakamura, H., Masutani, H., and Yodoi, J. (2005). The involvement of thioredoxin and thioredoxin binding protein-2 on cellular proliferation and aging process. *Annals of the NY Academy of Sciences.* 1055: 1-12.
- ⁸⁵ Woo, H.A., Chae, H.Z., Hwang, S.C., Yang, K.S., Kang, S.W., Kim, K., and Rhee, S.G. (2003). Reversing the inactivation of peroxiredoxins caused by cysteine sulfinic acid formation. *Science.* 200(5619): 653-6.
- ⁸⁶ Manevich, Y., Feinstein, S.I., and Fisher, A.B. (2004). Activation of the antioxidant enzyme 1-CYS peroxiredoxins requires glutathionylation mediated by heterodimerization with π GST. *Pro. Natl. Acad. Sci. USA.* 101(11): 3780-3785.
- ⁸⁷ Fisher, A.B., Dodia, C., Feinstein, S.I., and Ho, Y.S. (2005). Altered lung phospholipid metabolism in mice with targeted deletion of lysosomal-type phospholipase A2. *J Lipid Res.* 46: 1248-1256.
- ⁸⁸ Claiborne, A., Yeh, J.I., Mallett, T.C., Luba, J., Crane, E.J, 3rd., Charrier, V., and Parsonae, D. (1999). Protein-sulfenic acids: diverse roles for an unlikely player I enzyme catalysis and redox regulation. *Biochem.* 38(47): 15407-16.
- ⁸⁹ Neumann, C.A., Krause, D.S., Carman, C.V., Das, S., Dubey, D.P., Abraham, J.L., Bronson, R.T., Fujiwara, Y., Orkin, S.H., and Van Etten, R.A. (2003). Essential role for the peroxiredoxins Prdx1 in erythrocyte antioxidant defence and tumour suppression. *Nature.* 424(6948): 561-5.
- ⁹⁰ Dong, C., Li, B., Yang, D., Wang, G., Wang, X., and Bai, C. (2011). Overexpression of peroxiredoxin 6 protect mice from ovalbumin-induced airway inflammation and hypersecretion of MUC5AC by reducing ROS levels. *Euro. Res. J.* 38(55):970.
- ⁹¹ Mullen, L., Hanschmann, E.M., Lillig, C.H., Herzenberg, L.A., and Ghezzi, P. (2015). Cysteine oxidation targets peroxiredoxins 1 and 2 for exosomal release through a novel mechanism of redox-dependent secretion. *Mol. Med.* 21(1): 98-108.
- ⁹² Sohal, R.S., and Sohal, B.H. (1991). Hydrogen peroxide release by mitochondria increase during aging. *Mech. Ageing and Dev.* 57(2):187-202.
- ⁹³ Sohal, R.S. and Dubey, A. (1994). Mitochondrial oxidative damage, hydrogen peroxide release, and aging. *Free Rad. Biol. Med.* 16(5):621-626.

-
- ⁹⁴ Lim, J., and Luderer, U. (2011). Oxidative damage increases and antioxidant gene expression decreases with aging in the mouse ovary. *Biol. Reprod.* 84(4):775-82.
- ⁹⁵ Tadros, S.F., D'Souza, M., Zhu, X., and Frisina, R.D. (2014). Gene expression changes for antioxidants pathways in the mouse cochlea: relations to age-related hearing deficits. *PLOS One.* 10.1371/journal.pone.0090279.
- ⁹⁶ Baraibar, M.A., Liu, L., Ahmed, E.K., and Friguet, B. (2012), Protein oxidative damage at the crossroads of cellular senescence, aging, and age-related diseases. *Oxid. Med. Cellular Longevity.* Article ID 919832.
- ⁹⁷ Lobo, V., Patil, A., Phatak, A., and Chandra, N. (2010). Free radicals, antioxidants and functional foods: Impact on human health. *Pharmacogn Rev.* 4(8): 118-126.
- ⁹⁸ Lattanzio, V., Lattanzio, V.M.T., and Cardinali, A. (2006). Role of phenolics in the resistance mechanisms of plants against fungal pathogens and insects. *Phytochemistry: Advances in Research.* 23-67.
- ⁹⁹ Ruiz-García, Y., and Gómez-Plaza, E. (2013). Elicitors: A tool for improving fruit phenolic content. *Agriculture.* 3, 33-52.
- ¹⁰⁰ Constabel, C.P., Bergey, D.R., and Ryan, C.A. (1995). Systemin activates synthesis of wound-inducible tomato leaf polyphenol oxidase via the octadecanoid defense signalling pathway. *Proc Natl Acad Sci U S A.* 92(2): 407-11.
- ¹⁰¹ Tsao, R. (2010). Chemistry and biochemistry of dietary polyphenols. *Nutrients.* 2:1231-1246.
- ¹⁰² Harbone, J.B. and Williams, C.A. (2000). Advances in flavonoid research since 1992. *Phytochemistry.* 55: 481-504.
- ¹⁰³ Bravo, L. (1998). Polyphenols: Chemistry, dietary sources, metabolism, and nutritional significance. *Nutr. Rev.* 56: 317-333.
- ¹⁰⁴ Cheynier, V. (2005). Polyphenols in food are more complex than often thought. *Am. J. Clin. Nutr.* 81: 223S-229S.
- ¹⁰⁵ Pandey, K.B., and Rizvi, S.I. (2009). Plant polyphenols as dietary antioxidants in human health and disease. *Oxid. Med. Cell. Longev.* 2(5): 270-278.
- ¹⁰⁶ Bors, W., Heller, W, Michel, C., and Saran, M. (1990). Flavonoids as antioxidants: Determination of radical-scavenging efficiencies. *Methods Enzymol.* 186: 343-55.

-
- ¹⁰⁷ Ninfali, P., Mea, G., Giorgini, S., Rocchi, M., and Bacchiocca, M. (2004). Antioxidant capacity of vegetables, spices and dressings relevant to nutrition. *Brit. J. Nutr.* 93(2): 257-266.
- ¹⁰⁸ Pérez-Jiménez, J. Neveu, V., Vos, F., and Scalbert, A. (2010). Identification of the 100 richest dietary sources of polyphenols: an application of the Phenol-Explorer database. *Eur. J. Clin. Nutr.* 64: S112-S120.
- ¹⁰⁹ Scalbert, A., Morand, C., Manach, C., and Rémésy, C. (2002). Absorption and metabolism of polyphenols in the gut and impact on health. *Biomedicine & Pharmacotherapy.* 56(6): 276-282.
- ¹¹⁰ Guinane, C.M., and Cotter, P.D. (2013). Role of the gut microbiota in health and chronic gastrointestinal disease: understanding a hidden metabolic organ. *Therap. Adv. Gastroenterol.* 6(4):295-308.
- ¹¹¹ Marín, L., Miguélez, E.M., Villar, C.J., and Lombó, F. (2015). Bioavailability of dietary polyphenols and gut microbiota metabolism: antimicrobial properties. *BioMed Research International.* Article ID 905215.
- ¹¹² Arnott, J.A. and Planey, S.L. (2012). The influence of lipophilicity in drug discovery and design. *Expert Opin. Drug Disc.* 7(10): 863-875.
- ¹¹³ Bhawana, S., Basniwak, R.K.B., Butter, H.S., Jain, V.K., and Jain, N. (2014). Curcumin nanoparticles: Preparation, characterization, and antimicrobial study. *J. Agric. Food Chem.* 59(5): 2056-61.
- ¹¹⁴ Lim, K.J., Bisht, S., Bar, E.E., Maitra, A., and Ebergart, C.G. (2011). A polymeric nanoparticle formulation of curcumin inhibits growth, clonogenicity and stem-like fraction in malignant brain tumours. *Cancer Biol. Therap.* 11(5): 1-10.
- ¹¹⁵ Scalbert A, Morand C, Manach C *et al.* (2002) Absorption and metabolism of polyphenols in the gut and impact on health. *Biomedicine & Pharmacotherapy.* 56(6): 276-282.
- ¹¹⁶ Miene C, Weise A, & Gleit M (2011) Impact of polyphenol metabolites produced by colonic microbiota on expression of COX-2 and GSTT2 in human colon cells (LT97). *Nutrition and cancer.* 63(4): 653-622.
- ¹¹⁷ Queen BL & Tollefsbol TO (2010) Polyphenols and Aging. *Curr Aging Sci.* 3(1): 34-42.
- ¹¹⁸ Crozier A, Del Rio D, & Clifford MN (2010) Bioavailability of dietary flavonoids and phenolic compounds. *Molecular Aspects of Medicine.* 31: 446-467.

-
- ¹¹⁹ Del Rio, D., Stalmach, A., Calani, L., and Crozier, A. (2010). Bioavailability of coffee chlorogenic acids and green tea flavan-3-ols. *Nutrients*. 2: 820-833.
- ¹²⁰ Tzonis, X., Vulevic, J., Kuhnle, C.G., George, T., Leonczak, J., and Gibson, G.R. (2008). Flavanol monomer-induced changes to the human faecal microflora. *Br J Nutr*. 99: 782-92.
- ¹²¹ Teng, Z., Yuan, C., Zhang, F., Huan, M., Cao, W., Li, K., Yang, J., Cao, D., Zhou, S., and Mei, Q. (2012). Intestinal absorption and first-pass metabolism of polyphenol compounds in Rat and their transport dynamics in Caco-2 cells. *PLOS One*.
- ¹²² Notes, G., Nifli, A.P., Kampa, M., Pelekanou, V., Alexaki, V.I., Theodoropoulos, P., Vercauteren, J., and Castanas, E. (2012). Quercetin accumulates in nuclear structures and triggers specific gene expression in epithelial cells. *J Nutr Biochem*. 23: 656-66.
- ¹²³ Accomando, S., Pellitteri, V., and Corsello, G. (2010). Natural polyphenols as anti-inflammatory agents. *Front. Biosci*. 2: 318-31.
- ¹²⁴ Han, X., Shen, T., and Lou, H. (2007). Dietary polyphenols and their biological significance. *Int. J. Mol, Sci*. 8(9): 950-988.
- ¹²⁵ Chandran, B., and Goel, A. (2012). A randomized, pilot study to assess the efficacy and safety of curcumin in patients with active rheumatoid arthritis. *Phytother Res*. 26(11): 1719-25.
- ¹²⁶ Moon, D.O., Kim, M.O., Choi, Y.H., Park, Y.M., and Kim, G.Y. (2010). Curcumin attenuates inflammatory response in IL-1 β -induced human synovial fibroblast and collagen –induced arthritis in mouse model. 10(5): 605-610.
- ¹²⁷ Thomas, R., Williams, M., Sharma, H., Chaudry, A., and Bellamy, P. (2014). A double –blind, placebo-controlled randomised trial evaluating the effect of a polyphenols-rich whole food supplement on PSA progression in men with prostate cancer- the UK NCRN Pomi-T study. *Prostate Cancer and Prostatic Disease*. 17: 180-186.
- ¹²⁸ ATCC: The Global Bioresource center. Jurkat, Clone E6-1 (ATCC® TIB-152™), Culture method. LGC Standards, Middlesex, UK. [http://www.lgcstandards-atcc.org/products/all/TIB-152.aspx?geo_country=gb#culturemethod] (assessed 15.12.15).

¹²⁹ ATCC: The Global Bioresource center. THP-1 (ATCC® TIB-202™), Culture method. LGC Standards, Middlesex, UK [<http://www.lgcstandards-atcc.org/Products/All/TIB-202.aspx#culturemethod>] (assessed 15.12.15).

¹³⁰ Moeller, R., and Mason, A.Z. Quantification of reduced glutathione and glutathione disulphide using glutathione reductase and 2-vinylpyridine. NSF student research.
http://www.csulb.edu/~zedmason/students/current/research/rhondamoeller/moeller_introduction.html (assessed 15.01.15).

¹³¹ Zhonghua, Y., and Banerjee, R. (2011). Redox remodeling as an immunoregulatory strategy. *Biochem.* 49(6):1059.

¹³² Dimauro, I., Pearson, T., Caporossi, D., and Jackson, M.J. (2012). A simple protocol for subcellular fractionation of skeletal muscle cells and tissue. *BMC Technical notes.* 5:513.

¹³³ Sigma-Aldrich. Nuclear Protein Extraction Without the Use of Detergent. [<http://www.sigmaaldrich.com/technical-documents/protocols/biology/nuclear-protein-extraction.html>] (assessed 17.12.15)

¹³⁴ Active Motif. 'preparation of nuclear extracts'
[\http://www.activemotif.com/documents/41.pdf] (assessed 17.12.15).

¹³⁵ Banda, M., Bommineni, A., Thomas, R.A., Luckinbil, L.S., and Tucker, J.D. (2008). Evaluation and validation of housekeeping genes in response to ionizing radiation and chemical exposure for normalizing RNA expression in real-time PCR. *Mutat. Res.* 649(1-2):126-34.

¹³⁶ Lackie, J. (2010). *A Dictionary of Biomedicine: Cytokine.* Oxford University Press. ISBN 9780199549351.

¹³⁷ Niu, Q.X., Chen, H.Q., Chen, Z.Y., Fu, Y.L., Lin, J.L., and He, S.H. (2008). Induction of inflammatory cytokine release from human umbilical vein endothelial cells by agonist of proteinase-activated receptor-2. *Clin Exp Pharmacol Physiol.* 35(1): 89-96.

¹³⁸ Späte, U., Schulze, P.C. (2004). Proinflammatory cytokines and skeletal muscle. *Curr Opin Clin Nutr Metab Care.* 7(3):265-9.

¹³⁹ Apte, R.N. (1995). Mechanism of Cytokine Production by Fibroblast-Implication for Normal Connective Tissue Homeostasis and Pathological Conditions. *Folia Microbiol.* 40(4):392-404.

¹⁴⁰ Linton, P., and Thoman, M.L. (2001). T cell senescence. *Front Biosci.* 6:D248-61.

-
- ¹⁴¹ Ginaldi, G., Loreto, M.F., Corsi, M.P., Modesti, M., and Martinis, M.D. (2001). Immunosenescence and infectious diseases. *Microbes and Infection*. 3(10): 851-857.
- ¹⁴² Michaud, M., Balardy, L., Moulis, G., Gaudin, C., Peyrot, C., Vellas, B., Cesari, M., and Nourhashemi, F. (2013). Pro-inflammatory Cytokines, Aging, and Age-Related Diseases. *JAMDA*. 14(12):877-882.
- ¹⁴³ Calder, P.C., Field, C.J., and Gill, H.S. (2002) Nutrition and immune function: Nutrition and ageing of the immune system. 360.
- ¹⁴⁴ Pedersen, M., Bruunsgard, H., Weis, N., Hendel, H.W., Andreassen, B.U., Eldrup, E., Dela, F., and Pedersen, B.K. (2003). Circulating levels of TNF-alpha and IL-6- relation to truncal fat mass and muscle mass in healthy elderly individuals and in patients with type-2 diabetes. *Mech Ageing Dev*. 124(4):495-502.
- ¹⁴⁵ Alsadany, M.A., Shehata, H.H., Mohamad, M.I., and Mahfouz, R.G. (2013). Histone deacetylases enzyme, copper, and IL-8 levels in patients with Alzheimer's disease. *Am J Alzheimers Dis Othe Demen*. 28(1):54-61.
- ¹⁴⁶ Clark, J.A., and Peterson, T.C. (1994) Cytokine production and aging: overproduction of IL-8 in elderly males in response to lipopolysaccharide. *Mech Ageing Dev*. 77(2):127-39.
- ¹⁴⁷ Vauzour, D., Rodriguez-Meteos, A., Corona, G., Oruna-Concha, M.J., Spencer, J.P.E. (2010). Polyphenols and human health: Prevention of disease and mechanism of action. *Nutrients*. 2(11): 1106-1131.
- ¹⁴⁸ Chandran, B., and Goel, A. (2012). A randomized, pilot study to assess the efficacy and safety of curcumin in patients with active rheumatoid arthritis. *Phytother Res*. 26(11):1719-25.
- ¹⁴⁹ Ford, C.T., Richardson, S., McArdle, F., Lotito, S.B., Crozier, A., McArdle, A., and Jackson, M.J. (2016). Identification of (poly)phenol treatments that modulate the release of pro-inflammatory cytokines by human lymphocytes. *Br J Nutr*. 115 (10): 1699 – 1710.
- ¹⁵⁰ Manger, B., Hardy, K.J., Weiss, A., and Stobo, J.D. (1986). Differential effect of cyclosporin A on activation signalling in human T cell lines. *J Clin Invest*. 77(5): 1501-6.

-
- ¹⁵¹ Nantz, M.P., Rowe, C.A., Muller, C., Creasy, R., Colee, J., Khoo, C., and Percival, S.S. (2013). Consumption of cranberry polyphenols enhances human $\gamma\delta$ - T cell proliferation and reduces the number of symptoms associated with colds and influenza: a randomized, placebo-controlled intervention study. *Nutrition Journal*. 12:161.
- ¹⁵² Roe, S.D., and Pagidas, K. (2010). Epigallocatechin-3-gallate, a natural polyphenol, inhibits cell proliferation and induces apoptosis in human ovarian cancer cells. *Anticancer Res*. 30(7):2519-23.
- ¹⁵³ Yoo, K.Y., Choi, J.H., Hwang, I.K., Lee, C.H., Lee, S.O., Han, S.M., Shin, H.C., Kang, I.J., and Won, M.H. (2010). (-)-Epigallocatechin-3-gallate increases cell proliferation and neuroblasts in the subgranular zone of the dentate gyrus in adult mice. *Phytother Res*. 24(7):1065-70.
- ¹⁵⁴ Possemiers, S., Bolca, S., Verstraete, W., and Heyerick, A. (2011). The intestinal microbiome: A separate organ inside the body with the metabolic potential to influence the bioactivity of botanicals. *Fitoterapia*. 82(1):53-66.
- ¹⁵⁵ Kliem, C., Merling, A., Giaisi, M., Köhler, R., Krammer, P.H., and Li-Weber, M. (2012). Curcumin suppresses T cell activation by blocking Ca^{2+} mobilization and nuclear factor of activated T cells (NFAT) activation. *The Journal of biological chemistry*. 287(13): 10200-10209.
- ¹⁵⁶ Fisher, W.G., Yang, P., Medikonduri, R.K., and Jafri, M.S. (2006). NFAT and NF κ B activation in T lymphocytes: A model of differential activation of gene expression. *Ann Biomed Eng*. 34(11): 1712-1728.
- ¹⁵⁷ Manna, S.K., Mukhopadhyay, A., and Aggarwal, B.B. (2000). Resveratrol suppresses TNF-induced activation of nuclear transcription factor NF- κ B, activator protein-1, and apoptosis: potential role of reactive oxygen intermediates and lipid peroxidation. *Journal of immunology*. 164 (12): 6509-6519.
- ¹⁵⁸ Shen, C.L., Yeh, J.K., Cao, J.J., Tatum, O.L., Dagda, R.Y., and Wang, J.S. (2010). Synergistic effects of green tea polyphenols and alphacalcidol on chronic inflammation-induced bone loss in female rats. *Osteoporos Int*. 21(11): 1841-1852.
- ¹⁵⁹ Chung, H. Y., Cesari, M., Anton, S., Marzetti, E., Giovanni, S., Seo, A.Y., Carter, C., Yu, B.P., and Leeuwenburgh, C. Molecular inflammation: underpinnings of aging and age-related diseases. *Ageing research reviews* 8, 18–30 (2009).

-
- ¹⁶⁰ Chang, J., Rimando, A., Pallas, M., Camins, A., Porquet, D., Reeves, J., Shukitt-Hale, B., Smith, M.A., Joseph, J.A., and Casadesus, G. (2011). Low-dose pterostilbene, but not resveratrol, is a potent neuromodulator in aging and Alzheimer's disease.
- ¹⁶¹ Díaz-Chávez, J., Fonseca-Sánchez, M.A., Arechaga-Ocampo, E.A., Flores-Pérez, A., Palacios-Rodríguez, Y., Domínguez-Gómez, Marchat, L.A., Fuentes-Mera, L., Mendoza-Hernández, G., Gariglio, P., and López-Camarillo, C. (2013). Proteomic profiling reveals that resveratrol inhibits HSP27 expression and sensitizes breast cancer cells to doxorubicin therapy. *PLOS one*. 8(5): e64378.
- ¹⁶² Meng, X., Maliakal, P, Lu, H., Lee, M., and Yang, C.S. (2004). Urinary and plasma levels of resveratrol and quercetin in human, mice, and rats after ingestion of pure compounds and grape juice. *J. Agric. Food Chem.* 52: 935-942.
- ¹⁶³ Niles, R.M., Cook, C.P., Meadows, G.G., Fu, Y., McLaughlin, J.L., and Rankin, G.O. (2006). Resveratrol is rapidly metabolized in athymic (Nu/Nu) mice and does not inhibit human melanoma xenograft tumor growth. *J. Nutrition*. 136(10): 2542-2546.
- ¹⁶⁴ Mann, M. (2009). Comparative analysis to guide quality improvements in proteomics. *Nature Methods* 6, 717-719.
- ¹⁶⁵ Patel, V.J., Thalassinou, K., Slade, S.E., Connolly, J.B., Crombie, A., Murrell, J.C., and Scrivens, J.H. (2009). A comparison of labelling and label-free mass spectrometry-based proteomics approaches. *J. Proteome Res.* 8(7): 3752-3759.
- ¹⁶⁶ Sorriento, D., Fusco, A., Ciccarelli, M., Rungi, A., Anastasio, A., Carillo, A., Dorn, G.W., Trimarco, b., Laccarino, A. (2013). Mitochondrial G protein coupled receptor kinase 2 regulates pro-inflammatory responses in macrophages. *587 (21): 3487-3494.*
- ¹⁶⁷ Riganti, C., Gazzano, E., Polimeni, M., Aldieri, E., and Ghigo, D. (2012). The pentose phosphate pathway: An antioxidant defence and a crossroad in tumor cell fate. *Free Radical biology and Medicine*. 53: 421-436.
- ¹⁶⁸ Lo, S.C., and Hannink, M. (2008). PGAM5 tethers a ternary complex containing Keap1 and Nrf2 to mitochondria. *Exp Cell Res* 314(8): 1789-803.
- ¹⁶⁹ Wang, Z., Jiang, H., Chen, S., Du, F., and Wang, X. (2012). The mitochondrial phosphatase PGAM5 function at the convergence point of multiple necrotic death pathways. *Cell*. 148(1-2): 228-43.
- ¹⁷⁰ Guo, C., Liu, S., Greenaway, F., and Sun, M.Z. (2013). Potential role of annexin A7 in cancers. *Clin Chim Acta*. 423: 83-9.

-
- ¹⁷¹ Tew, K.D., Manevich, Y., Grek, C., Xiong, Y., Uys, J., and Townsend, D.M. (2012). The role of glutathione S-transferase P in signalling pathways and S-glutathionylation in cancer. *Free Radic Bio Med.* 51(2): 299-313.
- ¹⁷² Khalaf, H., Jass, J., and Olsson, P. (2010). Differential cytokine regulation by NF- κ B and AP-1 in Jurkat T-cells. *BMC Immunol.* 11:26.
- ¹⁷³ Penela, P., Murga, C., Ribas, C., Tutor, A.S., Peregrin, S., Mayor, F., Jr. (2006). Mechanism of regulation of G protein-coupled receptor kinases (GRKs) and cardiovascular disease. *Cardiovasc Res.* 69:46-56.
- ¹⁷⁴ Permont, R.T., Gainetdinov, R.R. (2007). Physiological roles of G protein-coupled receptor kinases and arrestins. *Annu Rev Physiol.* 69:511-534.
- ¹⁷⁵ Theilade, J., Strøm, C., Christiansen, T., Haunsø, S., and Sheikh, S.P. (2003). Differential G protein receptor kinase 2 expression in compensated hypertrophy and heart failure after myocardial infarction in the rat. *Basic Res Cardiol.* 98(2):97-103.
- ¹⁷⁶ Lymperopoulos, A., Rengo, G., and Koch, W.J. (2012). GRK2 inhibition in heart failure: something old, something new. *Curr Pharm Des.* 18(2):186-91.
- ¹⁷⁷ Corbi, G., Conti, V., Russomanno, G., Longobardi, G., Furgi, G., Filippelli, A., and Ferrara, N. (2013). Adrenergic signalling and oxidative stress: a role for sirtuins? *Front. Physiol.*
- ¹⁷⁸ Maravillas-Montero, J.L. and Santos-Argumedo, L. (2011). The myosin family: unconventional roles of actin-dependent molecular motors in immune cells. *JLB.*
- ¹⁷⁹ Fomproix, N., and Percipalle, P. (2004). An actin-myosin complex on actively transcribing genes. *Exp Cell Res.* 294(1):140-8.
- ¹⁸⁰ Van Dijk, S. J., Feskens, E. J., Bos, M. B., de Groot, L. C., de Vries, J. H., Müller, M., Afman, L., A. (2012). Consumption of a high monounsaturated fat diet reduces oxidative phosphorylation gene expression in peripheral blood mononuclear cells of abdominally overweight men and women. *Journal of nutrition.* 142 (7): 1219-25.
- ¹⁸¹ Iqbal, M., Sharma, S.D., Okazaki, Y., Fujisawa, M., and Okada, S. (2003). Dietary supplementation of curcumin enhances antioxidant and phase II metabolizing enzymes in ddY male mice: possible role in protection against chemical carcinogenesis and toxicity. *Pharmacol Toxicol.* 92(1): 33-8.
- ¹⁸² Jung, K.H., and Park, J.W. (2011). Suppression of mitochondrial NADP⁺ - dependent isocitrate dehydrogenase activity enhances curcumin-induced apoptosis in HCT116 cells. *Free Radical Research.* 45(4): 431-438.

-
- ¹⁸³ Nishinaka, T., Ichijo, Y., Ito, M., Kimura, M., Katsuyama, M., Iwata, K., Miura, T., Terada, T., and Yebe-Nishimura. (2007). Curcumin activates human glutathione S-transferase P1 expression through antioxidant response element. *Toxicology Letters*. 170(3): 238-247.
- ¹⁸⁴ Wiegand, H., Boesch-Saadatmandi, C., Regos, I., Treutter, D., Wolffram, S., and Rimbach, G. (2009). Effects of quercetin and catechin on hepatic glutathione-S-transferase (GST), NAD(P)H quinone oxidoreductase 1 (NQO1), and antioxidant enzyme activity levels in rats. *Nutrition and cancer*. 61(5): 717-722.
- ¹⁸⁵ Gorrini, C., Harris, I.S., Mak, T.W. (2013). Modulation of oxidative stress as an anticancer strategy. *Nature reviews: Drug discovery*. 12:31-947.
- ¹⁸⁶ Yang, J.H., Shin, B.Y., Han, J.Y., Kim, M.G., Wi, J.E., Kim, Y.W., Cho, I.J., Kim, S.C., Shin, S.M., and Ki, S.H. (2014). Isorhamnetin protects against oxidative stress by activating Nrf2 and inducing the expression of its target genes.
- ¹⁸⁷ Franceschi, C., Bonafè, M., Valensin, S., Olivieri, F., De Luca, M., Ottaviani, E., and De Benedictis, G. (2000). Inflamm-aging. An evolutionary perspective on immunosenescence. *Ann N Y Acad Sci*. 908:244-54.
- ¹⁸⁸ Balaban, R.S., Nemoto, S., and Finkel, T. (2005). Mitochondria, Oxidants, and Ageing. *Cell*. 120 (4), 483-495.
- ¹⁸⁹ Boveris, A., Oshino, N., and Chance, B. (1972). The cellular production of hydrogen peroxide. *Biochem. J*. 128(3):617-30.
- ¹⁹⁰ Finke, T. (1998). Oxygen radicals and signalling. *Curr. Opin Cell Biol*. 10(2):248-53.
- ¹⁹¹ Hardman, D. (1956). Aging: a theory based on free radical and radiation chemistry. *J Gerontol*. 11(3): 298-300.
- ¹⁹² Thannickal, V.J., and Fanburg, B.L. (2000). Reactive oxygen species in cell signalling. *Amer. J. of Physio*. 279(6):1005-1028.
- ¹⁹³ McInnes, I.B., and Schett, G. (2007). Cytokines in the pathogenesis of rheumatoid arthritis. *Nature Review Immunology*. 7: 429-442.
- ¹⁹⁴ Pedersen, M., Bruunsgard, H., Weis, N., Hendel, H.W., Andreassen, B.U., Eldrup, E., Dela, F., and Pedersen, B.K. (2003). Circulating levels of TNF-alpha and IL-6-

relation to truncal fat mass and muscle mass in healthy elderly individuals and in patients with type-2 diabetes. *Mech Ageing Dev.* 124(4):495-502.

¹⁹⁵ Alsadany, M.A., Shehata, H.H., Mohamad, M.I., and Mahfouz, R.G. (2013). Histone deacetylases enzyme, copper, and IL-8 levels in patients with Alzheimer's disease. *Am J Alzheimers Dis Othe Demen.* 28(1):54-61.

¹⁹⁶ Vieira de Almeida, L.M., Piñeiro, C.C., Leite, M.M., Brolese, G., Tramontina, F., Feoli, A.M., Gottfried, C., and Gonçalves, C.A. (2007). Resveratrol increases glutamate uptake, glutathione content, and S100B secretion in cortical astrocyte cultures. *Cell Mol Neurobiol.* 27: 661-668.

¹⁹⁷ Sayin, O., Arslan, N., and Guner, G. (2012). The protective effects of resveratrol on human coronary artery endothelial cell damage induced by hydrogen peroxide in vitro. *Acta Clin Croat.* 51(2): 227-35.

¹⁹⁸ Igbal, M., Sharma, S.D., Okazaki, Y., Fujisawa, M., and Okada, S. (2003). Dietary supplementation of curcumin enhances antioxidant and phase II metabolizing enzymes in ddY male mice: possible role in protection against chemical carcinogenesis and toxicity. *Pharmacol Toxicol.* 92(1): 33-8.

¹⁹⁹ González-Reyes, S., Guzmán-Beltán, S., Medina-Campos, O.N., and Pedraza-Chaverri, J. (2013). Curcumin pretreatment induces Nrf2 and an antioxidant response and prevent hemin-induced toxicity in primary cultures of cerebellar granule neurons of rats. *Oxi. Med. And Cell. Longevity.*

²⁰⁰ Ramyaa, P., Krishnaswamy, R., and Padma, V.V. (2014). Quercetin modulates OTA-induced oxidative stress and redox signalling in HepG2 cells – up regulation of Nrf2 expression and down regulation of NF- κ B and COX-2. *Biochimica et Biophysica Acta.* 681-692.

²⁰¹ Liu, X., Zhang, S., Whitworth, R.J., Stuart, J.J., and Chen, M. (2015). Unbalanced activation of glutathione metabolic pathway potential involvement in plant defence against the gall midge *Mayetiola destructor* in wheat. *Scientific reports.* 5: 8092.

²⁰² Elliot, A.J., Scheiber, S.A., Thomas, C., and Pardini, R.S. (1992). Inhibition of glutathione reductase by flavonoids: A structure-activity study. *Biochem. Pharm.* 44(8):1603-1608.

²⁰³ Hayes, J.D., and Pulford, D.J. (1995). The glutathione S-transferase supergene family: regulation of GST* and the contribution of the isoenzymes to cancer chemoprotection and drug resistance. *Critical Review in Biochem. and Mol. Biol.* 30(6):445-600.

-
- ²⁰⁴ Fisher, A.B. (2011). Peroxiredoxin 6: a bifunctional enzyme with glutathione peroxidase and phospholipase A2 activities. *Antioxid Redox Signal*. 15(3): 831-44.
- ²⁰⁵ Gorrini, C., Harris, I.S., and Mak, T.W. (2013). Modulation of oxidative stress as an anticancer strategy. *Nature Reviews Drug Discovery*. 12: 931-947.
- ²⁰⁶ Limonciel, A., and Jennings, P. (2014). A review of the evidence that ochratoxin A is an Nrf2 inhibitor: implications for nephrotoxicity and renal carcinogenicity. *Toxins (Basel)*. 6(1):371-9.
- ²⁰⁷ Turtinen, L.W., Prall, D.N., Bremer, L.A., Nauss, R.E., and Hartsel, S.C. (2004). Antibody array-generated profiles of cytokine release from THP-1 leukemic monocytes exposed to different amphotericin B formulations. *Antimicrob. Agents Chemother*. 48(2): 396-403.
- ²⁰⁸ Schildberger, A., Rossmanith, E., Eichhorn, T., Strassl, K., and Weber, V. (2013). Monocytes, peripheral blood mononuclear cells, and THP-1 cells exhibit different cytokine expression patterns following stimulation with lipopolysaccharide. *Mediators of inflammation*. ID 697972, 10 pages.
- ²⁰⁹ Chanput, W., Mes, J., Vreeburg, R.A.M., Savelkoul, H.F.J., and Wichers, H.J. (2010). Transcription profiles of LPS-stimulated THP-1 monocytes and macrophages: a tool to study inflammation modulating effects of food-derived compounds. *Food and function*. 1: 254-261.
- ²¹⁰ Xue, X., Lai, K.T.A., Huang, J.F., Gu, Y., Karlsson, L., and Fourie, A. (2005). Anti-inflammatory activity on vitro and in vivo of the protein farnesyltransferase inhibitor tipifarnib. *JPET*. 317(1): 53-60.
- ²¹¹ Namiki, M., Kawashima, S., Yamashita, T., Ozaki, M., Hirase, T., Ishida, T., Inoue, N., Hirata, K., Matsukawa, A., Morishita, R., Kaneda, Y., and Yokoyama, M. (2002). Local overexpression of monocyte chemoattractant protein-1 at vessel wall induces infiltration of macrophages and formation of atherosclerotic lesion: synergism with hypercholesterolemia. *Arterioscler Thromb Vasc Biol*. 22:115–120.
- ²¹² Wang, Z.M., Gao, W., Wang, H., Zhao, D., Nie, Z.L., Shi, J.Q., Zhao, S., Lu, X., Wang, L.S., and Yang, Z.J. (2014). Green tea polyphenol epigallocatechin-3-gallate inhibits TNF- α -induced production of monocyte chemoattractant protein-1 in human umbilical vein endothelial cells. *Cell Physiol Biochem*. 33(5): 1349-58.
- ²¹³ Michaud, M., Balardy, L., Moulis, G., Gaudin, C., Peyrot, C., Vellas, B., Cesari, M., and Nourhashemi, F. (2013). Proinflammatory cytokines, Ageing and Age-related diseases. *J Amer Med Direct Ass*. 14(12): 877-882.

-
- ²¹⁴ Cianciulli, A., Dragone, T., Calvello, R., Porro, C., Trotta, T., Lofrumento, D.D., and Panaro, M.A. (2015). IL-10 plays a pivotal role in anti-inflammatory effects of resveratrol in activated microglia cells. *Int Immunopharmacol.* 2: 369-76.
- ²¹⁵ Drummond, E.M., Harbourne, N., Marete, E., Martyn, D., Jacquier, J.C., O’Riordan, D., and Gibney, E.R. (2013). Inhibition of proinflammatory biomarkers in THP1 macrophages by polyphenols derived from chamomile, meadowsweet and willow bark. *Phytother Res.* 27(4): 588-94.
- ²¹⁶ Subbaramaiah, K., Sue, E., Bhardwaj, P., Du, B., Hudis, C.A., Giri, D., Kopelovich, L., Zhou, X.K., and Dannenberg, A.J. (2013). Dietary polyphenols suppress elevated levels of proinflammatory mediators and aromatase in the mammary gland of obese mice. *Cancer Prev Res* 6(9): 886- 97.
- ²¹⁷ Luo, Y., Sun, G., Dong, X., Wang, M., Qin, M., Yu, Y, and Sun, X. (2015). Isorhamnetin attenuates atherosclerosis by inhibiting macrophage apoptosis via PI3K/AKT activation and HO-1 induction. *PLoS One.* 10(3): e0120259.
- ²¹⁸ Oh, Y.C., Kang, O.H., Choi, J.G., Chae, J.G., Lee, Y.S., Brice, O.O., Jung, H.J., Hong, S.H., Lee, Y.M., and Kwon, D.Y. (2009), Anti-inflammatory effect of resveratrol by inhibition of IL-8 production in LPS-induced THP-1 cells. *Am J Chin Med.* 37(6):1203-14.
- ²¹⁹ Ouyang, W., Rutz, S., Crellin, N.K., Valdez, P.A., and Hymowitz, S.G. (2011). Regulation and functions of the IL-10 family of cytokines in inflammation and disease. *Annu. Rev. Immunol.* 29: 71-109.
- ²²⁰ Wong, C.P., Nguyen, .P., Noh, S.K., Bray, T.M., Bruno, R.S., and Ho, E. (2010). Induction of regulatory T cells by green tea polyphenols EGCG. *Immun. Letters.* 139(1-2):7-13.
- ²²¹ Caldwell, C.C., Kojima, H., Lukashev, D., Armstrong, J., Farber, M., Apasov, S.G., and Sitkovsky, M.V. (2001). Differential effects of physiologically relevant hypoxic conditions on T lymphocyte development and effector functions. *J Immunol.* 167: 61040-6149.
- ²²² Atkuri, K.R., Herzenberg, L., Niemi, A., Cowan, T., and Herzenberg, L.A. (2006). Importance of cultering primary lymphocytes at physiological oxygen levels. *PNAS.* 104(11): 4547-4552.
- ²²³ Ershler, W.B. (1993). Interleukin-6: a cytokine for gerontologists. *J Am Geriatr Soc.* 41(2):176-81.

-
- ²²⁴ Ershler, W.B., Sun, W.H., Binkley, N., Gravenstein, S., Volk, M.J., Kamoske, G., Klipp, R.G., Roecker, E.B., Daynes, R.A., and weindruch, R. (1993). Interleukin-6 and aging: blood levels and mononuclear cell production increase with advancing age and in vitro production is modifiable by dietary restriction. *Lymphokine Cytokine Res.* 12(4): 225-30.
- ²²⁵ Bruusgard, H., Skinhøj, P., Pedersen, A.N., Schroll, M., and Pedersen, B.K. (2000). Ageing, tumour necrosis factor-alpha (TNF α) and atherosclerosis. *Clin Exp Immunol.* 121(2): 255-260.
- ²²⁶ Spaulding, C.C., Walford, R.L., and Effros, R.B. (1997). Calorie restriction inhibits the age-related dysregulation of the cytokines TNF-alpha and IL-6 in C3B10RF1 mice. *Mech Ageing Dev.* 93(1-3):897-94.
- ²²⁷ Bruunsgaard, H., and Pedersen, B.K. (2003). Age-related inflammatory cytokines and disease. *Immunol Allergy Clin North Am.* 23(1): 15-39.
- ²²⁸ 10 facts on ageing and the life course. World Health Organization. [internet]. April 2011. (Assessed 07.5.13). [<http://www.who.int/features/factfiles/ageing/en/index.html>]
- ²²⁹ Kliem, C., Merling, A., Giaisi, M., Köhler, R., Krammer, P.H., and Li-Weber, M. (2012). Curcumin suppresses T cell activation by blocking Ca²⁺ mobilization and nuclear factor of activated T cells (NFAT) activation. *The Journal of biological chemistry.* 287(13): 10200-10209.
- ²³⁰ Fisher, W.G., Yang, P., Medikonduri, R.K., and Jafri, M.S. (2006). NFAT and NF κ B activation in T lymphocytes: A model of differential activation of gene expression. *Ann Biomed Eng.* 34(11): 1712-1728.
- ²³¹ Boesch-Saadatmandi, C., Loboda, A., Wagner, A.E., Stachrska, A., Jozkowicz, A., Dulak, J., Döring, F., Wolfram, S., and Rimbach, G. (2011). Effect of quercetin and its metabolites isorhamnetin and quercetin-3-glucuronide on inflammatory gene expression: role of miR-155. *Journal of Nutritional Biochemistry.* 22(3): 293 – 299.
- ²³² Capeleto, D., Barbisan, F., Azzolin, V., Dornelles, E.B., Rogalski, F., Teixeira, C.F., Machado, A., Cadoná, F.C., da Silva, T., Duarte, M.M., and da Cruz, I.B. (2015). The anti-inflammatory effects of resveratrol on human peripheral blood mononuclear cells are influenced by a superoxide dismutase 2 gene polymorphism. *Biogerontology.* 16(5):621-30.
- ²³³ Manna, S.K., Mukhopadhyay, A., and Aggarwal, B.B. (2000). Resveratrol suppresses TNF-induced activation of nuclear transcription factor NF- κ B, activator

protein-1, and apoptosis: potential role of reactive oxygen intermediates and lipid peroxidation. *Journal of immunology*. 164 (12): 6509-6519.

²³⁴ Park, W.H., Han, Y.H., Kim, S.H, and Kim, S.Z. (2007). Pyrogallol, ROS generator inhibits As4.1 juxtaglomerular cells via cell cycle arrest of G2 phase and apoptosis. *Toxicology*. 235(1-2): 130-9.

²³⁵ Kim, S.W., Han, Y.W., Lee, S.T., Jeong, H.J., Kim, I.H., Lee, S.O., Kim, D.G., Kim, S.H., Kim, S.Z., and Park, W.H. (2008). A superoxide anion generator, pyrogallol, inhibits the growth of HeLa cells via cell cycle arrest and apoptosis. *Mol Carcinog*. 47(2): 114-25.

²³⁶ Han, Y.H., Kim, S.Z., Kim, S.H., and Park, W.H. (2008). Pyrogallol as a glutathione depletory induces apoptosis in HeLa cells. *Int J Mol Med*. 21(6): 721-30.

²³⁷ Kim, J.E., Son, J.E., Jung, S.K., Kang, N.J., Lee, C.Y., Lee, K.W., and Lee, H.J. (2010). Cocoa polyphenols suppress TNF- α -induced vascular endothelial growth factor expression by inhibiting phosphoinositide 3-kinase (PI3K) and mitogen-activated protein kinase kinase-1 (MEK1) activities in mouse epidermal cells. *Br J Nutr*. 104(7): 957-64.

²³⁸ Roux, P.P., Shahbazian, D., Vu, H., Holz, M.K., Cohen, M.S., Taunton, J., Sonenberg, N., and Blenis, J. (2007). RAS/ERK signalling promotes site-specific ribosomal protein S6 phosphorylation via RSK and stimulates cap-dependent translation. *J Biol Chem*. 282(19):14056-64.

²³⁹ RPS6KA1 (ribosomal protein S6 kinase, 90kDa, polypeptide 1). Atlas of genetics and cytogenetics in oncology and haematology. Assessed July 2015. [<http://atlasgeneticsoncology.org/Genes/RPS6KA1ID43477ch1p36.html>]

²⁴⁰ Manczak, M., Park, B.S., Jung, Y, and Reddy, P.H. (2004). Differential expression of oxidative phosphorylation genes in patients with Alzheimer's disease: implications for early mitochondrial dysfunction and oxidative damage. *Neuromolecular Med*. 5(2): 147-62.

²⁴¹ Hayden, M.S., West, A.P. and Ghosh, S. (2006). NF-kappaB and the immune response. *Oncogene*. 25(51):6758-80.

²⁴² Kriete, A., and Mayo, K.L. (2009). Atypical pathways of NF-kappaB activation and aging. *Exp. Genontol*. 44(4): 250-5.

-
- ²⁴³ Ruiz, P.A., and Haller, D. (2006). Functional diversity of flavonoids in the inhibition of the proinflammatory NF-kappaB, IRF, and Akt signalling pathways in murine intestinal epithelial cells. *J. Nutr.* 136(3): 664-71.
- ²⁴⁴ Karunaweera, N., Raju, R., Gyengesi, E., and Münch, G. (2015). Plant polyphenols as inhibitors of NF-κB induced cytokine production – a potential anti-inflammatory treatment for Alzheimer’s disease? *Front. Mol. Neurosci.* 8:24.
- ²⁴⁵ Biswas, S.K., McClure, D., Jimenez, L.A., Megson, I.L., and Rahman, I. (2005). Curcumin induces glutathione biosynthesis and inhibits NF-kappaB activation and interleukin-8 release in alveolar epithelial cells: mechanism of free radical scavenging activity. *Antioxid Redox Signal.* 7(1-2): 32-41.
- ²⁴⁶ Sheehan, D., Meade, G., Foley, V.M. and Dowd, C.A. (2001). Structure, function and evolution of glutathione transferases: implications for classification of non-mammalian members of an ancient enzyme superfamily. *Biochem. J.* 15(360)(Pt1):1-16.
- ²⁴⁷ Fisher, A.B. (2011). Peroxiredoxin 6: a bifunctional enzyme with glutathione peroxidase and phospholipase A2 activities. *Antioxid. Redox Signal.* 15(3):831-44.
- ²⁴⁸ Dayer, R., Fischer, B.B., Eggen, R.I.L. and Lemaire, S.D. (2008). The peroxiredoxins and glutathione peroxidase families in *Chlamydomonas reinhardtii*. *Genetics.* 179(1):41-57.
- ²⁴⁹ Baird, L., and Dinkova-Kodtova, A. T. (2011). The cytoprotective role of the Keap1-Nrf2 pathway. *85*: 241-272.
- ²⁵⁰ Tanigawa, S., Fujii, M., and Hou, D.X. (2007). Action of Nrf2 and Keap1 in ARE-mediated NQO1 expression by quercetin. *Free Radic Biol Med.* 42(11):1690-703.
- ²⁵¹ Chen, C., Yu, R., Owuor, E.D., and Kong, A.T. (2000). Activation of antioxidant-response element (ARE), mitogen-activated protein kinases (MAPKs) and caspases by major green tea polyphenol components during cell survival and death. *Arch. Phar., Res.* 23(6):605-612.
- ²⁵² Mustacich, D., and Powis, G. (2000). Thioredoxin reductase. *Biochem. J.* 346 Pt 1: 1-8.
- ²⁵³ Rhee, S.G., Kang, S.W., Chang, T.S., Jeong, W., and Kim, K. (2001). Peroxiredoxin, a novel family of peroxidases. *IUBMB Life.* 52 (1-2): 35-41.
- ²⁵⁴ UniProt. Protein database. [<http://www.uniprot.org/>] accessed July 2015.

-
- ²⁵⁵ Megumi, M., Atsushi, I., Eriko, S., Shogo, O., and Toshisike, K. (2003). Mixed lineage kinase L2K and antioxidant protein-1 activate NF-kappaB synergistically. *Eur. J. Biochem (Germany)*. 270 (1): 76-83.
- ²⁵⁶ Schriener, S.E., Linford, N.J., Martin, G.M., Treuting, P., Ogburn, C.E., Emond, M., Coskun, P.E., Ladiges, W., Wolf, N., Van Remmen, H, Wallace, D.C., and Rabinovitch, P.S. (2005). Extension of murine life span by overexpression of catalase targeted to mitochondria. *Science*. 308(5730):1909-11.
- ²⁵⁷ Kegg Pathway Database [<http://www.genome.jp/kegg/pathway.html>] assessed Jan 2015.
- ²⁵⁸ Gorrini, C., Harris, I.S., and Mak, T.W. (2013). Modulation of oxidative stress as an anticancer strategy. *Nat Rev Drug Discov*. 12(12):931-47.
- ²⁵⁹ Hsieh, C.C., and Papaconstantinou, J. (2009). Dermal fibroblasts from long-lived Ames dwarf mice maintain their in vivo resistance to mitochondrial generated reactive oxygen species (ROS). *Aging (Albany NY)*. 1(9):784-802.
- ²⁶⁰ Masaki, M., Ikeda, A., Shiraki, E., Oka, S., and Kawasaki, T. (2003). Mixed lineage kinase L2K and antioxidant protein-1 activate NF-kappaB synergistically. *Eur. J. Biochem*. 270(1):76-83.
- ²⁶¹ Wang, T., Arifolu, P., Ronai, Z., and Tew, K.D. (2001). Glutathione S-transferase P1-1 (GSTP1-1) inhibits c-Jun N-terminal kinase (JNK1) signaling through interaction with the C terminus. *J. Biol. Chem*. 276(24):20999-1003.
- ²⁶² Han, X., Shen, T., and Lou, H. (2007). Dietary polyphenols and their biological significance. *Int. J. Mol. Sci*. 8(9):950-988.
- ²⁶³ Arnér, E.S., and Holmgren, A. (2000). Physiological functions of thioredoxin and thioredoxin reductase. *Eur. J. Biochem*. 267(20):6102-9.
- ²⁶⁴ Ambruso, D.R. (2013). Peroxiredoxin-6 and NADPH oxidase activity. *Methods Enzymol*. 527:145-67.
- ²⁶⁵ Khor, T.O., Huang, M.T., Kwon, K.H., Chan, J.Y., Reddy, B.S., and Kong, A.N. (2006). Nrf2-deficient mice have an increased susceptibility to dextran sulfate sodium-induced colitis. *Cancer Res*. 66(24):11580-4.
- ²⁶⁶ Kwak, M.K., Wakabayashi, N., Itoh, K., Motohashi, H., Yamamoto, M., and Kensler, T.W. (2003). Modulation of gene expression by cancer chemopreventative

dithiolethiones through the Keap1-Nrf2 pathway. Identification of novel gene clusters for cell survival. *J Biol Chem.* 278(10):8135-45.

²⁶⁷ Zheng, N., Felix, C.A., Pang, S., Boston, R., Moate, P., Scavuzzo, J., and Blair, I.A. (2004). Plasma etoposide catechol increases in pediatric patients undergoing multiple-day chemotherapy with etoposide. *Clin. Cancer. Res.* 10:2977.

²⁶⁸ Kim, H., Roh, H., Lee, H.J., Chung, S.Y., Choi, S.O., Lee, K.R., and Han, B. (2003). Determination of phloroglucinol in human plasma by high-performance liquid chromatography-mass spectrometry. *J Chromatography B.* 792(2): 307-312.

²⁶⁹ Urpi-Sarda, M., Monagas, M., Khan, N., Llorach, R., Lamuela-Raventós, R.M., Jáuregui, O., Estruch, R., Izquierdo-Pulido, M., Andrés-Lacueva, C. (2009). Targeted metabolic profiling of phenolics in urine and plasma after regular consumption of cocoa by liquid chromatography-tandem mass spectrometry. *J. Chrom. A.* 1216: 7258-7267.

²⁷⁰ Rodriguez-Gutiérrez, G., Wood, S., Guzmán, J.F.B., Duthie, G.G., and Roos, B. (2011). Determination of 3,4-dihydroxyphenylglycol, hydroxytyrosol and tyrosol purified from olive oil by-products with HPLC in animal plasma and tissue. *Food Chem.* 126(4) 1948-1952.

²⁷¹ Beving, H., Olsson, U., Bemgård, A., Kristensson, J., Palmborg, J., and Sollenberg, J. (1990), High-performance liquid chromatographic analysis of hippuric acid in human blood samples. *J Chromatography.* 535(1): 45-53.

²⁷² Clifford, M.N. (2000). Chlorogenic acids and other cinnamates – nature, occurrence, dietary burden, absorption and metabolism. *J. Sci. Food Agric.* 80: 1033-1043.

²⁷³ Gonthier, M.P., Verny, M.A., Besson, C., Rémésy, C., and Scalbert, A. (2003). Chlorogenic acid bioavailability largely depends on its metabolism by the gut microflora in rats. *J Nutr.* 133(6): 1853-9.

²⁷⁴ Deutsch, J.C. (1997). Determination of p-hydroxyphenylpyruvate, p-hydroxyphenyllactate and tyrosine in normal human plasma by gas chromatography-mass spectrometry isotope-dilution assay. *J Chromatography B Viomed Sci Appl.* 690(1-2):1-6.

²⁷⁵ Niles, R.M., Cook, C.P., Meadows, G.G., Fu, Y., McLaughlin, J.L., and Rankin, G.O. (2006). Resveratrol is rapidly metabolized in athymic (Nu/Nu) mice and does not inhibit human melanoma xenograft tumor growth. *J. Nutrition.* 136(10): 2542-2546.

-
- ²⁷⁶ Wiczowski, W., Romaszko, K., Bucinski, A., Szawara-Nowak, D., Honke, J., Zielinski, H., and Piskula, M.K. (2008). Quercetin from shallots (*Allium cepa* L. var. *aggregatum*) is more bioavailable than its glucosides. *J Nutr.* 138(5): 885-8.
- ²⁷⁷ Loke, W.M., Hodgson, J.M., Proudfoot, J.M., McKinley, A.J., Puddey, I.B. and Croft, K.D. (2008). Pure dietary flavonoids quercetin and (-)-epicatechin augment nitric oxide products and reduce endothelin-1 acutely in healthy men. *American J Clin Nutr.* 88(4): 1018-1025.
- ²⁷⁸ Lan, K., Jiang, X., and He, J. (2007). Quantitative determination of isorhamnetin, quercetin and kaempferol in rat plasma by liquid chromatography with electrospray ionization tandem mass spectrometry and its application to the pharmacokinetic study of isorhamnetin. *Rapid Commun. Mass Spectrom.* 21(2): 12-20.
- ²⁷⁹ Bone, K., and Mills, S. (2013). Principles and practice of phytotherapy, 2nd Ed. Modern herbal medicine. Churchill Livingstone Elsevier. pg. 603.
- ²⁸⁰ Farah, A., Monteiro, M., Donangelo, C.M., and Lafay, S. (2008). Chlorogenic acids from green coffee extract are highly bioavailable in humans. *J Nutr.* 138(12): 2309-2315.
- ²⁸¹ Sharma, R.A., Euden, S.A., Platton, S.L., Cooke, D.N., Shafayat, A., Hewitt, H.R., Marczylo, T.H., Morgan, B., Hemingway, D., Plummer, S.M., Pimohamed, M., Gescher, A.J., and Steward, W.P. (2004). Phase I clinical trial of oral curcumin biomarker of systemic activity and compliance. *Clin. Cancer Res.* 10: 6847.
- ²⁸² Vareed, S.K., Kakarala, M., Ruffin, M.T., Crowell, J.A., Normolle, D.P., Djuric, Z., and Brenner, D.E. (2008). Pharmacokinetics of curcumin conjugate metabolites in healthy human subjects. *Cancer Epidemiol Biomarkers Prev.* 17(6): 1411-1417.
- ²⁸³ Wu, X., Pittman, H.E. 3rd, and Prior, R.L. (2004). Peragonidin is absorbed and metabolized differently than cyaniding after marionberry consumption in pigs. *J Nutr.* 134(10): 2603-10.
- ²⁸⁴ Mullen, W., Edward, C.A., Serafini, M., and Crozier, A. (2008). Bioavailability of pelargonidin-3-O-glucoside and its metabolites in humans following the ingestion of strawberries with and without cream. *J Agric Food Chem.* 56(3): 713-9.
- ²⁸⁵ Cerdá, B., Llorach, R., Cerón, J.J., Esoin, J.C., and Tomás-Barberán, F.A. (2003). Evaluation of the bioavailability and metabolism in the rat of punicalagin, an antioxidant polyphenol from pomegranate juice. *Eur J Nutr.* 42(1): 18-28.
- ²⁸⁶ Ramachandran, L., Manu, K.A., Shanmugam, M.K., Li, F., Siveen, K.S., Vali, S., Kapoor, S., Abbasi, T., Surana, R., Smoot, D.T., Ashktorab, H., Tan, P., Ahn, K.S., Yap,

C.W., Kumar, A.P., and Sethi, G. (2012). Isorhamnetin inhibits proliferation and invasion and induces apoptosis through modulation of peroxisome proliferator-activated receptor γ activation pathway in gastric cancer. *J Biol Chem.* 287(45): 38028-38040.

²⁸⁷ Zhang, B., Wang, Y., Gong, H., Zhao, H., Lv, X., Yuan, G., and Han, S. (2015). Isorhamnetin flavonoid synergistically enhances the anticancer activity and apoptosis induction by cis-platin and carboplatin in non-small cell lung carcinoma (NSCLC). *Int J Clin Exp Pathol.* 8(1): 25-37.